

Bonding Interactions in Congested Molecules: A Study of the Interatomic Forces and the Molecular Electrostatic Potential

Stuart Raymond Colenzo von Berg



Dissertation presented for the degree of Doctor of Philosophy in the Faculty of Science at Stellenbosch University

Supervisor: Prof. Jan L. M. Dillen

December 2022

Declaration

By submitting this dissertation electronically, I declare that the entirety of the work contained therein is my own, original work, that I am the sole author thereof (save to the extent explicitly otherwise stated), that reproduction and publication thereof by Stellenbosch University will not infringe any third party rights and that I have not previously in its entirety or in part submitted it for obtaining any qualification.

December 2022

Abstract

The purpose of this research is to apply the quantum theory of atoms in molecules (QTAIM) to the molecular electrostatic potential (MEP) field and use the topology of the MEP to determine whether a stabilising interaction occurs between two hydrogens in a congested molecule. A method for comparing bond strength using the ratio of the nuclear and electronic components of the MEP is developed and applied to the congested molecules. The MEP ratio was used to associate the bond strength of the hydrogen-hydrogen interaction in congested molecules to that of a hydrogen bond between water molecules. Despite this result, analysis of the electron density, laplacian and kinetic energy created an equally compelling argument against the interaction being stabilising. Applying the QTAIM method to the MEP topology does not provide sufficient evidence to determine whether the hydrogen-hydrogen interaction in congested molecules forms a stabilising or destabilising interaction.

Opsomming

Die doel van hierdie navorsing is om die kwantumteorie van atome in molekules (QTAIM) toe te pas op die veld vir molekulêre elektrostatiese potensiaal (MEP) en die topologie van die MEP te gebruik om te bepaal of 'n stabiliserende interaksie tussen twee waterstowwe in 'n oorbelaste molekule voorkom. 'N Metode vir die vergelyking van bindingssterkte met behulp van die verhouding van die kern- en elektroniese komponente van die MEP word ontwikkel en toegepas op die oorbelaste molekules. Die MEP-verhouding is gebruik om die bindingssterkte van die waterstof-waterstof-interaksie in oorvol molekules te verbind met die van 'n waterstofbinding tussen watermolekules. Ten spyte van hierdie resultaat het analyse van die elektrondigtheid, laplakese en kinetiese energie 'n ewe dwingende argument geskep teen die stabilisering van die interaksie. Die toepassing van die QTAIM-metode op die MEP-topologie lewer nie voldoende bewyse om te bepaal of die waterstof-waterstofinteraksie in oorvol molekules 'n stabiliserende of destabiliserende interaksie vorm nie.

Acknowledgments

The author would like to acknowledge the generosity of the National Research Foundation (NRF) for the financial support of this research. The financial support provided by the University of Stellenbosch was greatly appreciated and helpful in completing the research.

Thank you to Prof. C. Esterhuysen for making herself available for discussions whenever needed. Thank you to Prof. J. Dillen for his endless amount of patience and understanding, his expansive knowledge motivated me to always be assessing my understanding and interpretation of the research.

A special thank you to my family whose mental support and encouragement went a long way in helping me to get through the sometimes frustrating world of research.

Contents

Declaration	i
Abstract	ii
Opsomming	iii
Acknowledgments	iv
List of Figures	vi
List of Tables	vii
List of Abbreviations and Symbols	viii
1 Introduction	1
1.1 Interactions in Molecules	1
1.2 Structure of Thesis	8
2 Background	9
2.1 Quantum Theory of Atoms in Molecules	9
2.1.1 Critical Points	9
2.1.2 Ellipticity	12
2.1.3 Poincaré-Hopf Rule	12
2.2 Molecular Graphs	13
2.2.1 Constructing Molecular Graphs	13
2.3 A Definition for Atoms and Bonds	15
2.3.1 Types of Atomic Interactions	18
2.4 Molecular Electrostatic Potential	18
2.4.1 Topology and the Molecular Electrostatic Potential	20
2.4.2 Computational Method	23
2.5 eDensity	27
3 Exploring the Topologies of Electron Density and Molecular Electrostatic Potential Scalar Fields	30
3.1 Comparing the Electron Density and Molecular Electrostatic Potential Scalar Fields	30
3.1.1 Extreme Examples of Methane	32
3.1.2 Iso-surface and Gradient Lines of the Methane Molecule	36
3.2 Using the Topology to Identify Molecular Properties	39
3.3 Exploring Degenerate Critical Points	54

3.4	Conclusions	63
4	Defining Atom Interactions in the Molecular Electrostatic Potential	64
4.1	Interactions in the Hydrogen Molecule	64
4.1.1	Interactions in the Singlet and Triplet State for a Hydrogen Molecule . .	64
4.1.2	Interactions with a Background Charge	68
4.2	Interactions Between Noble Gases	70
4.3	Using the Ratio of nucMEP : elecMEP in Order to Define an Interaction	72
4.4	Conclusions	77
5	Exploring Hydrogen-Hydrogen Bonding in Molecules	80
5.1	Analysing the Molecular Electrostatic Potential Topology of the 2-Butene Molecule	80
5.2	Analysing the Chrysene Molecule	83
5.3	The MEP Topology of the Biphenyl Molecule	93
5.4	Congested Molecules	97
5.4.1	Conclusion	102
6	Conclusion	104
	Appendix A	109
	Bibliography	120

List of Figures

2.1	<i>Adamantane has examples of the four different critical points of rank three, NA (sphere), BCP (cylinder), RCP (ring) and CCP (cube).</i>	11
2.2	<i>A hydrogen molecule calculated in the electron density with two atomic basins, one shown by gradient lines and the other a filled boundary, and an AIL connecting the two atoms (red line). The (3, -1) critical point is depicted as a red cylinder.</i>	14
2.3	<i>The twisted biphenyl molecule shows the linking of (3, +3) critical points (green cube) with a gradient line passing through a (3, +1) critical point (blue ring) in the MEP.</i>	15
2.4	<i>The dashed lines represent the eigenvectors that had a positive eigenvalue and the surface with the solid arrows represent the surface created by the two eigenvectors associated with the negative eigenvalues.</i>	16
2.5	<i>MEP topology of a methane molecule showing four minima (green cubes) positioned between the hydrogens and joined by four (3, +1) saddle points (blue rings). The benzene topology is shown with the critical points above and below the ring.</i>	20
2.5	<i>The MEP topology of three molecules consisting of aromatic rings. The position of the critical points are attributed to the dispersed nature of the electrons which are associated with these types of structures. The grey cylinders are (3, -1) critical points, green cubes are (3, +3) critical points and the blue rings are (3, +1) critical points. The red (3, -1) critical point and atomic interaction line show a hydrogen-hydrogen bond.</i>	21
2.6	<i>The MEP calculated for the ethylene molecule shows the minima above and below the molecule which signifies the pi bonding electrons. The 1,3-trans-butadiene has the minima showing the double bonds and the (3, +1) critical point (blue ring) shows that the electrons bridge the space over the single bond. The joining of the two minima with a saddle point is attributed to dispersed electrons.</i>	22
2.7	<i>MEP topology of an ethane molecule showing two minima (green cubes) positioned between the hydrogens, the same can be seen in cyclohexane</i>	23
2.8	<i>The four critical points in eDensity is represented by the sphere (NA), cylinder (BCP), disc (RCP) and a cube (CCP).</i>	27
2.9	<i>The creation of the inter atomic surface using gradient lines and triangles to connect the gradient lines.</i>	28
2.10	<i>The acetylene molecule has a (2, +2) critical point which becomes a ring and the chloro-ethyne molecule shows a (2, 0) saddle point between two (2, +2) critical points all of which form a ring.</i>	29

3.1	<i>The first set of ethane, ethylene and acetylene are calculated in the electron density scalar field. The second set of ethane, ethylene and acetylene are calculated in the MEP scalar field. The black spheres are nuclear attractors representing carbon atoms, grey spheres are hydrogen atoms. The pink sphere for acetylene is a non-nuclear attractor. The grey cylinders are (3, -1) critical points, green cubes are (3, +3) critical points and the pink sphere is a (3, -3) critical point. The ring surrounding the (3, -1) critical point is a (2, +2) ring.</i>	31
3.0	<i>The six groups of pictures show a comparison between the electron density (pictures on the left) and MEP (pictures on the right) scalar fields when calculating the methane molecule. The lengths are chosen at 2, 3, 3.5, 5 and 5.5 Angstroms because at these distances the topology of the MEP undergoes significant changes. The first set of pictures shows the fully optimised structure of the methane molecule, thereafter only the bond length is fixed. The black spheres represent carbon atom, grey spheres are hydrogen atoms. The grey cylinders are (3, -1) critical points, the blue rings are (3, +1) critical points and green cubes are (3, +3) critical points.</i>	34
3.1	<i>A MEP iso-surface of fully optimised methane.</i>	36
3.2	<i>A MEP iso-surface of methane with bond lengths of 2 Å.</i>	37
3.3	<i>A contour plot of the methane molecule with bond lengths of 2 Å. The white contour lines show negative MEP and the black contour lines show positive MEP. The grey cylinders are (3, -1) critical points, the blue rings are (3, +1) critical points and green cubes are (3, +3) critical points. The grey sphere is carbon and the white spheres are hydrogen atoms.</i>	38
3.4	<i>Gradient lines of the methane molecule, on the left is the optimised structure and on the right is the methane molecule with bond lengths of 2 Å. The grey cylinders are (3, -1) critical points, the blue rings are (3, +1) critical points and green cubes are (3, +3) critical points. The grey sphere is carbon and the white spheres are hydrogen atoms.</i>	39
3.5	<i>Assigned double bonds of naphthalene (left) and naphthacene (right) based on the locations of the minima. The grey cylinders are (3, -1) critical points, the blue rings are (3, +1) critical points and green cubes are (3, +3) critical points. The black spheres are carbon atoms and the white spheres are hydrogen atoms.</i>	40
3.6	<i>The minima above and below the carbon-carbon bond in 1,3-trans-butadiene are separated by a (3, +1) saddle point. This configuration could be attributed to delocalised electrons. The hydrogens out of the plane have been removed for the contour plot, the black lines correspond to the positive MEP and the white lines the negative MEP. The grey cylinders are (3, -1) critical points, the blue rings are (3, +1) critical points and green cubes are (3, +3) critical points. The black spheres are carbon atoms and the grey spheres are hydrogen atoms.</i>	41
3.7	<i>The water and ammonia molecules both showing minima which represent lone pairs, the minima associated with a lone pair in nitrogen is indicated with an arrow. The minima between the hydrogens of the ammonia molecule serves the same function as the minima seen in ethane. The grey cylinders are (3, -1) critical points and the green cubes are (3, +3) critical points. The red sphere is oxygen and the blue sphere is nitrogen, the white spheres are hydrogen atoms.</i>	42

- 3.8 *The top MEP contour plot of water is shown with the plane through the (3, +3) critical points, the hydrogens are shown extending out of the plane. The MEP contour plot on the bottom shows the water molecule with the plane through the oxygen and hydrogens, the minima are out of the plane. The black lines show the positive MEP and the white lines show the negative MEP. The grey cylinders are (3, -1) critical points, the blue rings are (3, +1) critical points and the green cubes are (3, +3) critical points. The red sphere is oxygen and the white spheres are hydrogen atoms. 43*
- 3.9 *The contour plot of the ammonia molecule with the black line representing positive MEP and the white lines the negative MEP. The minimum below the hydrogens exists in the positive MEP as shown by the black contour lines. The grey cylinders are (3, -1) critical points, the blue rings are (3, +1) critical points and the green cubes are (3, +3) critical points. The blue sphere is a nitrogen atom and the grey spheres are hydrogen atoms. 44*
- 3.10 *The ethane molecule on the top is calculated with B3LYP//Def2TZVPP and the ethane molecule on the bottom is calculated with HF//AUG-cc-pVTZ. The grey cylinders are (3, -1) critical points and the green cubes are (3, +3) critical points and the blue rings are (3, +1) critical points. The black spheres are carbon the grey spheres are hydrogen atoms. 45*
- 3.10 *In the first figure the black contour lines around the atoms show the positive MEP while the white contour lines around the minima show the negative MEP. The second image is the gradient lines of carbon and hydrogen and are represented on a plane passing through the carbon and two of the hydrogens. The grey cylinders are (3, -1) critical points and the green cubes are (3, +3) critical points and the. The black spheres are carbon atoms and the white spheres are hydrogen atoms. 47*
- 3.11 *The distance between the carbon and hydrogen is 1.086 Å, hydrogen to minimum is 1.981 Å, and the angle is $\alpha = 80.47$ degrees. The grey cylinders are (3, -1) critical points and the green cubes are (3, +3) critical points. The black spheres are carbon atoms and the grey spheres are hydrogen atoms. 48*
- 3.12 *Methane has a distance between carbon and hydrogen of 1.083 Å and the distance between hydrogen and the minimum is 1.998 Å forming a bond angle of $\alpha = 78.73$. cyclohexane has a distance between the carbon and hydrogen of 1.090 Å and the distance between hydrogen and the minimum is 1.595 Å forming a bond angle of $\alpha = 93.60$. The grey cylinders are (3, -1) critical points and the green cubes are (3, +3) critical points and the blue rings are (3, +1) critical points. The black spheres are carbon the grey spheres are hydrogen atoms. 49*
- 3.12 *cyclohexane (top) has minima outside the ring which can be attributed to hybridisation of the carbon atoms. The minima for the benzene molecule (bottom) are located inside the ring stabilising the molecule. The ring created by the minima and (3, +1) saddle points has a radius smaller than the radius of the benzene molecule. Benzotriyne is a hypothetical molecule showing the minima outside the ring which is associated with bond strain. The grey cylinders are (3, -1) critical points and the green cubes are (3, +3) critical points and the blue rings are (3, +1) critical points. The black spheres are carbon atoms and the grey spheres are hydrogen atoms. 51*

- 3.13 *The first image shows the contour lines of the MEP with the plane going through the minima and carbon atoms. The second image is the plane passing through the four hydrogens and shows no negative MEP. The black contour lines are positive MEP and the white lines are negative MEP. The grey cylinders are (3, -1) critical points and the green cubes are (3, +3) critical points. The grey spheres are carbon atoms and the white spheres are hydrogen atoms. 52*
- 3.14 *The symmetry of the ethylene molecule was distorted by rotating one of the CH₂ groups. The black contour lines are positive MEP and the white lines are negative MEP. The grey cylinders are (3, -1) critical points, the blue rings are (3, +1) critical points and green cubes are (3, +3) critical points. The black spheres are carbon atoms and the grey spheres are hydrogen atoms. 53*
- 3.15 *A comparison between the electron density and the MEP at the minima located around various molecules. 54*
- 3.16 *The acetylene molecule on the left is shown with a degenerate ring around the middle of the molecule. The gradient lines shown in the image on the right all terminate at the degenerate ring. The grey cylinders are (3, -1) critical points, the ring around the molecule is made up of connecting (2, +2) critical points. The black spheres are carbon atoms and the grey spheres are hydrogen atoms. . . 55*
- 3.17 *The contour plot of the acetylene molecule is shown with the negative region shown by the white lines. The D_{∞h} symmetrical nature of the molecule means that the negative region is a continuous band around the centre of the molecule. The black contour lines show the positive region of the molecule. The grey cylinders are (3, -1) critical points, the black spheres are carbon atoms and the grey spheres are hydrogen atoms. 55*
- 3.18 *The 1-butyne molecule is shown on the left and the 2-butyne molecule is shown on the right. The grey cylinders are (3, -1) critical points, the blue rings are (3, +1) critical points and green cubes are (3, +3) critical points. The black spheres are carbon atoms and the grey spheres are hydrogen atoms. 56*
- 3.19 *The 1-butyne molecule is shown on the top and the 2-butyne molecule is shown on the bottom. The rank one critical point is shown by the arrow. The grey cylinders are (3, -1) critical points, the blue rings are (3, +1) critical points and green cubes are (3, +3) critical points. The purple sphere is a (1, -1) critical point. The black spheres are carbon atoms and the grey spheres are hydrogen atoms. . . 57*
- 3.20 *Instead of minima as for the water molecule the hydroxy anion has a ring of degenerate critical points. The gradient lines of the molecule encapsulates the molecule. The grey cylinders are (3, -1) critical points, the ring around the molecule is made up of connecting (2, +2) critical points. The red sphere is an oxygen atom and the grey sphere is a hydrogen atom. 58*
- 3.21 *The first molecule on the left is the fluoro-ethyne molecule and the second molecule on the right is the chloro-ethyne molecule. The second set of pictures show the gradient lines for the molecules. The grey cylinders are (3, -1) critical points, the black spheres are carbon atoms and the white spheres are hydrogen atoms, fluorine is shown as a yellow sphere and the chlorine atom is shown in green. The (2, +2) degenerate ring is blue and the (2, 0) degenerate ring is shown in green. 59*

3.22	<i>The fluorine molecule highlights that the (2, 0) degenerate ring is a consequence of the two (2, +2) degenerate ring. The (2, 0) degenerate ring is missing from the hydrogen fluoride molecule. The grey cylinders are (3, -1) critical points, the blue ring is made up of connecting (2, +2) critical points and the green ring is made up of connecting (2, 0) critical points. The yellow sphere is fluorine and the grey sphere is a hydrogen atom.</i>	60
3.23	<i>The fluorine atom is added to ethane and ethylene, the interaction with the π electrons influences the topology of the fluorine molecule. The grey cylinders are (3, -1) critical points, the blue rings are (3, +1) critical points and the green cubes are (3, +3). The yellow sphere is fluorine, black spheres are carbon and the grey spheres are hydrogen atoms.</i>	61
3.24	<i>An example of linear molecules with triple bonds (which are both linked to degenerate rings) where no degenerate ring is calculated.. The grey cylinders are (3, -1) critical points, the green cubes are (3, +3). The blue sphere are nitrogen and the black black spheres are carbon atoms.</i>	62
4.1	<i>Energies of the hydrogen molecule in the singlet state (H_2) and in the triplet state (tH_2). Energies are taken at intervals of 0.5 Å, included in the graph are the optimised bond lengths of 0.735 Å (H_2) and 5.044 Å (tH_2).</i>	65
4.2	<i>The two graphs show the MEP at the nucleus as well as the (3, -1) saddle point for the hydrogen molecule in the singlet and the triplet states, shown on the top and bottom respectively. The nucMEP refers to the nuclear component of the MEP and the elecMEP refers to the electronic component. Also shown on the graph is the elecMEP of the hydrogen NA, the values for the critical points were calculated in the MEP field.</i>	66
4.3	<i>The electron density calculated for a single hydrogen NA and the (3, -1) critical point (BCP) are compared for the hydrogen molecule in the singlet and triplet states.</i>	67
4.4	<i>The changing of the Laplacian ($\nabla^2\rho(r)$) with regards to the distance between the hydrogen atoms is shown for the hydrogen molecule in the singlet (H_2) and triplet (tH_2) states, values are taken from the (3, -1) critical point.</i>	67
4.4	<i>The atoms hydrogen, helium, neon and argon are shown interacting with a positive background charge in the MEP field, both the contour plot and gradient lines are shown. The calculations shown are at 1 Å, the red contour lines represent a negative value.</i>	70
4.5	<i>The MEP at the (3, -1) saddle point is shown for the hydrogen molecule in the ground state as well as for the three noble gases; He_2, Ne_2 and Ar_2. The symbols that do not have a colour fill indicate the distance between the atoms when fully optimised.</i>	71
4.6	<i>The MEP at the (3, -1) critical point between a carbon and hydrogen is plotted against the distance between the two atoms. The hydrocarbons plotted are a mixture alkanes, alkenes, alkynes as well as cyclo-hydrocarbons and aromatic structures. The triangles are cyclic structures and the dots are aliphatic structures.</i>	73
4.7	<i>Comparing the ratio of the nuclear MEP : electronic MEP to the total MEP at the (3, -1) critical point between carbon and hydrogen for a series of hydrocarbons.</i>	74
4.8	<i>A compilation of various bond types and bond order with H_2 shown as the upper limit and tH_2 shown at the lower limit. The dashed line is set a ratio of 1.0000 and any value below this line is regarded as being a non-bonding interaction . . .</i>	77

5.1	<i>The molecular graph of 2-butene in the MEP has a possible hydrogen-hydrogen bond between H11 and H7 (shown in red). The bond between atoms C3 and C4 is a double bond. The black spheres are carbon and the white spheres are hydrogen atoms. The white cylinders are (3, -1) critical points, blue rings are (3, +1) saddle points and the green cubes are (3, +3) critical points.</i>	81
5.1	<i>On the top is contour plot of the space between the two interacting hydrogens. On the bottom is a contour plot of the plane containing the (3, +1) saddle point. The white contour lines are negative MEP and the black contour lines are positive MEP. The black spheres are carbon and the white spheres are hydrogen atoms. The white cylinders are (3, -1) critical points, blue rings are (3, +1) saddle points and the green cubes are (3, +3) critical points.</i>	82
5.2	<i>The gradient lines of 2-butene in the MEP shows that the hydrogens are able to dominate the space between them. The black spheres are carbon and the white spheres are hydrogen atoms. The white cylinders are (3, -1) critical points and the blue rings are (3, +1) saddle points.</i>	82
5.3	<i>The chrysene molecule is shown with all the calculated critical points, the possible hydrogen-hydrogen interaction is shown in red. The black spheres are carbon and the white spheres are hydrogen atoms. The white cylinders are (3, -1) critical points, blue rings are (3, +1) saddle points and the green cubes are (3, +3) critical points.</i>	84
5.4	<i>The chrysene molecule is shown with the three hydrogen-hydrogen interaction sites to be investigated. Site A is where a (3, -1) saddle point is calculated as well as an atomic interaction line which is not shown. The critical points that are normally calculated above and below the molecule have been removed for clarity. The black spheres are carbon and the white spheres are hydrogen atoms. The white cylinders are (3, -1) critical points and the blue rings are (3, +1) saddle points</i>	84
5.5	<i>The contour lines of the MEP for the chrysene molecule, the first plot is in the plane of the molecule and the second plot is perpendicular to the molecule and is positioned over the hydrogens being studied. The white contour lines are negative MEP and the black contour lines are positive MEP. The black spheres are carbon and the white spheres are hydrogen atoms. The white cylinders are (3, -1) critical points and blue rings are (3, +1) saddle points</i>	85
5.6	<i>The chrysene molecule is shown with the three hydrogen-hydrogen interaction site that are being investigated. The gradient lines show the interaction between the various atoms. The critical points that are normally calculated above and below the molecule have been removed for clarity. The black spheres are carbon and the white spheres are hydrogen atoms. The white cylinders are (3, -1) critical points and the blue rings are (3, +1) saddle points</i>	86
5.6	<i>The blue line is the nucMEP and the red line is the elecMEP. The values on the graphs indicate the approximate elecMEP on the hydrogen atom, the values are in atomic units.</i>	88
5.6	<i>The blue line is the electron density and the red line is the molecular electrostatic potential. The graphs on the left are plotted between the hydrogens while the graphs on the right are plotted passing through the mid point of the hydrogens. . .</i>	90
5.7	<i>The gradient lines of the MEP for the chrysene molecule at the three different sites. The white spheres are hydrogen atoms. The pink cylinder is a (3, -1) critical point.</i>	91

5.8	<i>The chrysene molecule is shown with four probes placed in positions where a (3, +1) and a (3, -1) critical point could be expected to be calculated. The black spheres are carbon atoms and the white spheres are hydrogen atoms. The cylinders are (3, -1) critical points, the blue rings are (3, +1) critical points and the yellow spheres are probes.</i>	92
5.9	<i>The gradient lines of the MEP for the planar biphenyl molecule with the hydrogen-hydrogen bond shown in red. The white spheres are hydrogen atoms and the black spheres are carbon.</i>	94
5.10	<i>The topology of the biphenyl molecule calculated in the MEP is shown with two probes (yellow spheres), one is positioned where a (3, -1) critical point would be in the planar structure and the second probe is placed in the centre to signify a (3, +1) critical point. The white spheres are hydrogen atoms and the black spheres are carbon, the cylinders are (3, -1) critical points.</i>	96
5.11	<i>The gradient lines of the ortho hydrogen for the twisted biphenyl molecule show that the hydrogens are still interacting but do not form a critical point.</i>	97
5.12	<i>The molecular structures of (1) exo-exo-tetracyclododecane, (2) Pentacyclododecane, (3) 1,6-dimethylmonosecododecahedrane, (4) bicyclononane, (5) cyclodecane, (6) cis-syn-cis-perhydroanthracene, (7) exo-exo-octacycloheneicosane, (8) 11,12-difluoro-exo-exo-tetracyclododecane, (9) 4,5,9,10,11,12-hexafluoro-exo-exotetracyclododecane, (10) 5,9-difluoro-pentacyclododecane, (11) 5,9,11,12-tetrafluoro-pentacyclododecane.</i>	97
5.13	<i>The molecules of cyclododecane (top) and cis-syn-cis-perhydroanthracene (bottom) with the main hydrogen interaction line shown in red, and labeled as A in table ??, and secondary interaction lines shown in blue, labeled as B in table ??.</i>	100

List of Tables

2.1	<i>An explanation of the four types of stable critical points found in the electron density.</i>	11
2.2	<i>Stable degenerate critical points in the molecular electrostatic potential.</i>	19
2.3	<i>The effects of method and basis set on the topology of the Molecular Electrostatic Potential (MEP). The values for MEP (3, -1) are values taken between the centre two carbon atoms with the exception of neon for obvious reasons. The energies and MEP (3, -1) are all in a.u.</i>	24
2.5	<i>A comparison of the MEP value for wavefunctions calculated using the counterpoise correction (CP) and without the correction (nCP). The MEP values are reported in a.u. and are for the (3, -1) critical point for the noble gases helium, neon and argon.</i>	26
3.1	<i>A comparison of the MEP, electron density and electrostatic potential (elecMEP) for the methane molecule calculated with the Hartree-Fock and Unrestricted Hartree-Fock method. Both methods used the basis set 6-311++G(d,p). The values are in atomic units with the exception of the bond lengths which are in Ångström. . .</i>	35
4.1	<i>The bond length, electronic MEP (elecMEP), MEP, ρ, $\nabla^2\rho(r)$ and Lagrangian kinetic energy (G) are reported for the optimised geometries of the three noble gases, He_2, Ne_2 and Ar_2 as well as H_2 and $^t\text{H}_2$. All values are calculated from the (3, -1) critical point and reported in atomic units with the exception of the bond length which is shown in Å.</i>	71
4.2	<i>A breakdown of known bond types into the MEP components as well as the MEP ratio. The hydrogen molecule in the singlet and triplet state are added for comparison. The MEP values are in atomic units and the bond length is in Å.</i>	75
5.1	<i>The MEP, ρ, $\nabla^2\rho(r)$ and kinetic energy values for 2-butene at the (3, -1) saddle point between C2 and C3, the (3, +1) saddle point and the (3, -1) saddle point between H7 and H11 are shown in the table. All values are given in atomic units with the exception of the MEP ratio.</i>	83
5.2	<i>The table shows the bond length, MEP, ratio, ρ, $\nabla^2\rho(r)$ and kinetic energy (G) for the (3, -1) critical points between the carbon atoms as well as the probes at locations that would match (3, +1) critical points and (3, -1) critical points between the hydrogens. The values are calculated in atomic units except for the bond length which is calculated in Angstroms.</i>	93
5.3	<i>The MEP, ratio, ρ, $\nabla^2\rho(r)$ and kinetic energy (G) values for the (3, -1) saddle point between the centre carbons and the ortho hydrogens as well as the (3, +1) saddle point formed by the closing of the ring. All values are calculated in atomic units except for the ratio.</i>	94

5.4	<i>The MEP, ratio, ρ, $\nabla^2\rho(r)$ and kinetic energy (G) values of the twisted biphenyl structure with two probes positioned between the ortho hydrogens and in the place of the (3, +1) critical point. All values are calculated in atomic units except for the ratio</i>	96
5.5	<i>The MEP, ratio, ρ, $\nabla^2\rho(r)$ and kinetic energy (G) values for interacting hydrogens in congested molecules. The A and B for molecules cyclododecane and cis-syn-cis-perhydroanthracene refer to two different hydrogen-hydrogen interactions which are shown in figures, ???. The main hydrogen-hydrogen interactions is shown in red and the secondary interaction is shown in blue. All values are calculated in atomic units except for the ratio.</i>	101
5.6	<i>The MEP, ratio, ρ, $\nabla^2\rho(r)$ and kinetic energy (G) values for interacting hydrogens in congested molecules with halogens. All values are calculated in atomic units except for the ratio.</i>	101

List of Abbreviations and Symbols

QTAIM	Quantum Theory of Atoms in Molecules
BCP	Bond Critical Point
AIL	Atomic Interaction Line
NA	Nuclear Attractor
NNA	Non-Nuclear Attractor
RCP	Ring Critical Point
CCP	Cage Critical Point
IQA	Interacting Quantum Atoms
ELF	Electron Localisation Function
VESPR	Valence Shell Electron Pair Repulsion
LED	Localised Electron Detector
LOL	Localised Orbital Locator
MEP	Molecular Electrostatic Potential
π	Pi- bonding electrons
σ	Sigma bonding electrons
ρ	Electron Density
∇	First Derivative
∇^2	Second Derivative
ϵ	Ellipticity
nucMEP	Nuclear Molecular Electrostatic Potential
elecMEP	Electronic Molecular Electrostatic Potential
HF	Hartree-Fock
MP2	Møller-Plesset
B3LYP	Becke, Lee, Yang and Parr three parameter function
DFT	Density Functional Theory

Chapter 1

Introduction

1.1 Interactions in Molecules

The Quantum Theory of Atoms in Molecules (QTAIM), which was developed by Bader and co-workers [1, 2], is used to analyse experimental and theoretical electron density distributions in molecules or crystals. Through this analysis the bonding interactions of atoms can be studied as well as the type of interactions taking place [3]. The premise for QTAIM is that if a system is in equilibrium, the presence of a bond critical point (BCP) and an atomic interaction line (AIL) between two nuclear attractors (NA) is a sufficient criterion for considering the two atoms to be connected by a bonding interaction [3, 4, 5, 6].

A molecule consists of atoms and their corresponding electrons, therefore when looking for a method to predict how atoms combine to form molecules, the electron density is a good start. The electron density can be calculated using quantum mechanics and is experimentally observable which is why the electron density is an ideal starting point. Electrons are known to group around nuclei and bonds between atoms generally have shared electrons. Topology is a branch of mathematics which is used to explain the shape of a mathematical field (a space of a certain dimension), through the use of critical points and, when coupled with the electron density, can predict a molecule consisting of individual atoms. Being able to define an atom, identifying an atom in a molecule (this is shown to be possible with the use of the virial theorem [7, 8, 9]), and show a bonding interaction [10], are three criteria laid out by Bader for a successful model, all of which QTAIM achieves [8, 11].

The QTAIM model describes atoms as nuclear attractors as they attract gradient lines towards them. These gradient lines, calculated as the first derivative of the scalar field (eg: electron density), defines the volume of the atom. When two atoms interact, a line path (this is also known as an atomic interaction line if the gradient lines originate from the bond critical point and terminate at the nuclear attractor) joining the two NA's is formed and is described as a chemical interaction. This chemical interaction can be associated with a chemical bond but the purpose of the paths is to show chemical linkages. Therefore a line path can not always be associated with a bond (a bond consisting of an electron pair) [11, 12] and this is a point of contention with the QTAIM model. The problem arises because two strongly interacting fragments that have a saddle point between them and a connecting bond path can represent either a bonding or repulsive interaction and is thus necessary, but not a sufficient criteria, for determining if a bond exists [10, 13]. Further criteria were introduced in order to determine

whether a bond path showed an attractive interaction or a repulsive interaction. Low electron density values and a positive Laplacian of the electron density are good indicators of repulsive interactions as well as the bond ellipticity being highly elongated in the plane formed by the ring saddle point [14].

The QTAIM method has been successful in predicting structures of relatively simple molecules and even going as far as to increase the understanding of molecular structures and reactions. However, when applied to molecules of ever increasing complexity, the results have been controversial and sparked debate within the scientific community. These debates seem to encompass every aspect of the QTAIM model, this not only includes the critical points and lines joining them but also the physical meaning associated with critical points. Cioslowski noted that one area of misinterpretation of bond paths was due to the seeming inability of QTAIM to differentiate between strong and weak bonds. It was suggested that strong bonds had a high electron density and coincided with intuitively acceptable interactions and weak bonds could be identified through the highly elliptical distribution of the electron density around the BCP and the positive electron Laplacian [14]. Following on from that study, further publications tried to show that the bond paths were always present when two atoms were in close enough contact with each other and as such the bond path also showed repulsive interactions [14, 15, 16, 17]. The reply to this investigation was to question the reliability of a system that seemed subjective in its nature [3].

When calculating the topology of the electron density for planar biphenyl, a BCP is calculated between the ortho-hydrogens along with an AIL originating at the BCP and terminating at the two hydrogen atoms [18], these meet the conditions of a bond, laid out by the QTAIM method. The interaction between the two hydrogens is referred to as a hydrogen-hydrogen bond which is characteristically different than a di-hydrogen bond. The di-hydrogen bond involves two hydrogen atoms, one of which has a net positive charge and the other has a net negative charge whereas the hydrogen-hydrogen bond consists of two hydrogens with similar charges.

A hydrogen-hydrogen bond is therefore a counter intuitive interaction because from a classical view point like charges should repel each other. The hydrogens in the ortho position of the biphenyl molecule are also in a sterically hindered state and as such claiming a stabilising interaction between the hydrogens can be a difficult concept to understand.

A paper by Poater, Solà and Bickelhaupt argued that the interaction between the ortho-hydrogens was destabilising (repulsive interaction). Their aim was to show that the sterically hindered ortho-hydrogens raised the energy of the molecule and forced the molecule from a planar geometry to a twisted geometry. In the paper the authors showed that by removing the ortho-hydrogens the biphenyl molecule preferred the planar geometry. By using bond energy decomposition analysis the researchers showed that Pauli repulsion prevented the biphenyl molecule from adopting the planar geometry. As a result of these findings the Poater *et al.* concluded that the introduction of the hydrogens in the ortho position caused the molecule to rotate to its equilibrium geometry which contains a twist of 35.5 degrees [19].

The response to this paper was a detailed explanation that the repulsive force between the hydrogen-hydrogen bond in biphenyl was due to a misinterpretation of the physics on which QTAIM is built and that no such repulsion exists in the planar biphenyl structure [3, 20, 21]. Bader explained that the argument presented was based on an arbitrary partitioning of the energy into contributions from unrealisable states of the system. In contrast to the unrealisable states of a system, Bader's explanation is presented in terms of the Feynman, Ehrenfest and virial theory all of which is routed in quantum mechanics and are observable properties.

Naturally this in turn resulted in a rebuttal from Poater, Solà and Bickelhaupt [22]. In their reply the researchers claimed that their molecular orbital model of the chemical bond with the energy decomposition approach provided insight and has predictive powers which is something they claim atom in molecules is lacking (no predictive power).

Hernández-Trujillo and Matta showed that the interaction between the ortho-hydrogens in biphenyl were locally stabilising and therefore the bond path was a result of a bonding interaction [18, 23]. In their paper, Hernández-Trujillo and Matta compared the atomic energy of every atom in planar biphenyl to the same atoms in the twisted biphenyl structure. The researchers showed that the carbon-carbon bond was destabilising and that the four ortho hydrogens were stabilising, this was due to the hydrogen-hydrogen bond. Eskandari and Alsenoy used Interacting Quantum Atoms (IQA) and Hirshfeld Atomic Energy Partitioning Methods to analyse the planar biphenyl molecule and found the H-H bond to be stabilising [24].

Another case of bond paths being disputed was in a study of the endohedral cage complex of helium with adamantane. In this case the topology of the electron density found connections between the helium atom and four carbon atoms of the adamantane cage. In their research Haaland et al. [25, 26] showed that the four interactions were deemed to be anti-bonding in nature. This led to the conclusion that atomic interaction lines sometimes represent destabilising or antibonding interactions. Bader countered this paper by demonstrating that an attractive Ehrenfest force was present for the caged complexes and thus countered the repulsive Hellmann-Feynman force [5, 27, 28].

Bader was not the only one to counter Haaland's research [29, 30]. Other evidence for bond paths being discovered, but not representing a bonding interaction, can be seen in the analysis of dimers in alkali metal derivatives that have the form M_2X_2 [31] and intra-molecular halogen · · oxygen interactions [32, 33]. In both cases a bond path is observed but for the dimers the interaction was shown to be repulsive and the halogen-oxygen interaction was shown to have non-bonding characteristics. Bader's response to the bond paths being associated with repulsive forces was to re-iterate that, at equilibrium the attractive Ehrenfest force and repulsive Feynman force neutralise each other and hence there can be no net repulsive force.

Through the analysis of the Laplacian, Bader explained that the withdrawal of the electron density from the BCP (a common trait for closed shell interactions) does not show repulsion of the atoms involved and that this was a common occurrence for van der Waals interactions, hydrogen bonds, ionic bonds and bonds in molecular crystals [4].

The debate around whether a bond path is the same as a chemical bond or just showing a stabilising interaction has led some to question if QTAIM introduces a new "type" of bond [32]. The follow on from this is, should an IUPAC commission be formed to make a ruling on a new type of bond [34, 35, 36].

Bond paths being linked to bonding interactions have not been the only problem identified with the QTAIM method. While critical points of (3,+3) are normally associated with nuclei (nuclear attractor, NA) there are a few cases where (3, +3) critical points are found that are not nuclei and are termed non-Nuclear Attractors (NNA). This was initially a problem because the occurrence of NNAs were a result of a sensitivity to the quality of basis sets and sometimes correlation effects [37, 38, 39, 40, 41, 42, 43]. A common example of finding NNAs is in metallic lithium and sodium, where the NNAs are found between the two nuclei [44, 45, 46].

A study involving lithium, sodium, potassium, rubidium and cesium crystals showed that the existence of the NNAs decreased in frequency as one moves from lithium to cesium. This led

to the conclusion that the lighter elements are more prone to show NNAs and that perhaps weak long range bonds involving atoms of low excitation energies have a high chance of showing NNAs [45].

Martín-Pendás *et al.* reached the conclusion that NNA's were not an oddity of the electron density but was a normal progression in the chemical bonding homonuclear groups [47]. A similar conclusion that NNAs were not artifacts but a feature of the electron density was reached by Azizi *et al.* where lithium clusters were studied [48]. The results showed that the NNAs acted as a "glue" between the lithium atoms, resisting the separation of the atoms [38].

Cao *et al.* also showed that the NNA acted as a pseudo atom and formed part of a network of lithium and sodium clusters by bridging the two metal atoms (thus acting as an "electronic glue") [39]. This was also discovered in metallic hexagonal closed-packed (h.c.p) beryllium. The h.c.p beryllium structure was shown to have no beryllium atoms bonded to one another but instead consisted of a three dimensional network of bonds between beryllium atoms and NNAs [49].

An explanation given by Gatti *et al.* showed that subspaces that do not contain a nucleus do exist. However, these subspaces still contain a location in their domain that acts as a focal point for the gradient vector field [38, 41].

In a paper by Bader and Platts the researchers showed that the F-centre in alkali halide crystals is a physical manifestation of the NNA in the electron density [50]. The researchers also showed that if the odd electron was primarily delocalised then no NNA would be found but instead a cage critical point (a minimum in the electron density) would be found [50].

Using high-resolution X-ray diffraction Platts *et al.* showed that NNAs in dimeric magnesium do exist thus confirming theoretical calculations [51]. NNAs were not only discovered in metallic structures, a hydrated, cavity bound electron in water clusters (anionic water clusters) produces a NNA in the electron density topology. These NNAs are determined to behave in the same way NNAs behave in metallic structures, namely stabilising ("gluing") the clusters [52]. The research surrounding NNAs all point towards systems that have small polarity differences [45, 47, 53, 54].

Martín Pendás has shown that the topologies of the electron density and Ehrenfest force are homeomorphic (the topologies of the electron density and the Ehrenfest forces are similar) [55] and thus proving that the controversial bonding interactions discussed above do exist. However, a paper by Dillen showed that this is not always the case [56]. In the paper Dillen showed that integration of the electron density over the force density basin resulted in substantial differences between the partial charges of the atoms as compared with the partial charges obtained from the electron density basins. This was shown for a number of hydrides, fluorides and chlorides of first row elements. The research ultimately concluded that in some cases the atomic interaction line in the electron density was not always mirrored in Ehrenfest force density.

Research into the modelling capabilities of QTAIM have also been questioned, explaining that due to the mathematics, two atoms in close proximity will always form a BCP and an AIL and as such cannot not be used as anything more than a suggestion of an interaction [17].

Hydrogen bonds play an important role in nature, they aid in the determination of molecular conformations and molecular aggregation and their effects can be seen in everything from inorganic to biological systems [57]. Hydrogens that are involved in bonding interactions can be very complicated and to illustrate this, hydrogen bonds can be split into conventional and non-conventional [58, 59, 60]. A paper by Espinosa *et al.* used the topology of the electron

density to describe and classify hydrogen bonds [61, 62]. The research compared the results from 83 experimentally observed hydrogen bonds using X-ray diffraction to results obtained through theoretical methods.

Hydrogen bonds are best explained as a Coulombic attraction, therefore non-conventional hydrogen bonds can be found in systems containing isonitriles, carbanions, carbenes, silynes and pi-systems [63, 64, 65, 66, 67, 68]. To gain a better understanding of the complex hydrogen bond the topology of the electron density was used to characterise the hydrogen bonds [69, 70, 71].

The dihydrogen bonds are formed between two hydrogens, one hydrogen has a positive and the other a negative charge. Normally the negatively charged hydrogen is bonded to a metal atom. The dihydrogen bonds have been seen in X-ray crystallographic structures of organometallics and neutron diffraction crystallography of BH_3NH_3 [72, 73, 74, 75, 76, 77, 78, 79, 80]. In the same way that a hydrogen bond has electrostatic properties so does the dihydrogen bond. In dihydrogen bonds the attractions are a result of dipole-monopole and dipole-dipole interactions leading to stabilising interactions.

Unlike hydrogen and dihydrogen bonds a third type of interaction exists involving hydrogen and that is the hydrogen-hydrogen bond. The hydrogen-hydrogen bond can be characterised as a closed shell interaction between electrically neutral hydrogens or at least hydrogens with similar charges. The similarity of the hydrogen charges is likely due to the symmetry of the electronic environment of the two hydrogens [81]. Experimental evidence of the hydrogen-hydrogen bond was obtained through low temperature neutron diffraction crystallography of the norbornene derivatives [82]. Another experimental study an isotropic interaction potential for $\text{CH}_4 \cdot \text{CH}_4$ was discovered [83, 84] which was backed up by a theoretical study of the CH_4 dimer [85].

In a study focusing on congested molecules, the energies of tetracyclododecane and its derivatives were compared with norbornane and norbornane derivatives. The difference in the energies between the tetracyclododecane and norbornane molecules were used to conclude a stabilising or destabilising interaction. It was determined that the calculations used, QTAIM and Interacting Quantum Atoms (IQA), showed no correlation between the existence of a bond path and the energies calculated by QTAIM or IQA [86]. This means that no conclusion can be reached on whether or not the BCP and AIL represent a bonding (attractive) or anti-bonding (repulsive) interaction.

The questions around what constitutes a bond have fuelled the drive to investigate multiple different scalar fields [9, 55, 56, 87, 88, 89, 90, 91]. The development of the electron localisation function (ELF), which accounts for the electron density, its gradient and kinetic energy density, can be used to visualise the valence shell electron pair repulsion theory (VESPR). The ELF focuses on the local pair probabilities of electrons and is thus useful in identifying lone pairs and electrons involved in bond formation [87].

The localised electrons detector (LED) focuses on the electron density and its gradient exclusively in order to identify core shells, bonding and valence regions [89, 92]. One of the benefits of the LED is that it can provide insight into the electronic structure inside the atomic basin. This means that an intrabasin population analysis based on the LED isocontours can be used to increase the understanding of atoms. The LED has been used to identify covalent and hydrogen bonding through the analysis of the region around the (3, -1) critical point between two NAs.

The Ehrenfest force calculates the force acting on an electron due to the other electrons in

the molecule [55]. The Ehrenfest force field has been shown to accurately reproduce the same topology as the electron density. However, the Ehrenfest force field is heavily dependent of the basis sets used and can sometime show incorrect long range topographical features.

The Localized Orbital Locator (LOL) has been used to show locations of bonding electron pairs and the expected σ and π orbital shapes as well as lone pairs [88]. This field has can be used to clearly display the locations of the VESPR electronic groups and atomic shells. The LOL can also be used to analyse non-covalent interactions.

The Coulomb potential density takes a point in the electron density and assess the Coulombic forces acting at that point, namely the attractive forces of the nuclei and the repulsive forces of the other electrons in the system [91]. While the Coulomb potential produce homeomorphic structures of the electron density its main feature is providing an energetic foundation for the existence of the NNA.

Many of these fields have allowed for the localisation of the electron density and in so doing revealed the sites of lone pairs [93]. Other fields utilise the kinetic energy [9] of the atoms to determine interactions and even the force created by the electrons and the impact it has on the nuclei.

One such field, the Molecular Electrostatic Potential (MEP), has been largely used due to the fact that it takes into account the potential from the nuclei and the electrons. The MEP has been used to identify areas in and around a molecule that have a negative or positive potential, therefore the MEP can be used to locate electron rich and deficient areas respectively [94]. It is for this reason that contour maps of the MEP have been used to identify sites of electrophilic attack by nucleophiles [95]. A benefit of using the MEP is that it is a physical property and can be observed through diffraction techniques [96, 97].

In organic molecules containing halogens it was noticed that inter-molecular interactions in crystals occurred in either a head-on or side-on approach, MEP maps were used to understand these directional approaches and indicated that electrophiles approached side-on and nucleophiles approached head on [98] in accordance with the negative and positive potentials. The MEP iso-surfaces are usually plotted on the contour of the electron density which is calculated at 0.001 a.u [99].

The idea of covalently bonded halogens being attracted to each other can at first seem peculiar as the halogens are often seen as being negative in their nature. However, through the use of MEP iso-surfaces it became apparent that the halogens formed a positive potential at the polar region of the atom (along the extension of the covalent bond) and a negative potential formed around the equatorial sides of the halogen [98, 100]. The linear interactions with nucleophiles and the lateral interactions with electrophiles could all be explained through the interaction of the positive outer region of the halogen with the negative site of another halogen [101, 102, 103, 104]. Understanding non-covalent bonds and in particular halogen bonding has had a large impact in medicinal and biological areas. These include but are not limited to protein-ligand interactions, drug design, docking processes and conformational stabilisation [105, 106, 107, 108, 109, 110].

Due to the information made available through the use of MEP surface and contour maps, it makes sense to use the QTAIM method in connection with the MEP. This has lead to molecular maps being surrounded by a diverse and sometimes heavily populated space of critical points. The abundance of critical points has "opened up" the nature of the molecules and the contributions from the atoms contained within them, this has resulted in many papers being

published linking these critical points to certain molecular characteristics. As mentioned before the MEP is useful for understanding non-covalent interactions but when coupled with atoms in molecules, atomic and molecular properties such as energies, covalent and anionic radii as well as electronegativities (chemical potentials) can be expressed [111, 112, 113].

A common result of the MEP is the appearance of (3, +3) critical points which coincide with π electrons, most notably in molecules with double and triple bonds and lone pairs [13, 111]. Analysis of the MEP topography can be used to predict the regions of an atom where lone pairs may exist as well as explain the directionality of lone pair - π interactions [114].

The alternating ring of (3, +3) and (3, +1) critical points above and below the benzene ring have been attributed to delocalised electrons and is synonymous with aromaticity [115]. The critical points of the MEP have also been shown to coincide with the ionic radii of ions and even define the shape of the ions [95].

Much like the electron density at a BCP can be used to characterise a bond in terms of bond order and possibly bond strain [115], the location of the (3, +3) minima in the MEP can be used to identify bond strain. Minima located around a BCP can depict a double bond, alternating (3, +3) and (3, +1) critical points around a BCP indicates a triple bond. The minima representing the pi system of double bonds could reveal repulsive interactions between the pi electrons, such is the case with cyclobutadiene where the minima are located on the outside of the ring structure [116]. The location of the minima for a ring structure can denote stability (minima positioned on the inside of the ring) and strain (minima positioned on the outside of the ring).

The use of (3, +3) minima have also been used to try and identify and rank sites that are susceptible to electrophilic attack [97, 117, 118, 119]. However this does not always work as calculations tend to leave out polarisation effects produced by an approaching electrophile [117, 120]. Another possibility that is considered is that not all negative regions consist of electrons that are the most reactive electrons in the molecule [121, 122, 123, 124].

To round off the the various critical points in the MEP topology, stable degenerate critical points are often present around linear, neutral or negatively charged molecules [13].

The diverse topology of the MEP illuminates the many characteristics of molecules and atoms, especially bonding interactions. It is for this reason that the MEP topology was chosen to better understand the interaction between hydrogen-hydrogen bonds in congested molecules.

The aim of this thesis is to use the QTAIM technique with the MEP to try and clarify the hydrogen-hydrogen interaction found in congested molecules. Due to the sometimes controversial nature of QTAIM and the classification of bonding interactions the research presented in this thesis starts with an investigation into the pitfalls of QTAIM and the many interpretations of the MEP topology. To address the issue of always finding a (3, -1) critical point between atoms an investigation is carried out to determine under which conditions (3, -1) saddle points are determined, this was done for both the electron density and molecular electrostatic potential. The research presented studies the topology and contour maps of the MEP to gain a better understanding of how and when bonds form using the QTAIM method.

An investigation into the topology of the MEP was also carried out, this was done with the intention of linking the topology to well known structural properties such as lone pairs, pi-bonds and aromaticity. This would reaffirm current literature on the MEP topology but also introduce some unexplained results such as minima with a positive potential and degenerate critical points.

In order to deal with inter atomic interactions a classification system for bond types needed to be established. The presented research attempts to classify inter atomic interactions solely on the MEP rather than tie the definition of a bond to energy criteria. To this end systems of increasing complexity were calculated and analysed. This included an analysis of the noble gases to understand closed shell interactions and how they are represented in the MEP topology. The more complex systems consisted of hydrocarbons and non-covalent interactions. A system of the hydrogen molecule in the singlet and triplet state were used to try and characterise a stabilising and non-stabilising interaction based on the MEP.

The research then focuses on planar molecules like chrysene, *cis*-1,4-butene, phenantrene and others. This introduces the issue of the hydrogen-hydrogen bond in congested molecules. The topology of the MEP is used to explore the concepts of delocalised electrons and their possibility of stabilising the hydrogen-hydrogen interaction and the molecule. The planar biphenyl molecule, both in the planar and twisted geometries, are then analysed. The research aims to use the fact that the MEP describes the effect that the whole molecule has on one point to understand the true nature of the hydrogen-hydrogen interaction.

The thesis concludes with an analysis of congested molecules and hydrogen-hydrogen interactions. An analysis of these interactions is presented in the context of electron density, Laplacian and kinetic energy in an attempt to answer the question of whether or not the hydrogens in congested molecules form a stabilising or destabilising interaction.

1.2 Structure of Thesis

Chapter 1 provided the background to the issues that will be studied in this thesis. The arguments, both for and against the use of QTAIM, were highlighted in the opening chapter and ended with a focus on congested hydrogen-hydrogen interactions. The following chapters further explore the use of QTAIM and its ability to identify chemical structures through the MEP field.

Chapter 2 aims to introduce the fundamental concepts that are used throughout the thesis as well as the computational methods used throughout the thesis. The concepts include identifying the topology and possible interpretations of critical points, the evolution of the Poincaré-Hopf equation and an introduction to the MEP. Focus is placed on the various scalar fields and the information they provide, this will be used to introduce some of the concepts of the MEP.

Chapter 3 highlights the differences between the topology of the electron density and molecular electrostatic potential fields. The current interpretations of the MEP topology is explored using contour plots and mapping out gradient paths for selected atomic interactions. The identification and interpretation of degenerative critical points in the MEP are also analysed.

Chapter 4 explores the numerical aspect of the interactions in the MEP field. An understanding of bonding interactions is studied and compared with bonding interactions like covalent, ionic and hydrogen bonds. A system to identify the type of intra atomic interactions using QTAIM and MEP is investigated.

Chapter 5 applies the concepts developed in previous chapters to planar and congested molecules. An analysis of hydrogen-hydrogen interactions in planar molecules, including biphenyl, and congested molecules is discussed.

Chapter 2

Background

2.1 Quantum Theory of Atoms in Molecules

The strength of Quantum Theory of Atoms in Molecules (QTAIM) is not only based on the fact that it uses quantum mechanics to describe a three dimensional space that contains nuclei and electrons, without assuming a pre-defined structure, but it also makes use of an observable quantity, namely the electron density. If the system being studied obeys the laws of quantum mechanics, the interaction between the atoms are valid and as a consequence, so are the molecular graphs (geometric structures) that are determined. While there can be many molecular graphs for a chemical system, not all of them are stable. The molecular graphs are useful in determining reaction pathways and transition structures which ultimately lead to molecular structures which are stable chemical system in the ground state. This feature has been shown in the Molecular Electrostatic Potential (MEP) as well with the summation of the atomic counterparts making up the molecule [111].

2.1.1 Critical Points

The molecular structure is determined by the distribution of the electron density, ρ , which can be measured experimentally, and is visualised through the use of the topology [125]. The mathematical field of topology is used to relate the values calculated through quantum mechanics to recognisable structures in chemistry. A component of topology, which is important for chemistry, is the use of critical points. Critical points are used in chemistry to define an atom as well as the geometry of a group of atoms. In this section the various types of critical points will be defined and discussed. In order to define a critical point, a scalar field needs to be calculated, an example of this would be the electron density or molecular electrostatic potential. The first derivative of the scalar field is then calculated, when the derivative is zero a critical point is located. Calculating the second derivative of the scalar field defines the type of critical point, whether it is a maximum, minimum or one of two types of saddle points.

The topological properties of the electron density can be characterised by calculating the gradient of the electron density ($\nabla\rho(r)$) [126]. This vector field is useful for characterising critical points because the vector field has a zero value as the vectors converge on a single point, $\nabla\rho = 0$. Calculating the derivative of the vector field (second derivative of the scalar field) describes the

shape of the space around the critical point and thus defines the critical point. The critical points in the ρ can take on four forms namely, maxima, minima and two saddle points.

In order to describe these critical points in three dimensional space there are nine second derivatives that need to be calculated. There are six unique derivatives that form the Hessian matrix which is shown in equation 2.1.

$$\begin{vmatrix} \frac{\partial^2 \rho}{\partial x^2} & \frac{\partial^2 \rho}{\partial xy} & \frac{\partial^2 \rho}{\partial xz} \\ \frac{\partial^2 \rho}{\partial yx} & \frac{\partial^2 \rho}{\partial y^2} & \frac{\partial^2 \rho}{\partial yz} \\ \frac{\partial^2 \rho}{\partial zx} & \frac{\partial^2 \rho}{\partial zy} & \frac{\partial^2 \rho}{\partial z^2} \end{vmatrix} \quad (2.1)$$

When the Hessian matrix is diagonalised, the values then describe the curvature of the critical point, shown in equation 2.2.

$$\Lambda = \begin{vmatrix} \frac{\partial^2 \rho}{\partial X^2} & 0 & 0 \\ 0 & \frac{\partial^2 \rho}{\partial Y^2} & 0 \\ 0 & 0 & \frac{\partial^2 \rho}{\partial Z^2} \end{vmatrix} = \begin{vmatrix} \lambda_1 & 0 & 0 \\ 0 & \lambda_2 & 0 \\ 0 & 0 & \lambda_3 \end{vmatrix} \quad (2.2)$$

When defining the critical points, two numbers are used, namely rank and signature. The rank of the critical point is equal to the number of non-zero axes of curvature, therefore a typical critical point will have a rank of three. This is not always the case, and when one of the second derivative vanishes (is equal to zero) in one or two directions, then the rank would be two or one respectively. These critical points (rank two or one) are then referred to as degenerate critical points. In the electron density these critical points are not found when in the ground state, as the degenerate critical points are unstable. This is true for the electron density but other scalar fields such as the MEP do contain stable degenerate critical points. The movement of a system through a chemical change, such as a transition where bonds are broken and formed, will result in a catastrophe point. A catastrophe point will have a rank of less than three, generally two. Therefore, it is unlikely to find a degenerate critical point in the electron density if the system is in equilibrium (ground state), however there are some examples where this may occur [11]. A structural change in a molecular system requires the system to pass through a catastrophe point [126]. This will result in the destruction of two critical points, a RCP and BCP for ring breaking, or the bifurcation of a single critical point into two critical points, a degenerate critical point bifurcating into a BCP and RCP for ring formation. The signature of the critical point is the algebraic sum of the signs of the eigenvalues in the diagonalised Hessian matrix. Therefore, if the slope at a critical point is negative in all three directions ($\nabla^2 \rho(r) < 0$, this would be a NA), then the signature is negative three. A saddle point between two nuclear attractors has one positive eigenvalue and two negative eigenvalues which would result in a signature of negative one. There are four possible stable critical points in the electron density and they are described in table 2.1.

Table 2.1: *An explanation of the four types of stable critical points found in the electron density.*

Critical Point	Description	Common Name
(3 , -3)	local maximum	Nuclear Attractor (NA)
(3 , -1)	saddle point	Bond Critical Point (BCP)
(3 , +1)	saddle point	Ring Critical Point (RCP)
(3 , +3)	local minimum	Cage Critical Point (CCP)

The local maxima are labeled as Nuclear Attractors (NA) because the critical point has a high concentration of electron density, this suggests the location of a nucleus. It is not always the case that a maximum denotes the site of a nucleus. When this occurs the critical point is given the name of a non-Nuclear Attractor (NNA) [44]. The (3, -3) critical point is a maximum in the electron density and the charge density will decrease in any direction moving away from the critical point [11]. Bond Critical Points (BCP) are typically found between two NA and fulfils one of the criteria for defining a bond [10]. At the BCP the vector field decreases in two directions and increases in the third, the increase is directed towards the NA's. Therefore a BCP is a maximum in two directions and a minimum in one direction [127]. When a ring structure is formed, as in cyclopropane, a Ring Critical Point (RCP) is found. A cyclic structure will form a ring surface on which the electronic distribution is a minimum at the (3, +1) critical point. The gradient paths which define this ring surface originate at the (3, +1) critical point and terminate at the (3, -3) and (3, -1) critical points on the surface [126, 127]. The RCP is a minimum in two directions and a maximum in one direction. The Cage Critical Point (CCP) is a minimum in all directions and is normally surrounded by four RCP's [128]. Figure 2.1 shows the four different critical points; the black and grey spheres are NA's, the grey cylinder denotes a BCP, the blue rings show the RCP and the green cube is the CCP.

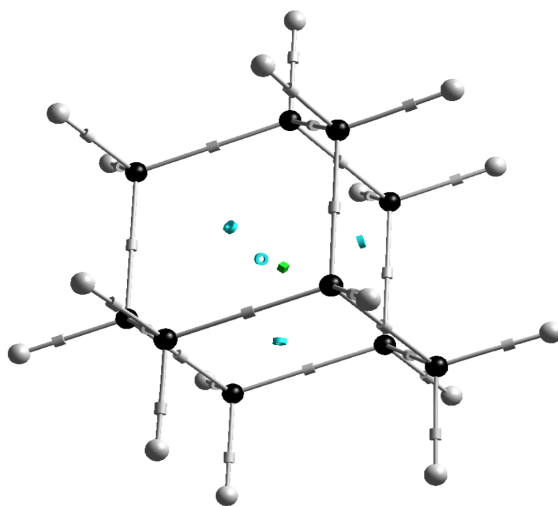


Figure 2.1: *Adamantane has examples of the four different critical points of rank three, NA (sphere), BCP (cylinder), RCP (ring) and CCP (cube).*

2.1.2 Ellipticity

When creating an image of a molecule using the topology of a scalar field (electron density or MEP) the single, double and triple bonds are visually identical, basically they are all represented by a single line. Some scalar fields such as the molecular electrostatic potential have extra information that is visible and can be used to identify double and triple bonds. The topology of the electron density does not have a visual way of distinguishing between the different bond orders and thus the ellipticity becomes useful. If the atomic interaction line is placed along the z-axis then the ellipticity is the measure of the electron distribution in the x- and y-axes, or rather, how the electron density is distributed in the planes perpendicular to the z-plane. The ellipticity is calculated from zero to one with zero being cylindrical and one being planar. This relationship can be summed up in the equation:

$$\epsilon = \frac{\lambda_1}{\lambda_2} - 1 \quad (2.3)$$

where $\lambda_1 > \lambda_2$. Using ethane and ethylene as examples for single and double bonds, the ellipticity is $\epsilon \approx 0$ and $\epsilon \approx 0.117$ respectively, with a double bond in benzene equal to $\epsilon \approx 0.094$.

2.1.3 Poincaré-Hopf Rule

The number and type of rank three critical points in a stable system with a finite number of nuclei is governed by the Poincaré-Hopf relationship. Through this relationship there exists a restraint on the set of structural parameters [126]. There is a link between the critical points calculated and the stability of a chemical system. It has been discussed earlier in section 2.1.1 that if a system contains two NA's close to each other there will be a BCP. If the BCP's form a ring then there will be a RCP, and if the RCP's enclose a space, forming a cage, then a CCP will be calculated. The connection between the critical points adheres to the mathematical equation developed by Poincaré and Hopf. This relationship is shown in equation 2.4.

$$n - b + r - c = \chi \quad (2.4)$$

In equation 2.4 the number of NA, BCP, RCP and CCP are denoted by n , b , r , c respectively and the Euler characteristic, denoted as χ , should equal one for a stable system in the electron density [127]. The Euler characteristic is invariant to the topology and is always an integer [116, 127, 129]. A number other than one for the electron density denotes an unstable system such as a transition state. While this equation is valid for critical points in the electron density, it does not account for the added critical points found in other fields such as the MEP. The Poincaré-Hopf equation can be adapted to account for the extra critical points calculated in the MEP which is shown in the following equation;

$$(n + n_{neg}) - b + r - (c + n_{pos}) = 0 \quad (2.5)$$

The asymptotic maxima (n_{neg}) and minima (n_{pos}) are the (3, -3) and (3, +3) critical points respectively and separating these critical points in equation 2.5 results in;

$$n - b + r - c = n_{neg} - n_{pos} \quad (2.6)$$

This equation is similar to equation 2.4, however $\chi = n_{neg} - n_{pos}$. The value of n_{neg} refers to the negative critical points associated with the asymptotic maxima and the n_{pos} refers to the positive critical points associated with the asymptotic minima of the scalar field [116, 130]. These asymptotic maxima and minima occur outside of the molecule (outside the skeletal structure of the molecule) as the MEP approaches zero away from the molecule. Positively charged systems have a Euler characteristic of -1 and negatively charged systems +1. The MEP of neutral systems approach zero at infinity and therefore the asymptotic minima and maxima are calculated on a sphere surrounding all critical points [116].

Degenerate critical points are not included within the Poincaré-Hopf rule as the critical points tend to form a ring on a surface perpendicular to the molecule and therefore can not be directly calculated. When the symmetry of the system is broken, the degeneracy is solved into non-degenerate critical points and can then be included in equation 2.6. The degenerate critical points in ground state molecules have been shown to have a vanishing contribution to equation 2.6 and therefore do not need to be accounted for in the Poincaré-Hopf equation [116].

More recently the Poincaré-Hopf equation was altered so that $\chi = n_o - n_i$, where n_o refers to critical points where the gradients show an outflux from the critical point ($\nabla V(r) \cdot dr > 0$) and n_i refers to critical points where the gradients show an influx to the critical point ($\nabla V(r) \cdot dr < 0$) [131].

2.2 Molecular Graphs

The combination of graph theory and topology is used to construct a chemical graph (molecular graph) which can be described as a network of bond paths that link neighbouring nuclei [4]. According to Bader *et al.* the molecular structure can not be compared with a point in nuclear configuration space. The geometrical parameters of a structure will change when the atoms move as a consequence of natural motion, the molecular structure is thus associated with a molecular graph which describes a region in configuration space [125]. Therefore, a chemical structure is a set of molecular graphs which have the same number of bond paths linking the same atoms [126].

2.2.1 Constructing Molecular Graphs

Once the critical points are calculated and defined, the next step would be to calculate which critical points interact with each other. To do this the gradient lines of the vector field (first derivative of the scalar field) are examined. The gradient lines of interest are those that originate at (3, -1) saddle points, are calculated along the direction of positive curvature and then terminate at (3, -3) critical points. The gradient lines of (3, +1) saddle points terminate at (3, -1) and (3, +3) critical points. The gradient lines of the (3, +3) minima terminate at all the other critical points. A line that links two (3, +3) critical points and passes through a (3, -1) critical point is known as an Atomic Interaction Line (AIL). An AIL is defined as having two gradient lines that start at a (3, -1) saddle point and terminate at a (3, +3) critical point. It

can therefore be predicted that when two atoms are in close proximity to one another, they would share an atomic surface and thus have an AIL [128].

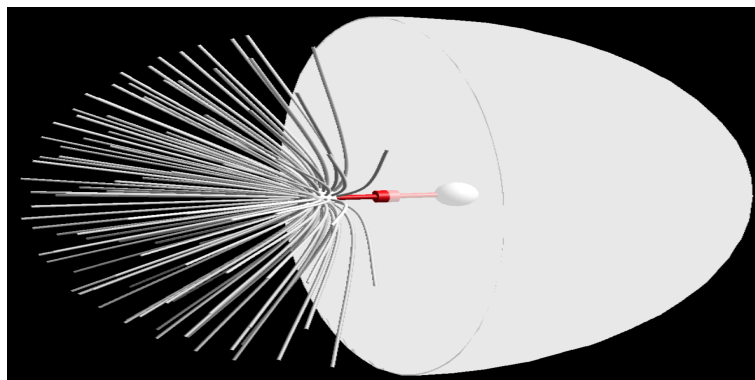


Figure 2.2: A hydrogen molecule calculated in the electron density with two atomic basins, one shown by gradient lines and the other a filled boundary, and an AIL connecting the two atoms (red line). The $(3, -1)$ critical point is depicted as a red cylinder.

The existence of a $(3, -1)$ critical point in the electron density between a pair of nuclei implies that the two atomic basins are neighbouring basins as they share a common atomic surface. The two basins are connected by a line in which the electron density is a maximum. This is a bond path and as such the neighbouring atoms are bonded. In general the bond path will not be coincident with the corresponding internuclear axis with the notable exception of bonds in molecules containing high symmetry. The bond paths reveal the stabilising or destabilising forces acting within the system [11]. A similar relationship exists between the $(3, +3)$ and the $(3, +1)$ critical points. When analysing the topology of the MEP it is noticed that whenever there is a pair of $(3, +3)$ critical points they are connected by a $(3, +1)$ critical point. There also exists a gradient line extending from the $(3, +1)$ critical point which will terminate at each of the $(3, +3)$ critical points. As minima in the electron density are only calculated when a molecule forms a cage structure like adamantane (figure 2.1) a string of minima and $(3, +1)$ saddle points similar to those found in the MEP do not occur. However, there is still a gradient line that is calculated in the electron density between the minimum and saddle point and should a molecule consist of multiple caged structures then the minima would be connected through $(3, +1)$ saddle points.

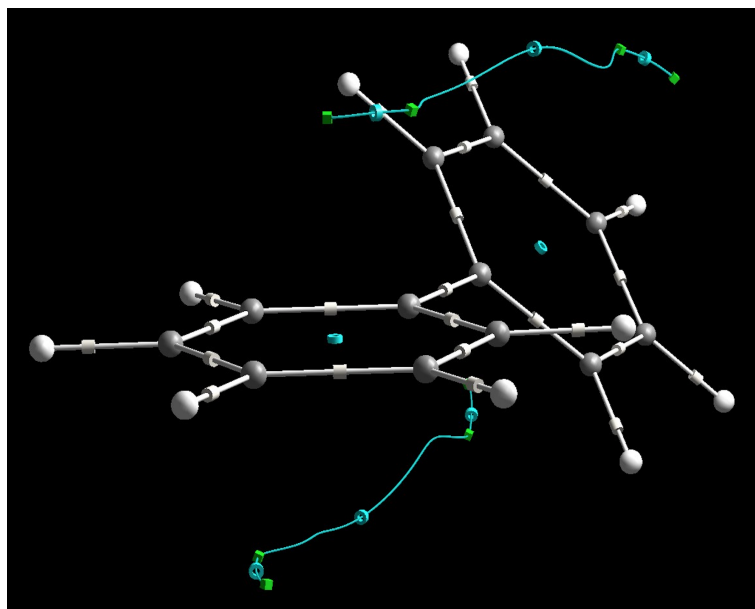


Figure 2.3: *The twisted biphenyl molecule shows the linking of (3, +3) critical points (green cube) with a gradient line passing through a (3, +1) critical point (blue ring) in the MEP.*

2.3 A Definition for Atoms and Bonds

There are three concepts that are important for the description of a chemical system. First, there needs to exist atoms (or functional groups consisting of atoms) in a molecule that can be determined by a set of characteristic properties. Second, the stability of the molecule through strong interactions between atoms in a molecule (bonding interactions). Lastly, the atoms and interactions need to resemble a molecular structure and molecular shape [126].

”To give substance to the notion of a bonded pair of atoms one must define the atoms as well as the bond” [125].

Based on the simple idea that opposite charges attract, when two atoms are close enough to each other the resulting positive charge will lead to an accumulation on negative charge between them by means of the electron density. This accumulation of electron density leads to a line of maximum density between the two atoms. This also allows for the formation of a surface that acts as a common boundary between the two atoms. This boundary intersects the line of maximum density at a point where the density reaches a minimum value, this point is known as a critical point and is described as a (3, -1) critical point [1, 4, 10, 11, 126, 132]. Mathematically this location is defined as a point where the gradient vector field of the electron density is zero.

$$\nabla\rho(r) = 0 \tag{2.7}$$

The (3, -1) critical point can be further defined by diagonalising the Hessian matrix. This will result in two negative eigenvalues and one positive eigenvalue, a more detailed explanation is provided in section 2.1.1. The two negative eigenvalues are linked to two eigenvectors which

create a surface upon which an infinite amount of gradient lines in the electron density, $\nabla\rho(r)$, terminate at the (3, -1) critical point. This surface is known as the interatomic surface, $S(r_s)$, and it separates the two atoms. The positive eigenvalue is associated with a pair of eigenvectors that originates at the (3, -1) critical point and terminates at one of the interacting nuclei. When compared to other possible paths between the two atoms the unique eigenvectors associated with the positive eigenvalue trace a path between the atoms that is a maximum in the electron density.

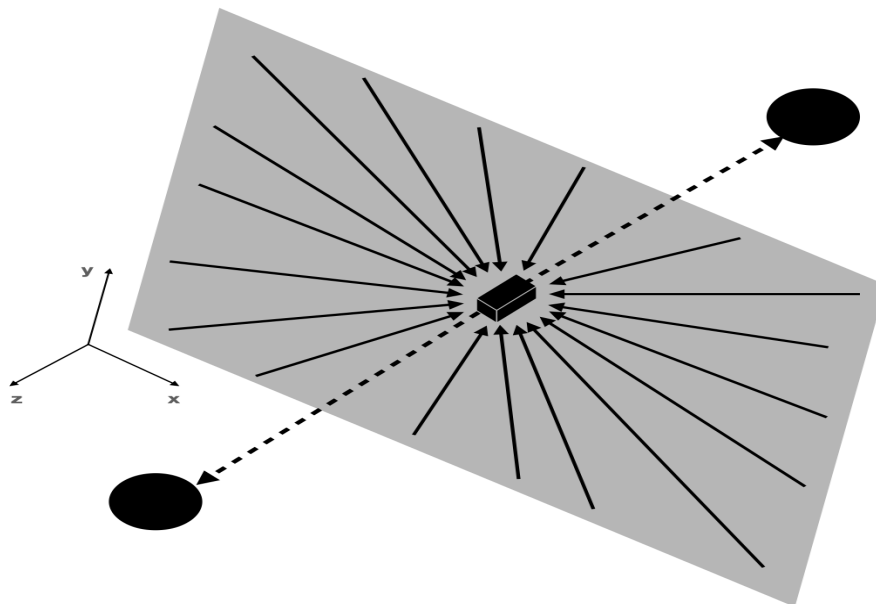


Figure 2.4: *The dashed lines represent the eigenvectors that had a positive eigenvalue and the surface with the solid arrows represent the surface created by the two eigenvectors associated with the negative eigenvalues.*

The interatomic surface, $S(r_s)$, is a zero flux surface which is calculated by taking the dot product of the gradients in the electron density vector field and a vector normal to the surface, the product is always equal to zero, equation 2.8. Interatomic surfaces can therefore be used with the electron density to partition molecules into their individual atoms based on physics alone [1, 133, 134].

$$\nabla\rho(r) \cdot \mathbf{n}(r) = 0 \quad \forall r \in S(r) \quad (2.8)$$

The gradient of the electron density is denoted as $\nabla\rho(r)$, $\mathbf{n}(r)$ is the normal surface vector and $S(r)$ is the surface. Any gradient lines in the electron density that extend to infinity naturally form a surface as the values are approximately zero [134].

The importance of the (3, -1) critical point and the gradient lines that originate from them to form an atomic interaction line is found in the energy of the system. When calculating the wave function for a system in the stationary state the final energy of the system is a minimum. Therefore the atomic interaction line (AIL) is linked to the minimised energy between a pair of atoms and the combination of the AIL and (3, -1) critical point implies the cancellation of the attractive and repulsive forces resulting in zero net forces [4]. The forces being balanced in a molecule is the Hellmann-Feynman force acting on the nuclei and the Ehrenfest force which

acts on the electrons. By calculating the virial of the Ehrenfest force the potential energy of the system can be analysed. The geometric structures calculated from the virial and electron density fields are homeomorphic. This implies that the line of maximum density between two atoms is matched by a line of maximum negativity for the potential energy which is a sign of stability [4]. At this point the (3, -1) critical point is referred to as a BCP and the AIL is now called a bond path.

All gradient paths in the electron density originate at infinity ($\nabla\rho = 0$) and terminate at the nucleus. The gradient lines terminating at a nucleus indicates the volume of space that the nucleus occupies and thus the atom [11, 126, 127], shown in figure 2.2. Bond paths are used to show interacting atoms and this is used to formulate a molecular graph. The bond paths can also be used to show molecular strain. When the bond paths of a molecule are curving in towards the centre of the molecule, the system is considered to be electron deficient. If the bond paths are curving out, away from the centre of the molecule, this indicates bond strain [125]. However, it has been shown that when analysing the energies of such a system, there is not always a correlation between the curving of the bond path and strain of the system [86].

An atom in a molecule can further be described as a combination of subsystems to create a complete system, a molecule. The subsystems themselves are defined by the averaging of an observable (as an example, the electron density) which is calculated through quantum mechanical principles. These subsystems are bound by a zero flux surface which is calculated using the gradient of a chosen field. The zero flux surfaces partition the molecule into a combination of disjointed mononuclear regions [135]. The set of surfaces created by (3, -1) critical points within a molecular system partition the space of the system into a collection of regions which can be identified as atomic-like regions [11].

The molecular structure and its stability can be viewed as a competition for the electron density between the various nuclei within a molecule. This would imply that the atoms which are competing for the electron density need to share an atomic surface and thus be bonded to each other [126]. The number of bond paths terminating at a nucleus is model independent. It is determined by the topological properties of the electron density distribution. The properties of the electron density distribution are in turn determined by the forces acting between the various nuclei [11]. The gradient lines that connect two neighbouring atoms originate at the (3, -1) critical point and terminate separately at the two atoms. An interatomic surface is formed around the (3, -1) critical point which separates the two interacting nuclei. The basins of two neighbouring nuclei are distinct as the gradient lines, which terminate at the nuclei, avoid the (3, -1) critical point with the exception of the gradient lines beginning at the (3, -1) critical point and terminating at the nuclei. The gradient lines originating at the (3, -1) critical point, along which the $\rho(r)$ is a minimum between the two NA's and a maximum in the direction perpendicular to the line linking the two NA's, is referred to as a bond path and the neighbouring atoms are now considered to have a bonding interaction [126, 127].

As systems, atoms or molecules, approach each other the zero flux surfaces (a partition/surface which is created by the (3, -1) saddle point) of the systems persist. The shape and volume of the system is however determined by the forces present in the new system. This implies that while the atomic basin of an atom will remain between different molecular systems, the volume and shape may change [11], therefore atoms maintain individuality in a molecule. It is therefore possible to expect that the properties of a subsystem, such as dipole moments and reactivity, are specific to the subsystem and are transferable. These transferable effects are carried over to define group properties as well [135].

2.3.1 Types of Atomic Interactions

There are two general classes of atomic interactions, as defined by the molecular structure definition, which are characterised by their mechanical properties. First, interactions between closed-shell atoms and molecules are governed by the contraction of the electron density towards each of the interacting nuclei. This is the case for noble gases, ionic bonds, hydrogen bonds and van der Waals molecules. The second class of interactions result from the sharing of electron density between atoms, these are governed by the contraction of the electron density towards the line of interaction joining the nuclei. Systems that represent this characteristic are covalent and polar bonds [132]. The Laplacian of the electron density at the (3, -1) critical point is negative for covalent and polar bonds at equilibrium. As the electron density is contracted along the line of interaction, it is shared by both nuclei involved and is referred to as shared interactions [132]. For closed-shell interactions the electron density and the (3, -1) critical point is low and therefore the Laplacian at this point is positive [132].

As systems, atoms or molecules, approach each other the zero flux surfaces of the systems persist. The shape and volume of the system is determined by the forces present in the new system. This implies that while the atomic basin of an atom will remain between different molecular systems, the volume and shape may change [11]. The distribution of electron density within a fragment is almost identical in different systems [8]. In the context of topology, the nuclei are considered to be relatively stable point attractors and as a consequence the identity of the atom is able to be conserved in different environments despite the changing electron density in the different environments [125].

2.4 Molecular Electrostatic Potential

Using scalar fields such as the electron density and molecular electrostatic potential are a good method for representing features such as bonding, molecular structure and bond strengths and the MEP going further by being able to identify lone pairs [115]. The MEP has also been used to explore many other properties of atoms and molecules such as reactivity [136].

The electron density for ground state atoms is positive everywhere and decreases steadily when moving away from the nucleus. The benefit of using the molecular electrostatic potential is that there are negative regions which are associated to the valence electron region. This feature is what allows the MEP to draw focus to chemical features such as lone pairs, π -bonds and aromaticity [115].

The Hellman-Feynman theorem applies to systems which use a fixed nucleus approximation and as such a force on a single nucleus will be determined by the electrostatic field of the electron density and the other nuclei in the system. The necessary condition for the nuclei to be bonded is that there needs to be at least one configuration of the nuclei for which the Hellmann-Feynman (electrostatic) force is zero for each nucleus [132].

The molecular electrostatic potential (MEP) is a scalar field and therefore the same rules apply for calculating the molecular graph as for the electron density. The MEP is calculated by moving a positive probe in the scalar field and calculating the potential at the various points. The aim of using this method is that it is possible to calculate the potential energy caused by the nuclei as well as the potential created by the electrons. The overall potential energy is then

calculated by subtracting the electron potential from the nuclei potential energy. This is shown in equation 2.9 in atomic units.

$$V(\mathbf{r}) = \sum_{A=1}^N \frac{Z_A}{|\mathbf{r} - \mathbf{R}_A|} - \int \frac{\rho(\mathbf{r}')}{|\mathbf{r} - \mathbf{r}'|} d^3\mathbf{r}' \quad (2.9)$$

In equation 2.9, $V(\mathbf{r})$ is the potential energy and Z and \mathbf{R} are the nuclear charge and nuclear position respectively. The position of the probe is given as \mathbf{r} and the position of the electron is \mathbf{r}' . The gradient lines (vector field) are determined by calculating the first derivative of the scalar field, this includes the calculation of the AIL. The gradient lines are useful for determining the molecular graph but when used in the MEP the gradient lines represent the electric field created by the atoms [131]. The second derivative is used to define the shape of the critical point. This is calculated in the Hessian matrix as described above. Unlike the electron density, it is possible to have degenerate critical points that are stable [116], they do not bifurcate or vanish with the vibrations of the atoms. It is therefore possible to have many more types of critical points which are shown in table 2.2.

Table 2.2: *Stable degenerate critical points in the molecular electrostatic potential.*

Critical Point	Description
(2 , -2)	local maximum
(2 , 0)	inflection point
(2 , +2)	local minimum
(1 , -1)	-
(1 , +1)	-

The degenerate critical points with rank 2 describe a curve while a rank 1 critical point describes a surface [116].

The "rules" for the critical points of rank three are different in the MEP compared to the electron density. While the (3, -3) critical points still represent the nuclei, the (3, -1) saddle points are not only found between nuclei but also serve the function of showing the shape of the system. An example of this is seen in the topology of benzene, the (3, -1) saddle point appears above and below the benzene ring surrounded by (3, +3) and (3, +1) critical points. The (3, +1) saddle points still appear in ring structures but also fulfil a similar function to (3, -1) saddle points. Instead of joining nuclei, the (3, +1) saddle points link minima together. The (3, +1) saddle point therefore does not need to be surrounded by (3, -1) saddle points as is the case in the electron density. Likewise, the minima are no longer restricted by having to be surrounded by (3, +1) saddle points. This presents a problem when using the Poincaré - Hopf rule because the critical points are no longer as dependant on each other as in the electron density. Degenerate critical points add to the complexity of the Poincaré-Hopf equation as they are acceptable in the MEP, therefore equation is no longer valid in its current form (this is discussed in an earlier section, 2.1.3).

2.4.1 Topology and the Molecular Electrostatic Potential

Topology is ideally suited to studying atoms and molecules as it characterises a scalar field using contours, gradient lines and critical points [115]. However, it is important to realise that sometimes having a general interpretation of the topology can lead to incorrect explanations of a system. The topology of the MEP can become very populated with critical points, even simple molecules such as methane, figure 2.5, can have a diverse range of critical points. It can be tempting to have general interpretations for the four main critical points, namely $(3, -3)$, $(3, -1)$, $(3, +1)$ and $(3, +3)$ however each critical point should be analysed on an individual basis. A common example for this is the benzene molecule where the delocalised pi-electrons are positioned above and below the ring, represented by alternating $(3, +3)$ and $(3, +1)$ critical points, in the middle of the ring of critical points is a $(3, -1)$ critical point, figure 2.5. This critical point is clearly not depicting a bond critical point like those present between the carbons (it is also missing any gradient lines connecting two $(3, -3)$ critical points), instead it is a representation of the deformed space above the molecule. The critical points above and below the benzene ring is a sign of aromaticity and the similar values of the critical point is an indication of flattening of the MEP. While it is tempting to always associate the ring of $(3, -1)$ and $(3, -3)$ critical points as representing aromaticity molecules such as triphenylene, phenanthrene and chrysene (figure 2.5) clearly lack the same ring of critical points above and below the ring such as with benzene. It is also easy to associate $(3, +3)$ critical points with regions of negative MEP but this is not always true.

The topology of the molecules shown in this section are not new but they have all been calculated using eDensity (explained in greater detail below). The wavefunctions were calculated using Gaussian09 with the HF and B3LYP theory and a combination of 6-311++G(d,p) and Def2TZVPP basis sets. Wavefunctions that are obtained using HF//6-311++G(d,p) and B3LYP//Def3TZVPP were used to calculate the topology of the molecules in the MEP. The molecules in the following section are from the HF//6-311++G(d,p) wavefunction only as the topologies from both methods are similar.

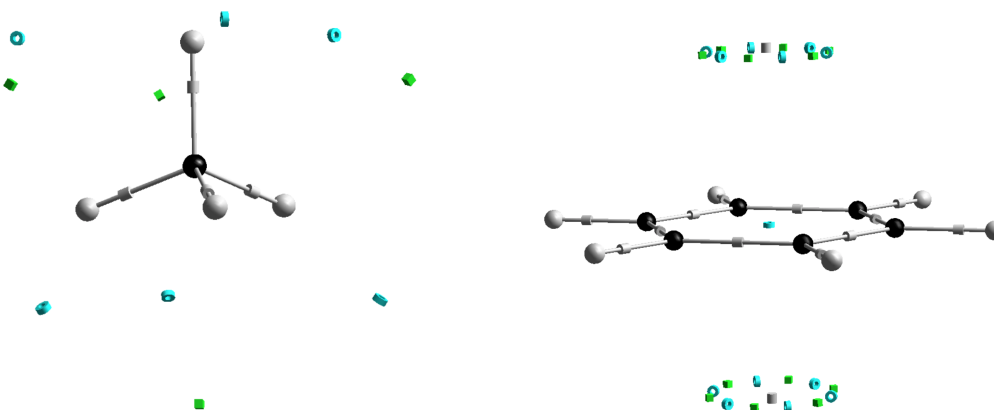


Figure 2.5: *MEP topology of a methane molecule showing four minima (green cubes) positioned between the hydrogens and joined by four $(3, +1)$ saddle points (blue rings). The benzene topology is shown with the critical points above and below the ring.*

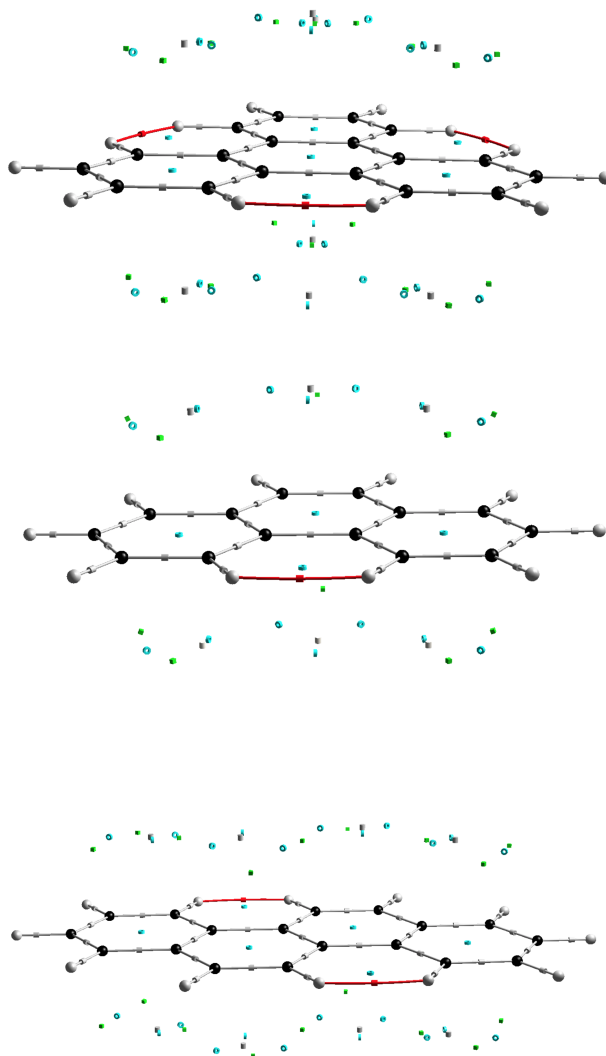


Figure 2.5: *The MEP topology of three molecules consisting of aromatic rings. The position of the critical points are attributed to the dispersed nature of the electrons which are associated with these types of structures. The grey cylinders are $(3, -1)$ critical points, green cubes are $(3, +3)$ critical points and the blue rings are $(3, +1)$ critical points. The red $(3, -1)$ critical point and atomic interaction line show a hydrogen-hydrogen bond.*

If the interpretation of the MEP topology is as diverse as the topology itself then the question arises, can it be useful? The topology of the electron density is a good way to highlight the bonding features of a molecule as the density values at the bond critical points can identify properties such as bond order and bond strain [115]. Unfortunately, using the MEP topology in the same way as using electron density topology can lead to problems. An example of this is the bending of bonding gradient lines, atomic interaction lines, which signify bond strain in the electron density. The bonding gradient lines in the MEP seldom deform. If the bond between atoms is electron deficient the nucMEP term (nuclear component of the MEP) of the MEP equation becomes dominant which results in a straight line connecting two atoms. When determining bond order in the MEP, double bonds are accompanied by two $(3, +3)$ critical points positioned above and below the bond. It has been suggested that the position of the $(3, +3)$

critical points can be used to identify systems that are strained. Interactions that take place at long distances (4 \AA or more) can have curved interaction lines, this is more of a representation of the outward expanding electric field rather than strain. The minima representing the pi system of double bonds can reveal repulsive interactions between the pi electrons, such as the case with cyclobutadiene where the minima are located on the outside of the ring structure [116]. This is opposite to the nature of the delocalised electrons of the benzene molecule, figure 2.5 (with the minima located within the cyclic structure) or having the minima directly above the double bonds as in ethylene, figure 2.6. The $(3, +1)$ saddle points located across a single bond between two double bonds (as in 1,3-trans-butadiene, figure 2.6) is yet another example of delocalisation of the pi electrons [116].

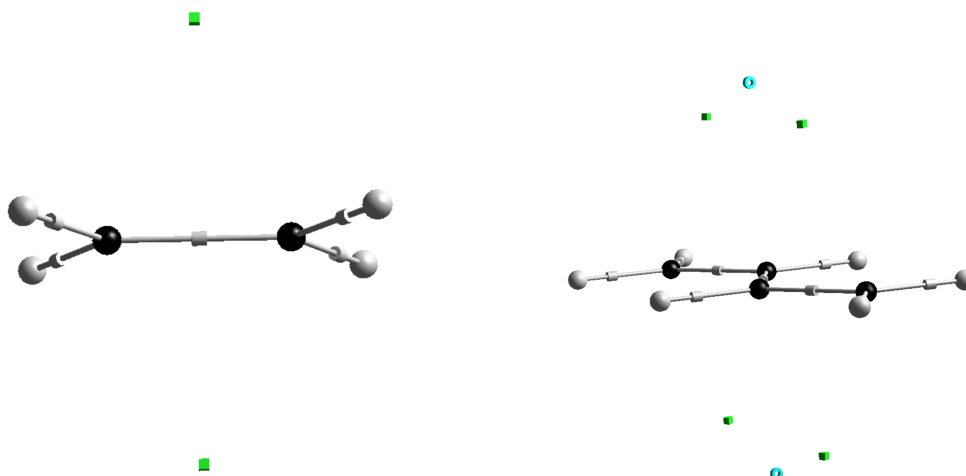


Figure 2.6: *The MEP calculated for the ethylene molecule shows the minima above and below the molecule which signifies the pi bonding electrons. The 1,3-trans-butadiene has the minima showing the double bonds and the $(3, +1)$ critical point (blue ring) shows that the electrons bridge the space over the single bond. The joining of the two minima with a saddle point is attributed to dispersed electrons.*

A downfall of using the electron density is that there are many features of an atom and molecule that are not present. Using a scalar field such as the laplacian and the MEP allows for a greater population of the space surrounding the atoms and molecules. In a paper by Kumar *et al.* the researchers used the laplacian to analyse critical points that represented lone pairs [93]. Lone pairs are not identified in the electron density even though one might expect to see a $(3, -3)$ critical point, a non-nuclear attractor, in a region with a high density of electrons. Lone pairs are identified in many other scalar fields including the laplacian and the MEP. While the laplacian highlights electron rich environments that are in accordance with the VESPR model, the MEP focuses on positive and negative regions in the scalar field and as such is able to locate minima in the electron rich regions [93]. Unfortunately the diverse topology of the MEP can have many local minima and they can not all be lone pairs. To distinguish between π -bonds, lone pairs and other minima Kumar *et al.* studied the eigenvalues and eigenvectors of the minima in relation to the nuclei. It was found that the eigenvalues (not the MEP values) were larger for lone pairs when compared with other minima. The eigenvector that is associated with the eigenvalue was also the largest eigenvalue and pointed towards the nucleus [93].

There are still further uses for the minima found in the MEP, the $(3, +3)$ critical points have been

used to assign double bonds in molecules containing multiple aromatic rings joined together, this forms part of Clar's sextet rule [137, 138, 139]. As each double bond in a molecule is represented by two (3, +3) critical points, above and below the bond, wherever these minima occur, a double bond is assigned. Even the minima found between the hydrogens of the methane molecule (figure 2.5) can be attributed to the sp^3 hybrid tails of the carbon atom [116] which can also be used to explain the minima found between the hydrogens of the ethane (figure 2.7) molecule. The minima associated with the hybridisation of the carbon atom seems to occur for many of the cyclic hydrocarbons as well, figure 2.7. The minima that form around a cyclic structure, such as cyclopropane, is as a result of the electron density being forced to the outside of the ring. This is also a sign of a strained ring structure [116].

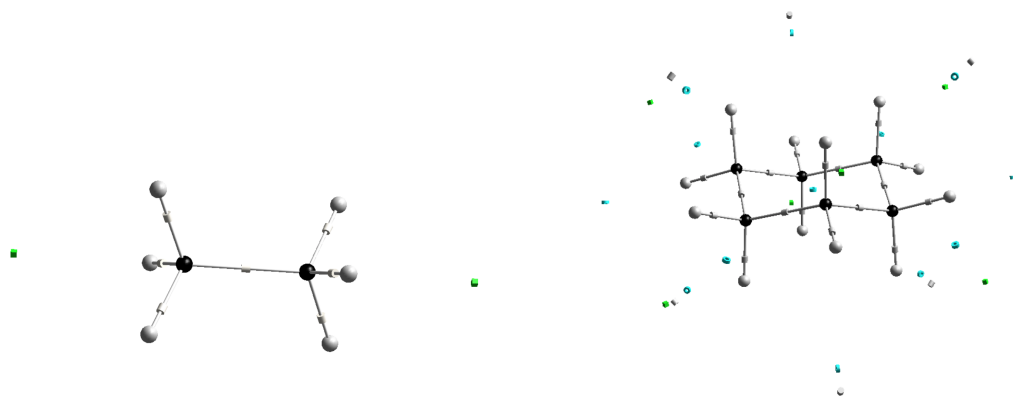


Figure 2.7: *MEP topology of an ethane molecule showing two minima (green cubes) positioned between the hydrogens, the same can be seen in cyclohexane*

Once again, there seem to be as many uses for the minima in the MEP topology as there are critical points. A pessimistic view of this might lead one to have doubts about many of the interpretations but a more optimistic view is that the range of explanations is a further testament to the ability of the MEP topology to explain complex systems in a way that offers even more insight than other methods.

2.4.2 Computational Method

In many cases choosing the correct method or basis set is important so that the properties being analysed are as close to the real value as possible while simultaneously being as cost effective in terms of computational time. It is for this reason that a simple study of a few methods and basis sets were carried out. The three main methods were Hartree-Fock (HF), second order Møller-Plesset (MP2) and the three parameter function Becke, Lee, Yang and Parr (B3LYP) and the triple zeta basis sets used were the 6-311++G(d,p), AUG-cc-pVTZ and Def2TZVPP. The combinations used were B3LYP//Def2TZVPP, MP2//6-311++G(d,p) and HF//AUG-cc-pVTZ, some of the calculations also included counterpoise correction. The overall goal was to test the effects of calculating the wave function from the Schrödinger equation as well as from a hybrid method which includes Density Functional Theory (DFT). The results for some of the calculations are presented in the table 2.3.

Table 2.3: *The effects of method and basis set on the topology of the Molecular Electrostatic Potential (MEP). The values for MEP (3, -1) are values taken between the centre two carbon atoms with the exception of neon for obvious reasons. The energies and MEP (3, -1) are all in a.u.*

Method//Basis set	MEP (3, -1)	(3, -3)	(3, -1)	(3, +1)	(3, +3)
Ne₂					
MP2//6-311++G(d,p)	0.0005	2	1	-	2
B3LYP//Def2TZVPP	0.0029	2	1	-	2
HF//AUG-cc-pVTZ	0.0005	2	1	-	2
HF//6-311++G(d,p)	0.0008	2	1	-	2
Ethane					
B3LYP//Def2TZVPP	0.6395	8	7	6	8
HF//AUG-cc-pVTZ	0.6204	8	7	6	8
HF//6-311++G(d,p)	0.6236	8	7	-	2
Ethylene					
B3LYP//Def2TZVPP	1.0397	6	5	-	2
HF//AUG-cc-pVTZ	1.0269	6	5	-	2
HF//6-311++G(d,p)	1.0399	6	5	-	2
Acetylene					
B3LYP//Def2TZVPP	1.4163	4	3	-	-
HF//AUG-cc-pVTZ	1.4424	4	3	-	-
HF//6-311++G(d,p)	1.4587	4	3	-	-
Butane					
B3LYP//Def2TZVPP	0.6276	14	17	6	4
HF//AUG-cc-pVTZ	0.6097	14	17	8	8
HF//6-311++G(d,p)	0.6128	14	17	6	4
cyclo-Hexane					
B3LYP//Def2TZVPP	0.6242	18	18	7	6
HF//AUG-cc-pVTZ	0.6056	18	18	7	6
HF//6-311++G(d,p)	0.6087	18	24	13	6
Benzene					
B3LYP//Def2TZVPP	0.9015	12	14	13	12
HF//AUG-cc-pVTZ	3.5804	12	12	1	-
HF//6-311++G(d,p)	0.8967	12	14	13	12

It was determined that the basis sets as well as method used did not play a significant role in determining the topological critical points that were calculated. In general the different methods and basis sets gave the same number of critical points but there were a few examples where extra critical points or fewer critical points were calculated. The extra critical points were associated with values that were considered to be too small to be significant. This determination was based on the values themselves being smaller than 10^{-5} and the critical points not showing in other methods and basis set combinations. A paper by Leboeuf *et al.* concluded that the topology obtained using DZVP and DZ-ANO were identical [116]. Roy *et al.* showed that for basis sets above 6-31G(d,p) there were no significant change in the topology and while the MEP values will change with different basis sets the general nature of the critical points remains the same [129].

After consideration of the results and previous publications [50, 140] it was decided that using the Hartree-Fock method with the 6-311++G(d,p) basis set was sufficient for the research proposed. This allowed for acceptable energy calculations, useful critical points (minimal critical point artefacts) and relatively cheap computational cost. The effect of adding in the counterpoise correction was tested on simple molecules as is shown in table 2.5 and was deemed unnecessary as no significant differences were noticed, however, the counterpoise correction would be better tested on more complex molecules which is beyond the scope of this thesis. The default geometry optimisation parameters for the Gaussian 09, Revision D.01 [141] program was used to calculate the wavefunction and the visualisation and MEP calculations were carried out using the eDensity [56] program. Initial calculations of the electron density and MEP were carried out using the AIMAll [142] software, this was done to ensure the values calculated using eDensity were accurate.

The expectation value was used in all the topology calculations as calculations using the tensor has been shown to produce critical point artefacts. The cutoff threshold for the MEP calculations was set at 1×10^{-5} a.u., this was done to account for the wider area of influence of the MEP in comparison to the electron density.

Table 2.5: A comparison of the MEP value for wavefunctions calculated using the counterpoise correction (CP) and without the correction (nCP). The MEP values are reported in a.u. and are for the (3, -1) critical point for the noble gases helium, neon and argon.

Distance (Å)	He ₂					
	B3LYP//Def2TZPP CP	B3LYP//Def2TZPP nCP	MP2//6-311++G(d,p) CP	MP2//6-311++G(d,p) nCP	RHF//AUG-cc-pVTZ CP	RHF//AUG-cc-pVTZ nCP
0.5	3.4013	3.4013	3.5624	3.5624	3.4721	3.4721
1.0	0.5940	0.5940	0.5910	0.5910	0.5857	0.5857
1.5	0.1269	0.1269	0.1246	0.1246	0.1230	0.1230
2.0	0.0278	0.0278	0.0282	0.0282	0.0274	0.0274
2.5	0.0058	0.0058	0.0062	0.0062	0.0064	0.0064
3.0	0.0012	0.0012	0.0013	0.0013	0.0015	0.0015

Distance (Å)	Ne ₂					
	B3LYP//Def2TZPP CP	B3LYP//Def2TZPP nCP	MP2//6-311++G(d,p) CP	MP2//6-311++G(d,p) nCP	RHF//AUG-cc-pVTZ CP	RHF//AUG-cc-pVTZ nCP
1.0	2.2184	2.2184	2.2444	2.2444	2.2772	2.2772
1.5	0.4557	0.4557	0.4618	0.4618	0.4294	0.4294
2.0	0.1028	0.1028	0.0978	0.0978	0.0954	0.0954
2.5	0.0214	0.0214	0.0174	0.0174	0.0208	0.0208
3.0	0.0039	0.0039	0.0025	0.0025	0.0039	0.0039

Distance (Å)	Ar ₂					
	B3LYP//Def2TZPP CP	B3LYP//Def2TZPP nCP	MP2//6-311++G(d,p) CP	MP2//6-311++G(d,p) nCP	RHF//AUG-cc-pVTZ CP	RHF//AUG-cc-pVTZ nCP
1.0	4.9330	4.9330	5.7733	5.7733	5.4278	5.4278
1.5	1.7095	1.7095	1.8189	1.8189	1.7780	1.7780
2.0	0.5551	0.5551	0.5899	0.5899	0.5640	0.5640
2.5	0.1779	0.1779	0.1928	0.1928	0.1789	0.1789
3.0	0.0554	0.0554	0.0598	0.0598	0.0570	0.0570

2.5 eDensity

The program eDensity is an in house program developed by J. Dillen with some alterations pertaining to the Molecular Electrostatic Potential made by the author. The program uses a Newton-Raphson minimiser/optimiser when searching for critical points. A Nuclear Attractor (NA) is represented by spheres, the colour of the sphere corresponds a specific element for example the carbon NA is displayed in black. The Bond Critical Point (BCP) is shown as cylinders. This is done with the intention that the long side of the cylinder points in the direction of the positive eigenvalue. A Ring Critical Point (RCP) is shown as disk. The plane of the disk matches the plane formed by the two positive eigenvectors. The Cage Critical Point (CCP) is represented as a cube which is orientated along the three eigenvectors.



Figure 2.8: *The four critical points in eDensity is represented by the sphere (NA), cylinder (BCP), disc (RCP) and a cube (CCP).*

The bond paths are calculated from the BCP in each direction upwards towards the NA's, this is step process with the gradient being evaluated after each step and is represented by flexible rods. Further information can be gathered from the bond paths such as the bond path length between two NA's as well as the distance from a NA to the BCP. Gradient paths are calculated from critical points and usually move from high value to low value regions in a specific field, normally electron density. These gradient lines have a cut-off value which is usually set to 0.001 a.u. but can be adjusted.

The eDensity program uses the Runge-Kutta method and calculates the bond paths by solving the following differential equation.

$$\frac{dx(s)}{ds} = -\frac{\nabla\rho(x(s))}{|\nabla\rho(x(s))|} \quad (2.10)$$

The Inter Atomic Surface (IAS) is visualised by calculating the gradient lines perpendicular to the plane of the BCP. These gradient lines are calculated every 10 degrees on this surface for a total of thirty six gradient lines. The program then fills the space between the gradient lines with triangles thus producing a surface.

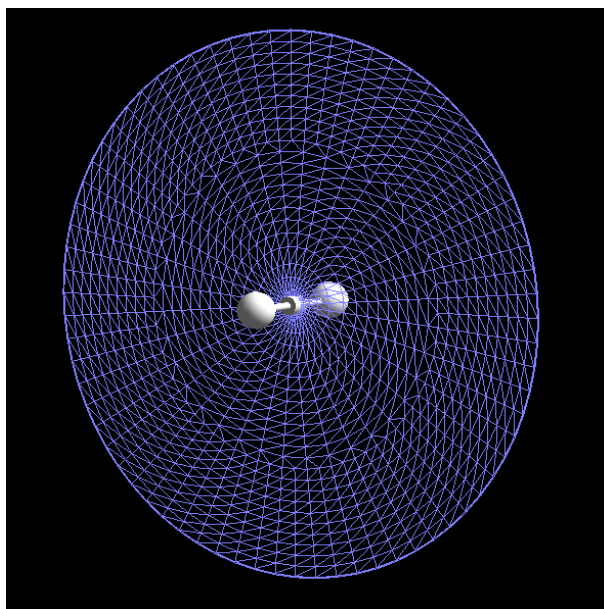


Figure 2.9: *The creation of the inter atomic surface using gradient lines and tringles to connect the gradient lines.*

The program uses the single Slater determinants to describe the wavefunction. The single electron orbitals are then expressed as a linear combination of a predefined basis function [143].

$$\Phi_i(\mathbf{r}) = \sum_j c_{ji} \chi_j(\mathbf{r}) \quad (2.11)$$

All contracted basis functions are expanded in the wavefunction file therefore the summations are over all primitives. The electron density is then defined as;

$$\rho(r) = \sum_i n_i \varphi_i^2(r) \quad (2.12)$$

The occupation number of each orbital is given by n_i and it is assumed that all molecular orbitals, $\varphi_i(r)$, and all constants, c_{ji} , are real ($\psi(r) = \psi^*(r)$).

The Laplacian function (negative of the Laplacian) of the electron density, $L(r)$, is defined by the equation below.

$$L(r) = -\frac{1}{4} \nabla^2 \rho(r) = -\frac{1}{2} [\psi(r) \nabla^2 \psi(r) + \nabla \psi(r) \cdot \nabla \psi(r)] \quad (2.13)$$

The Molecular Electrostatic Potential (MEP, $V_{MEP}(r)$) refers to the potential energy acting on a positive charge (hypothetical charge) positioned at r due to the interactions with all other particles in the system.

$$V_{MEP}(r) = \sum_A \frac{Z_A}{|\mathbf{r} - \mathbf{r}_A|} - \int \frac{\rho(\mathbf{r}')}{|\mathbf{r} - \mathbf{r}'|} d\mathbf{r}' \quad (2.14)$$

In the MEP equation the summation is over all nuclei and the integration is for all space, although this is impractical in terms of computational time. Therefore the second term of the equation is expanded in terms of the primitives.

Combining the wavefunction with the electron density gives the equation;

$$\rho(r) = \sum_i n_i \varphi_i^2(r) = \sum_i n_i \sum_r c_{ri} \chi_r(r) \cdot \sum_s c_{si} \chi_s(r) \quad (2.15)$$

Which gives;

$$\int \frac{\rho(\mathbf{r}')}{|\mathbf{r} - \mathbf{r}'|} d\mathbf{r}' = \sum_i n_i \sum_r \sum_s c_{ri} c_{si} \int \frac{\chi_r(r) \chi_s(r)}{|\mathbf{r} - \mathbf{r}'|} d\mathbf{r}' = \sum_i n_i \sum_r \sum_s c_{ri} c_{si} \langle \chi_r(r) | \frac{1}{|\mathbf{r} - \mathbf{r}'|} \chi_s(r) \rangle \quad (2.16)$$

If the primitives, $\chi(r)$, are Gaussian primitives then the nuclear attraction integrals (given in bracket notation) will have an analytical solution, however, if the primitives are slater type functionals the solutions do not exist.

The program has a unique function that allows for the calculation and visualisation of degenerate critical points. Critical points with rank two have a zero eigenvalue in the Hessian matrix, because of this a critical point is calculated in one of the planes as it meets the criteria of having a derivative equal to zero. Similar to how the bond path is calculated, eDensity calculates the gradient path in the surrounding area and traces a gradient path. As the critical points are rank two, this path becomes circular and therefore infinite.

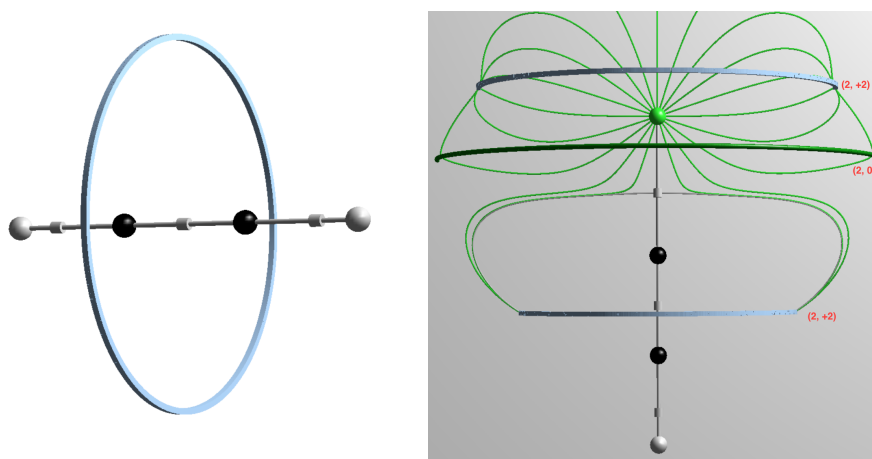


Figure 2.10: *The acetylene molecule has a (2, +2) critical point which becomes a ring and the chloro-ethyne molecule shows a (2, 0) saddle point between two (2, +2) critical points all of which form a ring.*

Chapter 3

Exploring the Topologies of Electron Density and Molecular Electrostatic Potential Scalar Fields

This chapter explores in more detail the topology of the electron density and Molecular Electrostatic Potential (MEP) fields, how they are different and what information can be gathered from the topologies. The uses for the topology of the MEP that were laid out in chapter two will be explored, this will include locating lone pairs and describing delocalised electrons. The degenerate critical points that are stable in the MEP and kinetic fields will be explored to determine if the critical points serve a purpose beyond describing a curved region of space.

The figures and tables in this chapter are calculated using Hartree-Fock level of theory with the 6-311++G(d,p) basis set unless otherwise stated. The values are reported in atomic units with the exception of the distance between atoms which is given in Angstroms.

3.1 Comparing the Electron Density and Molecular Electrostatic Potential Scalar Fields

The mathematical field of topology deals with folds in a given volume of space, therefore the more turbulent a field, the greater the number of critical points that are calculated. It is for this reason that the topology for the electron density has a relatively simple topology compared to the MEP. The MEP is the sum total of a nuclear component and an electronic component and therefore at any point in space one term could dominate the other resulting in a topology that represents an interacting positive and negative topology. The images in this section highlight the similarities and differences between the scalar fields of electron density (ρ) and the MEP.

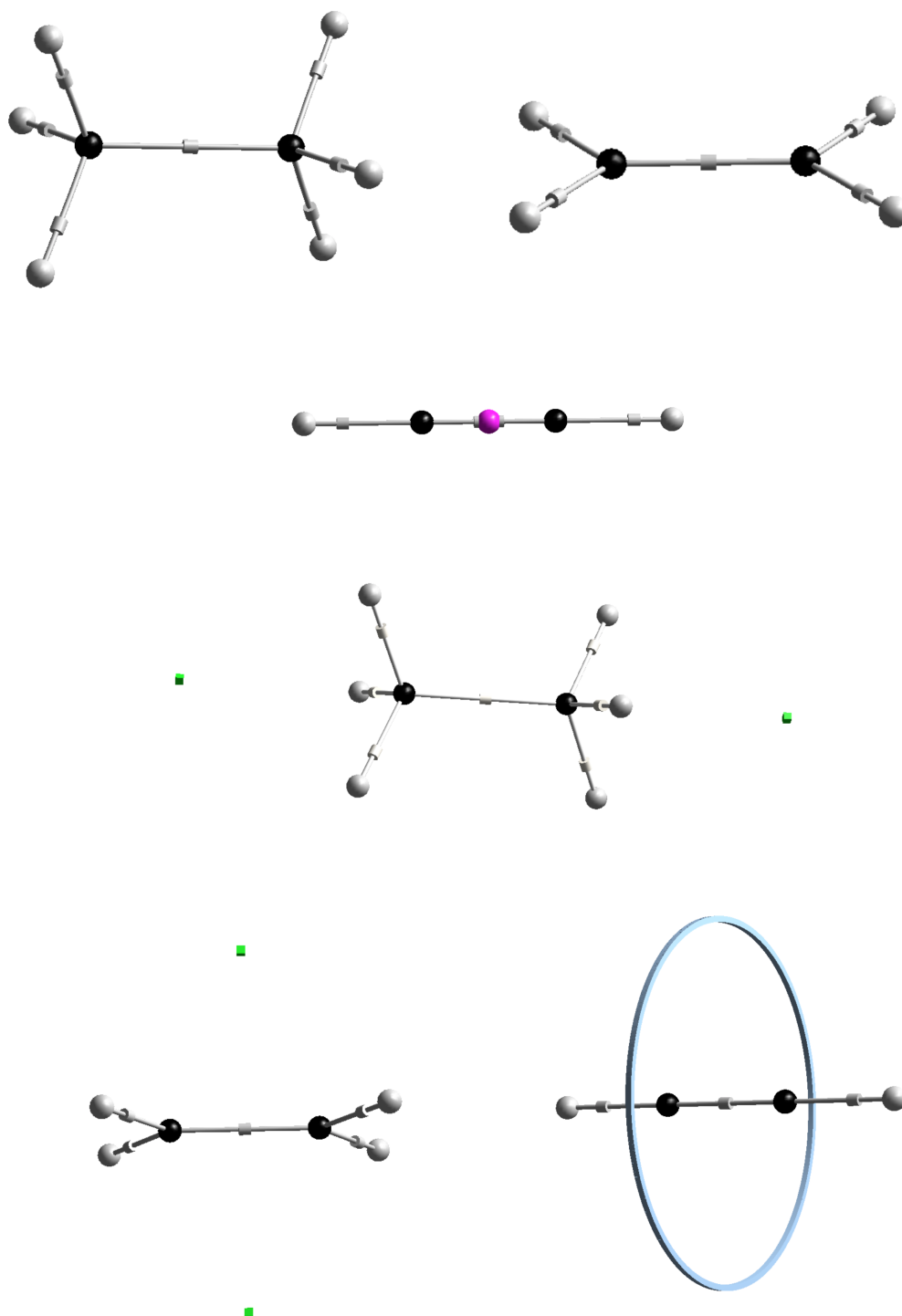
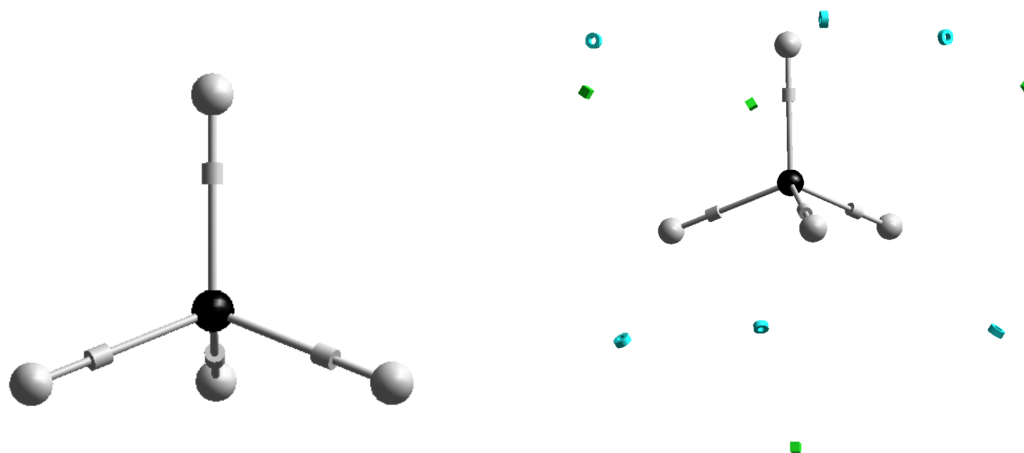


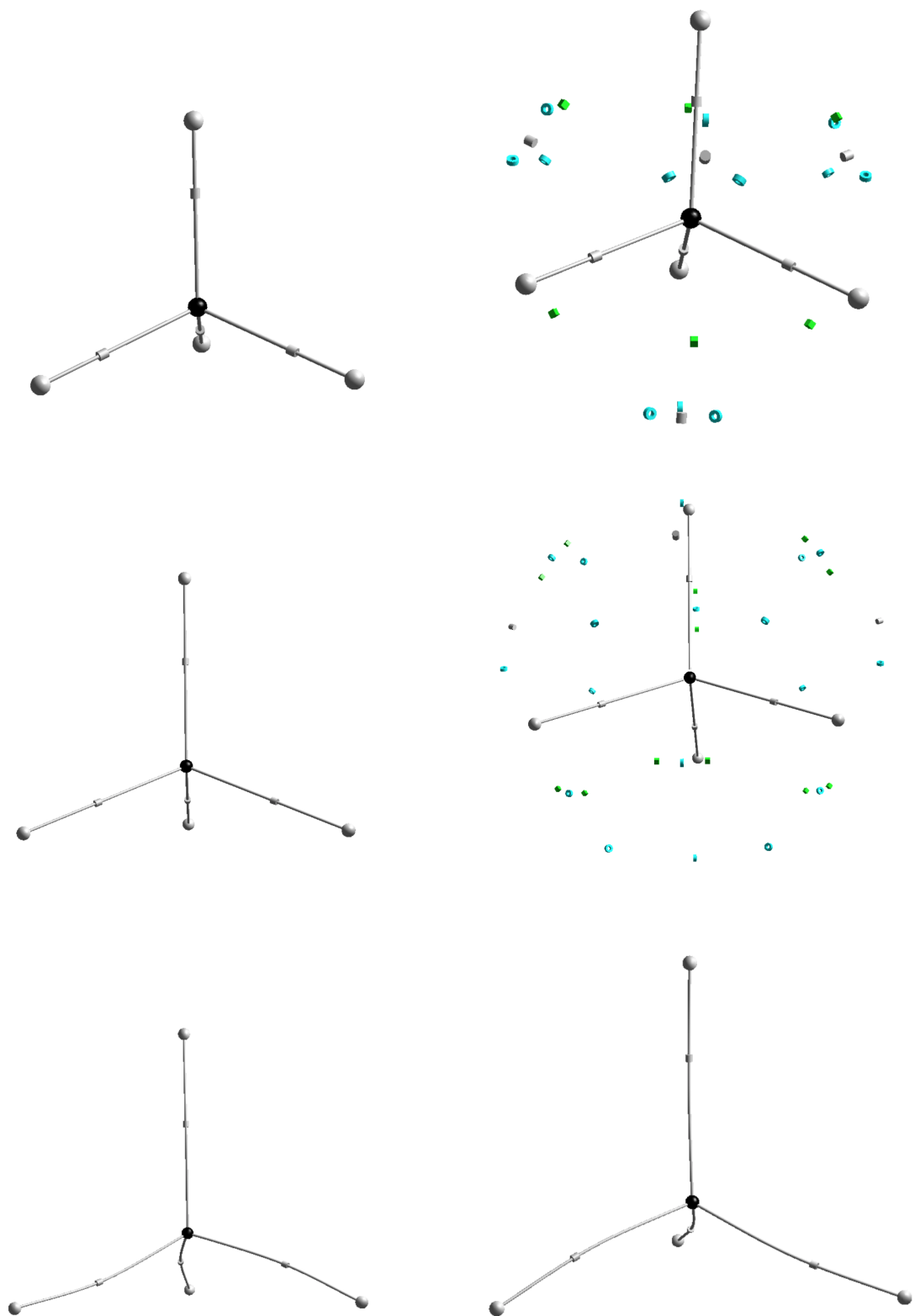
Figure 3.1: *The first set of ethane, ethylene and acetylene are calculated in the electron density scalar field. The second set of ethane, ethylene and acetylene are calculated in the MEP scalar field. The black spheres are nuclear attractors representing carbon atoms, grey spheres are hydrogen atoms. The pink sphere for acetylene is a non-nuclear attractor. The grey cylinders are $(3, -1)$ critical points, green cubes are $(3, +3)$ critical points and the pink sphere is a $(3, -3)$ critical point. The ring surrounding the $(3, -1)$ critical point is a $(2, +2)$ ring.*

The molecules in figure 3.1 show that even with a simple series like ethane, ethylene and acetylene there are differences between the topology of ρ and the MEP. The benefit of the MEP topology is shown in the ability to visually identify a double or triple bond. The symmetry of a molecule is also reflected in the MEP topology, this is easily seen with the molecules shown in figure 3.1 and in the methane molecule. The minima above and below the ethylene molecule is associated with the π - bonding electrons and the (2, +2) degenerate ring around the (3, -1) critical point is sometimes found around triple bonds. Not all of the critical points calculated in the MEP have a simple explanation, such as the minima between the hydrogens for ethane. These types of minima are calculated for a variety of alkanes and in this research a minimum is always calculated for hydrocarbons that have three hydrogens bonded to a carbon atom in a trigonal pyramidal configuration.

3.1.1 Extreme Examples of Methane

Calculating molecules allows for the opportunity to create extreme and unrealistic molecular structures. In this section the methane molecule is calculated with bond lengths between the hydrogens and carbon at distances ranging from 1 Å to 5.5 Å. The purpose for doing this is to better understand the topology of the MEP. When stretching bonds in ρ the topology remains the same but in the MEP the space around the atoms changes and so do the critical points. Figure 3.0 below show a side-by-side comparison of the methane molecule in the two fields, namely ρ and MEP, at predefined distances.





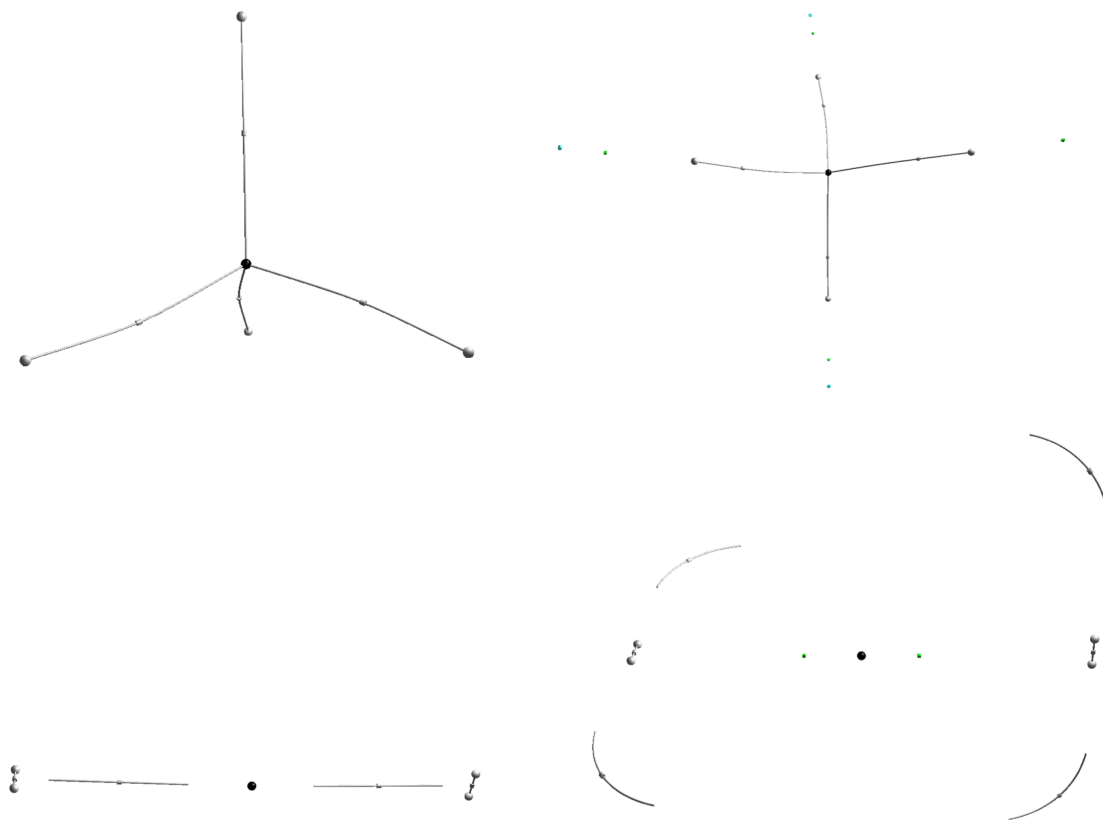


Figure 3.0: *The six groups of pictures show a comparison between the electron density (pictures on the left) and MEP (pictures on the right) scalar fields when calculating the methane molecule. The lengths are chosen at 2, 3, 3.5, 5 and 5.5 Angstroms because at these distances the topology of the MEP undergoes significant changes. The first set of pictures shows the fully optimised structure of the methane molecule, thereafter only the bond length is fixed. The black spheres represent carbon atom, grey spheres are hydrogen atoms. The grey cylinders are (3, -1) critical points, the blue rings are (3, +1) critical points and green cubes are (3, +3) critical points.*

The first figure is a comparison of the ρ and MEP for a fully optimised structure with no restrictions, all calculations were carried out using the Hartree-Fock method and a basis set 6-311++G(d,p). The other figures had the carbon-hydrogen bond lengths fixed and no other restrictions were put in place for the molecule. It is not surprising that there is very little change in the topology for the ρ scalar field, but the topology of the MEP scalar field goes through multiple changes.

At 2 Å the (3, +3) minimum is relocated to between two hydrogens, bridging the two hydrogens, and is no longer located between the three hydrogens. Where the minimum once was, a combination of three (3, +1) critical points are calculated and a single (3, -1) critical point is located in the middle of the saddle points.

The topology of the MEP scalar field at 3 Å is more spread out than the topology at 2 Å, this is mainly for the (3, +1) and (3, -1) critical points located between the three hydrogens. The

bridging minima between two hydrogen atoms splits into two minima with a (3, +1) saddle point between them. At 3.5 Å the topology of the ρ and MEP scalar fields are devoid of extra critical points and both topologies consist of similarly curved atomic interaction lines (bond paths).

At 5 Å the atomic interaction lines still have a curve for the ρ and MEP fields. However, (3, +3) and (3, +1) critical points are calculated above each hydrogen atom in the MEP field. When the bond length was increased to 5.5 Å the hydrogens were no longer in the spatial orientation of a methane molecule but rather the hydrogen atoms formed a diatomic molecule to which the carbon atom interacts. This was calculated for both scalar fields, the only difference is that for the MEP field the hydrogens formed a (3, -1) critical point between the hydrogen and the carbon, in the ρ field the carbon atom seems to interact with the (3, -1) critical point between the diatomic hydrogens. Two minima are also calculated on either side of the carbon atom in the MEP field.

The calculations were repeated using the unrestricted Hartree-Fock method with the same basis set (6-311++G(d,p)). The reason for this calculation is because the HF method calculates paired electrons in orbitals where as the unrestricted HF method calculates each electron in its own orbital and therefore might have an impact on how the stretched bond lengths are calculate. However there seems to be no difference between the two methods as they produced identical molecular topologies and the values at the (3, -1) saddle point are the same.

Table 3.1: *A comparison of the MEP, electron density and electrostatic potential (elecMEP) for the methane molecule calculated with the Hartree-Fock and Unrestricted Hartree-Fock method. Both methods used the basis set 6-311++G(d,p). The values are in atomic units with the exception of the bond lengths which are in Ångström.*

Distance (Å)	Methane					
	Hartree-Fock			Unrestricted Hartree-Fock		
	ρ	elecMEP	MEP	ρ	elecMEP	MEP
1.0	0.3326	-6.5526	1.0375	0.3326	-6.5526	1.0375
1.5	0.1294	-4.8481	0.2997	0.1294	-4.8481	0.2997
2.0	0.0499	-3.8397	0.0941	0.0499	-3.8397	0.0941
2.5	0.0200	-3.1365	0.0407	0.0200	-3.1365	0.0407
3.0	0.0093	-2.6156	0.0238	0.0093	-2.6156	0.0238
3.5	0.0034	-2.1058	0.1135	0.0034	-2.1058	0.1135
4.0	0.0020	-1.8470	0.0739	0.0020	-1.8470	0.0739
4.5	0.0014	-1.6389	0.0483	0.0014	-1.6389	0.0483
5.0	0.0011	-1.4713	0.0315	0.0011	-1.4713	0.0315
5.5 (C-H)	0.0000	-0.7883	0.0002	0.0000	-0.7996	0.0002
5.5 (H-H)	0.2661	-2.6321	0.9213	0.2661	-2.6320	0.9211

As a final note to this section, a comment should be made regarding the curved nature of the AIL. In later chapters the curved AIL is linked to strained atomic interaction but this is not the case for the methane molecule, the curved AIL in the methane molecule are due to an unstable wavefunction. This can be improved by adjusting the default convergence value for geometry optimisation, converting the input geometry to a Z-matrix with defined bond angles and lengths or by changing the level of theory from a single determinant approximation to multi-configurational calculation.

Constraining the bond length while allowing the rest of the molecular geometry to be optimised was intended to show, among other things, that there is some merit to the criticism that the QTAIM method will find AIL between two atoms no matter the distance between the atoms. Calculating a stable wavefunction and applying the QTAIM method would still produce AIL between the atoms and therefore the outcome will be the same. This is because no matter the distance, there will be a minimum between the atoms.

3.1.2 Iso-surface and Gradient Lines of the Methane Molecule

The topology of the MEP is good at identifying key locations in and around a molecule but much more information can be discovered through the use of gradient lines and contour maps. Methane is a simple molecule and yet the topology has been shown to be very populated especially when compared to molecules such as ethane or ethylene. Using the electrostatic potential iso-surface map it can be seen that a simple and repeating pattern emerges and it is clear that the topology only looks complex and is merely a result of T_d symmetry.

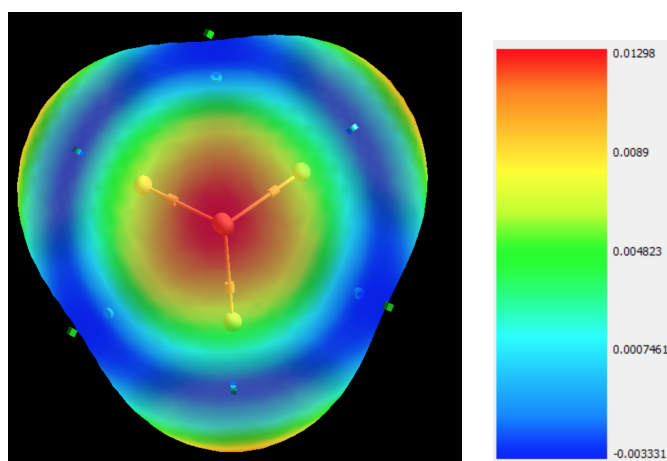


Figure 3.1: A *MEP iso-surface of fully optimised methane.*

The topology of the MEP at 2.0 \AA shows a shifting of the critical points, hence an electrostatic iso-surface, figure 3.2, was calculated for this methane molecule. When comparing figure 3.1 above with figure 3.2 it can be seen that the band of negative potential narrows and the centre point between the hydrogens coincides with a minimum. Similarly, the region where a minimum was previously calculated has also narrowed resulting in multiple critical points.

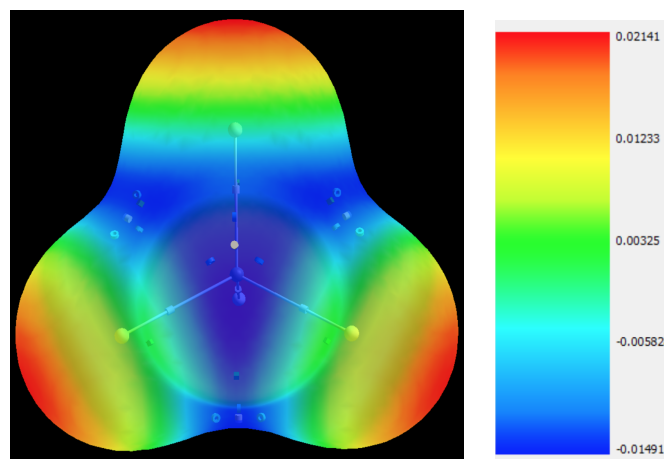


Figure 3.2: A *MEP iso-surface of methane with bond lengths of 2 Å*.

The MEP contour plot of the methane molecule, figure 3.3 with carbon hydrogen bond lengths of 2 Å is shown below. The plane passes through the carbon, two hydrogens and a minimum which is calculated between the hydrogens. The black lines indicate a positive MEP and the white lines a negative MEP. The minimum between the hydrogens has a negative MEP and shows a slice through a band of negative MEP, this band can be seen at the bottom of the figure passing through the minimum which is between the two out of plane hydrogens. These large areas of negative MEP are the same regions shown in blue in the MEP iso-surface.

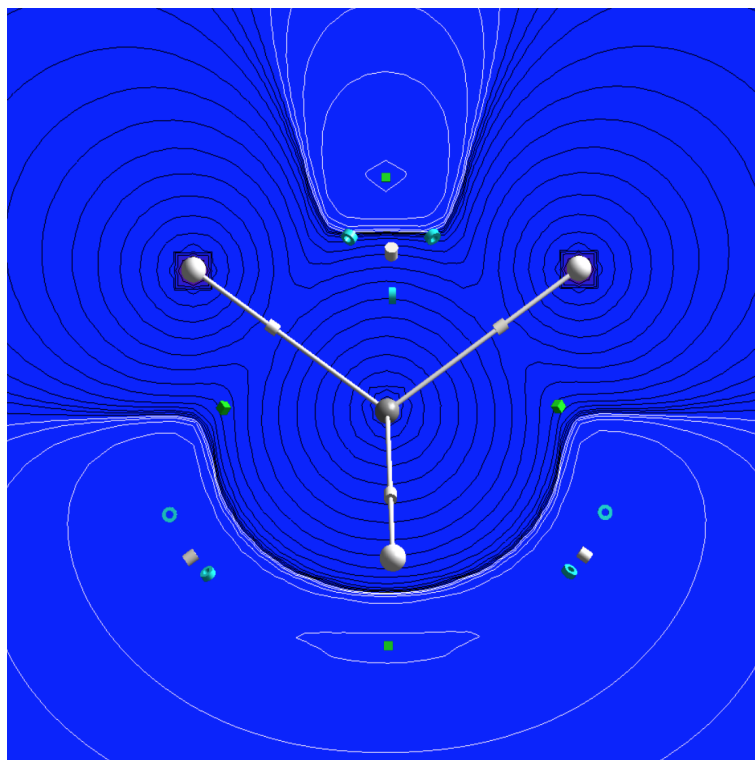


Figure 3.3: A contour plot of the methane molecule with bond lengths of 2 \AA . The white contour lines show negative MEP and the black contour lines show positive MEP. The grey cylinders are $(3, -1)$ critical points, the blue rings are $(3, +1)$ critical points and green cubes are $(3, +3)$ critical points. The grey sphere is carbon and the white spheres are hydrogen atoms.

While contour plots are useful for showing the changes of the MEP over the whole molecule, calculating gradient lines show the regions of the molecule that are dominated by individual atoms and the sometimes far reaching influence of the atoms.

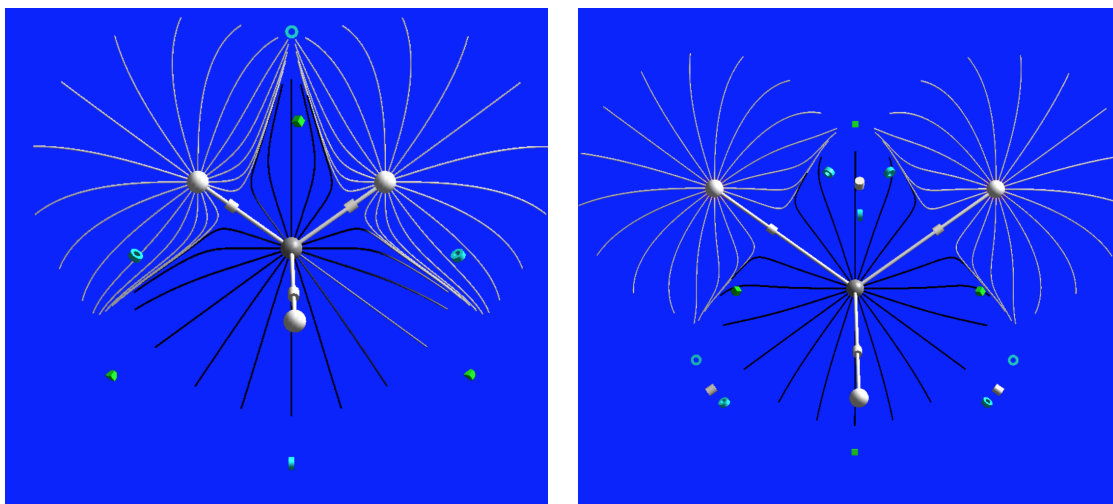


Figure 3.4: Gradient lines of the methane molecule, on the left is the optimised structure and on the right is the methane molecule with bond lengths of 2 Å. The grey cylinders are $(3, -1)$ critical points, the blue rings are $(3, +1)$ critical points and green cubes are $(3, +3)$ critical points. The grey sphere is carbon and the white spheres are hydrogen atoms.

The fully optimised methane molecule shows that the minima (which can be seen in the bottom left and right corners) are mostly as a result of the carbon atom. The hydrogen atoms force the influence of the carbon atom into narrow paths which result in narrow bands of negative MEP in the iso-surface pictures above. These narrow bands are also associated with the $(3, +1)$ saddle points. As the bond length is increased the gradient lines show that the atoms start to isolate from each other, this is represented by a more circular distribution of the gradient lines.

3.2 Using the Topology to Identify Molecular Properties

One of the simplest ways to interpret the $(3, +3)$ minima in the MEP field is when they are linked to double bonds. The minima are calculated above and below the atomic interaction line connecting two NAs and are associated with the location of the π -electrons, this is easily seen with the ethene molecule. Applying Clar's sextet rule using the MEP, if minima existed around a double bond then it should be possible to assign formal double bonds in molecules consisting of multiple aromatic rings [137, 138, 139], such as triphenylene, chrysene, phenanthrene, etcetera. Figure 3.5 shows the MEP topology of naphthalene and naphthacene as well as the proposed location of the double bonds based on the location of the $(3, +3)$ critical points, the pattern is consistent with symmetry.

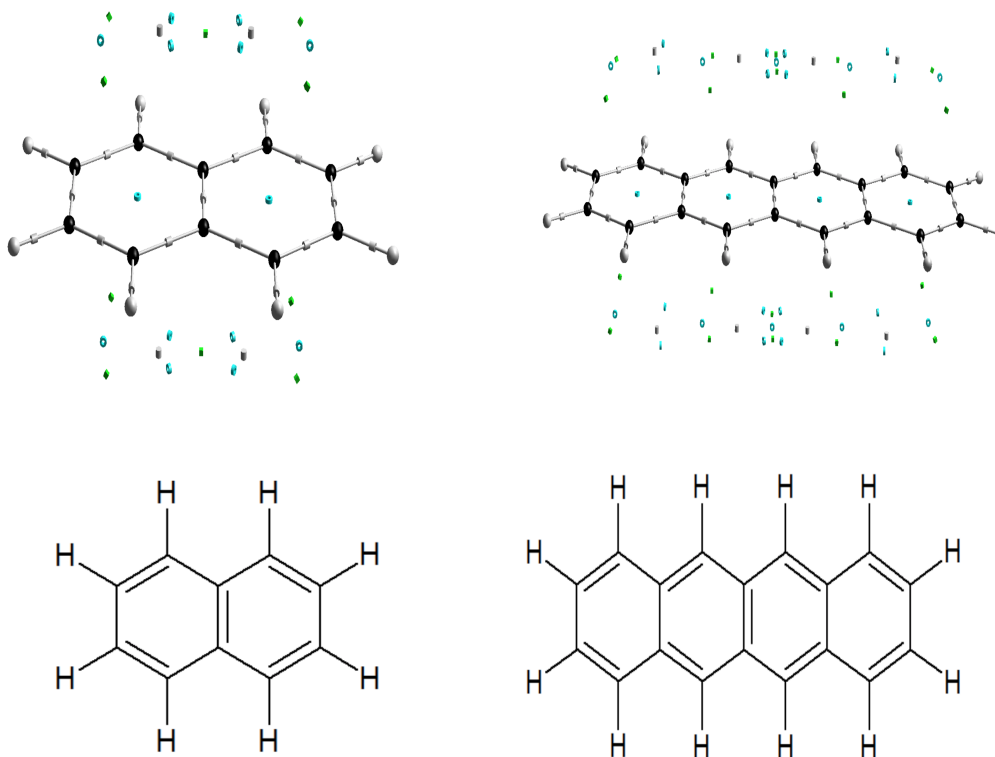


Figure 3.5: Assigned double bonds of naphthalene (left) and naphthacene (right) based on the locations of the minima. The grey cylinders are $(3, -1)$ critical points, the blue rings are $(3, +1)$ critical points and green cubes are $(3, +3)$ critical points. The black spheres are carbon atoms and the white spheres are hydrogen atoms.

When calculating the MEP topology of the benzene molecule, an alternating ring of six $(3, +3)$ and six $(3, +1)$ critical points with a $(3, -1)$ critical point in the middle, which appears above and below the molecule, is associated with an aromatic compound as well as an indication of delocalised electrons. The alternating $(3, +3)$ and $(3, +1)$ critical points are calculated for the majority of molecules consisting of multiple aromatic rings and therefore the pattern is attributed to delocalised electrons, this however allows for the possibility that any molecule with this repeating pattern has delocalised electrons, such as 1,3-butadiene.

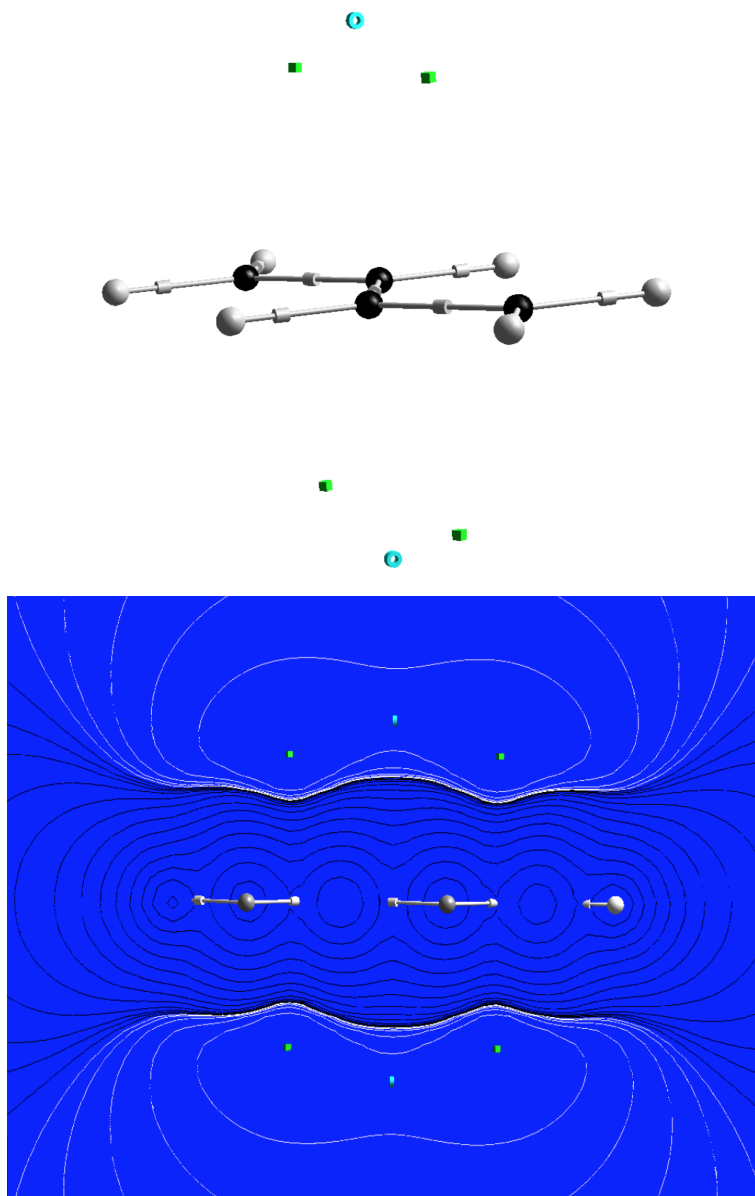


Figure 3.6: *The minima above and below the carbon-carbon bond in 1,3-trans-butadiene are separated by a $(3, +1)$ saddle point. This configuration could be attributed to delocalised electrons. The hydrogens out of the plane have been removed for the contour plot, the black lines correspond to the positive MEP and the white lines the negative MEP. The grey cylinders are $(3, -1)$ critical points, the blue rings are $(3, +1)$ critical points and green cubes are $(3, +3)$ critical points. The black spheres are carbon atoms and the grey spheres are hydrogen atoms.*

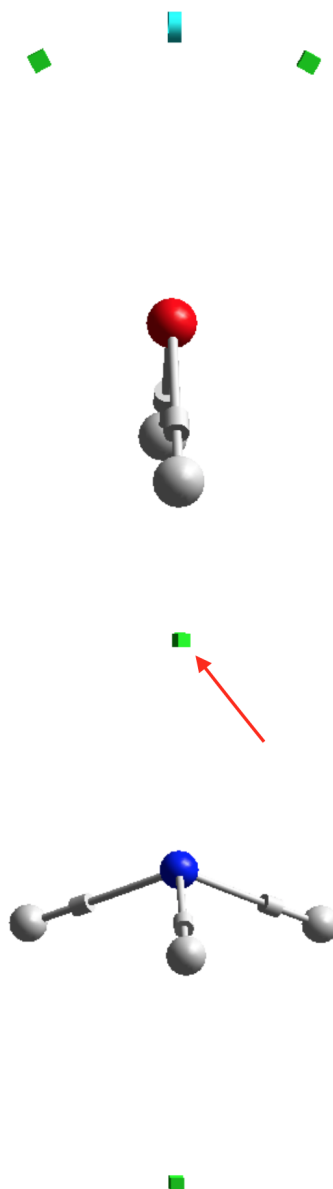


Figure 3.7: *The water and ammonia molecules both showing minima which represent lone pairs, the minima associated with a lone pair in nitrogen is indicated with an arrow. The minima between the hydrogens of the ammonia molecule serves the same function as the minima seen in ethane. The grey cylinders are $(3, -1)$ critical points and the green cubes are $(3, +3)$ critical points. The red sphere is oxygen and the blue sphere is nitrogen, the white spheres are hydrogen atoms.*

Lone pairs are also identified by a minimum, and Kumar *et al.* proposed that these can be identified by the angle at which the minimum is located relative to the atom [93]. One of the examples used was the lone pairs around the oxygen atom in a water molecule. However, a lone pair also exist for the ammonia molecule where the minimum is calculated directly over the nitrogen atom.

The contour plots for water in figure 3.8 show the large region around the oxygen atom as negative and this is associated with the lone pairs. However, the contour lines would suggest that rather than having two isolated regions for the lone pairs (expect to see contour lines circling the minima) there is instead a spread out region of space that the lone pairs exist in (shown by a single contour line around the minima). This could mean very little as the sensitivity of the calculations could mean that there is very little deviation in the MEP around the lone pairs and as such the cut off for calculating a contour line is not met.

The contour plot of the ammonia molecule in figure 3.9 showed that one of the calculated minima, above the nitrogen atom, is located in a negative region which can be associated to the lone pair. However, there is a second minimum calculated which is located below the three hydrogens in a similar position to the minima shown for the ethylene molecule. This minimum is positive and the dark contour lines show that this minimum exists as a minimum in the positive MEP. The electron density at the positive minimum is around 0.003 a.u. which is roughly 7 times lower than at the minimum above the nitrogen which is approximately 0.020 a.u.

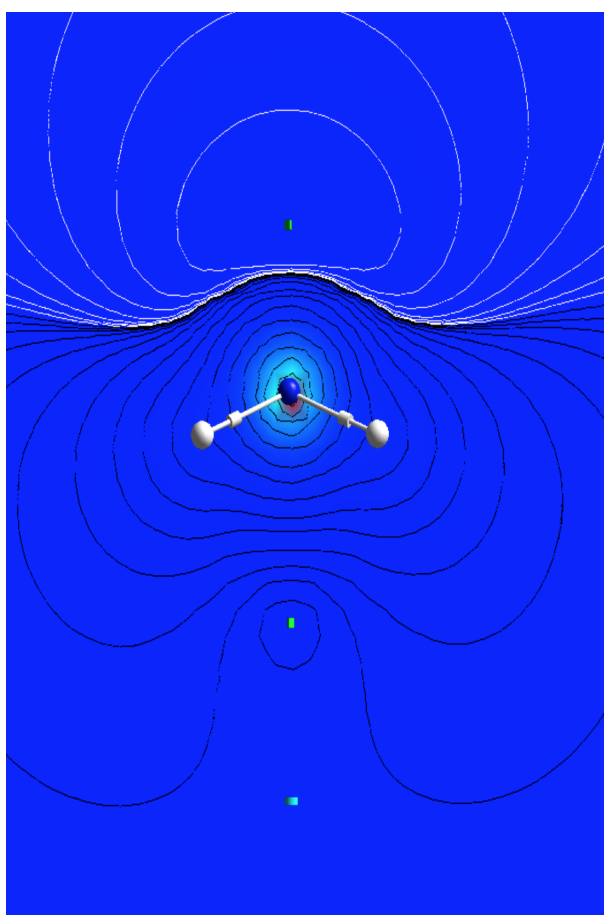


Figure 3.9: *The contour plot of the ammonia molecule with the black line representing positive MEP and the white lines the negative MEP. The minimum below the hydrogens exists in the positive MEP as shown by the black contour lines. The grey cylinders are (3, -1) critical points, the blue rings are (3, +1) critical points and the green cubes are (3, +3) critical points. The blue sphere is a nitrogen atom and the grey spheres are hydrogen atoms.*

The minima that are calculated between hydrogen atoms that form a trigonal pyramidal configuration has been attributed to the sp^3 hybridisation of the central atom that the hydrogens are bonded to, this can be seen for methane, ethane and even ammonia. However, changing the basis set or the theory used to calculate the molecule can have an effect on the location of the minimum or even produce multiple minima with saddle points. The molecular graphs in figure 3.10 show the ethane molecule calculated with the B3LYP theory and Def2TZVPP basis set as well as HF//AUG-cc-pVTZ calculation.

It is not unusual for some methods and basis sets to over calculate or under calculate the energy of a system which would result in the scalar field having different topologies. In the electron density these "extra" critical point are referred to as artefacts. In chapter 2 of this thesis different combinations of theory and basis sets were tested and the results showed that if extra critical points were calculated it was as a result of an over sensitivity to the changes in the MEP but did not add valuable information about the system. This is highlighted in figure 3.10 where instead of extra critical points being calculated the critical point locations are different. At a closer inspection the only critical points that move are the $(3, +1)$ saddle points that bridge the minima. It is difficult to find any reason why this would be significant as the saddle points indicate a change in the gradient of the MEP field but will always be calculated somewhere between the two minima. In terms of the research carried out in this thesis the theory and basis set used (HF//6-311++G(d,p)) sufficiently described the MEP field without creating confusion by over populating the molecule with critical points.

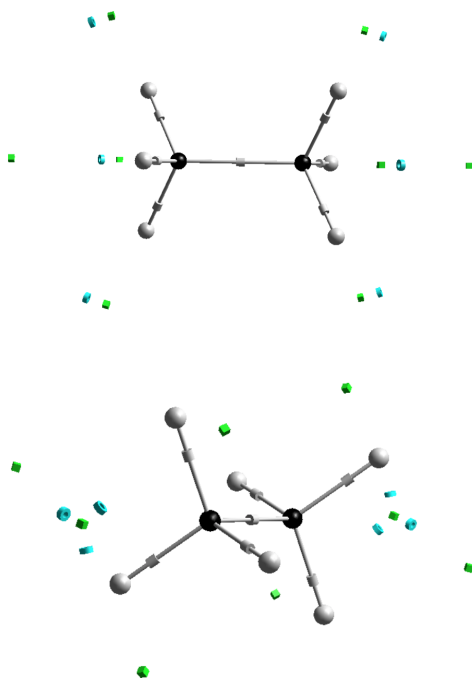
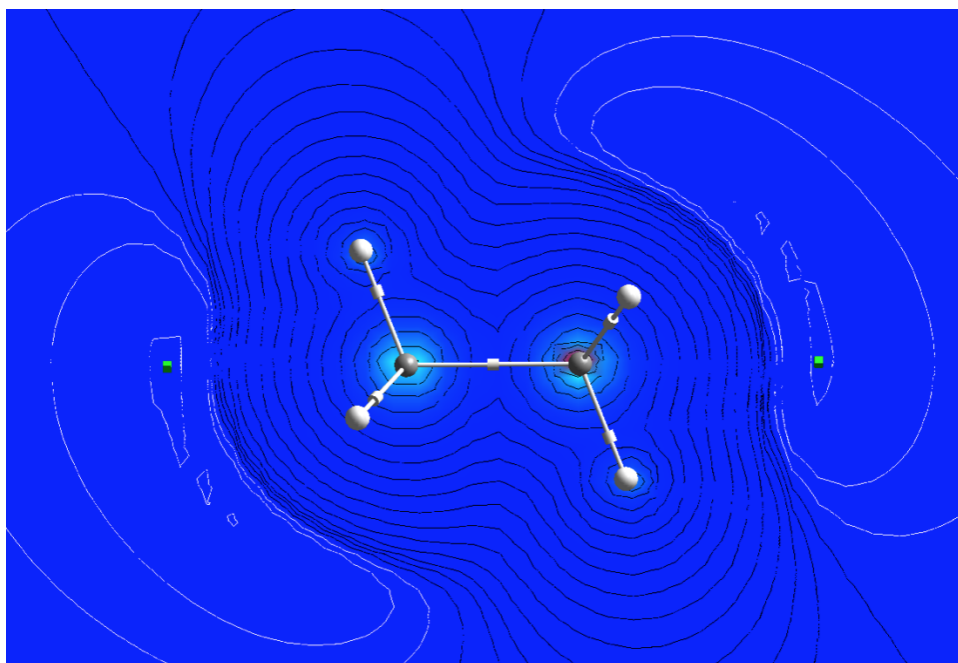


Figure 3.10: *The ethane molecule on the top is calculated with B3LYP//Def2TZVPP and the ethane molecule on the bottom is calculated with HF//AUG-cc-pVTZ. The grey cylinders are $(3, -1)$ critical points and the green cubes are $(3, +3)$ critical points and the blue rings are $(3, +1)$ critical points. The black spheres are carbon the grey spheres are hydrogen atoms.*

Figure 3.10 shows the contour plot for the ethane molecule with an optimised geometry and calculated with the Hartree-Fock method and 6-311++G(d,p) basis set. The minima are in the plane which passes through the carbons and two hydrogen atoms, the other hydrogens are out of the plane. The minima are located in a negative MEP which is indicated by the white contour lines, the black contour lines represent the positive MEP. The gradient lines, which are shown in the plane passing through the carbons and two of the hydrogens, are also shown for the ethane molecule where it can be seen that a combination of the carbon and hydrogen atoms are responsible for the minima.



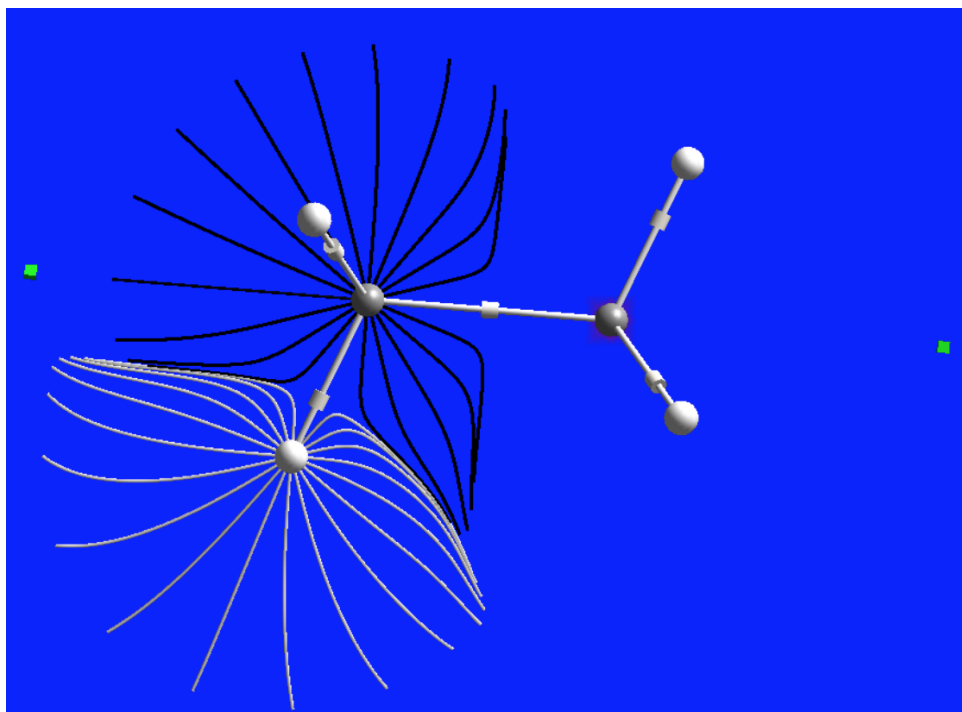


Figure 3.10: *In the first figure the black contour lines around the atoms show the positive MEP while the white contour lines around the minima show the negative MEP. The second image is the gradient lines of carbon and hydrogen and are represented on a plane passing through the carbon and two of the hydrogens. The grey cylinders are $(3, -1)$ critical points and the green cubes are $(3, +3)$ critical points and the. The black spheres are carbon atoms and the white spheres are hydrogen atoms.*

The minimum between the hydrogens of the ethane molecule is directly in line with the carbon atom but form an angle of 80.49 degrees ($\alpha = 80.47$) between the carbon, hydrogen and minimum with the angle measured at the hydrogen atom. The distance between the hydrogen and the minimum is 1.981 Å and the distance between the carbon and hydrogen is 1.086 Å.

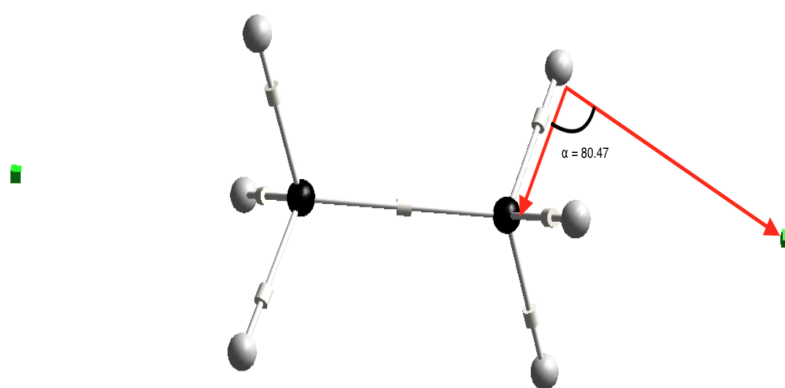


Figure 3.11: The distance between the carbon and hydrogen is 1.086 \AA , hydrogen to minimum is 1.981 \AA , and the angle is $\alpha = 80.47$ degrees. The grey cylinders are $(3, -1)$ critical points and the green cubes are $(3, +3)$ critical points. The black spheres are carbon atoms and the grey spheres are hydrogen atoms.

The angle formed at the hydrogen atom, formed from carbon, hydrogen and the minimum, for methane and cyclohexane are also calculated to see if there is a link between the location of the minimum and the sp^3 hybridisation. Figure 3.12 shows methane and cyclohexane with the calculated angles. The distance between the carbon-hydrogen and hydrogen-minimum for methane is calculated as 1.083 \AA and 1.998 \AA respectively with an angle of 78.73 degrees ($\alpha = 78.73$), for cyclohexane the distances are 1.090 \AA and 1.595 \AA with an angle of 93.60 degrees ($\alpha = 93.60$). The angles formed by the position of the minima show that the minimum between the hydrogens shifts further from the molecule when the number of atoms in the molecule is increased. The minima present in the *cis*-2-butene molecule show that the minimum between the hydrogens shifts away from the centre and is almost positioned between two hydrogens. The atoms in a molecule and the interactions between them naturally affect the MEP and the topology reflects these effects, it is therefore difficult to conclude that the minimum between the hydrogens is simply the hybridisation of the carbon atom. Looking at the contour lines it is more likely that the minima form as a result of the electronic component of the MEP being greater than the nuclear component before approaching zero.

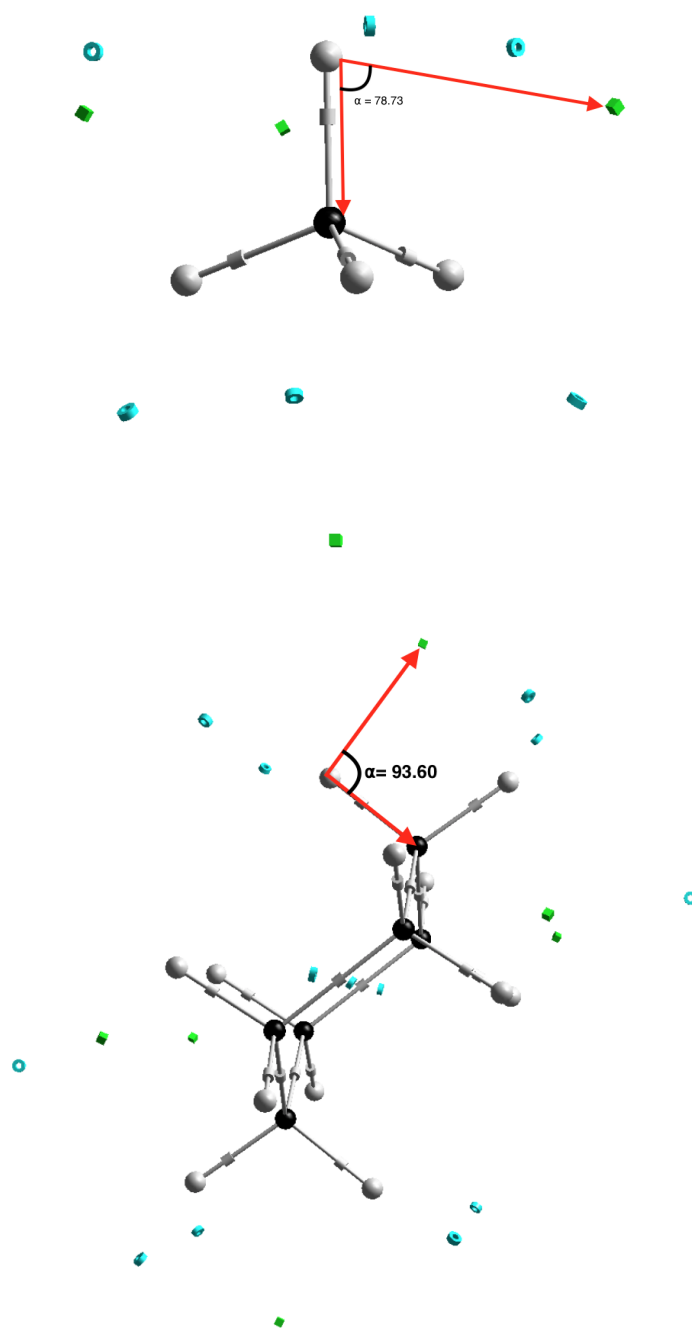
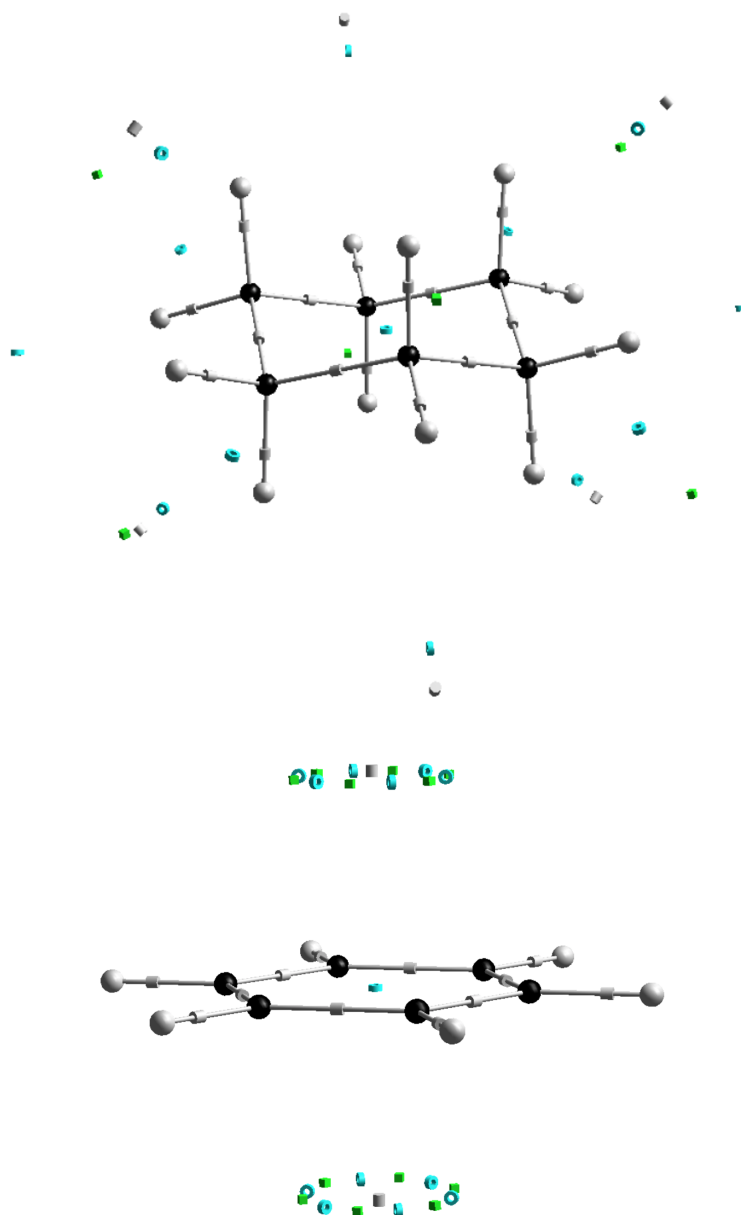


Figure 3.12: Methane has a distance between carbon and hydrogen of 1.083 \AA and the distance between hydrogen and the minimum is 1.998 \AA forming a bond angle of $\alpha = 78.73$. cyclohexane has a distance between the carbon and hydrogen of 1.090 \AA and the distance between hydrogen and the minimum is 1.595 \AA forming a bond angle of $\alpha = 93.60$. The grey cylinders are $(3, -1)$ critical points and the green cubes are $(3, +3)$ critical points and the blue rings are $(3, +1)$ critical points. The black spheres are carbon the grey spheres are hydrogen atoms.

Minima have also been linked to concepts such as bond strain in molecules [116]. The minima for strong stabilising bonds are located inside a cyclic molecule and minima outside the cyclic molecule are seen as showing a destabilising strained bond. Figure 3.12 shows cyclohexane with minima located outside the ring, this is explained by the hybridisation of the carbon atoms. Benzene shows the minima inside the ring indicating a strong stabilising bond while benzyne (a hypothetical molecule with triple bonds and no hydrogens) has minima outside the ring, possibly showing bond strain.



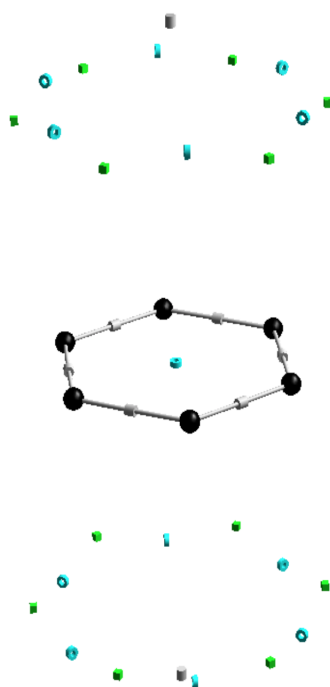


Figure 3.12: *cyclohexane* (top) has minima outside the ring which can be attributed to hybridisation of the carbon atoms. The minima for the benzene molecule (bottom) are located inside the ring stabilising the molecule. The ring created by the minima and $(3, +1)$ saddle points has a radius smaller than the radius of the benzene molecule. Benzotriyne is a hypothetical molecule showing the minima outside the ring which is associated with bond strain. The grey cylinders are $(3, -1)$ critical points and the green cubes are $(3, +3)$ critical points and the blue rings are $(3, +1)$ critical points. The black spheres are carbon atoms and the grey spheres are hydrogen atoms.

The π electrons for the ethylene molecule are represented in the topology of the MEP by two minima as shown in figure 3.13. These minima create a region of negative MEP but these two regions are isolated from one another, this is shown in figure 3.13. The first image shows a contour plot with the plane going through the carbon atoms and the minima. The black contour lines represent a positive MEP while the white lines represent the negative MEP. The second image shows the MEP contour lines in the plane running through the four hydrogens, in this image the minima are out of the plane. It can be seen that the negative region of the MEP extends outwards from the molecule and away from each other.

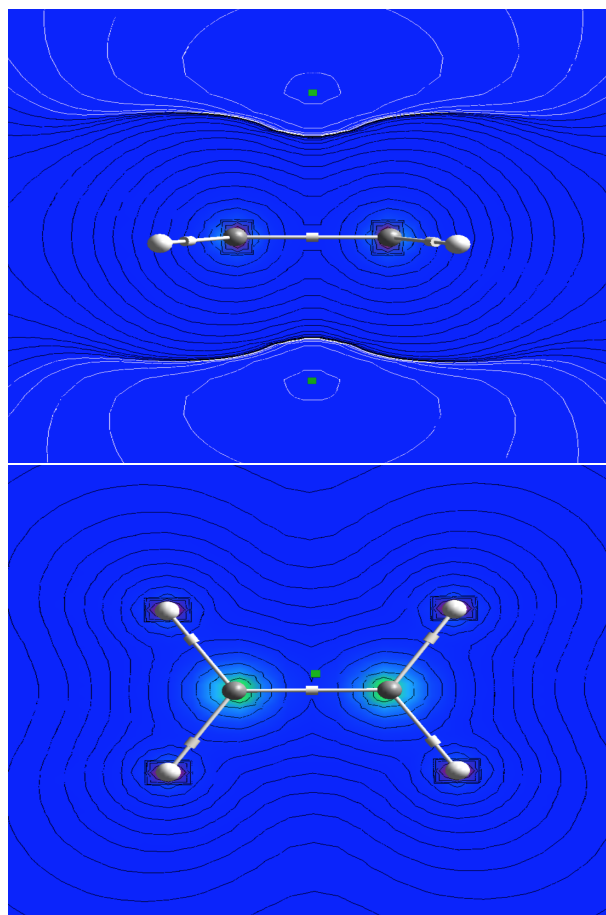


Figure 3.13: *The first image shows the contour lines of the MEP with the plane going through the minima and carbon atoms. The second image is the plane passing through the four hydrogens and shows no negative MEP. The black contour lines are positive MEP and the white lines are negative MEP. The grey cylinders are $(3, -1)$ critical points and the green cubes are $(3, +3)$ critical points. The grey spheres are carbon atoms and the white spheres are hydrogen atoms.*

If the symmetry of the ethylene molecule is altered and one of the CH_2 groups is rotated the π system is changed, the region in which the π electrons occupy is altered and this change is seen in the topology as shown in figure 3.14. While this molecule does not exist it may be useful in understanding the effects on a molecule should the symmetry of the system be changed or broken. The figure below shows this hypothetical molecule which was calculated using HF//6-311++G(d,p) and only the torsion angle between H-C-C-H fixed.

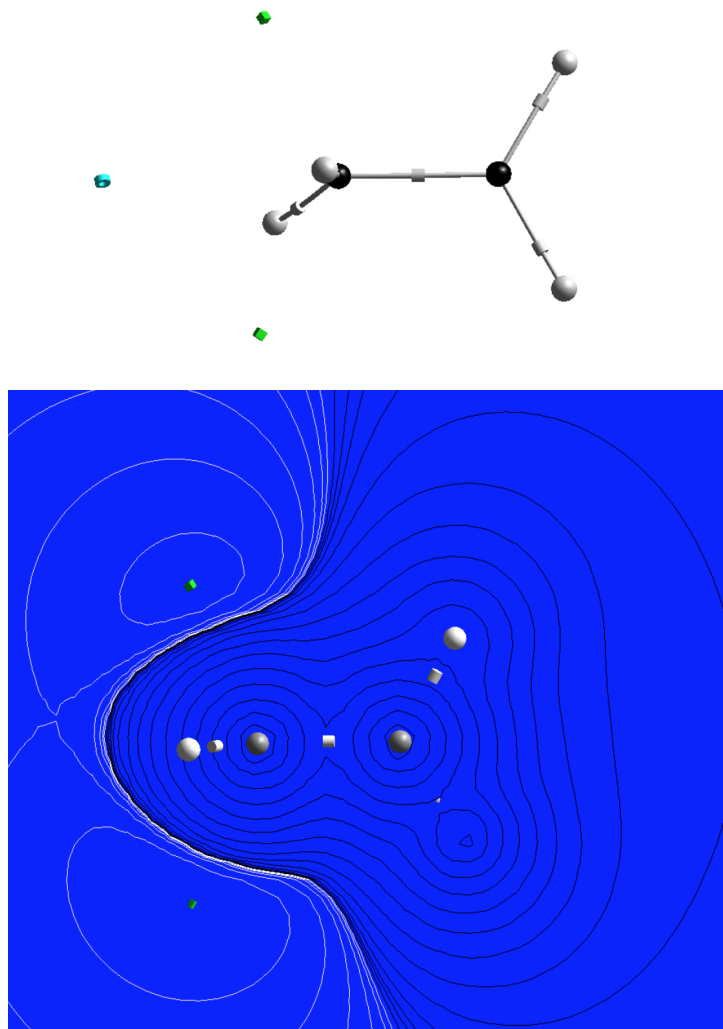


Figure 3.14: *The symmetry of the ethylene molecule was distorted by rotating one of the CH_2 groups. The black contour lines are positive MEP and the white lines are negative MEP. The grey cylinders are $(3, -1)$ critical points, the blue rings are $(3, +1)$ critical points and green cubes are $(3, +3)$ critical points. The black spheres are carbon atoms and the grey spheres are hydrogen atoms.*

The minima in the MEP topology is definitely useful for identifying properties of molecules as has been shown, but generally associating the minima with electrons or high concentrations of electron density can be problematic. The graph in figure 3.15 compares the MEP of the minima with the electron density of the minima, there is no correlation between the MEP of the minima and the electron density. The graph does highlight the problem that is mentioned in this section and that is that the explanation of the minima can not be generalised. While the majority of the graph does show a correlation between electron density and the MEP, this is a result of minima around double bonds and areas containing lone pairs. The values that show no correlation are a result of minima located in areas where the positive potential is dominant as well as minima calculated between three hydrogens as with the ethane molecule. The delocalised electrons for benzene are also represented on the graph differently to the delocalised electrons of *trans*-1,4-butene.

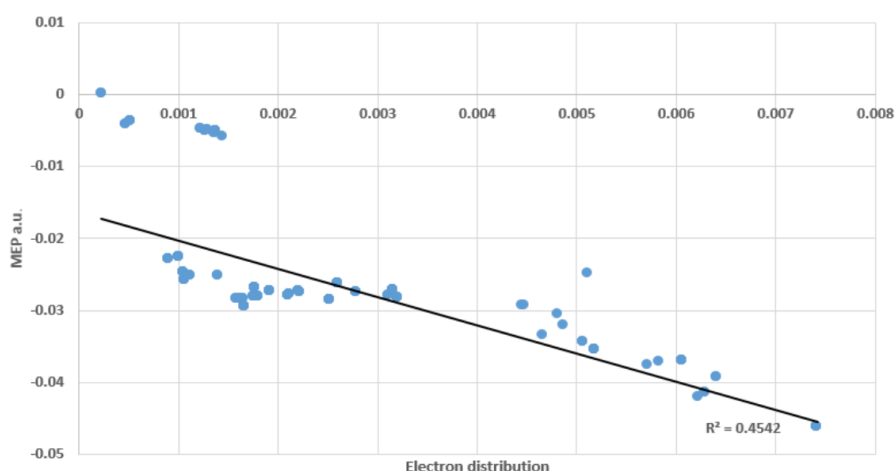


Figure 3.15: A comparison between the electron density and the MEP at the minima located around various molecules.

3.3 Exploring Degenerate Critical Points

Stable degenerate critical points have been reported in the topology of the MEP; this is in contrast to the electron density topology which tend to have degenerate critical points for molecules calculated in transition states. The degenerate critical points in the MEP topology tend to be of rank 2 and are common for linear molecules that have ($C_{\infty v}$ or $D_{\infty h}$) symmetry [116]. The degenerate critical points discussed in this section will be rank 2 critical points, this implies that they have one eigenvalue that is zero. If one eigenvalue is equal to zero then the degenerate critical points form a ring which can have a rank and signature of (2, -2), (2, 0) and (2, +2). The acetylene molecule is a good example of a molecule with a degenerate ring of critical points, the rank and signature is (2, +2). The inter-atomic surface (shown with a blue gradient line in the figure below) between the carbon and hydrogen atom encapsulates the carbon atom as it terminates at the degenerate ring. It can be seen that all the gradient lines calculated eventually terminate at the degenerate ring, the gradient lines of the hydrogen molecule may have far reaching loops but they return to and terminate at the degenerate ring.

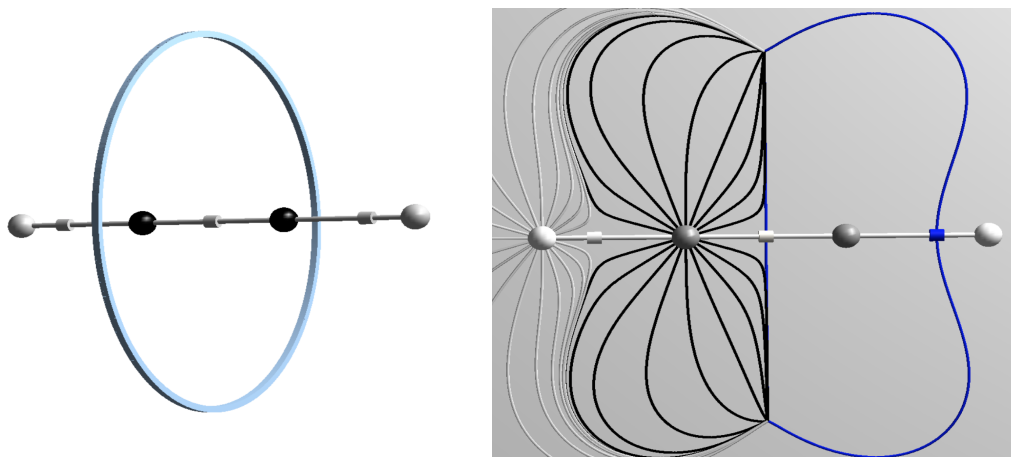


Figure 3.16: *The acetylene molecule on the left is shown with a degenerate ring around the middle of the molecule. The gradient lines shown in the image on the right all terminate at the degenerate ring. The grey cylinders are $(3, -1)$ critical points, the ring around the molecule is made up of connecting $(2, +2)$ critical points. The black spheres are carbon atoms and the grey spheres are hydrogen atoms.*

The contour plot of the acetylene molecule shows a similar pattern to that of the ethylene molecule, namely that a negative region exists around the outer edge of the centre of the molecule. The obvious difference is that due to the symmetry of the acetylene molecule, the negative region will continue uninterrupted around the molecule while the ethylene molecule has two distinct negative regions.

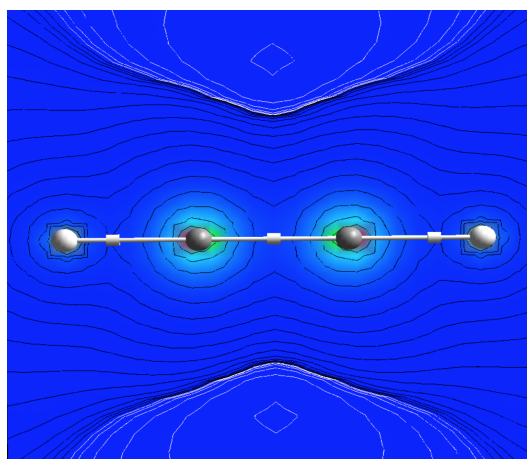


Figure 3.17: *The contour plot of the acetylene molecule is shown with the negative region shown by the white lines. The $D_{\infty h}$ symmetrical nature of the molecule means that the negative region is a continuous band around the centre of the molecule. The black contour lines show the positive region of the molecule. The grey cylinders are $(3, -1)$ critical points, the black spheres are carbon atoms and the grey spheres are hydrogen atoms.*

As pointed out by Leboeuf *et. al.*, once the symmetry is altered the degenerate critical points settle into a series of $(3, +3)$ and $(3, +1)$ critical points and therefore do not affect the Poincaré-Hopf rule [116], figure 3.18 demonstrates that this is true. When an ethyl group is added to one side of the acetylene molecule, the degenerate ring is broken into three $(3, +3)$ critical points which are connected by three $(3, +1)$ critical points. Changing the linearity of the acetylene molecule by adding a methyl group on either end of the molecule will also result in the degenerate ring breaking into a series of three $(3, +3)$ and three $(3, +1)$ critical points.

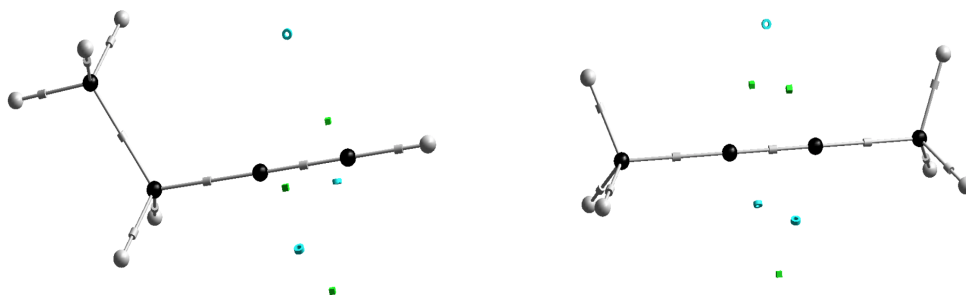


Figure 3.18: *The 1-butyne molecule is shown on the left and the 2-butyne molecule is shown on the right. The grey cylinders are $(3, -1)$ critical points, the blue rings are $(3, +1)$ critical points and green cubes are $(3, +3)$ critical points. The black spheres are carbon atoms and the grey spheres are hydrogen atoms.*

The minima around the ethylene molecule are used to identify the double bond and in much the same way, the degenerate ring that is perpendicular to the plane of the acetylene molecule can be used to identify the triple bond. Degenerate critical points of rank one were also calculated for some of the molecules but as can be seen from figure 3.19, these critical points are located at long distances from the molecule. The rank one critical points identified might be artefacts of the basis set used or they may play a role in molecular orientation during interactions between two molecules, either way the electron density and MEP for the critical points are close to zero.

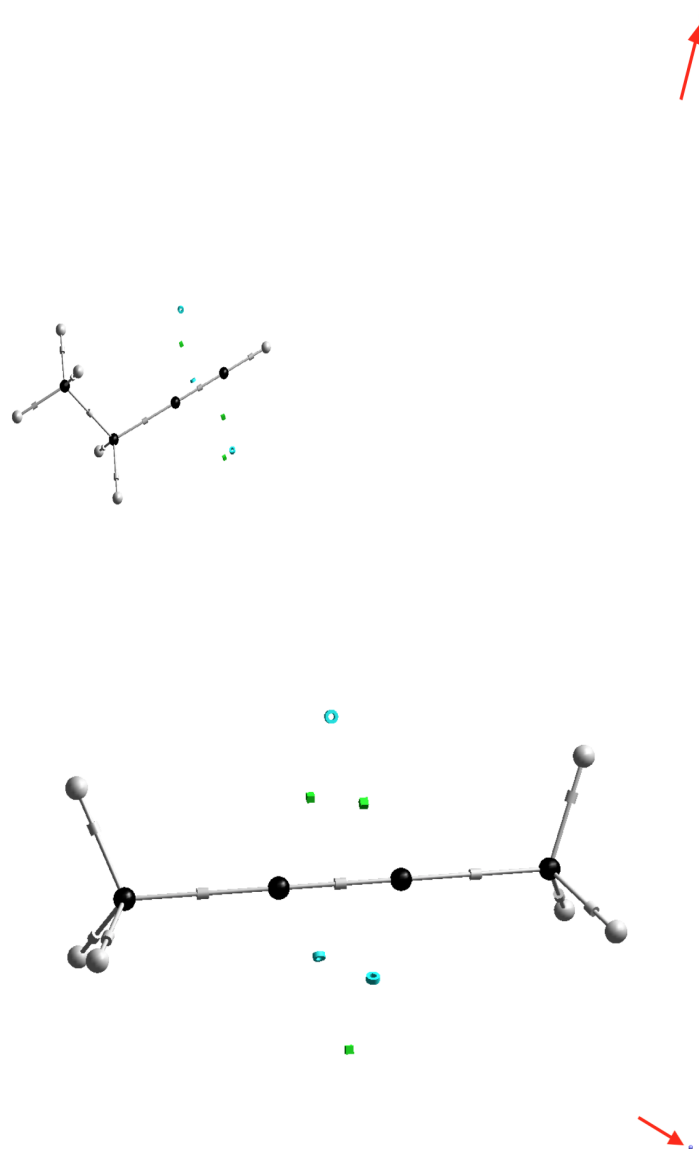


Figure 3.19: The 1-butyne molecule is shown on the top and the 2-butyne molecule is shown on the bottom. The rank one critical point is shown by the arrow. The grey cylinders are $(3, -1)$ critical points, the blue rings are $(3, +1)$ critical points and green cubes are $(3, +3)$ critical points. The purple sphere is a $(1, -1)$ critical point. The black spheres are carbon atoms and the grey spheres are hydrogen atoms.

Degenerate rings are not only linked to triple bonds as is shown in the hydroxy anion, OH^- , in figure 3.20. Instead of two minima as seen for the water molecule, the extra electron and the linear nature of the hydroxyl molecule create the right conditions to form a degenerate ring around the oxygen, this was hinted at in a paper by Kumar and Gadre [131]. The gradient lines formed from the oxygen atom terminate at either the $(3, -1)$ critical points or the degenerate ring. The gradient lines originating at the $(3, -1)$ critical point between the atoms also terminate at the degenerate ring, the gradient lines from the $(3, -1)$ critical points calculated on the outside of the molecule encapsulate the molecule and terminate at the degenerate ring.

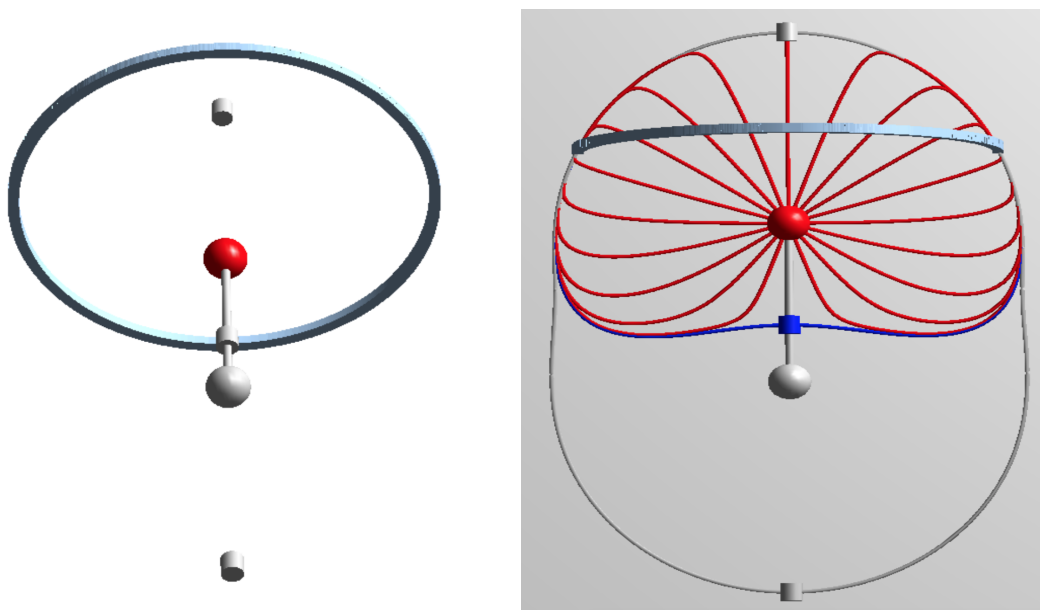


Figure 3.20: *Instead of minima as for the water molecule the hydroxy anion has a ring of degenerate critical points. The gradient lines of the molecule encapsulates the molecule. The grey cylinders are $(3, -1)$ critical points, the ring around the molecule is made up of connecting $(2, +2)$ critical points. The red sphere is an oxygen atom and the grey sphere is a hydrogen atom.*

Molecules containing halogens have two degenerate rings, one that is made up of connecting $(2, +2)$ critical points and one that has $(2, 0)$ critical points. This is shown in figure 3.21 where fluorine and chlorine replace one of the hydrogens in the acetylene molecule. The $(2, 0)$ degenerate ring is shown in green and it is positioned between two $(2, +2)$ degenerate rings. The molecules follow the same trend as the acetylene and hydroxyl anion in that the molecules are encapsulated.

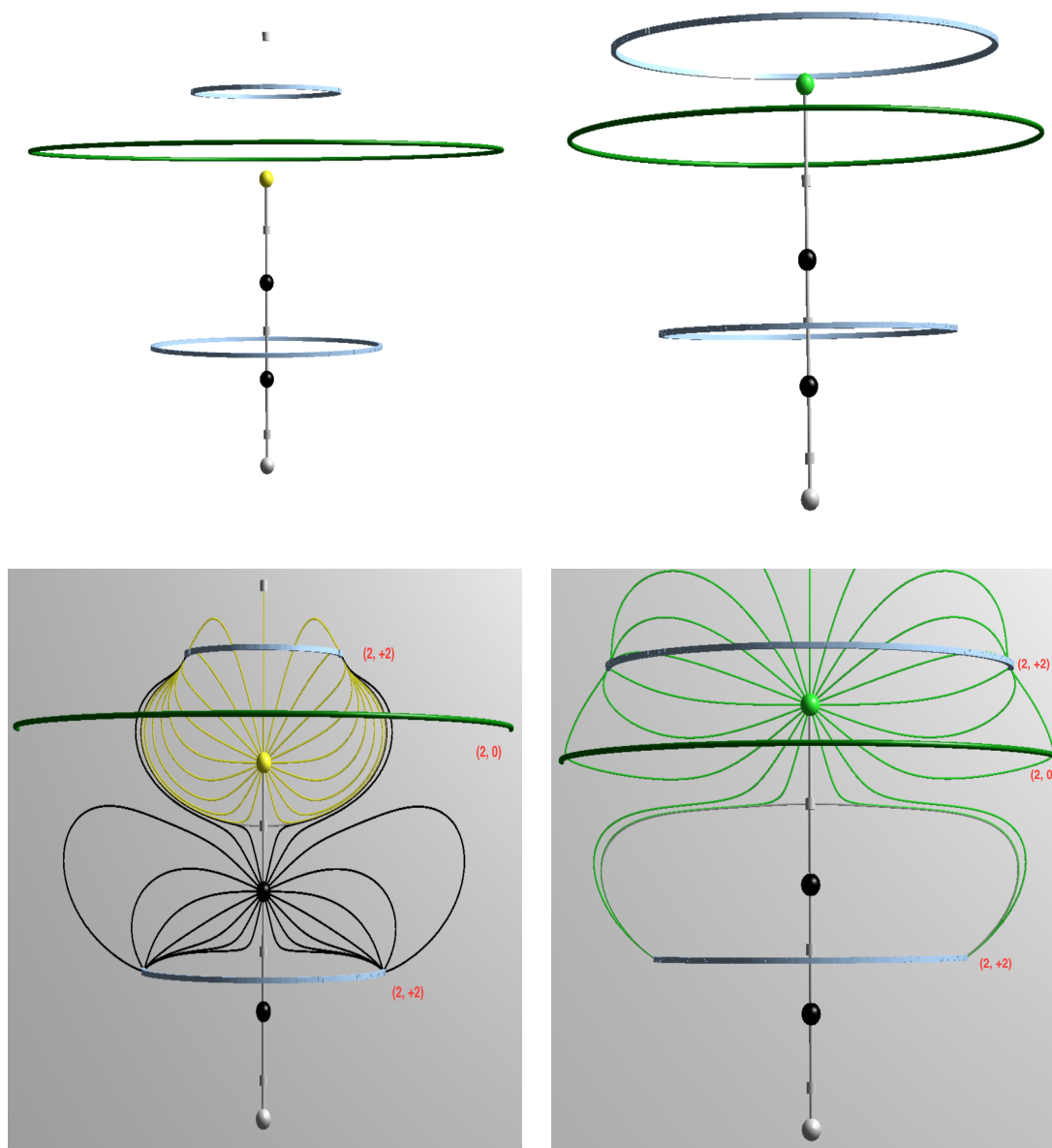


Figure 3.21: *The first molecule on the left is the fluoro-ethyne molecule and the second molecule on the right is the chloro-ethyne molecule. The second set of pictures show the gradient lines for the molecules. The grey cylinders are $(3, -1)$ critical points, the black spheres are carbon atoms and the white spheres are hydrogen atoms, fluorine is shown as a yellow sphere and the chlorine atom is shown in green. The $(2, +2)$ degenerate ring is blue and the $(2, 0)$ degenerate ring is shown in green.*

The $(2, 0)$ degenerate ring follows the same principle as the saddle points of rank three in that it exists to connect the $(2, +2)$ degenerate rings. To show this, a fluorine molecule (F_2) is calculated as well as a hydrogen fluoride molecule (HF), figure 3.22 shows these two molecules. The F_2 has two $(2, +2)$ degenerate rings around the fluorines which are separated by a $(2, 0)$ degenerate ring. When one of the fluorines is replaced with a hydrogen the only degenerate ring is calculated around the fluorine atom.

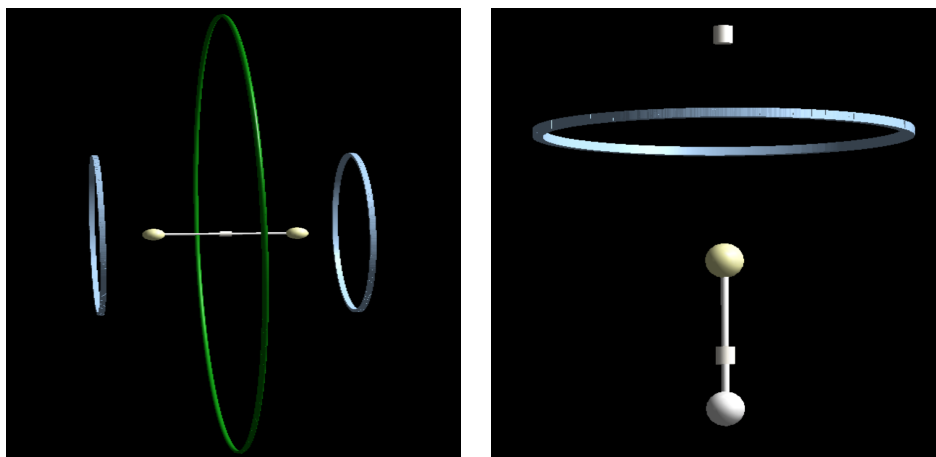


Figure 3.22: *The fluorine molecule highlights that the $(2, 0)$ degenerate ring is a consequence of the two $(2, +2)$ degenerate ring. The $(2, 0)$ degenerate ring is missing from the hydrogen fluoride molecule. The grey cylinders are $(3, -1)$ critical points, the blue ring is made up of connecting $(2, +2)$ critical points and the green ring is made up of connecting $(2, 0)$ critical points. The yellow sphere is fluorine and the grey sphere is a hydrogen atom.*

As mentioned before, the degenerate rings are common for linear molecules and this remains true for the fluorine atoms. When one hydrogen of ethane and ethylene are replaced with a fluorine atom, the topology around the fluorine atom changes. A noticeable difference between the fluoro-ethane and fluoro-ethene is that the π electrons influence the topology of the fluorine molecule, this is seen in figure 3.23.

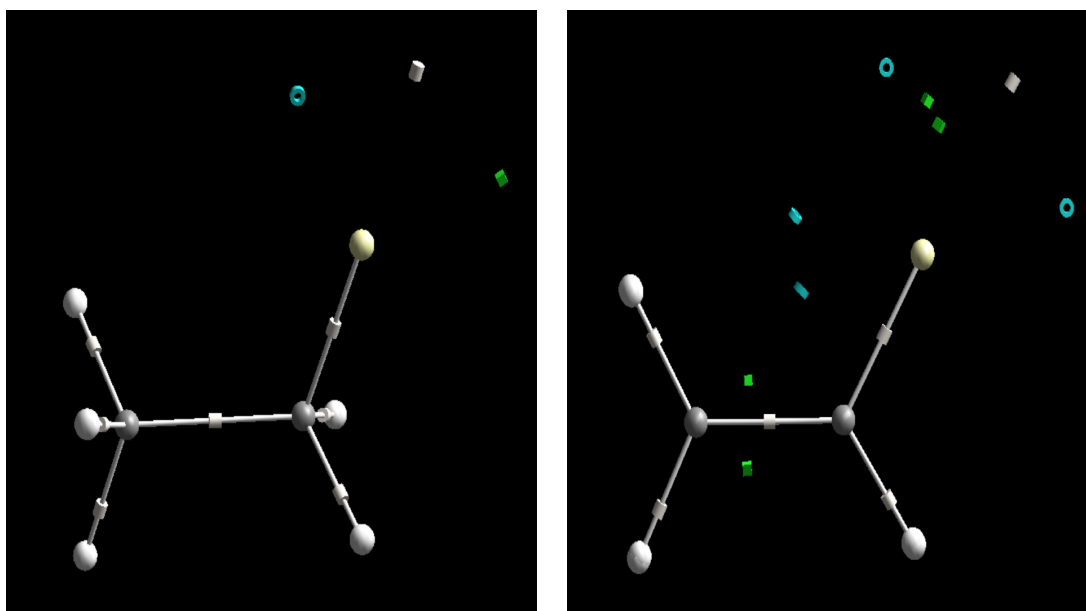


Figure 3.23: The fluorine atom is added to ethane and ethylene, the interaction with the π electrons influences the topology of the fluorine molecule. The grey cylinders are $(3, -1)$ critical points, the blue rings are $(3, +1)$ critical points and the green cubes are $(3, +3)$. The yellow sphere is fluorine, black spheres are carbon and the grey spheres are hydrogen atoms.

It may seem that degenerate rings and linear molecules go together but this is not always the case, nor is a degenerate ring always associated with triple bonds. Figure 3.24 highlights this by showing a nitrogen molecule (N_2) and a cyanogen molecule (C_2N_2), in both cases there is a linear molecule and a triple bond yet there are no degenerate rings. The contour plots show that while there are minima which are likely the result of the lone pairs on the nitrogen, there are no negative regions around the molecule that can be associated with a degenerate ring.

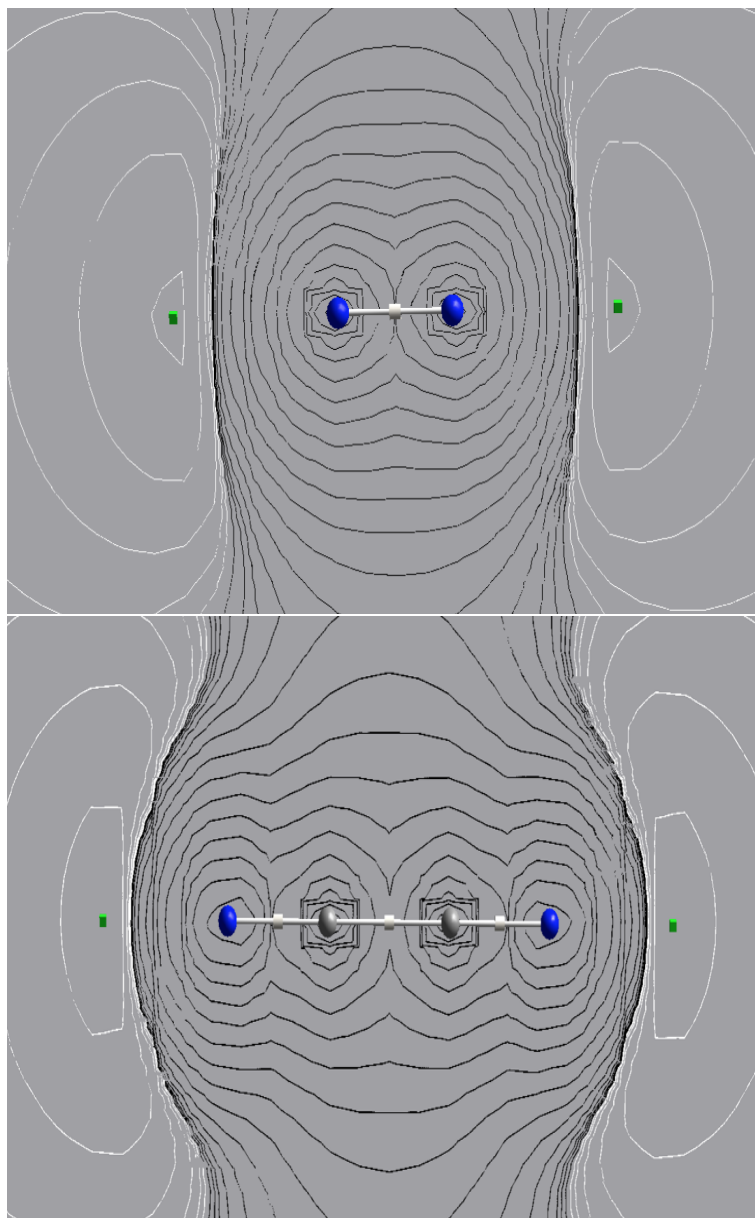


Figure 3.24: An example of linear molecules with triple bonds (which are both linked to degenerate rings) where no degenerate ring is calculated.. The grey cylinders are $(3, -1)$ critical points, the green cubes are $(3, +3)$. The blue spheres are nitrogen and the black spheres are carbon atoms.

3.4 Conclusions

This chapter makes it clear that compared to the electron density the topology of the molecular electrostatic potential (MEP) has a lot more information to offer. The methane molecule was a good example of how populated and confusing a simple molecule can become when the topology is analysed in the MEP. However, it also highlighted the need to have a simple understanding of the molecule being studied. In this example, knowing the symmetry of the molecule simplified the topology as the minima and saddle points were a result of a repeating pattern (symmetry). Calculating the hypothetical methane molecules (methane molecules with the bond length increased) also showed that the topology is reactive to the conditions of each calculation and something as simple as stretching the bond lengths of the hydrogens can have a varying effect on the MEP topology.

In the chapter the idea of associating minima to regions of electron density or even electrons is explored. It was shown that it is possible to use the minima to identify molecular properties such as double bonds and lone pairs, but an argument can be made that this is done with a basic understanding of the molecule that is calculated. Examples were given where associating a minimum with high electron density was false, the minimum between the hydrogens of ammonia, and no correlation was found between the MEP of the minima and electron density.

The degenerate critical points in the MEP topology were shown to fulfil a similar function to the minima in that it could also be used to identify molecular properties, namely triple bonds. However, the degenerate rings are not exclusively found around triple bonds as was shown with linear molecules containing halides. The two kinds of degenerate rings calculated in this chapter, namely $(2, +2)$ and $(2, 0)$, unsurprisingly operated the same way that the maxima/minima and saddle points operated. It was also shown that degenerate rings are not always calculated for linear molecules or even triple bonds. Degenerate critical points of rank one were calculated for very few of the molecules and given the nature of a rank one critical point, it has two zero eigenvalues, it is unlikely to ever feature in a molecule. In a scalar field such as the MEP a zero eigenvalue would indicate an equal distribution of the MEP in the plane of the eigenfunction (there is no increasing or decreasing gradient). It is for this reason that critical points of rank one were not investigated further in this research. However, it cannot be ruled out that it may play a role in long range interactions but it does not offer information on how atoms behave in a molecule.

Finally, this chapter highlighted that the MEP topology is rich in information and that the topology changes with the conditions of the molecules and the atoms present. It was also shown that making general assumptions about the topology can lead to false conclusions. Each molecule has unique conditions and this should be taken into consideration when analysing the topology.

Chapter 4

Defining Atom Interactions in the Molecular Electrostatic Potential

The aim of this chapter is to explore the concept of a bond using the topology of the molecular electrostatic potential (MEP). This chapter will focus on simple molecules and different types of bonds ranging from strong covalent bonds to weak hydrogen bonds. The topology of other scalar fields will be used to assess the results of the MEP in an attempt to improve the understanding of interactions between atoms. This chapter will lay the ground work for key concepts that are applied to all other molecules studied in this thesis.

The figures and tables in this chapter are calculated using Hartree-Fock level of theory with the 6-311++G(d,p) basis set unless otherwise stated. The values are reported in atomic units with the exception of the distance between atoms which is given in Angstroms.

4.1 Interactions in the Hydrogen Molecule

4.1.1 Interactions in the Singlet and Triplet State for a Hydrogen Molecule

The hydrogen molecule in the singlet state (H_2) and in the triplet state (tH_2) was chosen as a starting point as these two states represent a simple bonding interaction, H_2 , and a simple non-bonding interaction, tH_2 . In order to establish that the two systems demonstrate a typical bonding and non-bonding interaction, the energy of the two systems were calculated. The energies are calculated in intervals of 0.5 Å starting at 0.5 Å and ending at 3.0 Å. Included in the calculations were the fully optimised systems which resulted in a bond length of 0.735 Å for H_2 and 5.044 Å for tH_2 . The figure below shows the energies of the two systems.

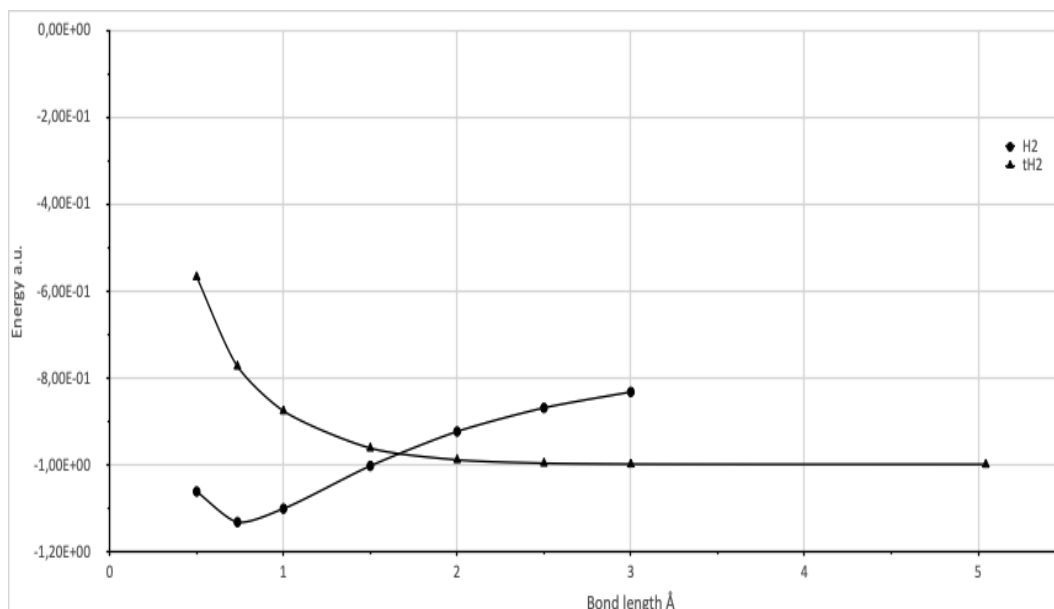


Figure 4.1: *Energies of the hydrogen molecule in the singlet state (H_2) and in the triplet state (tH_2). Energies are taken at intervals of 0.5 \AA , included in the graph are the optimised bond lengths of 0.735 \AA (H_2) and 5.044 \AA (tH_2).*

It can be seen in figure 4.1 that H_2 passes through a minimum energy which corresponds to the bonding of the two hydrogen atoms. The tH_2 does not pass through a minimum energy but rather the two atoms separate until both atoms have the characteristics of an isolated hydrogen atom. This energy graph gives a clear outline of repulsion ($l < 0.735 \text{ \AA}$), attraction ($l > 0.735 \text{ \AA}$) and bonding ($l = 0.735 \text{ \AA}$) energies for the hydrogen molecule in the singlet state. The topology of the MEP was calculated for the two hydrogen systems and as expected, at each distance a (3, -1) saddle point and atomic interaction lines were calculated. The two graphs below in Figure 4.2 show the MEP for the hydrogens in the singlet (top) and triplet (bottom) state, values for the nuclei as well as the saddle point are plotted.

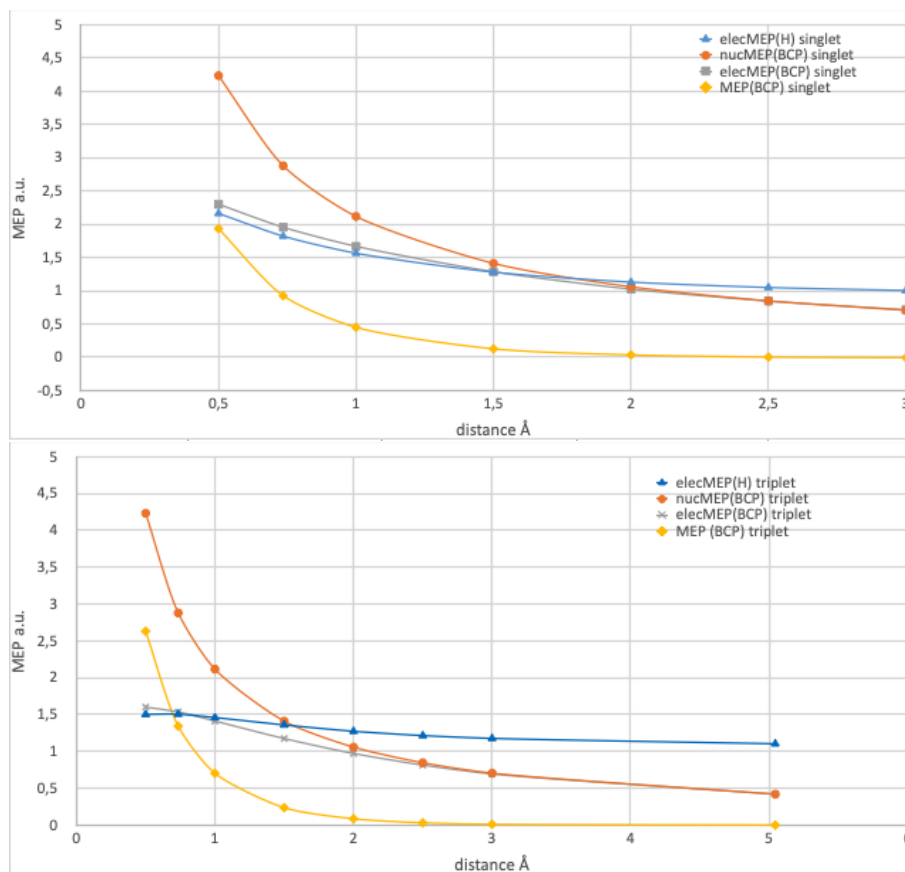


Figure 4.2: The two graphs show the MEP at the nucleus as well as the (3, -1) saddle point for the hydrogen molecule in the singlet and the triplet states, shown on the top and bottom respectively. The nucMEP refers to the nuclear component of the MEP and the elecMEP refers to the electronic component. Also shown on the graph is the elecMEP of the hydrogen NA , the values for the critical points were calculated in the MEP field.

The nucMEP refers to the nuclear component ($\sum_{A=1}^N \frac{Z_A}{|r-R_A|}$) of the MEP and the elecMEP refers to the electronic component ($\int \frac{\rho(r')}{|r-r'|} d^3r'$) of the MEP. The influence of separating the nuclear and electron component in the MEP equation can be seen in the graph in figure 4.2. As expected, the contribution of the nuclei are dominant and comparing the two graphs show that whether in the singlet or triplet state, the values at the (3, -1) critical point do not change. However, the same can not be said for the electronic values, the elecMEP for the H_2 ranges between 0.7 - 2.3 a.u. while the elecMEP for the tH_2 ranges from 0.4 - 1.6 a.u. at the (3, -1) critical point. Although it is obvious, given the equation of the MEP ($\sum_{A=1}^N \frac{Z_A}{|r-R_A|} - \int \frac{\rho(r')}{|r-r'|} d^3r'$), these differences in the elecMEP will result in different values for the total MEP at the (3, -1) saddle point, at least until the nucMEP and elecMEP values converge resulting in a zero MEP value. The rate of decline for the elecMEP at the (3, -1) critical should be noted because the rate of decrease for the H_2 is faster than the rate for the tH_2 . The differences in the rate of change, as well as the elecMEP at the (3, -1) critical point, can be associated with the high probability of locating an electron between the two hydrogens for the H_2 molecule as opposed to the low probability between the hydrogens in the tH_2 molecule.

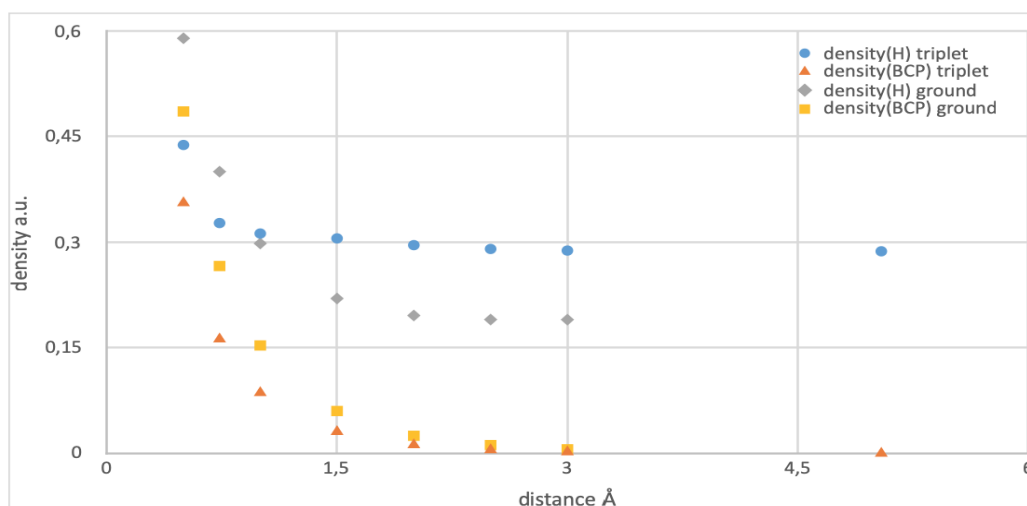


Figure 4.3: The electron density calculated for a single hydrogen NA and the (3, -1) critical point (BCP) are compared for the hydrogen molecule in the singlet and triplet states.

The electron density at the nuclei for the H_2 and tH_2 and the electron density at the (3, -1) critical point follow the same trend as is seen in the MEP, namely the values for H_2 are higher than tH_2 . When comparing the electron density at the (3, -1) critical point at a distance of 0.735 Å (the bonding length of H_2) the difference is 0.2661 a.u. for H_2 compared to 0.1624 a.u. for tH_2 . The lower electron density for tH_2 is another indication that the interaction between the hydrogens is weaker and that the electrons are distributed over a wider area. The ellipticity for the H_2 and tH_2 are both zero, indicating an equal distribution of the electron density in the two planes perpendicular to the plane of the interacting atoms.

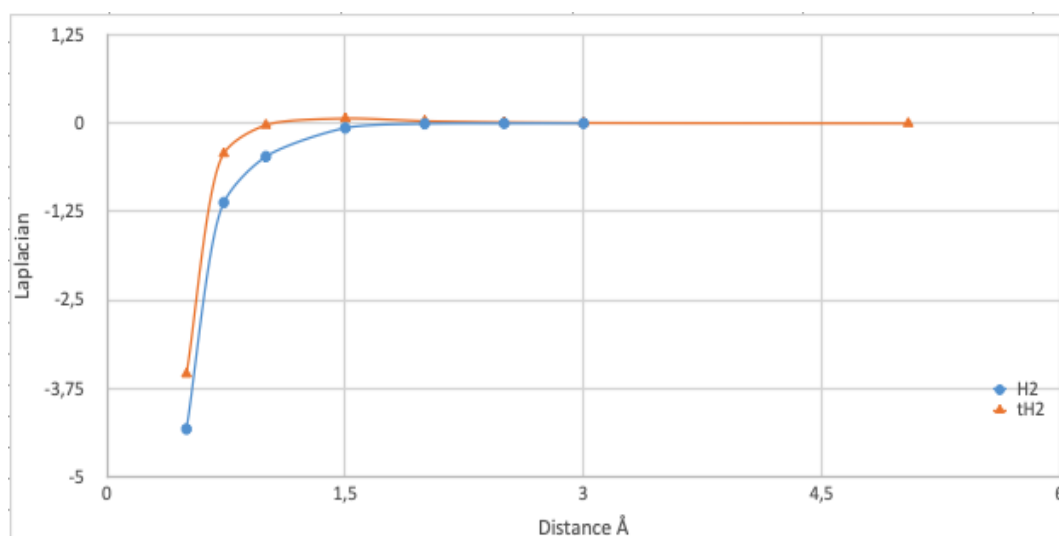
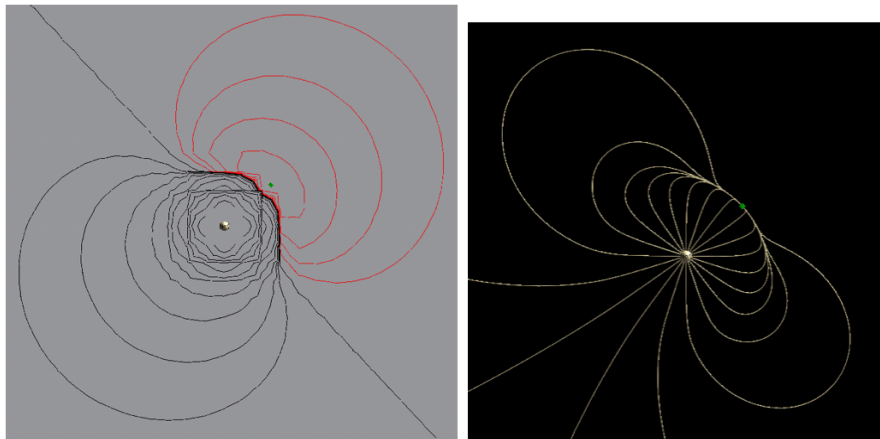
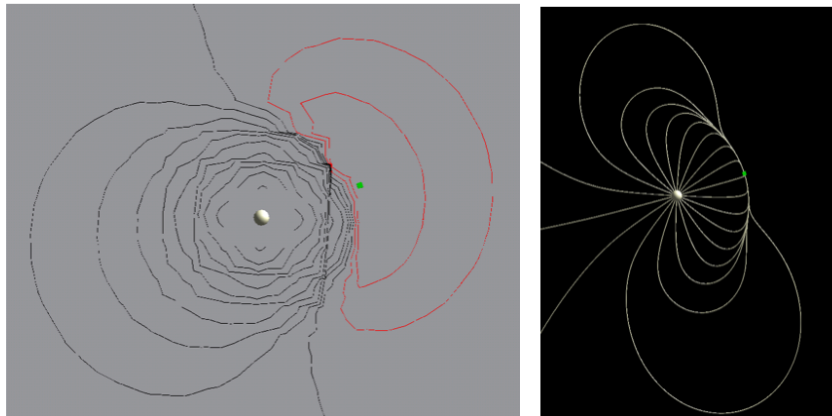
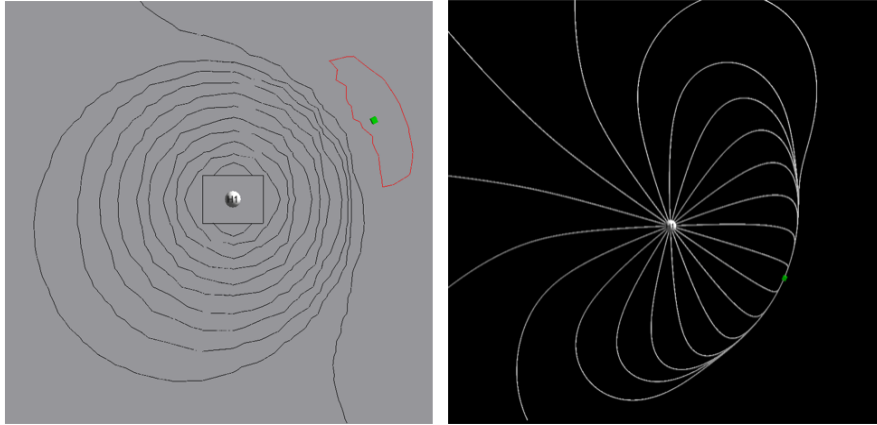


Figure 4.4: The changing of the Laplacian ($\nabla^2\rho(r)$) with regards to the distance between the hydrogen atoms is shown for the hydrogen molecule in the singlet (H_2) and triplet (tH_2) states, values are taken from the (3, -1) critical point.

The increasing value of the laplacian ($\nabla^2\rho(r)$) indicates a move to a more closed shell interaction, an interaction that is defined by a non-sharing of the electrons of each atom. At a distance of 0.735 Å it can be seen that the $\nabla^2\rho(r)$ is negative and thus indicates an open shell (sharing) system. As expected, the values for the $\nabla^2\rho(r)$ differ between the two hydrogen states with H₂ having a lower $\nabla^2\rho(r)$ value than ^tH₂. The "bonding" distance for H₂ is 0.735 Å and has a $\nabla^2\rho(r)$ of -1.1206 a.u. while the optimised geometry for ^tH₂ is 5.044 Å with a $\nabla^2\rho(r)$ of 0.0001a.u..

4.1.2 Interactions with a Background Charge

The previous chapters have shown that the topology of the MEP is diverse and can be misleading at times. Assigning chemical meaning to mathematical models can sometimes be problematic, especially when the model is unpredictable. The MEP equation separates the nuclear and electronic contributions, this is important to remember as it allows for the calculation of maxima and minima, even if the electronic part of the equation is removed. It is therefore worthwhile to investigate what would happen in the topology of the MEP if a positive background charge and an atom were calculated together. These interactions are shown in figure 4.4.



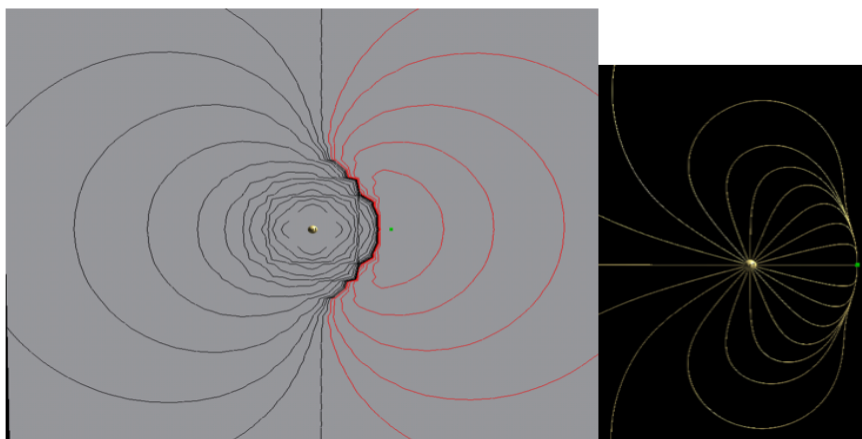


Figure 4.4: *The atoms hydrogen, helium, neon and argon are shown interacting with a positive background charge in the MEP field, both the contour plot and gradient lines are shown. The calculations shown are at 1 Å, the red contour lines represent a negative value.*

The positive background charge does not reflect in the electron density as it has no basis sets, but for reasons explained above, it does show in the MEP. The positive charge is calculated as a minimum and not a nucleus, this is most likely due to the fact that the background charge has no basis sets assigned to it and therefore, when calculating the wavefunction, it is not calculated as an atom. The contour plot shows the impact that the charge has on the MEP topology as there is a negative region calculated around the point charge. Interestingly the gradient lines for the atom terminate at the background charge, which is calculated as a minimum, which would suggest that the minima calculated in the MEP are not always associated with a negative charge (electron density). A paper by Wick and Clark further explored the effect that a proton would have on a hydrogen anion as well as how the topology would change if an atom was inside a strong electric field [144]. While the paper by Wick and Clark only focused on the electron density its aim was to show that QTAIM could not be used to reliably identify bonding interactions or at the very least caution should be used when applying the QTAIM method. This section focused on the effect that a positive background charge has on an atom in the MEP and because anions were not included in the calculations a direct comparison can not be made with the results of Wick and Clark. Even though a direct comparison can not be made the results point to a similar conclusion, care should be taken when assigning chemical significance to the results of the QTAIM method.

4.2 Interactions Between Noble Gases

The hydrogen molecule presented a simple system that could be easily analysed and therefore a basic interpretation of a "bond" and "non-bond" could be established for the MEP. In an attempt to build upon this foundation, three noble gases, helium, neon and argon, were studied. These gases provided systems of increasing size and complexity and have the added benefit of introducing a static interaction (London dispersion interaction), while not considered a "bond", it does account for a bond-like interaction between the noble gases. The figure below shows the MEP of the (3, -1) critical point located between the noble gases at various distances.

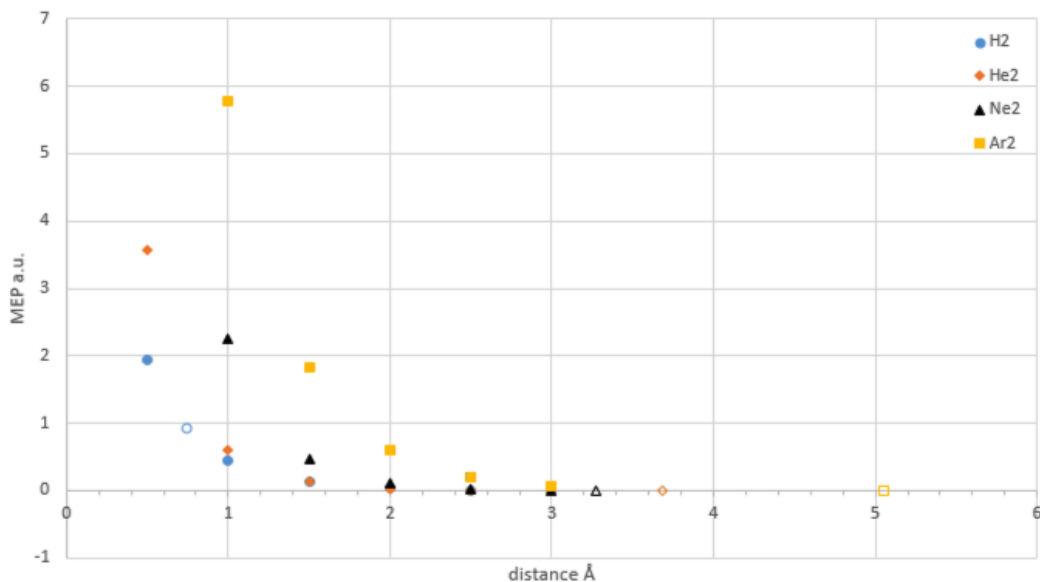


Figure 4.5: The MEP at the $(3, -1)$ saddle point is shown for the hydrogen molecule in the ground state as well as for the three noble gases; He_2 , Ne_2 and Ar_2 . The symbols that do not have a colour fill indicate the distance between the atoms when fully optimised.

The distance between the atoms are calculated in increments of 0.5 \AA up to a distance of 3.0 \AA , the systems were then optimised so that the distance between the atoms was at the lowest stable energy, these values can be seen on the graph as a non-filled marker. Comparing the energies of the various distances for each of the noble gases showed no discernible drop in energy that could be linked to a "bond". This is not surprising as the interaction between the atoms are long range interactions linked to dispersion forces. This does create an opportunity to understand the repulsive systems as well as dispersion forces. A break down of the values at the optimised geometries are represented in table 4.1.

Table 4.1: The bond length, electronic MEP (*elecMEP*), MEP, ρ , $\nabla^2\rho(r)$ and Lagrangian kinetic energy (*G*) are reported for the optimised geometries of the three noble gases, He_2 , Ne_2 and Ar_2 as well as H_2 and ${}^t\text{H}_2$. All values are calculated from the $(3, -1)$ critical point and reported in atomic units with the exception of the bond length which is shown in \AA .

Molecule	Bond Length	elecMEP	MEP	ρ	$\nabla^2\rho(r)$	<i>G</i>
H_2	0.735	-1.9542	0.9244	0.2661	-1.1206	$1.25\text{e}-34$
${}^t\text{H}_2$	5.044	-0.4195	0.0001	$5.04\text{e}-5$	0.0001	$2.48\text{e}-5$
He_2	3.682	-1.1496	0.0001	0.0001	0.0009	0.0001
Ne_2	3.274	-6.4647	0.0008	0.0010	0.0103	0.0017
Ar_2	5.050	-7.5444	0.0003	0.0002	0.0008	0.0001

Even though it is possible to form the molecules presented in table 4.1, this is normally under extreme conditions. The hydrogen molecule in the triplet state has a bond length of 5.044 \AA this is not a true value but rather a cut-off value. The true value would be infinity as the

two atoms repel each other, at this distance the value of the electron density and elecMEP on each atom are similar to that of an isolated hydrogen atom. The triplet hydrogen molecule is therefore a good example on a non-bonded molecule which has an AIL calculated using the QTAIM method.

The values for the MEP are close to zero which occurs when the MEP components have similar values which would indicate very weak interactions between the atoms. The $\nabla^2\rho(r)$ is positive which is an indication that any interaction would be a closed shell interaction and no sharing of electrons would take place. The low value of ρ and $\nabla^2\rho(r)$ is further evidence that it is unlikely to find electrons between the two atoms that can be attributed to a bonding interaction. The molecules presented here are optimised in the gas phase and the values at the (3, -1) critical point suggest that there is no clear bonding interaction between the noble gases.

If the hydrogen molecule is considered as the standard for a bonding interaction then it would be easy to adjust the distance between the atoms to increase the elecMEP, ρ to the point where the values mimic a bonding interaction. Yet, the optimised geometries and therefore lowest energy of the molecules represents a non-bonding interaction. However, the $\nabla^2\rho(r)$ for the noble gases becomes more positive as the atoms move closer together. This would suggest that the electrons of a closed shell system are not participating in a bonding interaction and are being forced together in a smaller volume of space resulting in a higher molecular energy.

4.3 Using the Ratio of nucMEP : elecMEP in Order to Define an Interaction

A predictable problem that can be noticed from the early calculations of the hydrogen and noble gas molecules is that the MEP at the (3, -1) critical point can not be used as a reliable measure to compare interactions between atoms. This is due to the fact that as systems become larger or more complex by adding in hetero-atoms, comparing the interactions becomes increasingly more difficult. A simple example of this is shown in figure 4.6 where multiple hydrocarbons were calculated and the MEP at the (3, -1) critical point between the carbon and hydrogen were plotted against the distance between the two atoms.

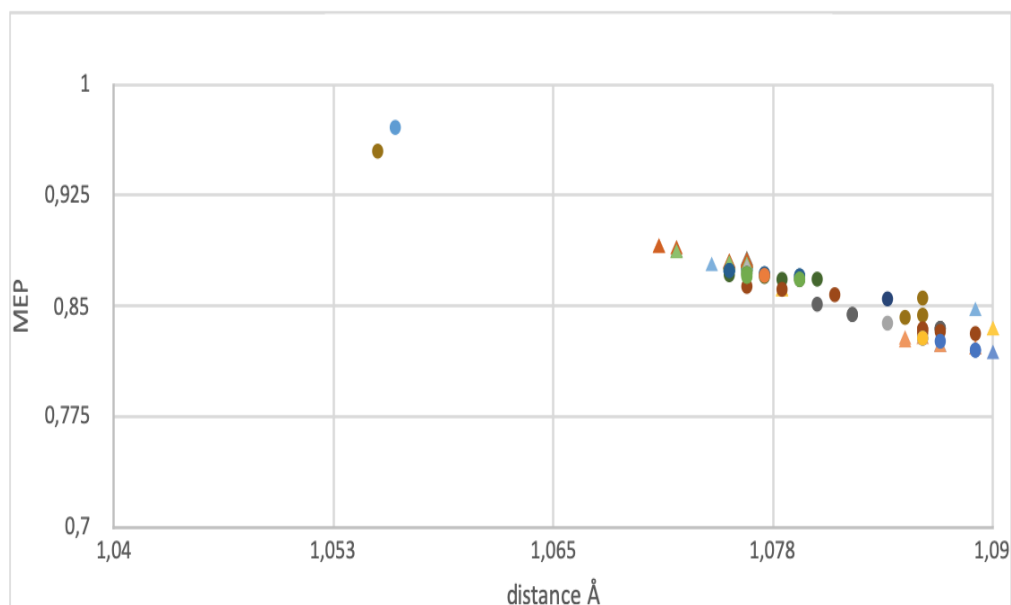


Figure 4.6: *The MEP at the (3, -1) critical point between a carbon and hydrogen is plotted against the distance between the two atoms. The hydrocarbons plotted are a mixture alkanes, alkenes, alkynes as well as cyclo-hydrocarbons and aromatic structures. The triangles are cyclic structures and the dots are aliphatic structures.*

The link between an increasing bond length and decreasing MEP is expected. The increasing distance between the atoms causes a decrease in the nucMEP and elecMEP at the (3, -1) critical point until the two components cancel each other. All the bonds in figure 4.6 are covalent bonds and with a clear spread of MEP values the question arises, is it possible to compare bonds such as polar-covalent bonds (dative bonds), ionic bonds or even identify hydrogen bonds? In an attempt to compare bond order and bond type the ratio of the nucMEP : elecMEP was calculated.

The logic behind using the MEP ratio is based on Coulombs law where the force exerted on a point charge is the product of two charges divided by the distance between them squared. As two positive charges move further apart the repulsive forces between them decreases. This would mean that the required negative charge between the two positive charges would likewise decrease in order to neutralise the repulsive forces. This suggests that an equilibrium for multiple charges can be calculated. While the nuclei are treated as point charges the electrons are calculated as a distribution of charge and this creates a problem when making direct charge comparisons. This is where the MEP ratio finds its niche. The MEP ratio makes it possible to discern the point where the electrostatic potential of two interacting atoms are stable. This concept is explored and explained in this section.

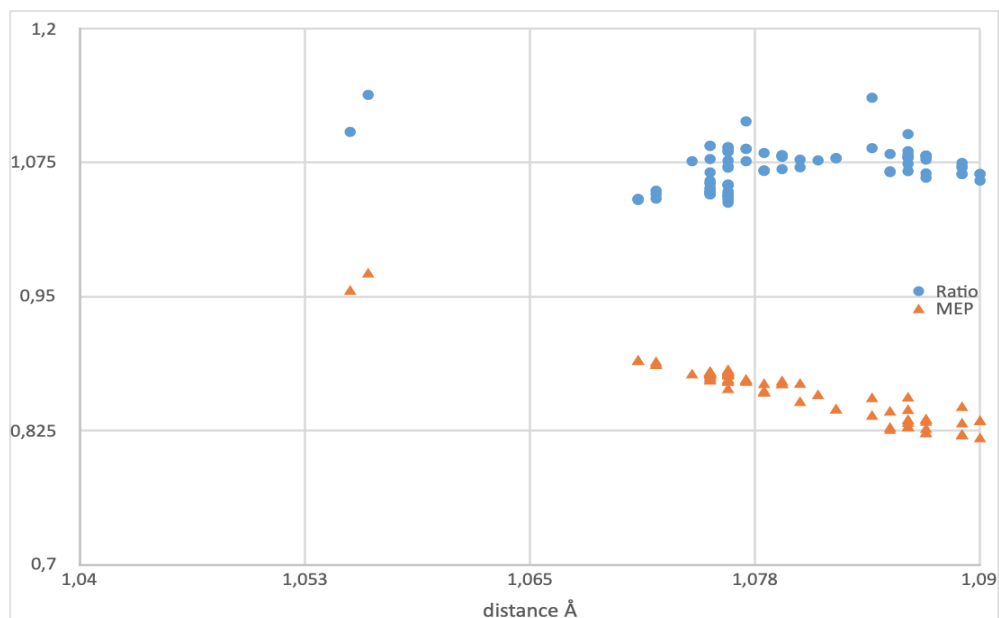


Figure 4.7: *Comparing the ratio of the nuclear MEP : electronic MEP to the total MEP at the (3, -1) critical point between carbon and hydrogen for a series of hydrocarbons.*

While there are some variations in the ratios, this is to be expected, what is important is that the more linear distribution of the ratio values over the different bond lengths provides a simple way to compare covalent bonds. The variation of the ratio can be attributed to the electronic structure of the molecules, if the hydrogen is bonded to a carbon in a linear, cyclic or aromatic molecule, the influence is seen in the MEP ratio. The MEP ratio for different bond types as well as bonding interactions between hetero-atoms were calculated and some of the results are shown in table 4.2.

Table 4.2: A breakdown of known bond types into the MEP components as well as the MEP ratio. The hydrogen molecule in the singlet and triplet state are added for comparison. The MEP values are in atomic units and the bond length is in Å.

Molecule	Bond Length	MEP	nucMEP	elecMEP	ratio	ρ	$\nabla^2\rho(r)$	G
H ₂	0.735	0.9244	2.8786	-1.9542	1.4730	0.2661	-1.1206	1.25e-34
^t H ₂	5.044	0.0001	0.4196	-0.4195	1.0004	5.04e-5	0.0001	2.48e-5
He ₂	3.682	0.0001	1.1498	-1.1497	1.0001	0.0001	0.0009	0.0001
Ne ₂	3.274	0.0008	6.4655	-6.4647	1.0001	0.0010	0.0103	0.0017
Ar ₂	5.050	0.0003	7.5448	-7.5444	1.0000	0.0002	0.0008	0.0001
~C—H ^a	1.079 (0.006)	0.86 (0.03)	15 (4)	-14 (4)	1.07 (0.02)	0.290(0.005)	-1.02(0.03)	0.040(0.001)
N≡N	1.071	2.0178	13.8403	-11.8224	1.1707	0.7321	-3.1341	0.6533
O=O	1.154	1.6855	14.6739	-12.9884	1.1298	0.6370	-1.5563	0.5614
O—O—O	1.194	1.5804	16.8689	-15.2885	1.1034	0.5746	-1.1322	0.4966
BH ₃ —H ₃ B ^b	1.323	0.6051	7.6446	-7.0396	1.0859	0.1491	-0.3161	0.0323
H ₃ B—BH ₃ ^c	1.783	0.5493	8.1991	-7.6498	1.0718	0.1116	-0.0445	0.0485
H ₂ O—H ₂ O	2.056	0.0261	7.6323	-7.6062	1.0034	0.0392	0.1588	0.0369
H ₃ N—BF ₃	1.670	0.5289	16.7504	-16.2215	1.0326	0.1876	-0.1761	0.0775
NC—CN	1.392	1.0899	13.1835	-12.0935	1.0901	0.3049	-1.0075	0.0699
H ₃ C—CH ₃	1.527	0.6236	10.3833	-9.7597	1.0639	0.2514	-0.6708	0.0511
H ₂ C=CH ₂	1.319	1.0399	11.0162	-9.9762	1.1042	0.3592	-1.1943	0.1400
HC≡CH	1.184	1.4587	11.3732	-9.9145	1.1471	0.4237	-1.3363	0.3034
Na ⁺ Cl ⁻	2.340	0.2218	16.8178	-16.5960	1.0134	0.0476	0.0960	0.0325

^a An average of all C-H bonds in hydrocarbons including aliphatic, cyclic and aromatic structures.

^b The values are taken from the saddle point between the hydrogen and both borons in the B₂H₆ molecule.

^c The values are taken from the saddle point between the two borons in the B₂H₆ molecule.

The values in table 4.2 are taken from the saddle point between the bonded atoms which are indicated in the first column. The bond that is analysed in the B_2H_6 (written as BH_3-H_3B in the table) molecule is between the hydrogen and both boron atoms and not between the two borons. A bond between the NH_3BF_3 molecule occurs between the nitrogen and the boron. It can also be seen that although most of the bonds in the table are covalent bonds, none of the ratio's come close to the value for H_2 , ratio ≈ 1.4 .

The covalent bond between the two carbons in ethane, ethylene and acetylene show that it is possible to use the MEP ratio to define bonding interactions. As the bond order changes from single to double and finally to a triple bond the ratio is increased, moving closer to the the ratio of 1.4. As none of the ratios come close to the ≈ 1.4 of H_2 , it is treated as the upper limit and any ratio exceeding 1.4 is treated as being indicative of an unstable interaction. The ratio of 1.4 being the upper limit of a bonding interaction is not just because no other bond ratio comes close to 1.4. The hydrogen molecule has the shortest bond length out of all the molecules and represents the simplest system, two protons and two electrons. By increasing the size of the atoms the repulsive force is naturally increased and this would increase the bonding distance and, as pointed out earlier, would decrease the ratio as the negative potential required to reach equilibrium would decrease. Decreasing the bond length for larger atoms would bring the MEP ratio closer to 1.4 but as is shown in figure 4.2 the positive potential increases much faster than the negative potential. One also needs to consider the repulsive nature that electrons exert on each other which may also account for the slower increase in the negative potential when atoms are forced together.

Table 4.2 shows that strong covalent bonds have a ratio of around 1.15, this is shown with the triple bonds. Coupling this information with the MEP ratio of 1.4 for hydrogen in the singlet state and a MEP ration of 1.0 for hydrogen in the triplet state it is possible to interpret any movement away from a MEP ratio of 1.15 as a weakening of a bonds strength.

The 4H_2 is treated as being an unstable interaction and therefore the ratio of 1.0000 is treated as threshold between a stabilising and non-stabilising interaction. A MEP ratio of 1.0 shows that the two opposite potentials are identical, this would point to atoms that are not influencing each other. The nuclei are not forced into creating a dipole which could result in attraction of repulsion. There is nothing to focus the electron density between the two atoms and without an external force the two atoms have no reason to interact with each other.

There are some interactions that were calculated where the MEP ratio at the (3, -1) saddle point was less than one. This is seen in figure 4.8 and the molecules were $HCCH-HLi$ and $HOH-NH_3$. This is treated as a non-stabilising interaction as the negative potential is higher than the positive potential. This could be an indication that the electron density between the atoms is creating a repulsive force due to the repulsive interactions between the electrons.

The C_2N_2 molecule was used to identify any effects that an electronegative atom would have on the MEP. The ratio of the (3, -1) saddle point between the carbons shows that there is more of a concentration of electronegativity than for the bonds between ethane and ethylene. The shorter bond length for the carbon-carbon bond in C_2N_2 results in a higher nucMEP at the saddle point and this contributes to the higher ratio. The nucMEP and elecMEP for the C_2N_2 is 13.1835 a.u. and -12.0935 a.u. respectively, this shows that the surrounding atoms can influence other bonds in the molecule.

The H_3N-BF_3 molecule was used to investigate the values for a polar-covalent (dative) bond as the bond is between the boron and nitrogen. A comparison between oxygen (O_2) and ozone

(O_3), which has a resonance structure, showed that the oxygen molecule has a slightly higher ratio than the ozone molecule and this could be attributed to the delocalised electron present in ozone. The B_2H_6 molecule was included to analyse the bifurcated hydrogen bond that links the borons together. The ratio for the bifurcated bond is 1.0859 and has a MEP of 0.6051 a.u. which places this bond in the same region as the carbon-carbon bond in ethane. The water molecule is a simple system that shows hydrogen bonding. The hydrogen bond is one of the weakest bonds and it is expected to have a low MEP ratio, the ratio is 1.0034 which is barely above the threshold for a non-stabilising interaction.

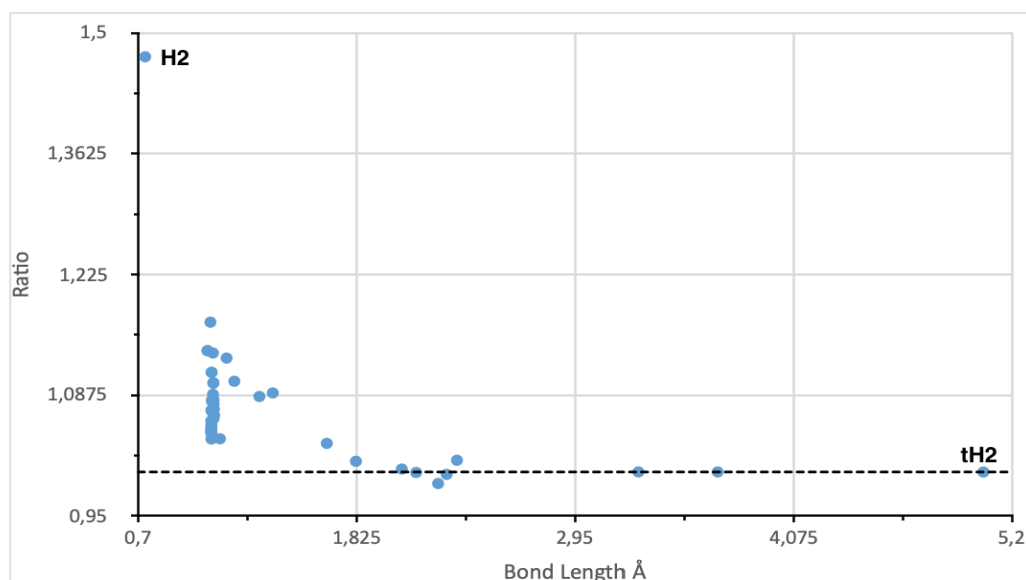


Figure 4.8: A compilation of various bond types and bond order with H_2 shown as the upper limit and tH_2 shown at the lower limit. The dashed line is set a ratio of 1.0000 and any value below this line is regarded as being a non-bonding interaction

The figure 4.8 is a collection of different bond types and bond order based on the MEP ratio compared to bond length. The first group of points in the graph, bond lengths between 0.7-1.4 Å, are all covalent bonds and the polar covalent bonds are seen trailing off the group with longer bond lengths, lengths greater than 1.5 Å. As the bond type becomes weaker, ionic and hydrogen bonds, the ratios decreases which is evident in the graph. It is clear from the graph that identifying bond type and order is not feasible because gathering a larger data set of bonds would blur the boundaries between the bond types. It is possible to see from the graph that there are definite cut-offs for stabilising and non-stabilising interactions (based on the hydrogen molecule in the singlet and triplet states) and could possibly be used to rank bond strength. Included in the figure 4.8 the ratios for halogen bonds as well as bonds for weak interacting molecules such as $HCCH \cdots HLi$ and $HOH \cdots NH_3$ which fall below the 1.0000 ratio threshold.

4.4 Conclusions

The hydrogen molecule was calculated in the singlet and triplet state with the intention of having two atoms that represented a stabilising interaction and a de-stabilising interaction. The comparison of these two results are used to set up thresholds in the MEP for similar interactions. The (3, -1) critical point between the atoms was analysed using the electron density (ρ), laplacian ($\nabla^2\rho(r)$), Lagrangian kinetic energy (G) and the molecular electrostatic potential (MEP) ratio.

The stabilising interaction is supported by the energy graph as well as the $\rho = 0.2661$ a.u. , the $\nabla^2\rho(r) = -1.1206$ which is an open shell interaction with electron concentration between the atoms. The ratio of the nuclear (nucMEP) and electronic (elecMEP) MEP was shown to be useful when comparing bonding interactions and the ratio for H_2 was 1.4730 which is treated as the upper limit for all stabilising interactions as a higher ratio would mean that there is an unstable interaction. The hydrogen molecule in the triplet state (${}^t\text{H}_2$) naturally had very different values. The $\rho \approx 0$ a.u. , the $\nabla^2\rho(r) = 0.0001$ a.u. and MEP ratio was 1.0004. The MEP ratio for ${}^t\text{H}_2$ is treated as the lower limit for a stabilising interaction.

The noble gases were studied because they introduced complexity in the form of larger nuclei and core electrons. The analysis showed that He_2 , Ne_2 and Ar_2 had a ratio of 1.0001, 1.0001 and 1.0000 respectively indicating the these were non-stabilising interactions based on the standard set up in this chapter. Ultimately the findings reinforced those of the hydrogen molecules and any real value would come from studying molecules consisting of hetero-atoms.

After analysing the hetero-atoms, bond orders and bond types it was determined that the ratio was a useful tool for identifying stabilising and destabilising interactions and could possibly be used to compare bond strengths. A stabilising interaction was shown to have a MEP ratio of around 1.12, increasing or decreasing this ratio led to ever weaker interactions until the ratio was more than 1.4 or less than 1.0. At a ratio of 1.1 the repulsive force of the nuclei are balance by the attractive force of the electrons in such a way that an equilibrium between the forces is reached.

As the ratio tends towards 1.4 the system changes and generally bond lengths decrease, this leads to weaker bonds. As the distance between atoms decreases the negative potential needs to increase at the same rate as the positive potential. The negative potential is a result of the electron density and trying to squeeze electrons into a smaller space cause an increase in repulsive forces, this time between the electrons. The interaction therefore becomes more unstable as the balance between the attractive and repulsive forces tends to be more repulsive.

As the ratio starts to decrease from 1.1 to 1.0 the interactions once again tend towards weaker and ultimately unstable interactions. This time it is a result of forces cancelling each other out rather than reaching an equilibrium. The negative potential reaches a point where it is equal to the positive potential, this suggests that the electron density around an atom is in equilibrium with the atom and is not being pulled towards the nucleus of a neighbouring atom. If there are no forces present between the atoms then it is difficult to argue that a bond exists.

Using the MEP ratio is therefore an appealing technique because each interaction between atoms can be judged solely on the ratio without having to compare to previously known bonding interaction.

Finally, it is worth mentioning that for two atoms to form a stable interaction the Coulomb forces need to be in equilibrium. The MEP between two atoms is almost always positive and

while this is to be expected, because nuclei are treated as point charges and the electrons are distributed in a volume of space, the nucMEP : elecMEP ratio is an indication that the total positive potential does not need to equal the total negative potential for the system to be in equilibrium. Therefore the molecular electrostatic potential can be used to discern between a stabilising and destabilising interaction.

Chapter 5

Exploring Hydrogen-Hydrogen Bonding in Molecules

In chapter one it was mentioned that there are differences between a hydrogen bond, di-hydrogen bond and a hydrogen-hydrogen bond, this chapter explores the hydrogen-hydrogen bond. The controversial nature of the hydrogen-hydrogen bond is rooted in the idea that two hydrogen atoms that have similar charges can form a stabilising interaction (a bond). The Quantum Theory of Atoms in Molecules (QTAIM) has been used to calculate a bond critical point (BCP) and an atomic interaction line (AIL) between two hydrogens of similar charge in the electron density and concluded that the interaction is stabilising, an example of this would be planar molecules and congested molecules [18, 145]. This is a contested finding as was discussed in chapter one but it has also lead to criticism of the QTAIM method in general with claims that there will always be a BCP and AIL between two atoms in close proximity to each other [144].

The figures and tables in this chapter are calculated using Hartree-Fock level of theory with the 6-311++G(d,p) basis set unless otherwise stated. The values are reported in atomic units with the exception of the distance between atoms which is given in Angstroms.

5.1 Analysing the Molecular Electrostatic Potential Topology of the 2-Butene Molecule

Previous chapters have discussed the different interpretations of the Molecular Electrostatic Potential (MEP) topology, mainly how the topology depicts delocalised electrons (a chain of minima and saddle points), bond strain (minima outside the ring) and stabilisation (minima inside the ring) [116]. These concepts as well as the values for the electron density (ρ), laplacian ($\nabla^2\rho(r)$) and the MEP ratio will be used to understand the type of interaction between the hydrogens in the cis-2-butene molecule.

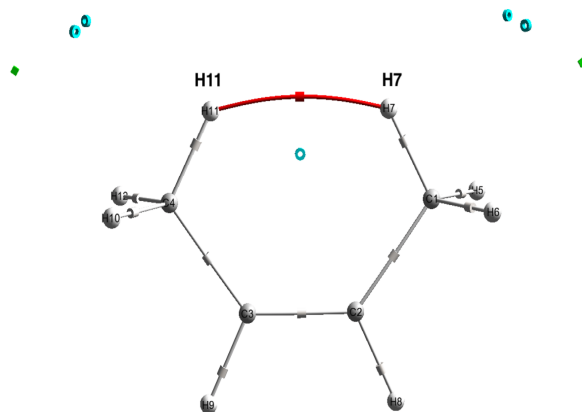
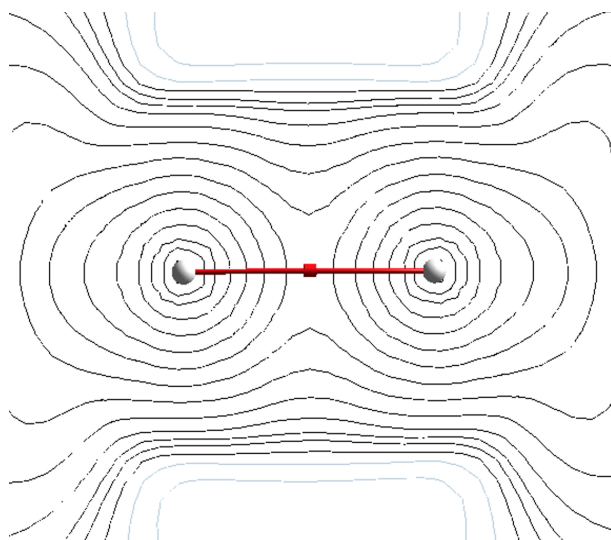


Figure 5.1: *The molecular graph of 2-butene in the MEP has a possible hydrogen-hydrogen bond between H11 and H7 (shown in red). The bond between atoms C3 and C4 is a double bond. The black spheres are carbon and the white spheres are hydrogen atoms. The white cylinders are (3, -1) critical points, blue rings are (3, +1) saddle points and the green cubes are (3, +3) critical points.*

The minima depicting the double bond are located above and below the bond, this would potentially rule out the idea that the molecule is under strain. The minima that normally appear in the middle of the CH₃ group are displaced and (3, +1) saddle points are calculated, the position of the saddle points may indicate that there is some delocalisation of the electrons.



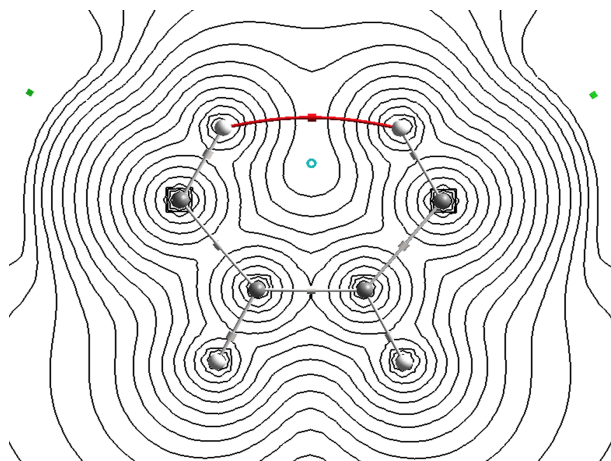


Figure 5.1: *On the top is contour plot of the space between the two interacting hydrogens. On the bottom is a contour plot of the plane containing the $(3, +1)$ saddle point. The white contour lines are negative MEP and the black contour lines are positive MEP. The black spheres are carbon and the white spheres are hydrogen atoms. The white cylinders are $(3, -1)$ critical points, blue rings are $(3, +1)$ saddle points and the green cubes are $(3, +3)$ critical points.*

The negative space above and below the hydrogen-hydrogen bond is similar to most bonds in aromatic structures, this is shown in figure 5.1 with the plane passing perpendicular to the hydrogen-hydrogen bond. It is noticed in the contour map that the negative MEP for aromatic structures tend to be pushed away from the nuclei and congregate around the saddle point (creating a wave pattern, this can be seen in the contour plot of 1, 3-butadiene, chapter 3), but for 2-butene the negative MEP does not follow the same pattern.

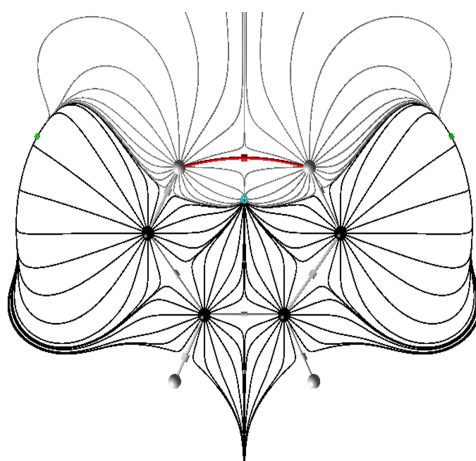


Figure 5.2: *The gradient lines of 2-butene in the MEP shows that the hydrogens are able to dominate the space between them. The black spheres are carbon and the white spheres are hydrogen atoms. The white cylinders are $(3, -1)$ critical points and the blue rings are $(3, +1)$ saddle points.*

The gradient lines show that the hydrogen atoms dominate the space between them and thus prevent any interference from the carbon atoms. This allows for the interaction of the two atomic

basins and the formation of the (3, -1) critical point and atomic interaction line (AIL).

Table 5.1: *The MEP, ρ , $\nabla^2\rho(r)$ and kinetic energy values for 2-butene at the (3, -1) saddle point between C2 and C3, the (3, +1) saddle point and the (3, -1) saddle point between H7 and H11 are shown in the table. All values are given in atomic units with the exception of the MEP ratio.*

	nucMEP	elecMEP	MEP	ratio	ρ	$\nabla^2\rho(r)$	G
(3, -1) C2-C3	14.7383	-13.7197	1.0187	1.0742	0.3355	-1.1507	0.1415
(3, +1)	9.4744	-9.4365	0.0379	1.0040	0.0093	0.0421	0.0083
(3, -1) H7-H11	8.0612	-8.0130	0.0482	1.0060	0.0079	0.0249	0.0053

The MEP decreases as one moves from the saddle point between the carbon atoms until reaching the (3, +1) saddle point, after which the MEP begins to increase. The ratio for the MEP at the saddle point, between the hydrogens, is above the recorded value for a hydrogen bond between two water molecules (1.0034); this would imply that there exists a stabilising interaction between the two hydrogens. While the laplacian is positive and thus indicating a closed shell interaction, the value does not rule out a stabilising interaction (laplacian for water hydrogen bond is 0.1588). The electron density value is low when compared to the hydrogen bond in a water molecule (water molecule $\rho=0.0392$ a.u.), this does not definitively prove that there is no stabilising interaction but points to an interaction that may be closer to a van der Waal interaction. The finding that the hydrogen-hydrogen interaction is stabilising agrees with a paper by Matta *et al.* [146]. The paper was in response to finding by Weinhold *et al.* where the hydrogen-hydrogen interaction was deemed to be repulsive in nature [147].

Comparing the values of the double bond with the double bond in ethylene it is noted that the values are lower in the cis-2-butene molecule. The MEP ratio for ethylene is 1.1042, $\rho = 0.3592$ a.u., $\nabla^2\rho(r) = -1.1943$ a.u. and the kinetic energy (G) is 0.1400 a.u.. The decrease in the laplacian can be interpreted as the electron density being shifted away from the centre of the double bond, the decrease in the electron density would support this observation. It is not unreasonable to interpret the results as the delocalisation of the electron density and the stabilisation of the ring formed by the hydrogen-hydrogen bond. Cioslowski demonstrated that the hydrogen-hydrogen interaction is not repulsive and that the delocalisation of the electrons stabilises the molecule [14].

An alternate explanation can be given where the decrease in the values is a result of the lengthening of the double bond to accommodate the hydrogen-hydrogen bond and therefore the hydrogen-hydrogen bond is viewed as being destabilising, a viewpoint that is expressed by Poater, Solà and Bickelhaupt [19]. However, this was already explained by Matta *et al.*, the conclusion was that locally the hydrogen-hydrogen bond was stabilising but the stretching of the carbon-carbon bond locally destabilising and ultimately the destabilising energy was greater than the stabilising energy [146].

5.2 Analysing the Chrysene Molecule

The chrysene molecule was chosen to analyse the differences between a pair of hydrogens that interact with each other and a pair that do not. The analysis included the distance between

the hydrogens, the topology, ρ , MEP ratio and a contour plots of the molecule. The chrysene molecule is shown in figure 5.3, the hydrogen-hydrogen interaction is shown in red.

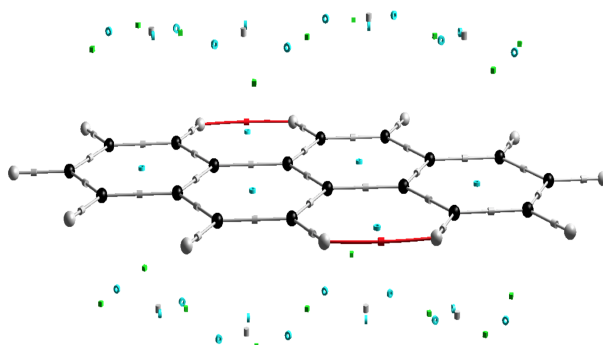


Figure 5.3: *The chrysene molecule is shown with all the calculated critical points, the possible hydrogen-hydrogen interaction is shown in red. The black spheres are carbon and the white spheres are hydrogen atoms. The white cylinders are $(3, -1)$ critical points, blue rings are $(3, +1)$ saddle points and the green cubes are $(3, +3)$ critical points.*

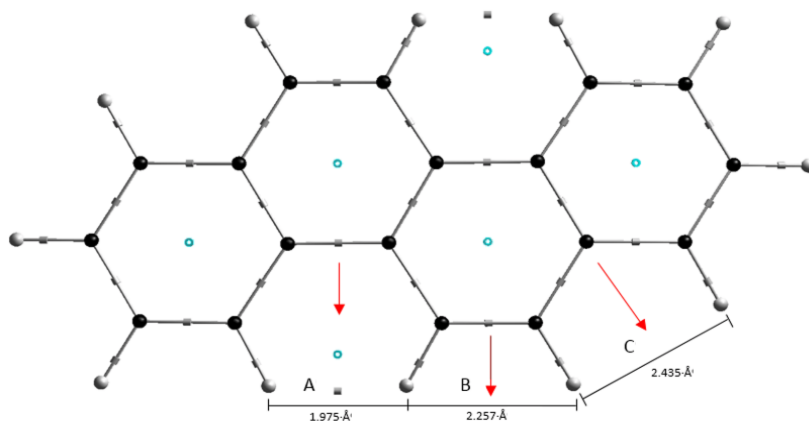


Figure 5.4: *The chrysene molecule is shown with the three hydrogen-hydrogen interaction sites to be investigated. Site A is where a $(3, -1)$ saddle point is calculated as well as an atomic interaction line which is not shown. The critical points that are normally calculated above and below the molecule have been removed for clarity. The black spheres are carbon and the white spheres are hydrogen atoms. The white cylinders are $(3, -1)$ critical points and the blue rings are $(3, +1)$ saddle points*

The critical points that are calculated out of the plane of the chrysene molecule, shown in figure 5.4, have been removed for clarity. Three sites are analysed which are marked as A, B and C, site A is where the only $(3, -1)$ critical point between two hydrogens was calculated along with an atomic interaction line which has been removed. Contour plots of the chrysene molecule are shown in figure 5.5, the first contour plot is in the plane of the molecule while the second plot

is in the plane perpendicular to the plane of the molecule and is positioned over the hydrogens being studied.

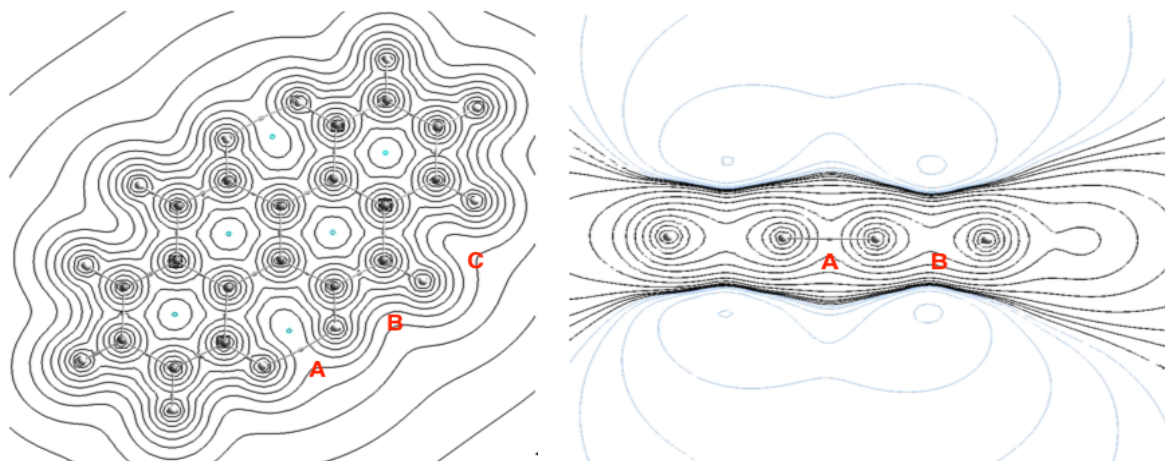


Figure 5.5: *The contour lines of the MEP for the chrysene molecule, the first plot is in the plane of the molecule and the second plot is perpendicular to the molecule and is positioned over the hydrogens being studied. The white contour lines are negative MEP and the black contour lines are positive MEP. The black spheres are carbon and the white spheres are hydrogen atoms. The white cylinders are $(3, -1)$ critical points and blue rings are $(3, +1)$ saddle points*

The contour plot over the hydrogens shows a similar pattern to aromatic molecules, possibly indicating the delocalised nature of the electrons. However, the contour plot in the plane of the molecule shows that the MEP between the three sites is different, with two of the sites showing a flattening of the MEP, while the third site (site A) shows the beginning of a ring formation. To get a better understanding of what is happening between the hydrogens, the gradient lines for the carbon and hydrogen atoms were calculated, and is shown in figure 5.6.

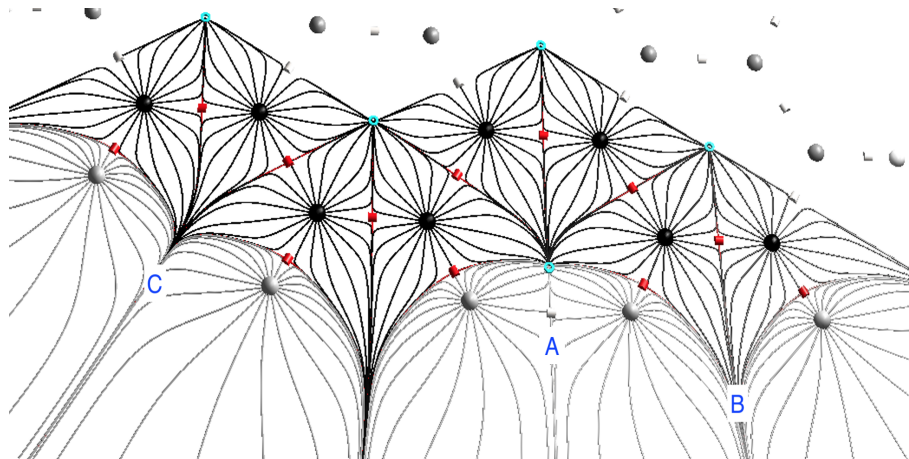
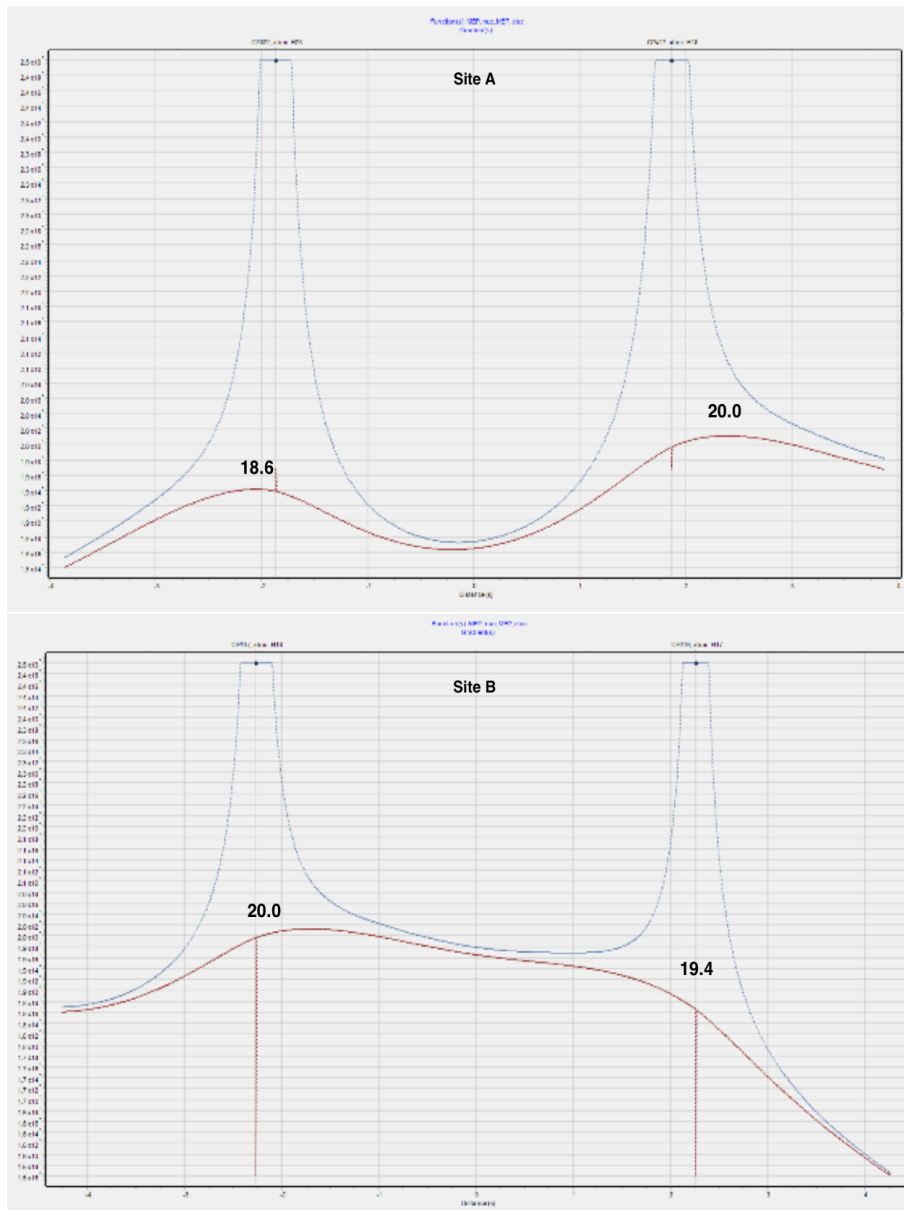


Figure 5.6: *The chrysene molecule is shown with the three hydrogen-hydrogen interaction site that are being investigated. The gradient lines show the interaction between the various atoms. The critical points that are normally calculated above and below the molecule have been removed for clarity. The black spheres are carbon and the white spheres are hydrogen atoms. The white cylinders are $(3, -1)$ critical points and the blue rings are $(3, +1)$ saddle points*

According to QTAIM the atoms in a molecule can be partitioned and therefore maintain their individuality, when a bonding interaction occurs between two atoms the atomic basins of the atoms touch [1]. The gradient lines show that at sites B and C the hydrogens do not interact as the influence of the carbon atoms passes through the space between them. At site A the two hydrogen atoms dominate the space between each other and thus exclude any interference from the carbon atoms. The nucMEP (blue line) and elecMEP (red line) were plotted for the space between the hydrogens and shown in figure 5.6.



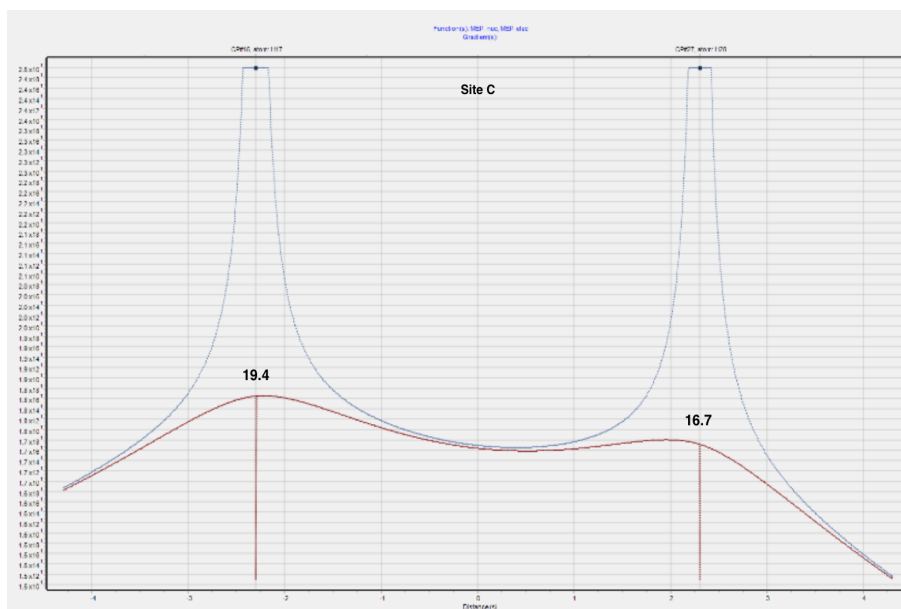
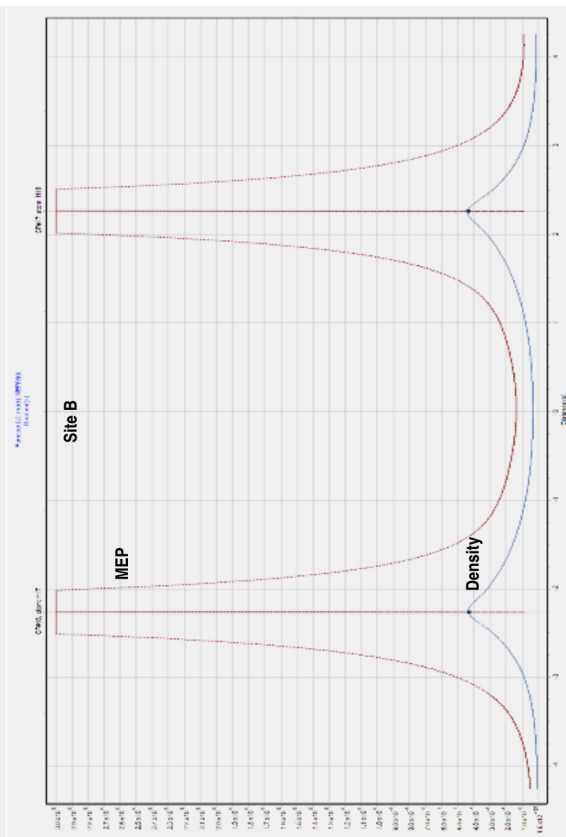
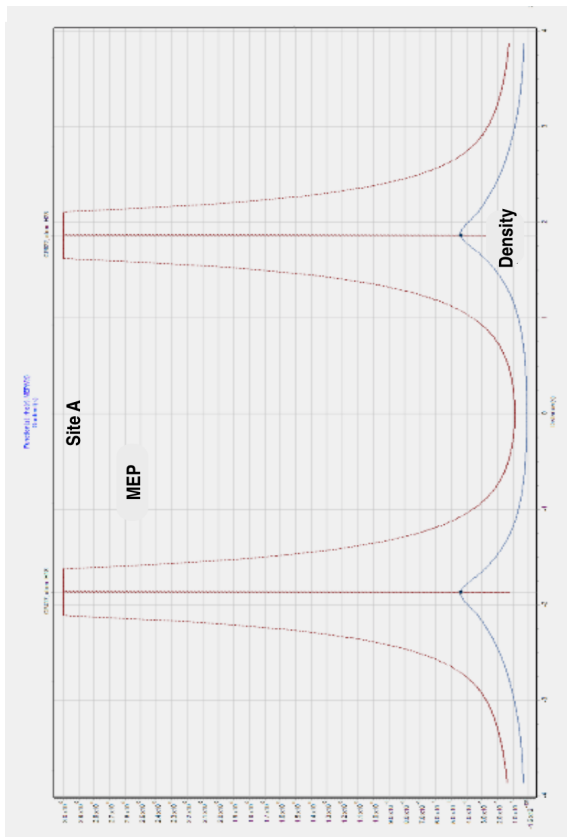
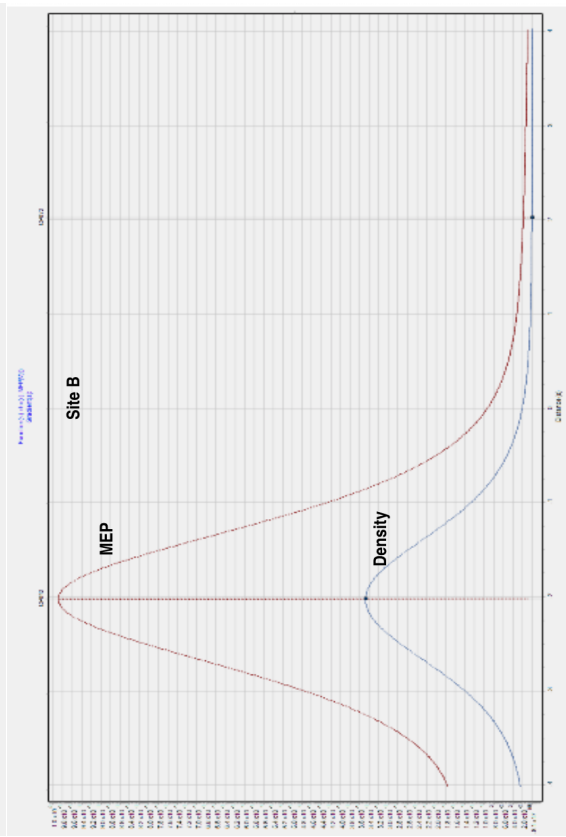
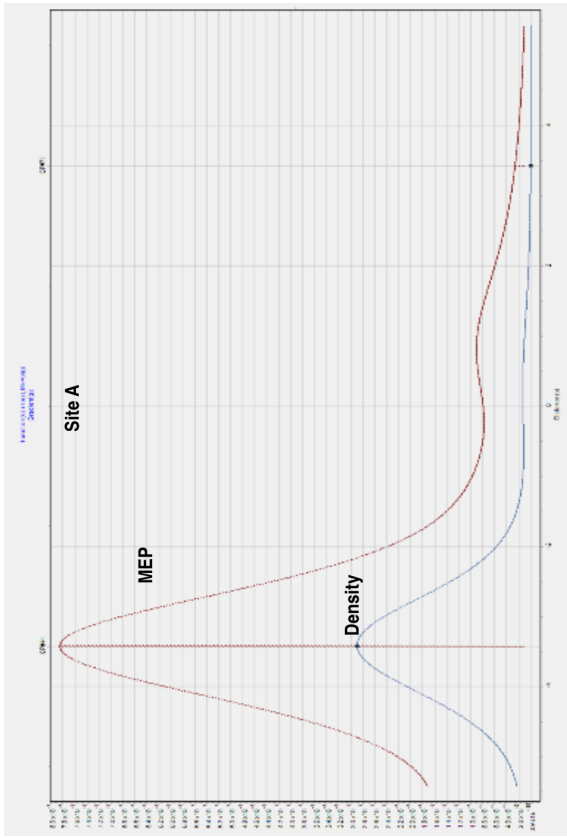


Figure 5.6: The blue line is the nucMEP and the red line is the elecMEP. The values on the graphs indicate the approximate elecMEP on the hydrogen atom, the values are in atomic units.

The differences in the elecMEP on the hydrogen atoms show that the hydrogens do not possess the same potentials and therefore the differences in the potentials could indicate an attractive interaction. While the elecMEP potentials do differ, it does not mean that the overall charge on the hydrogens are different. Site A is where the only (3, -1) saddle point was calculated and the graph shows the saddle point between the hydrogens. The graph for site B shows an inflexion point between the two hydrogens and this would rule out the possibility of locating a saddle point between the hydrogens. The graph for site C does show that a saddle point could be calculated but the contour plots and gradient plot show that the space between the hydrogens is interrupted by the carbon atoms.



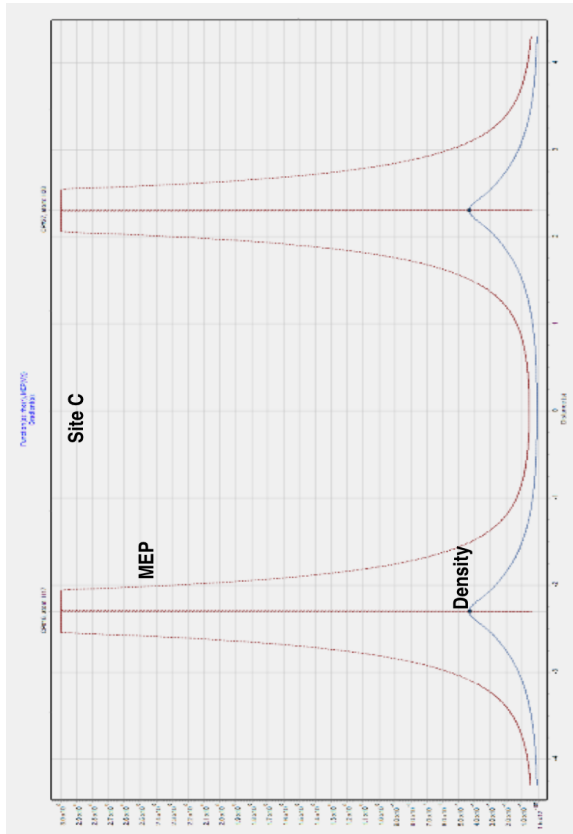
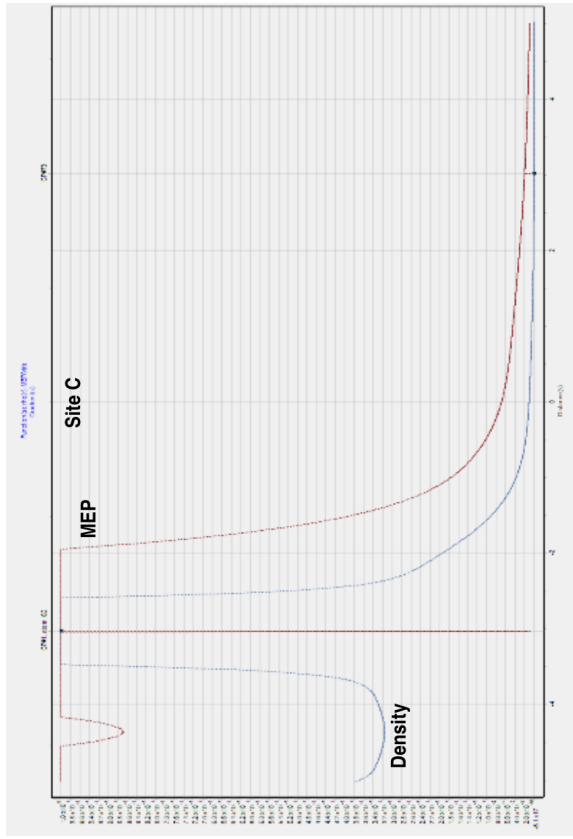


Figure 5.6: The blue line is the electron density and the red line is the molecular electrostatic potential. The graphs on the left are plotted between the hydrogens while the graphs on the right are plotted passing through the mid point of the hydrogens.

A (3, -1) critical point is defined as a minimum along one axis (normally between two NAs) and a maximum along the other two axes. The graphs in figure 5.8 show the MEP and ρ along the axis between the NAs (z-axis, graphs on the left) and along the axis perpendicular to the z-axis (graphs on the right). Sites B and C only show decreasing MEP and ρ along the perpendicular axis and therefore a saddle point will not be calculated. A comparison of the MEP and the ρ between the hydrogens, as well as through the probes (figure 5.8), is shown in figure 5.6. The electron density between the hydrogens at site A barely registers on the graph, but the plot of the MEP shows that a saddle point is calculated between the hydrogens. Sites B and C are clearly missing the saddle point when the MEP and electron density is calculated perpendicular to the molecule and passing between the hydrogens (values are plotted through the probes in figure 5.8).

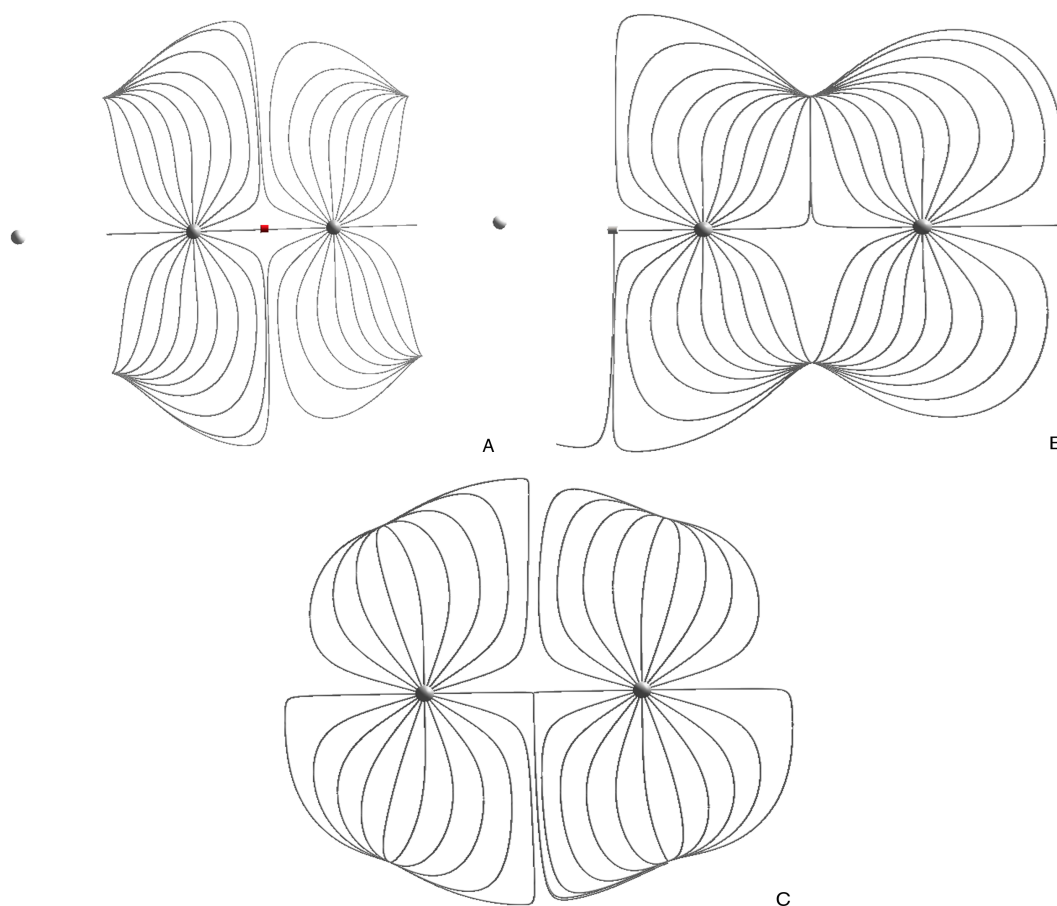


Figure 5.7: *The gradient lines of the MEP for the chrysene molecule at the three different sites. The white spheres are hydrogen atoms. The pink cylinder is a (3, -1) critical point.*

It may seem trivial to point out that the hydrogens at sites B and C do not dominate the space but looking at the contour plots calculated perpendicular to the plane of the molecule, sites A, B and C show that a turbulent MEP is the difference between calculating a critical point or not detecting one at all. This observation follows the explanation for a bond formation in QTAIM where the formation of a bond path is described as a competition between atoms to form an interatomic surface [4]. The gradient plots in figure 5.7 would suggest that there should be a critical point, possibly a (3, -1) critical point, above and below the hydrogens at site B. The

locations of these seemingly missing critical points are found in different positions for each site investigated. A targeted search for the critical points was carried out but no critical points were calculated. The program eDensity allows for a calculation to be carried out at a targeted location. This is done by restricting the boundary conditions to define the area of interest, visually this process looks like creating a box with a specific dimension. The calculation (in this instance it is the MEP) is then carried out with the new boundary conditions. This allows for a finer grid to be used when looking for critical points, the smaller step size in the calculation makes it easier to detect gradient changes and increases the chance of locating a critical point if one exists. It is likely that one or more of the first derivatives at these locations are non-zero which would result in no critical point.

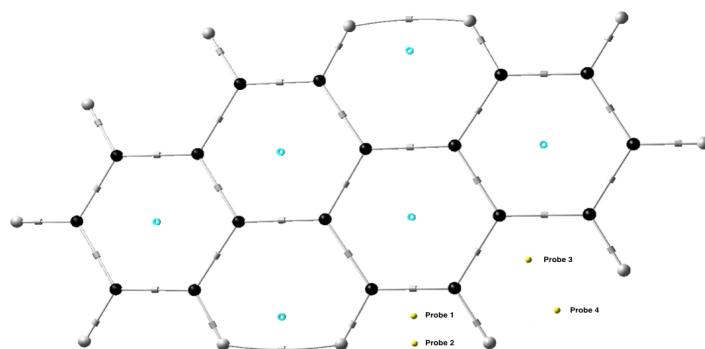


Figure 5.8: The chrysene molecule is shown with four probes placed in positions where a $(3, +1)$ and a $(3, -1)$ critical point could be expected to be calculated. The black spheres are carbon atoms and the white spheres are hydrogen atoms. The cylinders are $(3, -1)$ critical points, the blue rings are $(3, +1)$ critical points and the yellow spheres are probes.

Table 5.2: *The table shows the bond length, MEP, ratio, ρ , $\nabla^2\rho(r)$ and kinetic energy (G) for the (3, -1) critical points between the carbon atoms as well as the probes at locations that would match (3, +1) critical points and (3, -1) critical points between the hydrogens. The values are calculated in atomic units except for the bond length which is calculated in Angstroms.*

	length	nucMEP	elecMEP	MEP	ratio	ρ	$\nabla^2\rho(r)$	G
Site A								
C-C(3, -1)		27.9831	-27.1979	0.7852	1.0289	0.2896	-0.8516	0.0700
(3, +1)		20.5962	-20.5185	0.0777	1.0038	0.0124	0.0583	0.0117
H-H(3, -1)	1.975	18.4270	-18.3368	0.0903	1.0049	0.0114	0.0399	0.0083
Site B								
C-C(3, -1)		26.2704	-25.2811	0.9893	1.0391	0.3477	-1.1432	0.1226
probe 1		23.2403	-22.7231	0.5172	1.0228	0.1595	0.1613	0.1297
probe 2	2.257	19.7909	-19.6544	0.1365	1.0069	0.0331	0.1571	0.0376
Site C								
Carbon	-	-	-	-	-	-	-	-
probe 3		22.5808	-22.2758	0.3050	1.0137	0.0718	0.2584	0.0779
probe 4	2.435	17.4436	-17.3909	0.0528	1.0030	0.0069	0.0323	0.0063

The figures of the chrysene molecule show that it is possible for the QTAIM method to distinguish between an interacting and non-interacting pair of hydrogens and that (3, -1) critical points are not only dependent on whether or not two atoms are close together. The difference in the distances between the hydrogens at the three sites do not appear to be the deciding factor of whether a (3, -1) critical point is calculated or not calculated. Interestingly all the values calculated for site B, where the atoms seem to be the furthest from forming a ring structure, are higher than for site A. The MEP and electron density for probe 2 are higher than that of the (3, -1) critical point at site A. In contrast the values for probe 4 at site C are lower than the (3, -1) critical point at site A.

Comparing the values in Table 5.2 to a hydrogen bond in water the MEP ratio is higher for the hydrogen-hydrogen interaction (hydrogen bond = 1.0034), comparing the laplacian, the hydrogen-hydrogen interaction is 0.0399 a.u. compared with 0.1588 a.u. for a hydrogen bond. The ρ for the hydrogen-hydrogen bond is less than that of the hydrogen bond in water, 0.0114 a.u. and 0.0392 a.u. respectively. It should be pointed out that probe 2 (site B), which is located between two hydrogens, has a higher MEP ratio and ρ compared to the hydrogen-hydrogen interaction and actually has similar results (MEP ratio = 1.0069, ρ = 0.0331 a.u., laplacian = 0.1571 a.u.) to the hydrogen bond in water. This is interesting as no (3, -1) critical point is calculated between the hydrogens which shows that QTAIM and the topology of the MEP is reliant on more than just having atoms close together or the correct combination of values.

5.3 The MEP Topology of the Biphenyl Molecule

The biphenyl molecule in the planar conformation has a hydrogen-hydrogen interaction between the ortho hydrogens. This interaction has been the subject of debate [3, 18, 19, 20, 21, 22, 23]

as the interaction has been deemed to be a stabilising interaction, destabilising interaction and possibly an artefact of the Quantum Theory of Atoms in Molecules model [17, 144]. This section analyses the topology of the Molecular Electrostatic Potential (MEP), using the Quantum Theory of Atoms in Molecules (QTAIM).

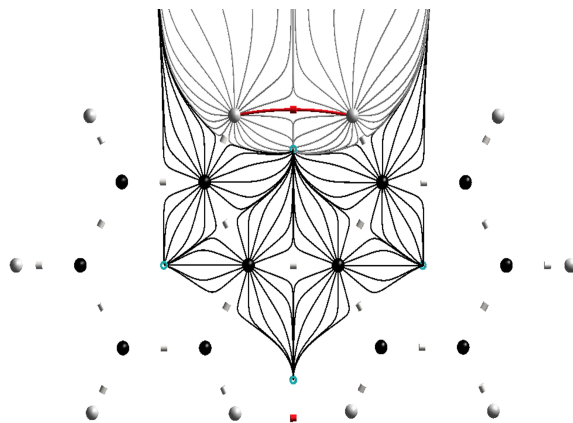


Figure 5.9: *The gradient lines of the MEP for the planar biphenyl molecule with the hydrogen-hydrogen bond shown in red. The white spheres are hydrogen atoms and the black spheres are carbon.*

In figure 5.9 the hydrogen-hydrogen interaction between the ortho hydrogens of the planar biphenyl molecule is shown in red. The gradient lines of the inner hydrogens show that the two atomic basin do interact and the interaction prevents the other carbon atoms from interfering with the interaction. The values for the (3, -1) critical point between the centre carbons and the two hydrogens are shown in table 5.3 along with the (3, +1) critical point formed by the closing of the ring.

Table 5.3: *The MEP, ratio, ρ , $\nabla^2\rho(r)$ and kinetic energy (G) values for the (3, -1) saddle point between the centre carbons and the ortho hydrogens as well as the (3, +1) saddle point formed by the closing of the ring. All values are calculated in atomic units except for the ratio.*

	nucMEP	elecMEP	MEP	ratio	ρ	$\nabla^2\rho(r)$	G
(3, -1) C-C	22.6800	-21.9737	0.7062	1.0321	0.2668	-0.7499	0.0535
(3, +1)	16.8904	-16.8153	0.0751	1.0045	0.0125	0.0593	0.0120
(3, -1) H-H	14.9821	-14.8941	0.0881	1.0059	0.0115	0.0402	0.0084

The values for the MEP ratio at the (3, -1) saddle point are comparable to a hydrogen bond in water (1.0034), the decrease in values for the central carbon-carbon bond compared to an ethylene molecule indicates delocalisation of the electrons. The delocalisation of the electrons is also seen in the topology of the MEP where the minima and (3, +1) saddle points have been previously linked to aromaticity. These delocalised electrons can stabilise the ortho hydrogen-hydrogen interaction causing the interaction to be stabilising [4, 20]. The low values for the ρ , $\nabla^2\rho(r)$ and kinetic energy (G) describe an interaction that is comparable to a van der Waals interaction [14].

However, Cioslowski showed that while the delocalised electrons in a molecular structure with a ring can lead to stabilisation of a weak bond, the low values for electron density and the laplacian can also be indicators of destabilising repulsive interactions [14]. This idea is supported by the laplacian which has a value of 0.0402 a.u., the positive value is interpreted as a closed shell interaction which means that the electrons are contracting away from the (3, -1) saddle point. This is reinforced by the low electron density which is 0.0115 a.u. and with a lower electron density between the hydrogens, it is possible that there is an increase in the positive charge, and therefore the interaction would be repulsive.

There is a different interpretation of the results which is based on the concept that as long as the repulsive forces (Feynman forces) are cancelled by the attractive forces (Ehrenfest force) then the interaction between two atoms is stabilising. The movement of the delocalised electrons to the region between the ortho hydrogens is sufficient to cancel the two opposing forces [18, 21]. This is seen in the results where the values for the carbon-carbon bond joining the rings is reduced compared to the ethylene molecule. The difference in the nucMEP at the (3, -1) critical point between the joining carbons and the (3, -1) critical point between the ortho hydrogens is 7.6979 a.u. and the elecMEP is -7.0796 a.u. The greater decrease in the nucMEP compared to the elecMEP may show that the electron density is held in the ring formed by the ortho hydrogens which would be stabilising. The MEP ratio should not be ignored as it directly shows the balance of the competing forces and a ratio of 1.0059 places the interaction as stabilising.

The discussion so far has been around whether or not the ortho hydrogen-hydrogen interaction is stabilising. The decrease in the electron density from the connecting carbon-carbon bond has been used to suggest that the movement of electrons was to stabilise the hydrogen-hydrogen interaction. Hernández-Trujillo and Matta have suggested that the hydrogen-hydrogen interaction is locally stabilising and that the changes in the carbon-carbon bond is locally destabilising [23]. Matta and co-workers also showed that the hydrogen-hydrogen interaction can be as strong, if not stronger, than a hydrogen bond [18].

Poater, Solà and Bickelhaupt tried to show that the hydrogen-hydrogen interaction was destabilising through a series of calculations, one of which was to fix the bonding lengths of all the atoms in biphenyl and then rotate the two rings [19]. The problem with this approach is that the atoms can not adjust to new forces being introduced via the rotation of the rings. This is a problem because Matta *et. al.* showed that while the connecting carbon-carbon bond showed signs of destabilisation, the rest of the molecule adjusted to a new equilibrium and therefore all the forces acting in the molecule were cancelled [18]. Poater, Solà and Bickelhaupt tried to prove the hydrogen-hydrogen interaction was repulsive by removing the hydrogens from the planar biphenyl and showed that the molecule was more stable. As has been seen in an earlier chapter, where the methane molecule was studied, changing bond length and bond angles can have a significant effect on the MEP topology and therefore removing the ortho hydrogens from the planar biphenyl molecule creates an entirely new topology. Comparing the two topologies would mean comparing two different systems and which would lead to incomplete conclusions, this conclusion has been reached by other researchers [18, 20, 23].

The biphenyl molecule in figure 5.10 is calculated in the optimised twisted geometry, one probe is placed between the ortho hydrogens and another probe is placed between the probe and the (3, -1) saddle point. The values for the two probes as well as for the (3, -1) critical point between the centre carbons is shown in table 5.4.

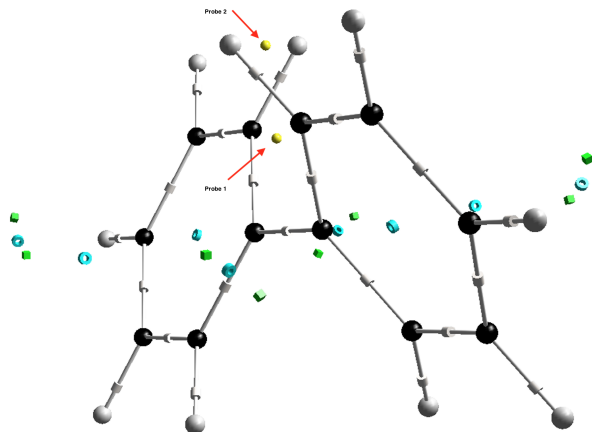


Figure 5.10: The topology of the biphenyl molecule calculated in the MEP is shown with two probes (yellow spheres), one is positioned where a $(3, -1)$ critical point would be in the planar structure and the second probe is placed in the centre to signify a $(3, +1)$ critical point. The white spheres are hydrogen atoms and the black spheres are carbon, the cylinders are $(3, -1)$ critical points.

Table 5.4: The MEP, ratio, ρ , $\nabla^2\rho(r)$ and kinetic energy (G) values of the twisted biphenyl structure with two probes positioned between the ortho hydrogens and in the place of the $(3, +1)$ critical point. All values are calculated in atomic units except for the ratio

	nucMEP	elecMEP	MEP	ratio	ρ	$\nabla^2\rho(r)$	G
$(3, -1)$ C-C	22.8277	-22.1113	0.7164	1.0324	0.2729	-0.7874	0.0546
probe 1	19.2296	-19.0978	0.1318	1.0069	0.0261	0.1320	0.0296
probe 2	15.5371	-15.5046	0.0325	1.0021	0.0061	0.0236	0.0047

In figure 5.10 it can be seen that there are delocalised electrons as depicted by the alternating minima and saddle points. As probe 1 is closer to the centre of the molecule it would make sense that the MEP and electron density is higher than the $(3, +1)$ counter part in the planar biphenyl structure. As the probe moves further away from the centre of the molecule, the values for probe 2 are less than for the $(3, -1)$ saddle point in the planar biphenyl. Bringing the hydrogens closer together increases the MEP and the electron density between them while the kinetic energy barely changes.

The difference in values between the planar and twisted biphenyl structures at the $(3, -1)$ critical point (probe 2 for the twisted geometry) could be explained by the delocalisation and redistribution of the electrons in the planar structure. The MEP ratio at probe 2 shows that the interaction between the hydrogens is slightly weaker than a hydrogen bond in water. No critical point is calculated between the ortho hydrogens for the twisted geometry and this has been explained by the two hydrogens moving too far away from each other [14]. As is shown in figure 5.11 the hydrogens are still close enough to influence each other, the space between them is also influenced by the carbon atoms which prevents a critical point from being calculated. A similar system was studied when analysing the chrysene molecule.

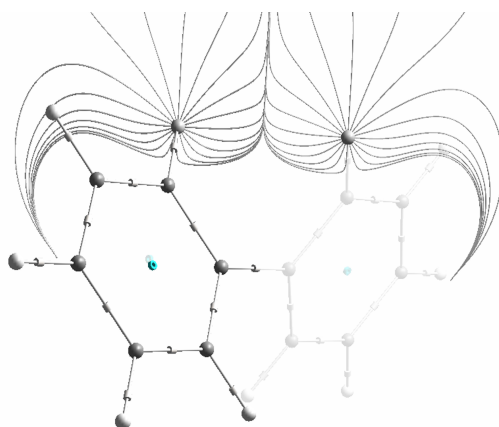


Figure 5.11: *The gradient lines of the ortho hydrogen for the twisted biphenyl molecule show that the hydrogens are still interacting but do not form a critical point.*

5.4 Congested Molecules

Congested molecules inevitably have atoms that are forced close together and in this section the congested hydrogens are of interest. A series of congested molecules are calculated and the congested hydrogens are analysed using the topology of the MEP. The congested molecules are also calculated with fluorine to better understand the influence that a halogen would have on the hydrogen-hydrogen interactions. A total of seven congested molecules are analysed and are listed below in figure 5.12 along with the fluorinated structures. The molecules were fully optimised and calculated with a basis set of 6-311G(d,p) and a Hartree-Fock level of theory. The author participated in an earlier study of congested molecules where four energy criteria were correlated with the appearance of a (3, -1) critical point and atomic interaction line [86].

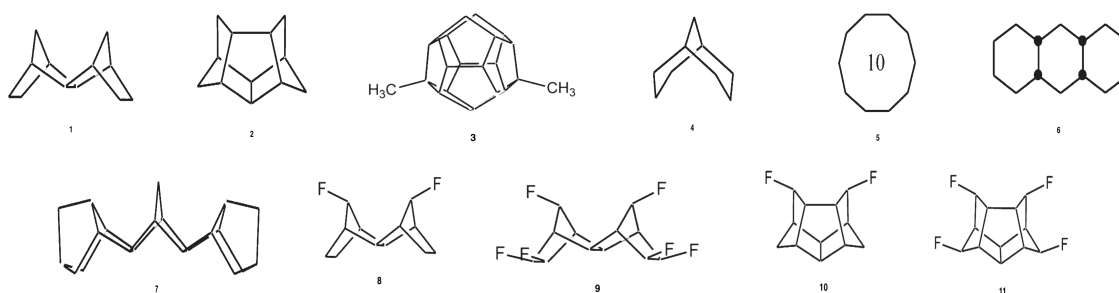


Figure 5.12: *The molecular structures of (1) exo-exo-tetracyclododecane, (2) Pentacyclododecane, (3) 1,6-dimethylmonosecododecahedrane, (4) bicyclononane, (5) cyclodecane, (6) cis-syn-cis-perhydroanthracene, (7) exo-exo-octacycloheneicosane, (8) 11,12-difluoro-exo-exo-tetracyclododecane, (9) 4,5,9,10,11,12-hexafluoro-exo-exotetracyclododecane, (10) 5,9-difluoro-pentacyclododecane, (11) 5,9,11,12-tetrafluoropentacyclododecane.*

Tables 5.5 and 5.6 show the values for all the hydrogen-hydrogen interactions calculated. The values of the nucMEP and elecMEP make it clear that the interactions in the molecule are

seen at the (3, -1) saddle point which is evident by the high MEP values when compared to a hydrogen molecule. The influence of the other atoms is also seen in the different values calculated for a hydrogen-hydrogen interaction. Some molecules, like cyclodecane and cis-syn-cis-perhydroanthracene, have multiple hydrogen-hydrogen interactions but these interactions are not equal which should be obvious because bond distance and atomic positions are different for the hydrogens. This all means that when analysing the hydrogen-hydrogen interaction, the effects that it has on the molecule are seen in the values at the (3, -1) critical point. Any strain on the molecule will be distributed throughout the molecule and will inevitably be seen in the hydrogen-hydrogen interaction. This means that only the hydrogen interaction needs to be analysed. If the interaction between the hydrogens is locally stabilising then the molecule will be stable and if the interaction is destabilising then the molecule will be unstable, this is not a unique concept [18].

It has been shown with the chrysene molecule that the hydrogens in the hydrogen-hydrogen interaction need to dominate the space between them, this follows a fundamental principle of QTAIM where two atomic basins need to share a common surface created by two interacting atoms [4]. The interaction between the hydrogens needs to be strong enough to prevent the carbon atoms from influencing the interaction at the (3, -1) saddle point. The problem that still needs to be addressed is, if the interaction shows signs of repulsion, this thesis has suggested that the ratio of nucMEP to elecMEP is a good indication of the nature of the interaction.

To test for a stabilising or destabilising interaction (attractive or repulsive) the focus needs to be on whether the repulsive positive charge is equalled by the attractive negative charge. The benefit of the MEP is that these two opposing forces are calculated together and the purpose of the MEP ratio is to find the balance between these forces that results in a stable interaction. This was done by comparing the ratios of various bond types and bond orders and for the hydrogen-hydrogen interaction, the comparison to a hydrogen bond in water was the best fit. The ratios for the hydrogen-hydrogen interaction in tetracyclododecane and pentacyclododecane are 1.0049 and 1.0048 respectively and when compared to the hydrogen bond in water, 1.0034, the interaction can be interpreted as not only being stabilising but also stronger than the hydrogen bond. The possibility of a hydrogen-hydrogen interaction being as strong, if not stronger, than a hydrogen bond has already been proposed [18].

The large positive value for the laplacian for tetracyclododecane and pentacyclododecane, 0.0503 a.u. and 0.0608 a.u. respectively, points to a contraction of the electron density away from the (3, -1) critical point, which is mirrored by the low electron density, 0.0149 a.u. and 0.0173 a.u. respectively. The contraction of the electron density away from the (3, -1) critical point could suggest that there would be an increase in the positive charge between the atoms and an overall repulsive interaction would occur, but the low value of the kinetic energy, 0.0107 a.u. and 0.0129 a.u., makes this unlikely. It is worth mentioning that the ellipticity for the hydrogen-hydrogen interactions is 0.1445 and 0.2053, these values are not consistent with destabilised interactions as the values indicate that the electron density is not greatly spread out in a plane perpendicular to the atomic interaction line between the hydrogens.

Cyclodecane and cis-syn-cis-perhydroanthracene have multiple hydrogen-hydrogen interactions yet the values for the secondary hydrogen-hydrogen interaction vary significantly, these molecules are shown in figure 5.13. The primary hydrogen-hydrogen interaction is shown in red and the secondary interactions in blue. The separation of the interactions into primary and secondary interactions was based on the MEP ratio with a stronger interaction being the primary hydrogen-hydrogen interaction. In table 5.5 the primary hydrogen-hydrogen interaction is labelled A and the secondary interaction B. The accumulation of electron density between the primary and

secondary hydrogen-hydrogen interactions in cyclododecane are almost identical however the focus of the nucMEP and elecMEP is between the hydrogens in the centre of the molecule. The ellipticity for the primary interaction in cyclododecane is 0.0726 indicating that the electron density is dispersed more along the atomic interaction line than in the planes perpendicular to the AIL. In contrast the secondary interaction has a ellipticity value of 0.3214 which would indicate a weaker interaction.

The differences in the primary and secondary interactions for cis-syn-cis-perhydroanthracene are more evident than in cyclododecane. The ratio for the primary hydrogen-hydrogen interaction is 1.0028 compared to 1.0000 for the secondary interaction. A value of 1 for the MEP ratio is an indication that the interacting hydrogens are self contained as the positive potential is equalled by the negative potential. The ellipticity for the secondary interaction is 0.7859 which is linked to an unstable (3, -1) saddle point, which is close to a catastrophe (joining with the (3, +1) critical point and disappearing). In contrast, the ellipticity for the primary interaction is 0.0784, which does indicate a stable critical point. The kinetic energy for the primary and secondary interactions is very low and this would suggest that the interaction between the hydrogens is very weak.

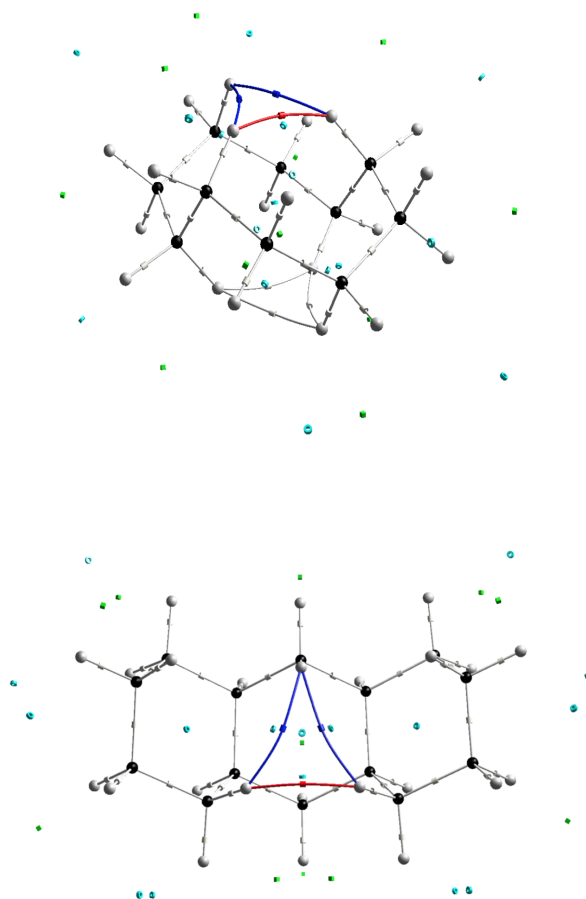


Figure 5.13: *The molecules of cyclododecane (top) and cis-syn-cis-perhydroanthracene (bottom) with the main hydrogen interaction line shown in red, and labeled as A in table 5.5, and secondary interaction lines shown in blue, labeled as B in table 5.5.*

Table 5.5: The MEP, ratio, ρ , $\nabla^2\rho(r)$ and kinetic energy (G) values for interacting hydrogens in congested molecules. The A and B for molecules cyclododecane and cis-syn-cis-perhydroanthracene refer to two different hydrogen-hydrogen interactions which are shown in figures, 5.13. The main hydrogen-hydrogen interactions is shown in red and the secondary interaction is shown in blue. All values are calculated in atomic units except for the ratio.

	nucMEP	elecMEP	MEP	ratio	ρ	$\nabla^2\rho(r)$	G
exo-exo-tetracyclododecane	17.2609	-17.1769	0.0840	1.0049	0.0149	0.0503	0.0107
Pentacyclododecane	17.1338	-17.0527	0.0812	1.0048	0.0173	0.0608	0.0129
1,6-dimethylmonosecododecahedrane	24.1977	-24.1205	0.0771	1.0032	0.0146	0.0492	0.0105
bicyclononane	14.6344	-14.5824	0.0520	1.0036	0.0108	0.0338	0.0074
cyclododecane A	16.6016	-16.5428	0.0588	1.0035	0.0107	0.0331	0.0073
B	16.0960	-16.0534	0.0426	1.0026	0.0086	0.0270	0.0059
cis-syn-cis-perhydroanthracene A	19.6033	-19.5490	0.0543	1.0028	0.0096	0.0286	0.0063
B	20.6315	-20.6315	0.0240	1.0000	0.0051	0.0166	0.0036
exo-exo-octacycloheneicosane	23.5170	-23.4576	0.0594	1.0025	0.0121	0.0391	0.0084

Table 5.6: The MEP, ratio, ρ , $\nabla^2\rho(r)$ and kinetic energy (G) values for interacting hydrogens in congested molecules with halogens. All values are calculated in atomic units except for the ratio.

	nucMEP	elecMEP	MEP	ratio	ρ	$\nabla^2\rho(r)$	G
11,12-difluoro-exo-exo-tetracyclododecane	20.5097	-20.3841	0.1255	1.0062	0.0158	0.0562	0.0118
4,5,9,10,11,12-hexafluoro-exo-exotetracyclododecane	24.2926	-24.1311	0.1615	1.0067	0.0171	0.0618	0.0130
5,9-difluoro-pentacyclododecane	20.5758	-20.4461	0.1296	1.0063	0.0192	0.0727	0.0153
5,9,11,12-tetrafluoro-pentacyclododecane	22.5718	-22.4186	0.1532	1.0068	0.0212	0.0802	0.0171

The addition of the fluorine atoms can immediately be seen in the nucMEP and elecMEP at the (3, -1) critical point between the congested hydrogens. The addition of the fluorine atom appear to increase the strength of the hydrogen-hydrogen interaction as the MEP ratio for tetracyclododecane and pentacyclododecane are increased from 1.0049 to 1.0062 and 1.0048 to 1.0063 respectively. The addition of even more fluorine atoms to the molecules further stabilised the hydrogen-hydrogen interaction. The increase in the kinetic energy is further evidence of a stabilising interaction. Despite this the laplacian at the (3, -1) critical point is increased with the addition of fluorine atoms which means there is more of a contraction of the electron density away from the critical point.

5.4.1 Conclusion

This chapter focused on two questions. First, whether or not the Quantum Theory of Atoms in Molecules (QTAIM) combined with the topology of the Molecular Electrostatic Potential (MEP) could be used to discern between interacting atoms and atoms that are merely close together. Secondly, could the topology and MEP surrounding the hydrogen-hydrogen interactions be enough to answer the question, is the hydrogen-hydrogen interaction a stabilising interaction or destabilising interaction?

Using the chrysene molecule it was shown that two atoms close to one another will not automatically result in a (3, -1) critical point and Atomic Interaction Line (AIL). The distance between the atoms was ruled out as the cause for no critical point being calculated, previous chapters have shown that a (3, -1) critical point and AIL can be calculated for atoms further than 3.0 Å apart. While the separation of the atoms is not the cause of no critical point being calculated, it is a contributing factor as it weakens the interaction between the interacting atoms, which allows for interference from other atoms in the molecule. The gradient plots of the cis-2-butene and chrysene molecules showed the importance that the interacting hydrogens dominate the space between them. The gradient plots of the chrysene molecule showed that while the atomic basins of the hydrogens did eventually touch, the influence of the carbon atoms disrupted the interaction to the extent that no critical point was calculated.

The topology of the electron density and the MEP for the congested molecules are homeomorphic (their geometric structures are the same) and as such the result is that the hydrogen-hydrogen interaction is stabilising. In terms of the values for the interacting hydrogens, the results are not as clear. The MEP ratio in most cases indicates an interaction that is stronger than a hydrogen bond and the low positive values of the laplacian, compared to the hydrogen bond in water, show that there is some contraction of the electron density but the laplacian is within the limits for a stabilising closed shell interaction.

The low values of the electron density as well as the kinetic energy can be used to argue that the interaction between the hydrogens is not stabilising and possibly destabilising as pointed out by Cioslowski. There are also two major issues for the MEP ratio that should be considered. First, an increase in the nucMEP indicates a build up of positive potential which would be repulsive but for an interaction like a hydrogen-hydrogen bond where the ratio is low, the increase in the nucMEP would increase the ratio but could still keep it below the ratio for a carbon-carbon bond, for example. The second issue is that there is no direct way to link a repulsive interaction to the MEP ratio. In an earlier chapter the hydrogen molecule in the triplet state was calculated at different interatomic distances and the fully optimised structure resulted in a bond length of 5.044 Å. However, it is possible to fix the bond length of the hydrogen atom in order to

calculate a favourable ratio and for congested molecules, where the hydrogens are forced into close proximity to each other, the MEP ratio could still indicate a favourable interaction.

In the end the MEP topology can not be used as a stand alone calculation to determine stabilising or destabilising interactions and should be used in conjunction with other scalar fields to determine the type of interaction taking place.

Chapter 6

Conclusion

The purpose of the thesis was to answer two questions. First, can the quantum theory of atoms in molecules (QTAIM) discern between interacting molecules or do all nuclear attractors in close proximity to each other result in a bond critical point (BCP) and atomic interaction line (AIL) being calculated? Secondly, is it possible to use QTAIM with the topology of the molecular electrostatic potential (MEP) to determine if hydrogen-hydrogen interactions in congested molecules are stabilising or destabilising?

The first question is an important one for any computational study. Unlike with physical experiments where the molecules obey the laws of nature, molecules that are calculated obey the laws of the variables set by the researcher to describe the laws of nature. Being able to control the variables and calculate the exact molecule desired has its benefits and can be used to answer difficult questions, but relies on the researchers to decide if the molecules are feasible in reality and this can pose a real problem. An example of this problem is a bond between atoms that is strained, strained bonds do exist in nature but as is highlighted in this thesis there is a lot of discussion around how much strain is too much to be believed.

There is of course a way to measure the strain of a bond and relate it to destabilising the molecule, that is to measure the energy of the molecule without the bond in question and compare it to the energy of the molecule when the bond is present. If the energy of the molecule is higher when the bond is present the interaction is deemed destabilising and if the energy is lower the bond is stabilising. The question then arises, how does one measure a molecule without a bond between two atoms and then with a bond between the atoms. One way is to split the molecule into two halves and measure the energy of the two molecules and add them together and then compare to the energy of the molecule created by combining the two halves.

Another way is to simply remove the atoms that have the bond in question and create a molecule with radicals and compare the energies of the two molecules. Comparing two systems that are different introduces a few problems one of which is that the forces present in the different systems are exactly that, different. To demonstrate the sensitivity of the MEP topology to changes the methane molecule was studied. Simply stretching the bonds of methane altered the topology and changing a single atom altered the topology of the rest of the molecule, this is due to the disruption of the symmetry of the molecule. The symmetry of a molecule is mirrored by the symmetry of the topology of the MEP. It should also be mentioned that there is the situation where the strained bond can be locally stabilising but globally destabilising, how does

a researcher decide which energy is more important and which method is more accurate.

The molecular electrostatic potential is ideally suited for the task of comparing forces in a molecule due to the charges present as it consists of the nuclear and electronic potentials. Through the study of common molecules and more specifically the types of bonds that are between hydrogens and other atoms (including hydrogen atoms) a standard can be set up that solely relies on the MEP and no preconceived ideas. This is explored in chapter 4 but first the topology of the MEP needed further investigating and explaining. The MEP is appealing as it is calculated from both the nuclear potential and the electronic potential and allows for a direct comparison of the two competing forces. However, the MEP topology can often be populated by many critical points and this can lead to many interpretations of the topology. This is explained in chapter 2 but explored further in chapter 3.

The critical points can be confusing as they represent focal points in the MEP which are regions in the field that are significant but not always for the same reason. A (3, -1) critical point between two (3, -3) critical points is mathematically similar to a (3, -1) critical point located outside the molecule (look at benzene for a good example of this). Even though these critical points are similar, both signify a similar shape of the field, they are interpreted differently. This is perhaps more noticeable with the (3, +3) critical points as these critical points are present in both a negative potential field as well as a positive potential field and can further be attached to the location of lone pairs.

The research presented in chapter 3 agreed with previous studies that minima around bonded carbon atoms can be used to show pi-bonding (for double bonds). The alternating minima and (3, +1) saddle points do show the delocalisation of the electrons in a molecule when located parallel to the molecule (an example is *trans*-1,3-butadiene or more commonly, benzene). When located in a ring around a (3, -1) saddle point (in a plane perpendicular to the bond), the alternating critical points show the location of a triple bond.

When analysing the minima in the MEP topology it was noticed that the minima are not always associated with a negative MEP. The ammonia molecule is calculated with two minima, one is negative and can be associated with a lone pair and the second minima is positive. The positive (3, +3) critical point is a result of the MEP being a minimum in a region of the molecule that is dominated by the nuclear potential of the MEP.

It has been suggested that the minima calculated between the hydrogens of a methyl group is a result of the sp^3 hybridisation. It was noticed that the minima calculated were dependent on the size of the molecule as well as the shape of the molecule. When the bond lengths in the methane molecule were lengthened the minima associated with sp^3 hybridisation was calculated at different positions. The *cis*-2-butene molecule also showed a shifting of the minima when one of the hydrogens was involved in a possible hydrogen-hydrogen interaction.

These anomalies with the minima lead to the conclusion that the minima calculated in the MEP topology can not immediately be associated with locations of high electron density. This conclusion does not mean that there is no electron density present in the area but serves as more of a warning about equating minima in the MEP field with electrons. It is possible that the minima located between the methyl groups and in positive potential regions of a molecule serve as a way for molecules to identify and orientate themselves for reactions but this type of research is beyond the scope of this study.

Another aspect explored in chapter 3 was the degenerate critical points. These critical points of rank 2 were commonly found in linear molecules with triple bonds and served as a way of

identify triple bonds but even though it is common it is not always true. The C_2N_2 molecule is a linear symmetrical molecule with triple bonds yet no degenerate ring is calculated around the molecule. Even associating a ring of degenerate critical points with a triple bond is not always correct as is shown with linear molecules consisting of halides or the hydroxyl anion. In all these cases the degenerate ring is an indication of the symmetry of the molecule and the rings are broken into minima and (3, +1) saddle points when the symmetry is disrupted.

The main goal of chapter 4 is to set up a method to understand bonding interactions between atoms, a method that is separate from human intuition. Building on Coulombs law the balance between the positive nuclear potential and negative electronic potential between atoms was explored in more detail. There should be a common ratio of positive to negative charge that is consistent through all types of interacting atoms, a ratio that implies a balance of repulsive and attractive forces. The ratio of positive and negative charges at equilibrium is an alternative representation of the concept of repulsive Hellmann-Feynman forces and attractive Ehrenfest forces.

The first approach in chapter 4 was to see if QTAIM would consistently find a saddle point between two nuclear attractors and this was tested by stretching the bond length in a diatomic molecule. This was done with hydrogen molecules in the singlet and triplet state as well as with diatomic noble gases. Predictably a saddle point was always calculated between the nuclear attractors and while basis sets and theory used in the calculation may influence this, mathematically there should always be a saddle point when only two nuclear attractors are present. This is due to the simple fact that a line of maximum density will always exist between two nuclear attractors in a diatomic molecule, unless the cut off value for locating critical points is set high as this would prevent a program from calculating the small changes in density at large distances. However, what is shown later in the chapter and in chapter 5 is that competing forces from other nuclear attractors influences where saddle points are calculated and simply having two nuclear attractors side by side is no longer sufficient to have a saddle point with an atomic interaction line, the two nuclear attractors need to be interacting with each other.

This interaction leads into the main discussion of what it means for two atoms to interact and form a bonding interaction. In order for the nuclear attractors to be interacting they need to share a common boundary, this would be the surface of the atomic basin of each nuclear attractor. The forces that are present are now solely between the two nuclear attractors as they have excluded the influence of all other nuclear attractors that may be present. If these forces are in equilibrium then a saddle point with atomic interaction line is present and if not then the nuclear attractors separate enough for other nuclear attractors to interfere.

What became clear early on is that the MEP value alone was not a good indicator of a stable interaction as it fluctuated (rather predictably) with the type of atoms present. This also prevented a direct comparison between different bond types and bonds between hetero atoms. This made the use of the MEP ratio more appealing because larger atoms did introduce more electrons but also a larger nucleus which translated into a larger positive potential. Chapter 4 showed that the ratio made comparing interactions possible and could also be used in identifying bond types. The changes in bond lengths are reflected in the MEP ratio and can be used to identify single, double and triple bonds between carbon atoms. Hydrogens bonded to carbons that are part of single, double or triple bonds (also noticed for carbons that are part of an aromatic ring) are reflected in the MEP ratio at the (3, -1) critical point between the hydrogen and carbon.

It is also shown that the MEP ratio can be used to study different bond types including covalent,

polar covalent (dative), ionic and hydrogen bonds. By comparing the MEP ratios for different bond types and bond orders the Coulomb forces in these interactions could be understood and associated with equilibrium forces. This can then be applied to controversial atomic interactions such as hydrogen-hydrogen interactions.

While chapter 4 seems to introduce a method that solves the problems of what makes an interaction between atoms a bonding interaction it did introduce some problems. When analysing the hydrogen molecule in the triplet state the MEP ratio not only passed through the ratio of a stable singlet hydrogen molecule but also the ratio of most other covalent bonds. This shows that just because the ratio shows a balance between positive and negative potentials it does not always represent the forces present in the molecule. This problem is raised in chapter 5 when discussing congested hydrogens. An argument could be made that the result between the triplet hydrogens only tested what occurs in a diatomic molecule and as stated earlier, when other atoms are present they introduce competing forces that may disrupt the interaction between the hydrogens.

Chapter five uses the concepts developed in the previous chapters and applies them to understanding when a (3, -1) critical point is calculated between two nuclear attractors (NA) and if the hydrogen-hydrogen interaction in congested molecules is stabilising or destabilising.

The chrysene molecule is used to determine if the QTAIM model can discern between two interacting atoms in the MEP topology. The results showed that it is possible for the QTAIM method to distinguish between interacting atoms and non-interacting atoms. It is shown that this is not a result of the distance between the atoms as chapter three showed that even at distances of 4 Å a (3, -1) critical point can be calculated. The difference between calculating a (3, -1) saddle point and not calculating a saddle point was due to the ability of the interacting atoms to dominate the space between them. This follows from one of the criteria of QTAIM: the atomic basins need to touch in order to form an interatomic surface. If the forces between two interacting atoms are not strong enough to prevent interference from other atoms in a molecule then a (3, -1) saddle point will not be calculated. This is shown with the chrysene and planar biphenyl molecules.

The contour and gradient plots of the planar biphenyl molecule show that interaction between the ortho hydrogens is strong enough to form a ring. The MEP ratio for the hydrogen-hydrogen interaction is as strong as a hydrogen bond. When the biphenyl molecule is calculated in the twisted geometry it is clear the hydrogens no longer have an interaction that is strong enough to prevent the carbon atoms from disrupting the interaction. This is also reflected in the ratio which is 1.0059 for planar biphenyl and 1.0021 for the twisted biphenyl.

When the concepts developed in previous chapters are applied to hydrogen-hydrogen interactions in congested molecules, the results show limited success. The MEP ratio can be applied to differentiate between primary and secondary hydrogen-hydrogen interactions as is shown for molecules cyclodecane and cis-syn-cis-perhydroanthracene. In each case the congested hydrogens dominated the space between them and the MEP ratios were similar to the ratio for a hydrogen bond with the exception of the secondary hydrogen-hydrogen interaction in cis-syn-cis-perhydroanthracene. The addition of fluorine to the congested molecules resulted in an apparent stabilisation of the hydrogen-hydrogen interaction as the ratios increased.

The ellipticity for the (3, -1) critical point between the NAs show that the electron density is concentrated along the atomic interaction line as opposed to spread out in the plane of the ring. This would indicate that the interaction is a stable one. The positive laplacian values indicate that the interaction is closed shell interaction, but this is a common trait for hydrogen

bonds and polar interactions. The low values for the electron density support the results of the laplacian but this too is a common occurrence for closed shell interactions. The low values for the kinetic energy reveal that there is no significant repulsion between the hydrogens.

Unfortunately, these results can also be associated with a repulsive interaction. Low values of electron density are also common for interactions that are destabilising as the interaction could be interpreted as being repulsive as a result of not having a sufficient negative charge between the atoms. A positive laplacian is a result of a contracting electron density away from the saddle point and this could support the idea the atoms are repelling each other. The low values of kinetic energy can also be interpreted as a consequence of atoms that are simply not interacting with each other.

Even the MEP ratio is not conclusive. As was shown in chapter four, by calculating H_2 in the triplet state, it is possible to create a favourable ratio by fixing the distance between the NAs. This argument can then be applied to congested molecules where the hydrogens are forced into a close proximity. This can create a MEP ratio that indicates a favourable interaction that is ultimately incorrect.

The final conclusion of this thesis is that QTAIM and the MEP topology are a powerful tool for understanding the interactions and properties of atoms. However, the interpretation of the topology requires an understanding of the molecules being analysed in order to properly interpret the result and this can introduce human bias. The QTAIM method with the MEP topology is not sufficient to determine if the hydrogen-hydrogen interaction in congested molecules is stabilising or destabilising.

The research covered in this thesis answered the two questions asked at the beginning of this chapter, QTAIM can be used effectively to differentiate between interacting and non interacting atoms. As for whether the MEP topology can be used to identify stabilising or destabilising interactions between congested hydrogens, the answer is that it adds value to the discussion of these types of interactions. As with most research when attempting to answer a question one inevitably finds more questions than answers. This research showed or re-affirmed that there are many types of interactions between atoms, interactions that have a stabilising effect on a molecule. However, not all of these weak interactions are considered as bonding by the scientific community and perhaps this is because some interactions do not match with the notion of what a bond should be ie: consisting of shared electrons.

At times it seemed that there was a battle between classic and quantum mechanics, the notion of negative point charges (electrons) between positive point charges (nuclei) being a description of a bond excludes the other types of interactions that equally important for the formation of molecular structures like crystals or polymers. Using quantum mechanic, as QTAIM does, provides a much more comprehensive explanation of what occurs between atoms in molecule and in a bonding interaction, it introduces and quantifies the contribution that atoms in molecule have towards a bonding interaction somewhere else in the molecule.

Finally, while this research could not definitively conclude if the hydrogen-hydrogen interaction in congested molecules is stabilising or destabilising it did show the possibilities of using the topology of MEP, not just in understanding the interactions between atoms but also the complexity of the molecules. Even though the research presented did not focus on chemical reaction pathways the topology of the MEP can definitely increase the understanding of reaction pathways and hopefully change the way we consider bonding interactions.

Appendix A

The author of this thesis was part of another study involving interactions of atoms in congested molecules. The study involved the analysis of a bond path between two non-bonded atoms in a series of sterically crowded derivatives of tetracyclododecane. Four energetic criteria were compared and correlated with the calculation of the bond path.

The conclusion of this research was that the bond paths that were calculated had little to do with changes in the atomic energies but was instead a consequence of the quantum theory of atoms in molecules (QTAIM) model and the scalar field it was applied to.

The authors contribution to this paper was to apply the QTAIM method to the different scalar fields used in this research. This paper was not included as a chapter as the main calculations (the wavefunctions for the molecules) was carried out by D. Myburgh.



A Comparison of Energetic Criteria to Probe the Stabilizing Interaction Resulting from a Bond Path Between Congested Atoms

Dirkie Myburgh, Stuart von Berg, and Jan Dillen *

Four energetic criteria, all rooted in the partitioning of a molecule into atomic basins based on the properties of the electron density, are compared and correlated with the presence of a bond path between two nonbonded atoms in a series of sterically crowded derivatives of the same tetracyclododecane molecule. It was found that there is no correlation between the

selected energetic criteria and the existence of a bond path between the congested atoms, nor with the existence of Ehrenfest force, virial, or Coulomb potential paths between those atoms. © 2018 Wiley Periodicals, Inc.

DOI:10.1002/jcc.25547

Introduction

In his work on the Quantum Theory of Atoms in Molecules (QTAIM), Bader^[1,2] describes how the topology of the electron density, $\rho(\mathbf{r})$, and its gradient provides a mapping to the fundamental concept of molecular structure. This results in the quantum definition of an atom, and atomic statements of the Ehrenfest force law and the virial theorem.

Since then, the topology of a variety of scalar and vector fields has been studied.^[3–10] The purpose of many of these fields is to localize the electrons in a system. Popelier et al.^[11] refer to these topological investigations as quantum chemical topology (QCT).

According to Bader's theory, the presence of a bond path in the electron density and a corresponding critical point, where the gradient of the latter is zero, is an indicator of a stabilizing interaction.^[12–15] However, in recent years, some controversial QTAIM topologies have resulted in sometimes heated debates.

Cioslowski and Mixon^[16–19] have stated that bond paths between sterically crowded molecules should be interpreted as nonbonding repulsive interactions.

Haaland and coworkers^[20,21] have suggested that the interaction between a helium atom included in an adamantane cage and its surrounding atoms is antibonding. This resulted in a number of different counter arguments.^[13,22,23]

Bickelhaupt and coworkers^[24] argued that the nature of the interaction between the ortho-hydrogens in planar biphenyl opposes the concept of a hydrogen–hydrogen bond as proposed by Bader and coworkers.^[25] This sparked several additional articles.^[26–29]

Bader has stated that although a bond path indicates a stabilizing interaction, it is not to be confused with a bond.^[12,30] This has prompted the question^[31] whether QTAIM introduces a “new” type of bonding and even whether we need another IUPAC commission to decide on this.^[32–34]

Despite the above mentioned discussions, it seems rational to determine the attractive or repulsive nature of an interaction

on the basis of energetic arguments. In the case of intermolecular interactions this is relatively straightforward, but in the case of intramolecular interactions this requires a reference state, unless one can calculate the interaction directly.

In this work, we investigate the interactions between the congested atoms in hetero-atom derivatives of the hydrocarbon molecule *exo-exo*-tetracyclo[6.2.1.1^{3,6}.0^{2,7}]dodecane, shown in Scheme 1.

We have chosen derivatives of one molecule only to minimize the effect of a different chemical environment of the interactions. In addition, the energetic arguments employed to determine the presence of an interaction between two classically nonbonded atoms connected by a bond path, are rooted in the QTAIM itself.

Theory and Methods

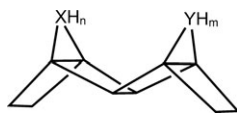
After application of the Born–Oppenheimer approximation, the Hamiltonian of a many electron system is, in atomic units, equal to

$$\hat{H} = -\frac{1}{2} \sum_i \nabla_i^2 - \sum_j \sum_{\alpha} \frac{Z_{\alpha}}{|\mathbf{r}_j - \mathbf{R}_{\alpha}|} + \sum_i \sum_{j>i} \frac{1}{|\mathbf{r}_i - \mathbf{r}_j|} + \sum_{\alpha} \sum_{\beta>\alpha} \frac{Z_{\alpha} Z_{\beta}}{|\mathbf{R}_{\alpha} - \mathbf{R}_{\beta}|} \quad (1)$$

where the summations run over all the electrons i and j and over all the nuclei α and β . The atomic number of a specific nucleus is Z , the symbol \mathbf{R} refers to its position and \mathbf{r} to the position of an electron.

The first term in this expression refers to the kinetic energy of the electrons. The second and third term are operators

[a] D. Myburgh, S. von Berg, J. Dillen
Department of Chemistry and Polymer Science, Stellenbosch University,
Private Bag X1, maTieland, Stellenbosch 7600, South Africa
E-mail: jldm@sun.ac.za



Scheme 1. Derivatives of tetracyclododecane.

representing the nucleus–electron and electron–electron interactions, respectively, whereas the last term refers to the nucleus–nucleus repulsion.

The Ehrenfest force operator is defined as

$$\hat{\mathbf{F}}_1 = -\nabla_1 \hat{V} = -\sum_{\alpha} Z_{\alpha} \frac{\mathbf{r}_1 - \mathbf{R}_{\alpha}}{|\mathbf{r}_1 - \mathbf{R}_{\alpha}|^3} + \sum_{j>1} \frac{\mathbf{r}_1 - \mathbf{r}_j}{|\mathbf{r}_1 - \mathbf{r}_j|^3} \quad (2)$$

where \hat{V} is the electronic coulomb operator, only including the second and third term in eq. 1. The subscript “1” refers to the fact that the operator works on an arbitrary electron “1” only.

The Ehrenfest force density is the expectation value of this operator,^[8] resulting in.

$$\mathbf{F}(\mathbf{r}) = N \langle \psi | -\nabla_1 \hat{V} | \psi \rangle' = -\rho(\mathbf{r}) \sum_{\alpha} Z_{\alpha} \frac{\mathbf{r} - \mathbf{R}_{\alpha}}{|\mathbf{r} - \mathbf{R}_{\alpha}|^3} + \int \rho_2(\mathbf{r}, \mathbf{r}') \frac{\mathbf{r} - \mathbf{r}'}{|\mathbf{r} - \mathbf{r}'|^3} d\mathbf{r}' \quad (3)$$

where the single quote means an integration over the spin coordinates of all the electrons in the system, and over the spatial coordinates of all the electrons except for electron 1. Because electrons are indistinguishable, all electrons contribute the same amount to this function as electron 1, hence the introduction of the scale factor N in front of this expression. The factor $\rho_2(\mathbf{r}, \mathbf{r}')$ is the second-order reduced density matrix.

The Ehrenfest force density is the average force acting on a point in the electron density as a result of its interactions with all the particles in the system. Its topology can be described in similar terms^[8,9,35] as that of the electron density, featuring critical points, and atomic interactions lines. A *force path* is, similarly to a bond path in the electron density, a line of steepest ascent or descent in force, connecting a critical point, where the Ehrenfest force density is zero, with the two adjacent maxima in the force density, both coinciding with atomic nuclei.

The average electronic, or Ehrenfest force exerted on an atom is obtained by integrating the force density over the atomic basin, A ,

$$\mathbf{F}(A) = \int_A \mathbf{F}(\mathbf{r}) d\mathbf{r} \quad (4)$$

For a stationary state, the Ehrenfest force density is also related to the stress tensor, $\sigma(\mathbf{r})$, through the relation^[1]

$$\mathbf{F}(\mathbf{r}) = -\nabla \cdot \sigma(\mathbf{r}) \quad (5)$$

From a computational point of view, this expression is much less time consuming to calculate than eq. 3, but it results in a bad topology of the force density due to various basis set artifacts.^[8,9] However, the advantage of this relation is that it allows

the calculation of the surface contribution to the Ehrenfest force, $\mathbf{F}(B|A)$, via application of Gauss’s theorem

$$\mathbf{F}(B|A) = - \int_{S(B|A)} \sigma(\mathbf{r}) \cdot \mathbf{n}(\mathbf{r}) d\mathbf{r} \quad (6)$$

where $S(B|A)$ is the zero flux surface separating atomic basins B and A , and $\mathbf{n}(\mathbf{r})$ is the normal to this surface. The zero flux surface is also known as an interatomic surface (IAS). Related is the contribution of the nucleus with basin B to the surface virial, $\mathcal{V}_s(A)$, via the expression

$$\mathcal{V}_s(B|A) = \int_{S(B|A)} \mathbf{r}_B \cdot \sigma(\mathbf{r}) \cdot \mathbf{n}(\mathbf{r}) d\mathbf{r} \quad (7)$$

In a similar fashion as for the Ehrenfest force density, the electronic Coulomb potential density is defined^[10] as the expectation value of the electronic Coulomb operator, \hat{V} ,

$$V_C(\mathbf{r}) = N \langle \psi | \hat{V} | \psi \rangle' = -\rho(\mathbf{r}) \sum_{\alpha} \frac{Z_{\alpha}}{|\mathbf{r} - \mathbf{R}_{\alpha}|} + \int \frac{\rho_2(\mathbf{r}, \mathbf{r}')}{|\mathbf{r} - \mathbf{r}'|} d\mathbf{r}' \quad (8)$$

This field represents the average Coulomb interaction experienced by a point in the electron density due to the interactions with all the particles in the system. In this work, we use the *additive* Coulomb potential density^[10,36] which differs from eq. 8 by a factor 1/2 in the last term

$$V_{\text{addC}}(\mathbf{r}) = -\rho(\mathbf{r}) \sum_{\alpha} \frac{Z_{\alpha}}{|\mathbf{r} - \mathbf{R}_{\alpha}|} + \frac{1}{2} \int \frac{\rho_2(\mathbf{r}, \mathbf{r}')}{|\mathbf{r} - \mathbf{r}'|} d\mathbf{r}' \quad (9)$$

so that the integration of $V_{\text{addC}}(\mathbf{r})$ over an atomic basin results in the correct Coulomb potential by that atom. The topology of the additive Coulomb potential density was recently studied by one of us^[10] showing it to be mainly homeomorphic with that of the electron density.

The total energy of a molecule can be written as

$$E(\text{mol}) = G(\text{mol}) + V(\text{mol})$$

where G is the kinetic energy and V the potential energy. For a molecule in a stationary state where the net forces acting on the nuclei vanish, the virial theorem is valid, that is,

$$V(\text{mol}) + \gamma G(\text{mol}) = 0$$

where, in theory, $\gamma = 2$, but in computational practice, γ is very close, but not exactly equal to 2.

If, as in the QTAIM,^[1,2] the molecule is partitioned in atomic basins which are based on the properties of the electron density, one can also write that

$$E(A) = G(A) + V(A) \quad (10)$$

and because the atomic basins, A , are nonoverlapping regions in space, one finds that

$$E(\text{mol}) = \sum_A^{\text{mol}} E(A) = \sum_A^{\text{mol}} G(A) + \sum_A^{\text{mol}} V(A)$$

where the summation runs over all the atomic basins in the molecular system. In this work, we will refer to $E(A)$ as the atomic energy. Typically, the potential energy term $V(A)$ contains contributions from particles in the atomic basin, A , but also from particles outside this basin. This can be highlighted by the notation $V(A,B)$ resulting in

$$V(A) = V(A, \text{mol}) = \sum_B^{\text{mol}} V(A,B)$$

where the term $V(A, \text{mol})$ emphasizes the fact that interactions between A and all the basins in the molecule are involved.

To correct for double counting, it is convenient to define

$$V_{ee}(A) = \frac{1}{2} V_{ee}(A, \text{mol}) \quad \text{and} \quad V_{nn}(A) = \frac{1}{2} V_{nn}(A, \text{mol})$$

but

$$V_{en}(A) = V_{en}(A, \text{mol})$$

From this it follows that

$$V_{ee}(\text{mol}) = \sum_A^{\text{mol}} V_{ee}(A) = \frac{1}{2} \sum_A^{\text{mol}} V_{ee}(A, \text{mol}) = \frac{1}{2} V_{ee}(\text{mol}, \text{mol})$$

$$V_{nn}(\text{mol}) = \sum_A^{\text{mol}} V_{nn}(A) = \frac{1}{2} \sum_A^{\text{mol}} V_{nn}(A, \text{mol}) = \frac{1}{2} V_{nn}(\text{mol}, \text{mol})$$

$$V_{en}(\text{mol}) = \sum_A^{\text{mol}} V_{en}(A) = \sum_A^{\text{mol}} V_{en}(A, \text{mol}) = V_{en}(\text{mol}, \text{mol})$$

Note that the additive Coulomb potential V_{addC} , integrated over the atomic basin A equals to

$$V_{\text{addC}}(A) = V_{en}(A, \text{mol}) + \frac{1}{2} V_{ee}(A, \text{mol})$$

In this work, three approaches to calculate the total energy of an atomic basin, $E(A)$, are explored, each differing by the way the potential energy, $V(A)$, is calculated.

In the traditional, virial based QTAIM method promoted by Bader,^[1,2] referred to as atoms in molecules (AIM) in the equations below, we have that

$$V_{\text{AIM}}(A) = V_{\text{addC}}(A) + V_{nn}^{\text{vir}}(A) = \mathcal{V}(A) \quad (11)$$

where $\mathcal{V}(\mathbf{r})$ is the virial density, and which satisfies the local virial condition $\mathcal{V}(A) + 2G(A) = 0$, which is valid if the molecule is in a stationary state. From this, it follows that

$$E_{\text{AIM}}(\text{mol}) = - \sum_A^{\text{mol}} G(A) = \frac{1}{2} \sum_A^{\text{mol}} \mathcal{V}(A)$$

Because of computational efficiency, it is common to utilize the summation in terms of the kinetic energy, G . Unless $\gamma = 2$ exactly,

it is found that $E_{\text{AIM}}(\text{mol}) \neq E(\text{mol})$, but this is easily rectified by rescaling the total potential energy so that

$$E_{\text{AIM}}^{\text{scaled}}(\text{mol}) = (1-\gamma) \sum_A^{\text{mol}} G(A)$$

Note that in this approach, the nuclear–nuclear repulsion term, $V_{nn}^{\text{vir}}(A)$ is not calculated from actual nuclear–nuclear repulsion interactions, but its value is derived to satisfy the local virial condition $V_{\text{addC}}(A) + V_{nn}^{\text{vir}}(A) + 2G(A) = 0$.

In the interacting quantum atoms (IQA) approach of Martín Pendás and coworkers^[37–39] the potential energy integrated over the atomic basin A is defined as

$$V_{\text{IQA}}(A) = \frac{1}{2} V_{en}(A, \text{mol}) + \frac{1}{2} V_{ne}(A, \text{mol}) + \frac{1}{2} V_{ee}(A, \text{mol}) + \frac{1}{2} V_{nn}(A, \text{mol}) \quad (12)$$

Because $V_{en}(\text{mol}, \text{mol}) = V_{ne}(\text{mol}, \text{mol})$, we find that $V_{\text{IQA}}(\text{mol}) = V_{en}(\text{mol}) + V_{ee}(\text{mol}) + V_{nn}(\text{mol})$ and hence that, within the precision of the numerical integrations over atomic basins, $E_{\text{IQA}}(\text{mol}) = E(\text{mol})$.

Finally, we define the *additive* potential energy, V_{add} , as

$$V_{\text{add}}(A) = V_{\text{addC}}(A) + V_{nn}(A) = V_{en}(A, \text{mol}) + \frac{1}{2} V_{ee}(A, \text{mol}) + \frac{1}{2} V_{nn}(A, \text{mol}) \quad (13)$$

This definition shares with the IQA potential energy that $V_{nn}(A, \text{mol})$ is calculated as the Coulomb repulsion of the nucleus in basin A with all the other nuclei in the molecule and, as in the QTAIM method, it uses the additive electron Coulomb potential integrated over the atomic basin. For this definition we also have that, within the precision of the numerical integrations, $E_{\text{add}}(\text{mol}) = E(\text{mol})$.

From this discussion, it follows that each of the three methods partitions the total energy of the molecule into contributions from atomic basins. Each atomic energy, $E(A)$, shares the same kinetic energy component, $G(A)$, but differs in the contribution of the potential energy $V(A)$. For all the three methods, the sum of the contributions of the atomic basins gives the total energy of the molecule if the molecule is in a stationary state. The IQA and additive methods also result in the correct value for $E(\text{mol})$ if the molecule is not in a stationary state.

Computational Details

All energy calculations were performed with the Gaussian09 program^[40] and the 6–311++G(d,p) basis set at the B3LYP level of theory.^[41–43] Default values were used for convergence criteria and grids. Topologies of the various fields were studied with our inhouse computer program eDensity.^[9,10] The topologies of the Ehrenfest force density were calculated using the expectation value, eq. 3. For the calculation of both the Ehrenfest force and the Coulomb field density, the Müller approximation^[44] was used to calculate the exchange contribution to the electron–electron

repulsion term. The AIMAll program^[45] was used to calculate energetic terms requiring integrations over atomic basins. This program uses the B3LYP functional to calculate the exchange–correlation term of the electron–electron repulsion term, resulting in correct energy values.^[39] Default values were used for the integration grids over the atomic basins. The maximum value for the magnitude of $L(A)$ varied from 1.14×10^{-4} to 4.18×10^{-4} au. Details are given in the Supporting Information.

Result and Discussion

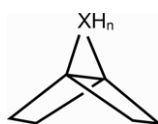
In this work, a number of derivatives of *exo-exo*-tetracyclo[6.2.1.1^{3,6}.0^{2,7}]dodecane, shown in Scheme 1, are considered. The molecules studied are combinations where the groups XH_n and YH_m ($n, m = 1, 2$) are CH_2 , NH_2^+ , BH_2^- , OH^+ , and NH . For the groups OH^+ and NH , which only have one hydrogen atom, the latter can either point inwards or outwards the molecule, denoted as NH_{in} and OH_{in}^+ , or NH_{out} and OH_{out}^+ resulting in a total of 22 molecules which we will identify with the short hand notation (XH_n, YH_m). A few theoretically possible combinations were left out because they did not result in stable molecules.

Except for two, all the molecules studied show signs of steric congestion between the XH_n and YH_m groups as is evident in the deformation of the geometries compared to the norbornane derivatives shown in Scheme 2. This deformation can be quantised by the angles as defined in Scheme 3, showing an increase in the values α_{in} and β_{in} combined with a decrease in α_{out} and β_{out} and also an increase in γ and δ , compared to the norbornane derivative, as summarized in Table 1. The exceptions are that only the BH_2^- unit in (NH_2^+, BH_2^-) shows a noticeable deformation, whereas in (NH_2^+, NH_{out}), the data suggest an attractive interaction between the XH_n and YH_m groups.

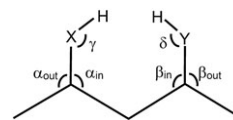
It should be emphasized that these angles only give an overall impression of possible steric hindrance and that they do not allow individual interactions to be identified. In addition, the phrase “steric congestion” does not imply that there is a net repulsive interaction between these groups, as the molecules are in a geometry that minimizes the total energy of the system and hence, the total force acting on each atom is zero.

For each molecule, the topology of the electron density, $\rho(\mathbf{r})$, the virial density, $\mathcal{V}(\mathbf{r})$, the force density, $\mathbf{F}(\mathbf{r})$, and the additive Coulomb potential density, $V_{addC}(\mathbf{r})$, was studied. In all the molecules, maxima in the magnitude of the field were found at or near (depending on the field) the atomic nuclei. With all the fields considered, these maxima were connected by interaction lines creating a molecular graph coinciding with the accepted molecular structure of the molecule.

However, in all molecules except for (OH_{in}^+, OH_{in}^+), an additional bond path was found to exist in the electron density between one atom of the XH_n group and one of the YH_m group. For (XH_2, YH_2), the bond path is always between two



Scheme 2. Norbornane derivatives considered.



Scheme 3. Definition of deformation angles.

hydrogen atoms whereas for the (XH_2, YH) and (XH, YH) compounds, bond paths between $H \cdots Y$ or $X \cdots Y$ were found to occur depending on the orientation of the hydrogen atom.

As mentioned earlier, according to the Quantum Theory of Atoms and Molecules,^[1,2] these bond paths are indicative of a bonding, and hence stabilizing, interaction between the two atoms.^[12–15] In addition, 19 of the molecules show an extra virial path, this being a line of maximum (in magnitude) potential energy density^[6] between the same nuclei as where a bond path was found. A total of 16 molecules exhibit a force path,^[8,9] and 21 have a Coulomb potential path^[10] between XH_n and YH_m . Especially for the latter, the atoms involved are not always the same as for the former two. As a representative example, the molecular graphs of *exo-exo*-tetracyclo[6.2.1.1^{3,6}.0^{2,7}]dodecane for all the fields considered are shown in Figure 1.

Because the values of both the virial and the electronic potential densities are negative along these interaction lines, one could argue that these represent a line of maximal stabilizing interaction between the nuclei. Similar arguments can be made for the force path. The exact position of the critical point along the interaction lines differ for each field, and we will limit ourselves to the properties of the critical point in the electron density, known as the bond critical point, \mathbf{r}_b , and summarized in Table 2.

If one or two hydrogen atoms are involved in the bond path, then the distance between the two nuclear attractors, r_{NA} , is larger than that between the two nuclei, r_{At} , indicating a shift of the point of maximum electron density toward the atom where the hydrogen is attached to.

The low values of $\rho(\mathbf{r}_b)$, the positive values of the Laplacian, $\nabla^2\rho(\mathbf{r}_b)$, and the energy density $H(\mathbf{r}_b)$ are indicative of closed shell interactions. Two entries, (NH_2^+, BH_2^-) and (NH_2^+, NH_{out}), have a negative value of $H(\mathbf{r}_b)$, a relative higher value of the magnitude of the virial density, $|\mathcal{V}(\mathbf{r}_b)|$, the force density, $|\mathbf{F}(\mathbf{r}_b)|$, the Coulomb potential density, $V_{addC}(\mathbf{r}_b)$, and also the delocalization index, $\delta(\mathbf{r}_b)$. According to the criteria of Nakanishi et al.^[46] these interactions can be classified as closed shell containing covalency.

Despite the fact that the bond paths are not always between the same type of nuclei, there is a good linear correlation between $V_{addC}(\mathbf{r}_b)$ and the electron density $\rho(\mathbf{r}_b)$ ($r^2 = 0.982$) and also between $V_{addC}(\mathbf{r}_b) + G(\mathbf{r}_b)$ and $\rho(\mathbf{r}_b)$ ($r^2 = 0.984$), as shown in Figure 2.

This correlation is remarkable, especially considering the chemical difference between the congested groups, and hence also the classical view of the resulting interactions between them.

In his work on $H \cdots H$ and $F \cdots F$ interactions, Matta et al.^[14,25,47] proposed to use the atomic energy, $E(A)$, as a quantitative tool to determine the strength of the interaction between the two atoms involved. Indeed, it was noticed that the presence of a

Table 1. Deviations of the angles (degrees) defined in Scheme 3 for the molecules (XH_n , YH_m), relative to the related norbornane derivatives.

XH_n	YH_m	$\Delta\alpha_{out}$	$\Delta\alpha_{in}$	$\Delta\gamma$	$\Delta\delta$	$\Delta\beta_{in}$	$\Delta\beta_{out}$
CH ₂	CH ₂	-3.1	5.8	3.7	3.7	5.8	-3.1
CH ₂	NH ₂ ⁺	-2.9	5.7	6.5	0.2	3.4	-1.4
CH ₂	BH ₂ ⁻	-2.4	4.4	0.3	6.9	8.4	-5.1
NH ₂ ⁺	NH ₂ ⁺	-2.6	5.8	6.3	6.3	5.8	-2.6
NH ₂ ⁺	BH ₂ ⁻	1.1	0.1	-5.3	6.0	6.6	-4.3
BH ₂ ⁻	BH ₂ ⁻	-5.4	8.7	6.7	6.7	8.7	-5.4
CH ₂	NH _{in}	-3.1	5.5	4.1	2.4	4.1	-1.9
CH ₂	NH _{out}	-1.7	4.1	0.8	-0.4	3.1	-1.4
CH ₂	OH _{in} ⁺	-2.5	4.8	6.6	-3.4	2.0	-0.6
CH ₂	OH _{out} ⁺	-1.2	3.8	3.4	-1.0	3.0	-1.5
NH ₂ ⁺	NH _{in}	-0.9	2.7	-0.6	18.1	4.1	-1.2
NH ₂ ⁺	NH _{out}	2.0	-0.5	-7.6	1.5	-0.2	0.3
NH ₂ ⁺	OH _{in} ⁺	-1.8	4.7	5.0	23.1	4.1	-1.2
NH ₂ ⁺	OH _{out} ⁺	-0.5	2.9	2.4	-0.8	0.9	0.1
BH ₂ ⁻	NH _{in}	-4.3	7.1	6.1	-4.2	2.4	-1.2
BH ₂ ⁻	NH _{out}	-2.4	5.3	4.2	3.8	1.9	-6.0
NH _{in}	NH _{in}	-2.0	4.1	3.6	3.6	4.1	-2.0
NH _{in}	NH _{out}	-0.1	1.8	-2.9	-0.2	2.2	-1.1
NH _{out}	NH _{out}	-1.3	3.8	-0.5	-0.5	3.8	-1.3
OH _{in} ⁺	OH _{in} ⁺	-1.1	3.9	17.8	17.8	3.9	-1.1
OH _{in} ⁺	OH _{out} ⁺	0.5	1.6	3.8	-0.7	0.2	0.5
OH _{out} ⁺	OH _{out} ⁺	0.7	1.2	-0.7	-0.7	1.2	0.7

bond path between either H···H or F···F would lower the atomic energy, $E(A)$, of the atoms involved compared to the other hydrogen or fluorine atoms in the molecule, resulting in stabilizing values of up to ~10 kcal/mol for H···H and ~14 kcal/mol for the F···F interactions.

We have calculated the atomic energies for each atom in all the molecules with the three methods mentioned earlier and defined in eqs. 11–13. As a reference, we choose the atoms in the corresponding XH_n and YH_m groups of the norbornane derivatives shown in Scheme 2. The sum of the energies $E(A)$ of the pair of atoms connected by a bond path in the (XH_n , YH_m) molecules is compared with the sum of the atomic energies of the corresponding atoms in the isolated norbornane derivatives, and the difference is taken as a measure of stabilization or destabilization. The results are shown in Table 3. Although

the (OH_{in}^+ , OH_{in}^+) molecule does not show a bond path between the congested hydrogen atoms, it has a force path between those atoms, and is, therefore, treated as all the other molecules in this table.

When using $E_{AIM}(A)$ as a criterion, 7 out of the 22 molecules do not show a lowering of the energies between the nuclei connected by an interaction line. The presence of a CH₂ group always lowers the sum of the energies of the pair of atoms. It is also noted that the energy is lowered if the XH_n and YH_m groups are equal, and if XH equals YH with the same orientation of the hydrogen atoms, with OH_{in}^+ as an exception. If the bond path is between two hydrogen atoms, this would imply a hydrogen–hydrogen bonding.^[25,47] Because the presence of a bond path may also affect the basin energies of the surrounding atoms, we also compared the energies of the

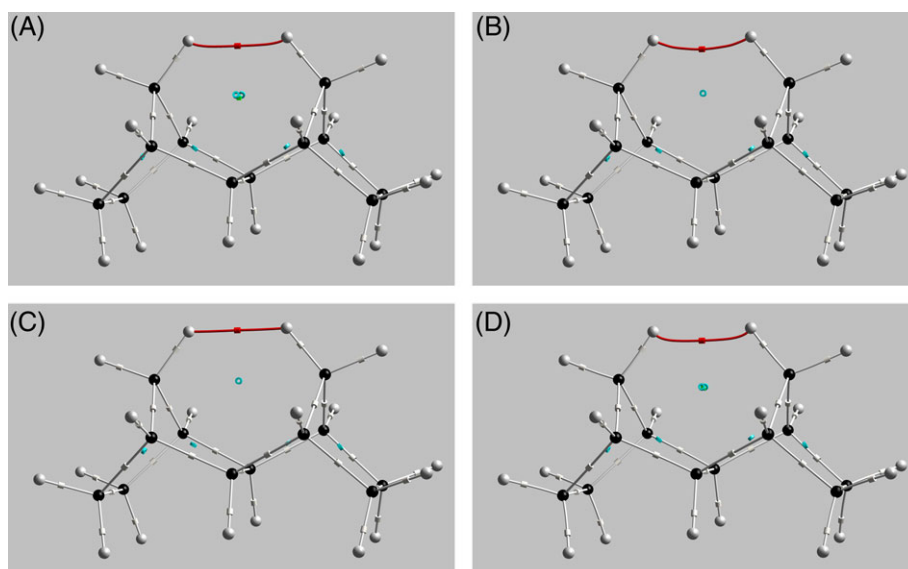


Figure 1. Molecular graphs of *exo-exo*-tetracyclo[6.2.1.1^{3,6}.0^{2,7}]dodecane for A) the electron density, $\rho(\mathbf{r})$, B) the virial density, $V(\mathbf{r})$, C) the Ehrenfest force, $\mathbf{F}(\mathbf{r})$, and D) the additive electronic Coulomb potential, $V_{addc}(\mathbf{r})$. The extra path between the congested hydrogen atoms is shown in red. [Color figure can be viewed at wileyonlinelibrary.com]

Table 2. Properties of the bond critical point, \mathbf{r}_b , along the bond paths between nuclei At_1 and At_2 .

XH_n	YH_m	At_1	At_2	r_{At}	r_{NA}	ρ	$\nabla^2\rho$	H	G	\mathcal{V}	$ F $	V_{addC}	ϵ	δ
CH_2	CH_2	H	H	1.801	1.818	1.78	5.91	0.24	1.24	-1.00	0.06	-16.44	0.167	0.043
CH_2	NH_2^+	H	H	1.668	1.689	2.19	6.98	0.21	1.54	-1.33	0.35	-21.48	0.156	0.042
CH_2	BH_2^-	H	H	1.816	1.831	2.00	5.60	0.17	1.23	-1.07	0.23	-17.43	0.140	0.076
NH_2^+	NH_2^+	H	H	1.964	1.985	0.98	3.70	0.17	0.76	-0.59	0.03	-9.78	0.191	0.011
NH_2^+	BH_2^-	H	H	1.328	1.345	5.94	5.08	-1.77	3.04	-4.81	2.84	-58.02	0.104	0.168
BH_2^-	BH_2^-	H	H	2.147	2.157	1.20	3.13	0.09	0.69	-0.60	0.01	-9.56	0.155	0.071
CH_2	NH_{in}	H	H	1.776	1.796	1.83	5.83	0.19	1.27	-1.08	0.11	-17.43	0.196	0.035
CH_2	NH_{out}	H	N	2.319	2.325	1.80	6.04	0.20	1.31	-1.11	0.19	-17.93	0.153	0.063
CH_2	OH_{in}^+	H	H	1.588	1.613	2.59	7.32	0.06	1.77	-1.70	0.59	-26.15	0.160	0.045
CH_2	OH_{out}^+	H	O	2.318	2.322	1.53	5.91	0.21	1.27	-1.07	0.05	-15.84	0.204	0.044
NH_2^+	NH_{in}	H	H	1.812	1.834	1.80	5.44	0.16	1.20	-1.03	0.25	-18.16	0.415	0.020
NH_2^+	NH_{out}	H	N	1.796	1.810	4.82	10.76	-0.71	3.40	-4.11	2.16	-53.09	0.028	0.139
NH_2^+	OH_{in}^+	H	O	2.594	2.601	0.89	3.29	0.10	0.72	-0.61	0.04	-9.37	1.082	0.018
NH_2^+	OH_{out}^+	H	O	2.208	2.217	1.64	6.60	0.23	1.42	-1.18	0.21	-17.78	0.185	0.035
BH_2^-	NH_{in}	H	H	1.664	1.684	2.68	6.62	0.02	1.64	-1.61	0.51	-24.52	0.144	0.085
BH_2^-	NH_{out}	H	N	2.633	2.635	1.21	3.61	0.10	0.80	-0.69	0.04	-11.17	0.218	0.066
NH_{in}	NH_{in}	H	H	1.800	1.823	1.73	5.17	0.12	1.17	-1.05	0.09	-16.93	0.241	0.024
NH_{in}	NH_{out}	H	N	2.166	2.176	2.28	7.27	0.14	1.67	-1.53	0.37	-23.61	0.106	0.067
NH_{out}	NH_{out}	N	N	2.866	2.866	1.33	4.75	0.15	1.03	-0.88	0.12	-14.10	0.025	0.067
OH_{in}^+	OH_{in}^+	H	H	2.288	2.306									0.001
OH_{in}^+	OH_{out}^+	H	O	2.219	2.229	1.64	6.26	0.15	1.41	-1.25	0.19	-18.33	0.293	0.026
OH_{out}^+	OH_{out}^+	O	O	2.697	2.697	1.36	6.00	0.18	1.32	-1.14	0.11	-15.46	0.084	0.050

Distance between the nuclei, r_{At} , and the nuclear attractors, r_{NA} , in Å. All other properties in atomic units $\times 10^2$, except for the ellipticity, ϵ , and the delocalization index, δ , which are in atomic units (au).

complete XH_n and YH_m groups with those of the unstrained molecules, also shown in Table 3. For some molecules, this results in the opposite conclusion as above, although the presence of a CH_2 group still always lowers the sum of the energies of the pair. There is no linear correlation ($r^2 = 0.005$) between group based interaction energies and the atom based interaction energies.

Atomic energies based on the IQA method and calculated according to eq. 12 are shown in column 7 of Table 2. About half (12) of the 22 molecules show an increase in the atomic energies of the pair of nuclei connected by an interaction line. There is a larger spread in the numerical values, but no linear correlation ($r^2 = 0.131$) with the QTAIM-based results.

Finally, additive based energies were compared. As is evident from Table 3, the numerical values show a dramatic increase in magnitude and are, from a chemical point of view, very unrealistic to serve as a measure for the stabilization or destabilization of a closed shell interaction between two atoms. In 8 of the 22 molecules, the energy of the atom pair is higher than in the unstrained reference molecules, but there is no linear correlation ($r^2 = 0.001$) with QTAIM-based, nor with IQA-based energies ($r^2 = 0.139$).

One of the major advantages of the IQA method is that it allows the calculation of $V(A,B)$, that is, the potential energy resulting from the interaction between two atomic basins A and B , regardless of the presence of an interaction line or not.

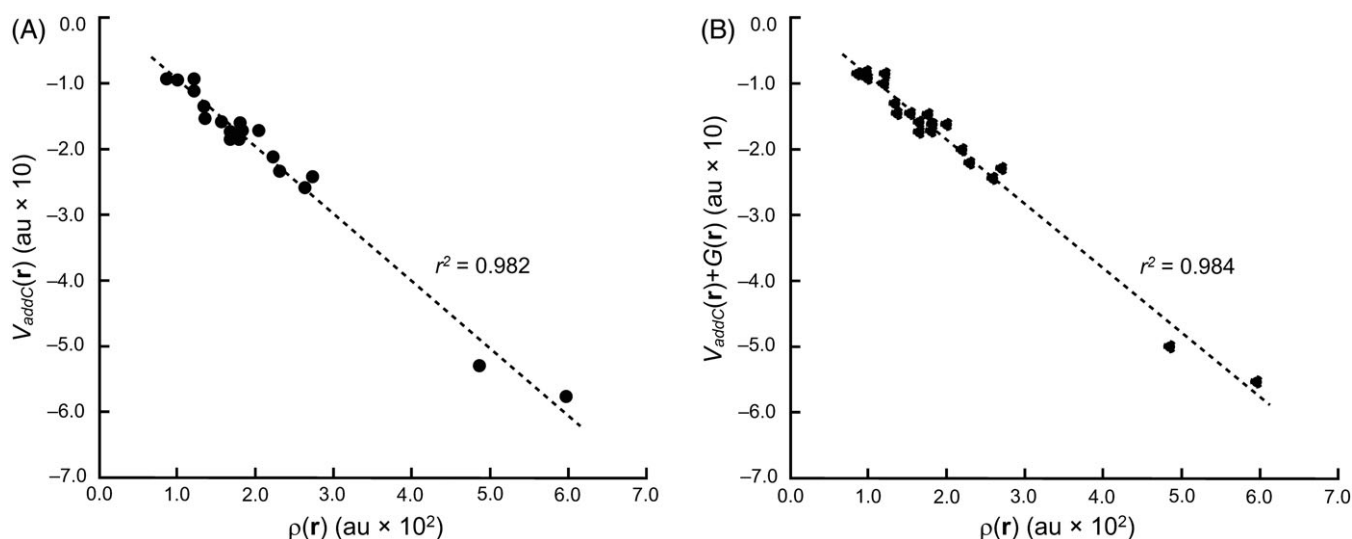


Figure 2. A) The additive electronic Coulomb potential, $V_{\text{addC}}(\mathbf{r})$, versus the electron density, $\rho(\mathbf{r})$, at the bond critical point, \mathbf{r}_b , between the congested atoms as given in Table 1. B) The sum of the Coulomb potential, $V_{\text{addC}}(\mathbf{r})$, and the kinetic energy, $G(\mathbf{r})$, as a function of the electron density at the same critical point.

Table 3. Differences in the atomic energies (kcal/mol) relative to the equivalent nucleus or group in the corresponding norbornane derivative, summed over the pair of nuclei ($At_1 + At_2$) or the complete group ($XH_n + YH_m$).

XH_n	YH_m	Pair		QTAIM		IQA		Additive
		At_1	At_2	$At_1 + At_2$	$XH_n + YH_m$	$At_1 + At_2$	$V(At_1 + At_2)$	$At_1 + At_2$
CH ₂	CH ₂	H	H	-14.4	-20.0	2.3	-5.7	-65.5
CH ₂	NH ₂ ⁺	H	H	-18.0	-19.2	-8.2	-12.8	374.0
CH ₂	BH ₂ ⁻	H	H	-1.7	-24.5	4.7	-14.9	-625.6
NH ₂ ⁺	NH ₂ ⁺	H	H	-20.8	17.2	25.9	22.2	998.9
NH ₂ ⁺	BH ₂ ⁻	H	H	17.6	-55.3	-53.9	-91.4	20.0
BH ₂ ⁻	BH ₂ ⁻	H	H	-24.0	-9.4	56.4	49.2	-1680.6
CH ₂	NH _{in}	H	H	-12.7	-20.9	0.4	-7.2	422.7
CH ₂	NH _{out}	H	N	-3.6	-6.7	6.1	-13.3	-1245.2
CH ₂	OH _{in} ⁺	H	H	-20.1	-17.9	-14.4	-18.4	621.4
CH ₂	OH _{out} ⁺	H	O	-18.5	-3.9	6.5	-4.9	-638.4
NH ₂ ⁺	NH _{in}	H	H	-1.0	-39.1	13.6	17.5	1188.5
NH ₂ ⁺	NH _{out}	H	N	8.0	-11.2	-53.3	-112.6	-1152.6
NH ₂ ⁺	OH _{in} ⁺	H	O	-26.4	6.6	-31.8	-52.6	-1637.2
NH ₂ ⁺	OH _{out} ⁺	H	O	6.6	32.7	-26.9	-64.3	-1220.2
BH ₂ ⁻	NH _{in}	H	H	4.6	-12.9	-15.6	-53.1	-160.5
BH ₂ ⁻	NH _{out}	H	N	-21.4	-25.1	48.2	67.7	-1898.2
NH _{in}	NH _{in}	H	H	-10.4	-20.7	1.0	10.2	952.9
NH _{in}	NH _{out}	H	N	8.4	0.4	-1.1	-62.0	-786.3
NH _{out}	NH _{out}	N	N	-4.0	-6.1	12.5	92.2	-2693.6
OH _{in} ⁺	OH _{in} ⁺	H ^[a]	H ^[a]	9.8	-3.7	61.3	55.4	2010.0
OH _{in} ⁺	OH _{out} ⁺	H	O	21.9	25.6	-22.3	-90.8	-893.7
OH _{out} ⁺	OH _{out} ⁺	O	O	-1.4	18	-81.0	93.9	-4057.3

[a] Does not show a bond path in the electron density between the two nuclei.
This text was in the header.

This calculation is not possible with the QTAIM or additive method because the electron–electron repulsion term in the additive Coulomb potential implies an integration over all space. The results are also shown in Table 3. Eight of the 22 molecules show a positive energy, indicating a repulsive interaction between the two atomic basins. The results are consistent with the partial charges obtained by a numerical integration of the

electron density over the atomic basins involved. There is no linear correlation between the IQA interactions energies and the results obtained using atomic energies with either the QTAIM method ($r^2 = 0.198$), IQA ($r^2 = 0.239$), or additive-based energies ($r^2 = 0.041$).

Bader^[12,13,48] has stressed the importance of the Ehrenfest force on determining the attraction between two atomic basins,

Table 4. Contribution of a nucleus (At_1 and At_2) to the surface virial \mathcal{V}_s of the other nucleus, and to the Ehrenfest force \mathbf{F} . ($\text{au} \times 10^2$)

XH_n	YH_m	At_1	$\mathcal{V}_s(At_1 At_2)$	At_2	$\mathcal{V}_s(At_2 At_1)$	$\mathbf{n} \cdot \mathbf{F}^{[a]}$
CH ₂	CH ₂	H	-1.87	H	-1.87	1.10
CH ₂	NH ₂ ⁺	H	-1.35	H	-1.06	0.76
CH ₂	BH ₂ ⁻	H	-2.51	H	-2.29	1.40
NH ₂ ⁺	NH ₂ ⁺	H	-0.89	H	-0.89	0.48
NH ₂ ⁺	BH ₂ ⁻	H	-4.83	H	-2.77	3.03
BH ₂ ⁻	BH ₂ ⁻	H	-2.59	H	-2.59	1.28
CH ₂	NH _{in}	H	-1.82	H	-1.61	1.02
CH ₂	NH _{out}	H	-2.56	N	-4.18	1.54
CH ₂	OH _{in} ⁺	H	-1.44	H	-0.87	0.77
CH ₂	OH _{out} ⁺	H	-2.35	O	-3.98	1.45
NH ₂ ⁺	NH _{in}	H	-1.46	H	-1.28	0.80
NH ₂ ⁺	NH _{out}	H	-2.56	N	-4.18	1.54
NH ₂ ⁺	OH _{in} ⁺	H	-1.06	O	-1.59	0.54
NH ₂ ⁺	OH _{out} ⁺	H	-2.35	O	-3.98	1.45
BH ₂ ⁻	NH _{in}	H	-2.58	H	-1.97	1.44
BH ₂ ⁻	NH _{out}	H	-2.66	N	-4.04	1.35
NH _{in}	NH _{in}	H	-1.65	H	-1.65	0.97
NH _{in}	NH _{out}	H	-2.25	N	-4.13	1.56
NH _{out}	NH _{out}	N	-3.12	N	-3.12	1.15
OH _{in} ⁺	OH _{in} ⁺			no bond path ^[b]		
OH _{in} ⁺	OH _{out} ⁺	H	-2.54	O	-1.37	0.93
OH _{out} ⁺	OH _{out} ⁺	O	-3.13	O	-3.13	1.23

[a] $\mathbf{n} \cdot \mathbf{F}$ is the contribution to the force where the direction of the normal vector is chosen for each nucleus in a pair so that $\mathbf{n} \cdot \mathbf{F} > 0$ implies an attractive contribution. The numerical value is the same for each nucleus in a pair.

[b] The absence of a BCP prevents the definition of an IAS.

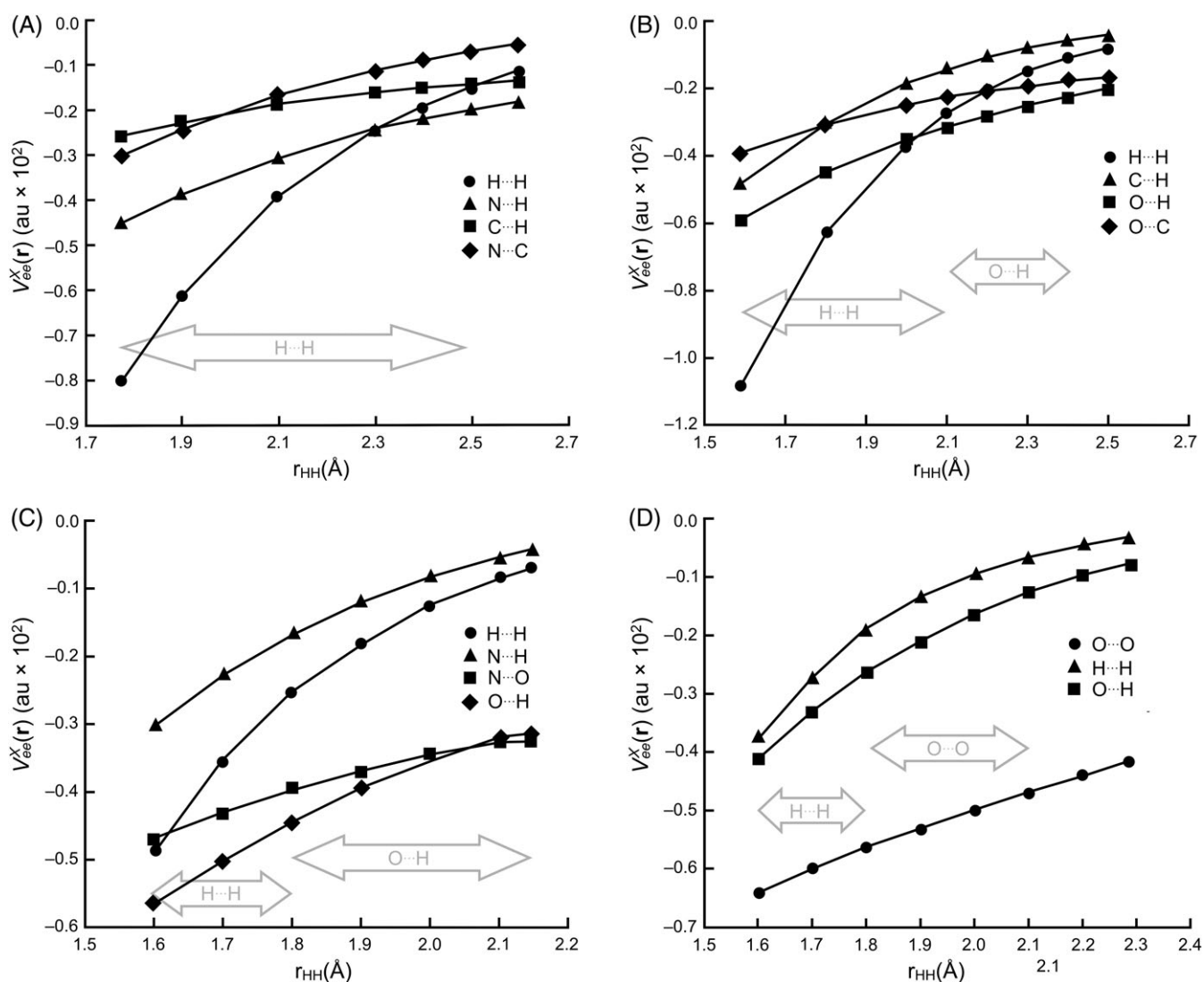


Figure 3. Exchange-correlation potential as a function of the H...H distance for various atom pairs in A) (CH_2 , NH_n), B) (CH_2 , OH_{in}^+), C) (NH_2^+ , OH_{in}^+), and D) (OH_{in}^+ , OH_{in}^+). The presence of a bond path is indicated by a gray arrow.

specifically the contribution of the zero-flux surface that separates the two atomic basins to the total force exerted on each basins calculated via eq. 6. That contribution should be attractive and, in addition, the surface should contribute to a lowering of the total surface virial, eq. 7, of the atomic basin.

The results are shown in Table 4, indicating that these requirements are fulfilled for all molecules where a bond path between XH_n and YH_m is observed.

However, a few comments should be made to place these results in perspective. One is that the expression for the Ehrenfest force density as shown in eq. 5, and also its surface contribution as expressed in eq. 6, assumes that the time-dependent Schrödinger equation can be solved and hence, strictly speaking, that it is only valid for an eigenfunction of that equation. The calculation via the expectation value, eq. 3, is valid for each wavefunction, ψ . As a result, even for the hydrogen atom, large basis sets are required in eq. 5 for the resulting numerical values to converge to the same result as obtained with the expectation value, eq. 3.

Secondly, especially the use of Gaussian basis sets, but also of Slater-type basis sets in conjunction with eq. 5 results in a topology of the Ehrenfest force density displaying a large number of spurious critical points and unrealistic molecular graphs when using eq. 5, casting some doubts on the physical meaning of the interpretation of the integration of Ehrenfest forces.^[8,9]

In addition, it should be remembered that the definition of the Ehrenfest force density, as evident in eq. 3, but also that of the additive Coulomb potential density in eq. 8, only involves the electronic part of the Coulomb operator, thus ignoring any contributions from nuclear-nuclear repulsions. The importance of the latter can be demonstrated by removing its contribution from the $V_{QA}(A,B)$ term in Table 3, turning all tabled interactions into stabilizing ones.

Finally, given the fact that the results above do not show a correlation between the existence of any of the calculated atomic interaction lines between the XH_n and YH_m groups and a stabilizing change in atomic energies of the nuclei involved,

nor with the IQA pair potential between those nuclei, we tested the hypothesis of Martín Pendás et al.^[49] that bond paths are privileged exchange channels, determined by a competition amongst exchange-correlation energies.

To this effect, we calculated the exchange-correlation part of the electron–electron repulsion energy, V_{ee}^X , of a number of atom pairs as a function of the H···H distance in the molecules (CH₂, NH_{i,n}) and (CH₂, OH⁺), where the short equilibrium H···H distance was gradually increased, and the molecules (NH₂⁺, OH⁺) and (OH⁺, OH⁺), where the long H···H distance was decreased. For these four molecules, which we believe to be representative for the whole set, bond paths, virial and force paths, and Coulomb potential paths were monitored. Figure 3 shows the exchange-correlation energy of several atom pairs for each molecule and the formation or disappearance of bond paths in the electron densities as a function of the H···H distance. The exchange-correlation contribution is always negative, increasing in magnitude at shorter distances because it shares the same $1/r$ dependence as the Coulomb contribution. More details can be found in the Supporting Information.

As can be seen from Figure 3, there is only a weak qualitative correlation between the presence of a bond path, and the atom pair having the lowest value of V_{ee}^X . As shown in the Supporting Information, a similar weak correlation is observed with the delocalization index.

Conclusions

In this work, four energetic criteria were employed to calculate the stabilizing interactions which, according to the QTAIM,^[1,2] exist between a classically nonbonded, and sterically congested, pair of atoms in a series of derivatives of tetracyclododecane. Despite the chemical differences between the congested groups, all the molecules studied display either a bond path in the electron density, an Ehrenfest force, virial, and/or Coulomb potential density path between the congested pair of atoms.

In three of the methods used, the energy integrated over the atomic basin of each nucleus in the pair is compared with the corresponding values obtained for the same pair in a norbornane derivative that is used as a reference. The three methods have in common the calculation of the kinetic energy and the electron–electron repulsion energy, but differ by the calculation of the remaining terms of the potential energy which are based on the local virial theorem,^[1,2] the IQA formalism,^[37–39] and the additive Coulomb potential,^[10,36] respectively. The fourth criterion involves the direct calculation of the potential energy between the two atomic basins according to the IQA method.^[37–39]

It was found that there does not exist a correlation between the presence of a bond path in the electron density between the sterically congested atoms and any of the energetic criteria used. Nor is there a linear correlation between the numerical data obtained with any of the methods used. Given that the Ehrenfest force density, virial, and Coulomb potential density are formulated in terms of the potential energy or the gradient thereof, the results support the view that the interaction line observed between the nuclei of the congested atoms should be interpreted as being a line of increasing magnitude in the

value of the field, with a minimum value along the direction of the line at the line critical point, and a maximum near or at the nuclei, without any consequences on the atomic energy, as calculated by integrating over the atomic basin, of the atoms involved. It hence appears that a similar conclusion is to be made about the bond path in the electron density.

Conversely, if calculated as the negative divergent of the stress tensor, eq. 5, the Ehrenfest force of the zero-flux surface indicates an attractive interaction between the two atomic basins and the contribution to the surface virial is stabilizing.

National Research Foundation (NRF), Grant Number: 91553 Reference no CSUR13091136352

Keywords: atoms in molecules · interacting quantum atoms · Ehrenfest force · bond path

How to cite this article: D. Myburgh, S. von Berg, J. Dillen. *J. Comput. Chem.* **2018**, 9999, 1–10. DOI: 10.1002/jcc.25547

 Additional Supporting Information may be found in the online version of this article.

- [1] R. F. W. Bader, *Atoms in Molecules. A Quantum Theory*, Oxford University Press, Oxford, **1990**.
- [2] R. F. W. Bader, *Chem. Rev.* **1991**, 91, 893.
- [3] A. D. Becke, K. E. Edgecombe, *J. Chem. Phys.* **1990**, 92, 5397.
- [4] H. L. Schmirer, A. D. Becke, *J. Mol. Struct. THEOCHEM* **2000**, 527, 51.
- [5] H. J. Bohórquez, C. F. Matta, R. J. Boyd, *Int. J. Quantum Chem.* **2010**, 110, 2418.
- [6] T. A. Keith, R. F. W. Bader, Y. Aray, *Int. J. Quantum Chem.* **1996**, 57, 183.
- [7] E. R. Johnson, S. Keinan, P. Mori-Sánchez, J. Contreras-García, A. J. Cohen, W. Yang, *J. Am. Chem. Soc.* **2010**, 132, 6498.
- [8] A. Martín Pendás, J. Hernández-Trujillo, *J. Chem. Phys.* **2012**, 137, 134101.
- [9] J. Dillen, *J. Comput. Chem.* **2015**, 36, 883.
- [10] L.-M. Ferreira, A. Eaby, J. Dillen, *J. Comput. Chem.* **2017**, 38, 2784.
- [11] P. L. A. Popelier, F. M. Aicken, *Chem. Phys. Chem.* **2003**, 4, 824.
- [12] R. F. W. Bader, *J. Phys. Chem. A* **1998**, 102, 7314.
- [13] R. F. W. Bader, D. C. Fang, *J. Chem. Theory Comput.* **2005**, 1, 403.
- [14] C. F. Matta, N. Castillo, R. J. Boyd, *J. Phys. Chem. A* **2005**, 109, 3669.
- [15] R. F. W. Bader, *J. Phys. Chem. A* **2010**, 114, 7431.
- [16] J. Cioslowski, S. T. Mixon, *Can. J. Chem.* **1992**, 70, 443.
- [17] J. Cioslowski, S. T. Mixon, *J. Am. Chem. Soc.* **1992**, 114, 4382.
- [18] J. Cioslowski, L. Edgington, B. B. Stefanov, *J. Am. Chem. Soc.* **1995**, 117, 10381.
- [19] J. Cioslowski, S. T. Mixon, W. D. Edwards, *J. Am. Chem. Soc.* **1991**, 113, 1083.
- [20] A. Haaland, D. J. Shorokhov, N. V. Tverdova, *Chemistry* **2004**, 10, 4416.
- [21] T. Strenalyuk, A. Haaland, *Chemistry* **2008**, 14, 10223.
- [22] M. Von Hopffgarten, G. Frenking, *Chemistry* **2008**, 14, 10227.
- [23] S. G. Wang, Y. X. Qiu, W. H. E. Schwarz, *Chemistry* **2009**, 15, 6032.
- [24] J. Poater, M. Solà, F. M. Bickelhaupt, *Chemistry* **2006**, 12, 2889.
- [25] C. F. Matta, J. Hernández-Trujillo, T. H. Tang, R. F. W. Bader, *Chemistry* **2003**, 9, 1940.
- [26] R. F. W. Bader, *Chemistry* **2006**, 12, 2896.
- [27] J. Poater, M. Solà, F. M. Bickelhaupt, *Chemistry* **2006**, 12, 2902.
- [28] K. Eskandari, C. Van Alsenoy, *J. Comput. Chem.* **2014**, 35, 1883.
- [29] J. Hernández-Trujillo, C. F. Matta, *Struct. Chem.* **2007**, 18, 849.
- [30] R. F. W. Bader, *J. Phys. Chem. A* **2009**, 113, 10391.
- [31] M. Jabłoński, *J. Phys. Chem. A* **2012**, 116, 3753.
- [32] J. D. Dunitz, *IUCrJ.* **2015**, 2, 157.
- [33] C. Lecomte, E. Espinosa, C. F. Matta, *IUCrJ.* **2015**, 2, 161.
- [34] T. S. Thakur, R. Dubey, G. R. Desiraju, *IUCrJ.* **2015**, 2, 159.

- [35] J. R. Maza, S. Jenkins, S. R. Kirk, J. S. M. Anderson, P. W. Ayers, *Phys. Chem. Chem. Phys.* **2013**, 15, 17823.
- [36] A. Martín Pendás, E. Francisco, A. Gallo Bueno, J. M. Guevara Vela, A. Costales, In *Emergent Scalar and Vector Fields in Quantum Chemical Topology*. R. Chauvin, C. Lepetit, B. Silvi, E. Alikhani, Eds., Springer, Switzerland, **2016**, p. 131.
- [37] M. A. Blanco, A. Martín Pendás, E. Francisco, *J. Chem. Theory Comput.* **2005**, 1, 1096.
- [38] E. Francisco, A. Martín Pendás, M. A. Blanco, *J. Chem. Theory Comput.* **2006**, 2, 90.
- [39] P. Maxwell, A. Martín Pendás, P. L. A. Popelier, *Phys. Chem. Chem. Phys.* **2016**, 18, 20986.
- [40] M. J. Frisch, G. W. Trucks, H. B. Schlegel, G. E. Scuseria, M. A. Robb, J. R. Cheeseman, G. Scalmani, V. Barone, B. Mennucci, G. A. Petersson, H. Nakatsuji, M. Caricato, X. Li, H. P. Hratchian, A. F. Izmaylov, J. Bloino, G. Zheng, J. L. Sonnenberg, M. Hada, M. Ehara, K. Toyota, R. Fukuda, J. Hasegawa, M. Ishida, T. Nakajima, Y. Honda, O. Kitao, H. Nakai, T. Vreven, J. A. Montgomery, Jr., J. E. Peralta, F. Ogliaro, M. Bearpark, J. J. Heyd, E. Brothers, K. N. Kudin, V. N. Staroverov, R. Kobayashi, J. Normand, K. Raghavachari, A. Rendell, J. C. Burant, S. S. Iyengar, J. Tomasi, M. Cossi, N. Rega, J. M. Millam, M. Klene, J. E. Knox, J. B. Cross, V. Bakken, C. Adamo, J. Jaramillo, R. Gomperts, R. E. Stratmann, O. Yazyev, A. J. Austin, R. Cammi, C. Pomelli, J. W. Ochterski, R. L. Martin, K. Morokuma, V. G. Zakrzewski, G. A. Voth, P. Salvador, J. J. Dannenberg, S. Dapprich, A. D. Daniels, O. Farkas, J. B. Foresman, J. V. Ortiz, J. Cioslowski, D. J. Fox, Gaussian 09 Rev D.01, Gaussian, Inc., Wallingford, CT, **2009**.
- [41] A. D. Becke, *J. Chem. Phys.* **1993**, 98, 5648.
- [42] C. Lee, W. Yang, R. G. Parr, *Phys. Rev. B* **1988**, 37, 785.
- [43] B. Miehlich, A. Savin, H. Stoll, H. Preuss, *Chem. Phys. Lett.* **1989**, 157, 200.
- [44] A. M. K. Müller, *Phys. Lett. A* **1984**, 105, 446.
- [45] T. A. Keith, *AIMAll*, Version 16.01.09; TKGrismill Software, Overland Park, **2016**.
- [46] W. Nakanishi, S. Hayashi, K. Narahara, *J. Phys. Chem. A* **2008**, 112, 13593.
- [47] C. F. Matta, *Hydrogen-Hydrogen Bonding: The Non-Electrostatic Limit of Closed-Shell Interaction Between Two Hydrogen Atoms. A Critical Review*, Springer, The Netherlands, **2006**.
- [48] R. F. W. Bader, *J. Phys. Chem. A* **2008**, 112, 13717.
- [49] A. Martín Pendás, E. Francisco, M. A. Blanco, C. Gatti, *Chemistry* **2007**, 13, 9362.

Received: 7 June 2018

Revised: 11 July 2018

Accepted: 11 July 2018

Bibliography

- [1] R. F. W. Bader, *Atoms in Molecules: A Quantum Theory*. Clarendon Press, Oxford, 1994.
- [2] R. W. F. Bader, "A quantum theory of molecular structure and its applications," *Chemical Reviews*, vol. 91, pp. 893–928, 1991.
- [3] ———, "Defintion of molecular structure: By choice or by appeal to observation," *The Journal of Physical Chemistry A*, vol. 114, pp. 7431–7444, 2010.
- [4] ———, "A bond path: A universal indicator of bonded interactions," *The Journal of Physical Chemistry A*, vol. 102, pp. 7314–7323, 1998.
- [5] R. F. W. Bader and D. Fang, "Properties of atoms in molecules: Caged atoms and the ehrenfest force," *Journal of Chemical Theory and Computation*, vol. 1, pp. 403–414, 2005.
- [6] C. F. Matta, N. Castillo, and R. J. Boyd, "Characterization of a closed-shell fluorine-fluorine bonding interaction in aromatic compounds on the basis of the electron density," *Journal of Chemical Physics A*, vol. 109, no. 3669-3681, 2005.
- [7] R. W. F. Bader and G. R. Runtz, "Virial partitioning of polyatomic systems," *Molecular Physics: An International Journal at the Interface Between Chemistry and Physics*, vol. 30, pp. 117–128, 1975.
- [8] R. F. W. Bader and P. M. Beddall, "Virial field relationship for molecular charge distributions and the spatial partitioning of molecular properties," *The Journal of Chemical Physics*, vol. 56, pp. 3320–3329, 1972.
- [9] T. A. Keith, R. F. W. Bader, and Y. Aray, "Structural homeomorphism between the electron density and the virial field," *International Journal of Quantum Chemistry*, vol. 57, pp. 183–198, 1996.
- [10] G. R. Runtz, R. F. W. Bader, and R. R. Messer, "Definition of bond paths and bond directions in terms of the molecular charge distribution," *Canadian Journal of Chemistry*, vol. 55, pp. 3040–3045, 1977.
- [11] R. F. W. Bader, S. G. Anderson, and A. J. Duke, "Quantum topology of molecular charge distributions. I," *Journal of the American Chemical Society*, vol. 101, pp. 1389–1395, 1979.
- [12] R. W. F. Bader, "Bond paths are not chemical bonds," *Journal of Physical Chemistry A*, vol. 113, pp. 10391–10396, 2009.
- [13] S. R. Gadre, "Molecular electrostatic potentials: A topographical study," *Journal of Chemical Physics*, vol. 96, pp. 5253–5260, 1992.

- [14] J. Cioslowski and S. T. Mixon, "Topological properties of electron density in search of the steric interactions in molecules: Electronic structure calculations on ortho-substituted biphenyls," *Journal of the American Chemical Society*, vol. 114, pp. 4382–4387, 1992.
- [15] —, "Universality among topological properties of electron density associated with the hydrogen-hydrogen nonbonding interactions," *Canadian Journal of Chemistry*, vol. 70, pp. 443–449, 1992.
- [16] J. Cioslowski, L. Edgington, and B. B. Stefanov, "Steric overcrowding in perhalogenated cyclohexanes, dodecahedranes and [60]fulleranes," *Journal of the American Chemical Society*, vol. 117, pp. 10 381–10 384, 1995.
- [17] J. Cioslowski, S. T. Mixon, and W. D. Edwards, "Weak bonds in the topological theory of atoms in molecules," *Journal of the American Chemical Society*, vol. 113, pp. 1083–1085, 1991.
- [18] C. F. Matta, J. Hernández-Trujillo, T.-H. Tang, and R. F. W. Bader, "Hydrogen-hydrogen bonding: A stabilizing interaction in molecules and crystals," *Chemistry A European Journal*, vol. 9, pp. 1940–1951, 2003.
- [19] J. Poater, M. Solà, and F. M. Bickelhaupt, "Hydrogen-hydrogen bonding in planar biphenyl, predicted by atoms-in-molecules theory, does not exist," *Chemistry A European Journal*, vol. 12, pp. 2889–2895, 2006.
- [20] R. W. F. Bader, "Pauli repulsion exists in the eye of the beholder," *Chemistry A European Journal*, vol. 12, pp. 2896–2901, 2006.
- [21] J. Hernández-Trujillo, F. Cortés-Guzmán, D. Fang, and R. W. F. Bader, "Forces in molecules," *Faraday Discuss*, vol. 135, pp. 79–95, 2007.
- [22] J. Poater, M. Solà, and F. M. Bickelhaupt, "A model of the chemical bond must be rooted in quantum mechanics, provide insight, and possess predictive power," *Chemistry A European Journal*, vol. 12, pp. 2902–2905, 2006.
- [23] J. Hernández-Trujillo and C. F. Matta, "Hydrogen-hydrogen bonding in biphenyl revisited," *Structural Chemistry*, vol. 18, pp. 849–857, 2007.
- [24] K. Eskandari and C. van Alsenoy, "Hydrogen-hydrogen interaction in planar biphenyl: A theoretical study based on the interacting quantum atoms and hirshfeld atomic energy partitioning methods," *Journal of Computational Chemistry*, vol. 35, pp. 1883–1889, 2014.
- [25] A. Haaland, D. J. Shorokhov, and N. V. Tverdova, "Topological analysis of electron densities: Is the presence of an atomic interaction line in an equilibrium geometry a sufficient condition for the existence of a chemical bond," *Chemistry A European Journal*, vol. 10, pp. 4416–4421, 2004.
- [26] T. Strenalyuk and A. Haaland, "Chemical bonding in the inclusion complex of he in adamantane (he@adam): The origin of the barrier to dissociation," *Chemistry A European Journal*, vol. 14, pp. 10 223–10 226, 2008.
- [27] R. P. Feynman, "Forces in a molecule," *Physical Review*, vol. 56, pp. 340–343, 1939.
- [28] H. Hellmann, *Einführung in die Quantenchemie*. Leipzig and Vienna: Deuticke, 1937.
- [29] M. von Hopffgarten and G. Frenking, "Chemical bonding in the inclusion complex of he

- in adamantane, he@adam: Antithesis and complement,” *Chemistry A European Journal*, vol. 14, pp. 10 227–10 231, 2008.
- [30] S. G. Wang, Y. X. Qiu, and W. H. E. Schwarz, “Bonding or nonbonding? description or explanation? ”confinement bonding” of he@adamantane,” *Chemistry A European Journal*, vol. 15, pp. 6032–6040, 2009.
- [31] P. Dem’yanov and P. Polestshuk, “A bond path and an attractive ehrenfest force do not necessarily indicate bonding interactions: Case study on $m \times 2$ ($m = \text{li, na, k; x} = \text{h, oh, f, cl}$),” *Chemistry A European Journal*, vol. 18, pp. 4982–4993, 2012.
- [32] M. Jabłoński, “Energetic and geometrical evidence of nonbonding character of some intramolecular halogen···oxygen and other y···y interactions,” *The Journal of Physical Chemistry A*, vol. 116, pp. 3753–3764, 2012.
- [33] M. Jabłoński and M. Palusiak, “The halogen-oxygen interaction in 3-halogenopropenal revisited – the dimer model vs. qtaim indications,” *Chemical Physics*, vol. 415, pp. 207–213, 2013.
- [34] J. D. Dunitz, “Intermolecular atom-atom bonds in crystals,” *IUCrJ*, vol. 2, pp. 157–158, 2015.
- [35] T. S. Thakur, R. Dubey, and G. R. Desiraju, “Intermolecular atom-atom bonds in crystals - a chemical perspective,” *IUCrJ*, vol. 2, pp. 159–160, 2015.
- [36] C. Lecomte, E. Espinosa, and C. F. Matta, “On atom-atom ‘short contact’ bonding interactions in crystals,” *IUCrJ*, vol. 2, pp. 161–163, 2015.
- [37] M. A. Spackman and E. N. Maslen, “Chemical properties from the promolecule,” *Journal of Physical Chemistry*, vol. 90, pp. 2020–2027, 1986.
- [38] C. Gatti, P. Fantucci, and G. Pacchioni, “Charge density topological study of bonding in lithium clusters,” *Theoretical chimica acta*, vol. 72, pp. 433–458, 1987.
- [39] W. L. Cao, C. Gatti, P. J. MacDougall, and R. W. F. Bader, “On the presence of non-nuclear attractors in the charge distributions of li and na clusters,” *Chemical Physics Letters*, vol. 141, pp. 380–385, 1987.
- [40] J. Cioslowski, “Nonnuclear attractors in the lithium dimeric molecule,” *Journal of Physical Chemistry*, vol. 94, pp. 5496–5498, 1990.
- [41] R. Glaser, R. F. Waldron, and K. B. Wiberg, “Origin and consequences of the nonnuclear attractor in the ab initio electron density functions of dilithium,” *Journal of Physical Chemistry*, vol. 94, pp. 7357–7362, 1990.
- [42] K. E. Edgecombe, R. O. Esquivel, V. H. Smith, and F. Müller-Plathe, “Pseudoatoms of the electron density,” *Journal of Chemical Physics*, vol. 97, pp. 2593–2599, 1992.
- [43] G. I. Bersuker, C. Peng, and J. E. Boggs, “The nature of the covalent bond: The existence and origin of nonnuclear attractors,” *Journal of Chemical Physics*, vol. 97, pp. 9323–9329, 1993.
- [44] C. Mei, K. E. Edgecombe, and C. H. Smith, “Topological analysis of the charge density of solids: bcc sodium and lithium,” *International Journal of Quantum Chemistry*, pp. 287–293, 1993.

- [45] V. Luaña, P. Mori-Sánchez, A. Costales, M. A. Blanco, and A. M. Pendás, “Non-nuclear maxima of the electron density on alkaline metals,” *Journal of Chemical Physics*, vol. 119, pp. 6341–6350, 2003.
- [46] G. K. H. Madsen, P. Blaha, and K. Schwarz, “On the existence of non-nuclear maxima in simple metals,” *Journal of Chemical Physics*, vol. 117, pp. 8030–8035, 2002.
- [47] A. M. Pendás, M. A. Blanco, A. Costales, P. Mori-Sánchez, and V. Luaña, “Non-nuclear maxima of the electron density,” *Physical Review Letters*, vol. 83, pp. 1930–1933, 1999.
- [48] A. Azizi, R. Momen, T. Xu, S. R. Kirk, and S. Jenkins, “Non-nuclear attractors in small charged lithium clusters, $Li(m)(q)$ ($m = 2-5$, $q = +- 1$), with qtaim and the ehrenfest force partitioning,” *Physical Chemistry Chemical Physics*, vol. 20, pp. 24 695–24 707, 2018.
- [49] B. B. Iversen, F. K. Larsen, M. Souhassou, and M. Takata, “Experimental evidence for the existence of non-nuclear maxima in the electron-density distribution of metallic beryllium. a comparative study of the maximum entropy method and the multipole refinement method,” *Acta Crystallographica*, vol. B51, pp. 580–591, 1995.
- [50] R. W. F. Bader and J. A. Platts, “Characterization of an fcenter in an alkali halide cluster,” *Journal of Chemical Physics*, vol. 107, pp. 8545–8553, 1997.
- [51] J. A. Platts, J. Overgaard, C. Jones, B. B. Iversen, and A. Stasch, “First experimental characterization of a non-nuclear attractor in a dimeric magnesium(i) compound,” *Journal of Chemical Physics A*, vol. 115, pp. 194–200, 2011.
- [52] A. Taylor, C. F. Matta, and R. J. Boyd, “The hydrated electron as a psuedo-atom in cavity bound water clusters,” *Journal of Chemical Theory and Computation*, vol. 3, pp. 1054–1063, 2007.
- [53] L. A. Terrabuio, T. Q. Teodoro, C. F. Matta, and R. L. A. Haiduke, “Non-nuclear attractors in heteronuclear diatomic systems,” *The Journal of Physical Chemistry A*, vol. 120, pp. 1168–1174, 2016.
- [54] Q. K. Timerghazin and G. H. Peslherbe, “Non-nuclear attractor of electron density as a manifestation of the solvated electron,” *The Journal of Chemical Physics*, vol. 127, p. 064108, 2007.
- [55] A. M. Pendás and J. Hernández-Trujillo, “The ehrenfest force field: Topology and consequences for the defintion of an atom in a molecule,” *The Journal of Chemical Physics*, vol. 137, p. 134101, 2012.
- [56] J. Dillen, “The topology of the ehrenfest force density revisited. a different perspective based on slater-type orbitals,” *Journal of Computational Chemistry*, vol. 36, pp. 883–890, 2015.
- [57] T. Steiner, “The hydrogen bond in the solid state,” *Angewandte Chemie International Edition*, vol. 41, pp. 48–76, 2002.
- [58] N. V. Belkova, E. S. Shubina, and L. M. Epstein, “Diverse world of unconventional hydrogen bonds,” *Accounts of Chemical Research*, vol. 38, pp. 624–631, 2005.
- [59] I. Alkorta, I. Rozas, and J. Elguero, “Non-conventional hydrogen bonds,” *Chemical Society Reviews*, vol. 27, pp. 163–170, 1998.

- [60] M. J. Calhorda, "Weak hydrogen bonds: Theoretical studies," *Chemical Communications*, vol. 10, pp. 801–809, 2000.
- [61] E. Espinosa, E. Molins, and C. Lecomte, "Hydrogen bond strengths revealed by topological analysis of experimentally observed electron densities," *Chemical Physics Letters*, vol. 285, pp. 170–173, 1998.
- [62] E. Espinosa, M. Souhassou, H. Lachekar, and C. Lecomte, "Topological analysis of the electron density in hydrogen bonds," *Acta Crystallographica*, vol. B55, pp. 563–572, 1999.
- [63] I. Alkorta, I. Rozas, and J. Elguero, "Isocyanides as hydrogen bond acceptors," *Theoretical Chemistry Accounts*, vol. 99, pp. 116–123, 1997.
- [64] I. Rozas, I. Alkorta, and J. Elguero, "Inverse hydrogen-bonded complexes," *Journal of Chemical Physics A*, vol. 101, pp. 4236–4244, 1997.
- [65] J. A. Platts, S. T. Howard, and K. Wozniak, "Quantum chemical evidence for c-h-c hydrogen bonding," *Chemical Communications*, vol. 1, pp. 63–64, 1996.
- [66] J. A. Platts and S. T. Howard, "C-h-c hydrogen bonding involving ylides," *Journal of the Chemical Society, Perkin Transactions 2*, vol. 11, pp. 2241–2248, 1997.
- [67] I. Alkorta and J. Elguero, "Carbenes and silylenes as hydrogen bond acceptors," *Journal of Physical Chemistry*, vol. 100, pp. 19 367–19 370, 1996.
- [68] I. Rozas, I. Alkorta, and J. Elguero, "Unusual hydrogen bonds: H- π interactions," *Journal of Physical Chemistry A*, vol. 101, pp. 9457–9463, 1997.
- [69] U. Koch and P. L. A. Popelier, "Characterization of c-h-o hydrogen bonds on the basis of the charge density," *Journal of Physical Chemistry*, vol. 99, pp. 9747–9754, 1995.
- [70] S. J. Grabowski, "Ab initio calculations on conventional and unconventional hydrogen bonds-study of the hydrogen bond strength," *Journal of Physical Chemistry A*, vol. 105, pp. 10 739–10 746, 2001.
- [71] —, "Hydrogen bonding strength - measures based on geometric and topological parameters," *Journal of Physical Organic Chemistry*, vol. 17, pp. 18–31, 2004.
- [72] R. H. Crabtree, "A new type of hydrogen bond," *Science*, vol. 282, pp. 2000–2001, 1998.
- [73] J. C. J. Lee, E. Peris, A. L. Rheingold, and R. H. Crabtree, "An unusual type of h-h interaction: Ir-h-h-o and ir-h-h-n hydrogen bonding and its involvement in sigma-metathesis," *Journal of the American Chemical Society*, vol. 116, pp. 11 014–11 019, 1994.
- [74] T. B. Richardson, S. de Gala, and R. H. Crabtree, "Unconventional hydrogen bonds: Intermolecular b-h-h-n interactions," *Journal of the American Chemical Society*, vol. 117, pp. 12 875–12 876, 1995.
- [75] R. H. Crabtree, P. E. M. Siegbahn, O. Eisenstein, A. L. Rheingold, and T. F. Koetzle, "A new intermolecular interaction: Unconventional hydrogen bonds with element-hydride bonds as proton acceptor," *Accounts of Chemical Research*, vol. 29, pp. 348–354, 1996.
- [76] W. T. Klooster, T. F. Koetzle, P. E. M. Siegbahn, T. B. Richardson, and R. H. Crabtree, "Study of the n-h-h-b dihydrogen bond including the crystal structure of bh_3nh_3 by neutron diffraction," *Journal of the American Chemical Society*, vol. 121, pp. 6337–6343, 1999.

- [77] R. H. Crabtree, "Dihydrogen complexes: Some structural and chemical studies," *Accounts of Chemical Research*, vol. 23, pp. 95–101, 1990.
- [78] R. C. Stevens, R. Bau, D. Milstein, O. Blum, and T. F. Koetzle, "Concept of the h(+)-h(-) interaction. a low temperature neutron diffraction study of cis-[irh(oh)(pme3)4]pf6," *Journal of the Chemical Society, Dalton Transactions*, vol. 4, pp. 1429–1432, 1990.
- [79] S. Park, R. Ramachandran, A. J. Lough, and R. H. Morris, "A new type of intramolecular h-h-h interaction involving nh-h(ir)-hn atoms. crystal and molecular structure of [irh(n1-sc5h4nh)2(n2sc5h4n)(pcy3)]bf3-0.72ch2cl2," *Journal of the Chemical Society, Chemical Communications*, vol. 19, pp. 2201–2202, 1994.
- [80] G. J. Kubas, "Molecular hydrogen complexes: Coordination of a sigma bond to transition metals," *Accounts of Chemical Research*, vol. 21, pp. 120–128, 1988.
- [81] C. F. Matta, *Hydrogen Bonding - New Insights*. Springer, 2006, ch. 9, pp. 337–375.
- [82] O. Ermer and S. A. Mason, "Extremely short non-bonded h-h distances in two derivatives of exo, exo-tetracyclo[6.2.1.1(3,6).o(2,7)] dodecane," *Journal of the Chemical Society, Chemical Communications*, vol. 1, pp. 53–54, 1983.
- [83] B. P. Reid, M. J. O'Loughlin, and R. K. Sparks, "Methane-methane isotropic interaction potential from total differential cross sections," *Journal of Chemical Physics*, vol. 83, pp. 5656–5662, 1985.
- [84] R. Righini, K. Maki, and M. L. Klein, "An intermolecular potential for methane," *Chemical Physics Letters*, vol. 80, pp. 301–305, 1981.
- [85] J. J. Novoa, M. H. Whangboo, and J. M. Williams, "Interaction energies associated with short intermolecular contacts of c-h bonds. ii. ab initio computational study of the c-h-h-c interactions in methane dimers," *Journal of Chemical Physics*, vol. 94, pp. 4835–4841, 1991.
- [86] D. Myburgh, S. von Berg, and J. Dillen, "A comparison of energetic criteria to probe the stabilizing interaction resulting from a bond path between congested atoms," *Journal of Computational Chemistry*, vol. 39, pp. 2273–2282, 2018.
- [87] A. D. Becke and K. E. Edgecombe, "A simple measure of electron localisation in atomic and molecular systems," *The Journal of Chemical Physics*, vol. 92, pp. 5397–5403, 1990.
- [88] H. L. Schmider and A. D. Becke, "Chemical content of the kinetic energy density," *Journal of Molecular Structure (Theochem)*, vol. 527, pp. 51–61, 2000.
- [89] H. J. Bohórquez, C. F. Matta, and R. J. Boyd, "The localized electrons detector as an ab initio representation of molecular structures," *International Journal of Quantum Chemistry*, vol. 110, pp. 2418–2425, 2010.
- [90] E. R. Johnson, S. Keinan, P. Mori-Sánchez, J. Contreras-García, A. J. Cohen, and W. Yang, "Revealing noncovalent interactions," *Journal of the American Chemical Society*, vol. 132, pp. 6498–6506, 2010.
- [91] L. Ferreira, A. Eaby, and J. Dillen, "The topology of the coulomb potential density. a comparison with the electron density, the virial energy density and the ehrenfest force density," *Journal of Computational Chemistry*, vol. 38, pp. 2784–2790, 2017.

- [92] H. J. Bohórquez and R. J. Boyd, "A localized electrons detector for atomic and molecular systems," *Theoretical Chemistry Accounts*, vol. 127, pp. 393–394, 2010.
- [93] A. Kumar, S. R. Gadre, N. Mohan, and C. H. Suresh, "Lone pairs: An electrostatic viewpoint," *The Journal of Physical Chemistry A*, vol. 118, pp. 526–532, 2014.
- [94] S. D. Kahn, C. F. Pau, and W. J. Hehre, "Models of chemical reactivity: Mapping of intermolecular potentials onto electron density surfaces," *International Journal of Quantum Chemistry*, vol. 34, pp. 575–591, 1988.
- [95] S. R. Gadre and I. H. Shrivastava, "Shapes and sizes of molecular anions via topographical analysis of electrostatic potential," *The Journal of Chemical Physics*, vol. 94, pp. 4384–4390, 1991.
- [96] R. F. Stewart, "On the mapping of electrostatic properties from bragg diffraction data," *Chemical Physics Letters*, vol. 65, pp. 335–342, 1979.
- [97] P. Politzer and D. G. Truhlar, *Chemical Applications of Atomic and Molecular Electrostatic Potentials*. New York: Plenum Press, 1981.
- [98] T. Brinck, J. S. Murray, and P. Politzer, "Surface electrostatic potential of halogenated methanes as indicators of directional intermolecular interactions," *International Journal of Quantum Chemistry: Quantum Biology Symposium*, vol. 19, pp. 57–64, 1992.
- [99] R. F. W. Bader, M. T. Carroll, J. R. Cheeseman, and C. Chang, "Properties of atoms in molecules: Atomic volumes," *Journal of the American Chemical Society*, vol. 109, pp. 7968–7979, 1987.
- [100] P. Politzer, J. S. Murray, and T. Clark, "Halogen bonding and other sigma - hole interactions: A perspective," *Physical Chemistry Chemical Physics*, vol. 15, pp. 11 178–11 189, 2013.
- [101] J. S. Murray, K. Paulsen, and P. Politzer, "Molecular surface electrostatic potentials in the analysis of non-hydrogen-bonding noncovalent interactions," *Proceedings of the Indian Academy of Sciences - Chemical Sciences*, vol. 106, pp. 267–275, 1994.
- [102] P. Murray-Rust and W. D. S. Motherwell, "Computer retrieval and analysis of molecular geometry. 4. intermolecular interactions," *Journal of the American Chemical Society*, vol. 101, pp. 4374–4376, 1979.
- [103] P. Murray-Rust, W. C. Stallings, C. T. Monti, R. K. Preston, and J. P. Glusker, "Intermolecular interactions of the c-f bond: The crystallographic environment of fluorinated carboxylic acids and related structures," *Journal of the American Chemical Society*, no. 105, pp. 3206–3214, 1983.
- [104] N. Ramasubbu, R. Parthasarathy, and P. Murray-Rust, "Angular preferences of intermolecular forces around halogen centers: Preferred directions of approach of electrophiles and nucleophiles around carbon-halogen bond," *Journal of the American Chemical Society*, vol. 108, pp. 4308–4314, 1986.
- [105] P. Auffinger, F. A. Hays, E. Westhof, and P. S. Ho, "Halogen bonds in biological molecules," *Proceedings of the National Academy of Sciences*, vol. 101, pp. 16 789–16 794, 2004.

- [106] P. Metrangolo, H. Neukirch, T. Pilati, and G. Resnati, "Halogen bonding based recognition processes: A world parallel to hydrogen bonding," *Accounts of Chemical Research*, vol. 38, pp. 386–395, 2005.
- [107] J. S. Murray, K. E. Riley, P. Politzer, and T. Clark, "Directional weak intermolecular interactions: sigma hole bonding," *Australian Journal of Chemistry*, vol. 63, pp. 1598–1607, 2010.
- [108] P. Politzer and J. S. Murray, "Halogen bonding: An interim discussion," *ChemPhysChem*, vol. 14, pp. 278–294, 2013.
- [109] J. S. Murray and P. Politzer, *Quantum Medicinal Chemistry*. Wiley-VCH, Weinheim, 2003, ch. 8, pp. 233–254.
- [110] P. Politzer, J. S. Murray, and Z. Peralta-Inga, "Molecular surface electrostatic potentials in relation to noncovalent interactions in biological systems," *International Journal of Quantum Chemistry*, vol. 85, pp. 676–684, 2001.
- [111] P. Politzer and J. S. Murray, "The fundamental nature and role of the electrostatic potential in atoms and molecules," *Theoretical Chemistry Accounts*, vol. 108, pp. 134–142, 2002.
- [112] K. D. Sen and P. Politzer, "Characteristic features of the electrostatic potentials of singly negative monoatomic ions," *Journal of Chemical Physics*, vol. 90, pp. 4370–4372, 1989.
- [113] P. Politzer, J. S. Murray, and P. Lane, "Electrostatic potentials and covalent radii," *Journal of Computational Chemistry*, vol. 24, pp. 505–511, 2003.
- [114] N. Mohan, C. H. Suresh, A. Kumar, and S. R. Gadre, "Molecular electrostatics for probing lone pair-pi interactions," *Physical Chemistry Chemical Physics*, vol. 15, pp. 18 401–18 409, 2013.
- [115] P. Balanarayan and S. R. Gadre, "Topography of molecular scalar fields. I. algorithm and poincaré-hopf relation," *Journal of Chemical Physics*, vol. 119, pp. 5037–5043, 2003.
- [116] M. Leboeuf, A. M. Köster, and K. Jug, "Topological analysis of the molecular electrostatic potential," *Journal of Chemical Physics*, vol. 111, pp. 4893–4905, 1999.
- [117] P. Politzer and K. C. Daiker, *The Force Concept in Chemistry*. Van Nostrand Reinhold, New York, 1981, ch. 6.
- [118] E. Scrocco and J. Tomasi, "The electrostatic molecular potential as a tool for the interpretation of molecular properties," *New Concepts II*, pp. 95–170, 2005.
- [119] —, "Electronic molecular structure, reactivity and intermolecular forces: An euristic interpretation by means of electrostatic molecular potentials," *Advances in Quantum Chemistry*, vol. 11, pp. 115–193, 1978.
- [120] D. Chou and H. Weinstein, "Electron charge redistribution following electrophilic attack on heterocycles: Nitrogen as a charge transducer," *Tetrahedron*, vol. 34, pp. 275–286, 1978.
- [121] T. Brinck, J. S. Murray, and P. Politzer, "Molecular surface electrostatic potentials and local ionization energies of group v-vii hydrides and their anions: Relationships for aqueous and gas-phase acidities," *International Journal of Quantum Chemistry*, vol. 48, pp. 73–88, 1993.

- [122] J. S. Murray and Z. Peralta-Inga, *Theoretical Organic Chemistry*. Elsevier, Amsterdam, 1998, ch. 7, pp. 189–199.
- [123] J. S. Murray, Z. Peralta-Inga, P. Politzer, K. Ekanayake, and P. LeBreton, “Computational characterization of nucleotide bases: Molecular surface electrostatic potentials and local ionization energies, and local polarization energies,” *International Journal of Quantum Chemistry*, vol. 83, no. 245-254, 2001.
- [124] P. Politzer, J. S. Murray, and M. C. Concha, “The complimentary roles of molecular surface electrostatic potentials and average local ionization energies with respect to electrophilic processes,” *International Journal of Quantum Chemistry*, vol. 88, pp. 19–27, 2002.
- [125] R. F. W. Bader, Y. Tal, S. G. Anderson, and T. T. Nguyen-Dang, “Quantum topology: Theory of molecular structure and its change,” *Israel Journal of Chemistry*, vol. 19, pp. 8–29, 1980.
- [126] R. F. W. Bader, T. T. Nguyen-Dang, and Y. Tal, “Quantum topology of molecular charge distributions. II. molecular structure and its change,” *The Journal of Chemical Physics*, vol. 70, pp. 4316–4329, 1979.
- [127] K. Collard and G. G. Hall, “Orthogonal trajectories of the electron density,” *International Journal of Quantum Chemistry*, vol. 12, pp. 623–637, 1977.
- [128] R. G. A. Bone and R. W. F. Bader, “Identifying and analyzing intermolecular bonding interactions in van der waals molecules,” *The Journal of Physical Chemistry*, vol. 100, pp. 10 892–10 911, 1996.
- [129] D. Roy, P. Balanarayan, and S. R. Gadre, “An appraisal of poincaré-hopf relation and application to topography of molecular electrostatic potentials,” *The Journal of Chemical Physics*, vol. 129, pp. 174 103–174 109, 2008.
- [130] A. Kumar, S. R. Gadre, X. Chenxia, X. Tianlv, S. R. Kirk, and S. Jenkins, “Hybrid qtaim and electrostatic potential-based quantum topology phase diagrams for water clusters,” *Physical Chemistry Chemical Physics*, vol. 17, pp. 15 258–15 273, 2015.
- [131] A. Kumar and S. R. Gadre, “Exploring the gradient paths and zero flux surfaces of molecular electrostatic potential,” *Journal of Chemical Theory and Computation*, vol. 12, pp. 1705–1713, 2016.
- [132] R. F. W. Bader and H. Essén, “The characterization of atomic interactions,” *Journal of Chemical Physics*, vol. 80, pp. 1943–1960, 1984.
- [133] R. F. W. Bader, “Principle of stationary action and the definition of a proper open system,” *Physical Review B*, vol. 49, pp. 13 348–13 356, 1994.
- [134] R. W. F. Bader, “Everyman’s derivation of the theory of atoms in molecules,” *Journal of Physical Chemistry A*, vol. 111, pp. 7966–7972, 2007.
- [135] R. F. W. Bader, A. Larouche, C. Gatti, M. T. Carroll, and P. J. MacDougall, “Properties of atoms in molecules: Dipole moments and transferability of properties,” *The Journal of Chemical Physics*, vol. 87, pp. 1142–1152, 1987.
- [136] R. K. Pathak and S. R. Gadre, “Maximal and minimal characteristics of molecular electrostatic potentials,” *The Journal of Chemical Physics*, vol. 93, pp. 1770–1773, 1990.

- [137] C. H. Suresh and S. R. Gadre, "Clar's aromatic sextet theory revisited via molecular electrostatic potential topography," *Journal of Organic Chemistry*, vol. 64, pp. 2505–2512, 1999.
- [138] E. Clar, *Aromatic Sextet*. London: Joh Wiley and Sons ltd, 1972.
- [139] G. M. Badger, *Aromatic Character and Aromaticity*. Cambridge: Cambridge University Press, 1969.
- [140] S. R. Gadre, S. A. Kulkarni, C. H. Suresh, and I. H. Shrivastava, "Basis set dependence of the molecular electrostatic potential topography. a case study of substituted benzenes," *Chemical Physics Letters*, vol. 239, pp. 273–281, 1995.
- [141] M. J. Frisch, G. W. Trucks, H. B. Schlegel, G. E. Scuseria, M. A. Robb, J. R. Cheeseman, G. Scalmani, V. Barone, G. Mennucci, A. Petersson, H. Nakatsuji, M. Caricato, X. Li, H. P. Hratchian, A. F. Izmaylov, J. Bloino, G. Zheng, J. L. Sonnenberg, M. Hada, M. Ehara, K. Toyota, R. Fukuda, J. Hasegawa, M. Ishida, T. Nakajima, Y. Honda, O. Kitao, H. Nakai, T. Vreven, J. A. M. Jr, J. E. Peralta, F. Ogliaro, M. Bearpark, J. J. Heyd, E. Brothers, K. N. Kudin, V. N. Staroverov, T. Keith, R. Kobayashi, J. Normand, K. Raghavachari, A. Rendell, J. C. Burant, S. S. Iyengar, J. Tomasi, M. Cossi, N. Rega, J. M. Millam, M. Klene, J. E. Knox, J. B. Cross, V. Bakken, C. Adamo, J. Jaramillo, R. Gomperts, R. E. Stratmann, O. Yazyev, A. J. Austin, R. Cammi, C. Pomelli, J. W. Ochterski, R. L. Martin, K. Morokuma, V. G. Zakrzewski, G. A. Voth, P. Salvador, J. J. Dannenberg, S. Dapprich, A. D. Daniels, O. Farkas, J. B. Foresman, J. V. Ortiz, J. Cioslowski, and D. J. Fox, "Gaussian, inc," *Wallingford CT*, 2013.
- [142] T. A. Keith, "Aimall, version 16.01.09," *TKGrismill Software, Overland Park*, 2016.
- [143] M. Springborg, *Methods of Electronic-Structure Calculations from Molecules to Solids*. Baffins Lane, Chichester: John Wiley and Sons ltd, 2000.
- [144] C. R. Wick and T. Clark, "On bond-critical points in qtaim and weak interactions," *Journal of Molecular Modeling*, vol. 24, pp. 142–151, 2018.
- [145] J. Dillen, "Congested molecules. where is the steric repulsion? an analysis of the electron density by the method of interacting quantum atoms," *International Journal of Quantum Chemistry*, vol. 113, pp. 2143–2153, 2013.
- [146] C. F. Matta, S. A. Sadjadi, D. A. Braden, and G. Frenking, "The barrier to the methyl rotation in cis-2-butene and its isomerization energy to trans-2-butene, revisited," *Journal of Computational Chemistry*, vol. 37, pp. 143–154, 2015.
- [147] F. Weinhold, P. von Ragué Schleyer, and W. C. McKee, "Bay-type h-h "bonding" in cis-2-butene and related species: Qtaim versus nbo description," *Journal of Computational Chemistry*, vol. 35, pp. 1499–1508, 2014.